Theses and Dissertations

2012

Structural features of fluoroquinolone-class antibiotics that affect lethal activities and DNA binding

Heidi Ann Schwanz
University of Iowa

STRUCTURAL FEATURES OF FLUOROQUINOLONE-CLASS ANTIBIOTICS

THAT AFFECT LETHAL ACTIVITIES AND DNA BINDING

by

Heidi Ann Schwanz

An Abstract

Of a thesis submitted in partial fulfillment
of the requirements for the Doctor of
Philosophy degree in Pharmacy (Medicinal and Natural Products Chemistry)
in the Graduate College of
The University of Iowa

July 2012

Thesis Supervisor: Associate Professor Robert J. Kerns

ABSTRACT

Fluoroquinolones, broad-spectrum bactericidal antibiotics, exert their effects by inhibiting type II topoisomerases through the formation of a fluoroquinolone-DNA-topoisomerase ternary complex. Recently, newer, structurally unique fluoroquinolones have been shown to kill bacteria by promoting chromosomal fragmentation in the presence and absence of protein synthesis, thus allowing fluoroquinolones to potentially be used in the treatment of microorganisms that go into a dormant state. There is a need to further understand the structure activity relationships (SAR) of fluoroquinolones to develop new antibiotics that can kill dormant bacteria and are active against current resistant strains. The hypothesis that structurally unique fluoroquinolones interact with the DNA- fluoroquinolone-topoisomerase ternary complex in a unique way that leads to different killing pathways is the basis of this work.

The first approach to understand SAR for fluoroquinolones to kill non-growing bacteria was to evaluate the effect of modifications at the C-8 and C-5 positions on lethality. Novel, synthetically-derived and commercially-available fluoroquinolones were evaluated for ability to kill *Escherichia coli* in the presence and absence of chloramphenicol, a known protein synthesis inhibitor used to simulate non-growing bacteria.

The second study was to understand SAR of fluoroquinolone-class agents necessary to maintain antibacterial activity against common fluoroquinolone resistance-causing bacterial mutations on topoisomerase IV. A panel of novel fluoroquinolones, 2,4-quinazoline diones, and fluoroquinolone-like analogues with unique substitution combinations at C-8 and C-7 was synthesized and evaluated for ability to poison wild-type and mutant *Bacillus anthracis* topoisomerase IV.

The third study to understand the contribution of SAR of fluoroquinolone-class agents to novel killing mechanisms was to evaluate the binding interaction of

fluoroquinolones to double-stranded and nicked DNA. Binding affinities of fluoroquinolones to DNA were determined; fluoroquinolones were found to bind different DNA types with varied affinities. The ability of a series of C-8 and C-7 modified fluoroquinolones to stabilize or destabilize DNA was assessed.

The results of these studies also add broadly to the understanding of SAR associated with fluoroquinolone-class antibiotics for killing in the presence and absence of protein synthesis, maintaining activity in the presence of resistance-causing mutations in the target enzymes, and increasing binding interactions with different types of DNA.

Abstract Approved: _____

                                  Thesis Supervisor

                                 _____

                                  Title and Department

                                 _____

                                  Date

STRUCTURAL FEATURES OF FLUOROQUINOLONE-CLASS ANTIBIOTICS

THAT AFFECT LETHAL ACTIVITIES AND DNA BINDING

by

Heidi Ann Schwanz

A thesis submitted in partial fulfillment
of the requirements for the Doctor of
Philosophy degree in Pharmacy (Medicinal and Natural Products Chemistry)
in the Graduate College of
The University of Iowa

July 2012

Thesis Supervisor: Associate Professor Robert J. Kerns

Graduate College
The University of Iowa
Iowa City, Iowa

CERTIFICATE OF APPROVAL

_____

PH.D. THESIS

_____

This is to certify that the Ph.D. thesis of

Heidi Ann Schwanz

has been approved by the Examining Committee
for the thesis requirement for the Doctor of Philosophy
degree in Pharmacy (Medicinal and Natural Products Chemistry) at the July
2012 graduation.

Thesis Committee: _____
                    Robert J. Kerns, Thesis Supervisor

                _____
                    Jonathan A. Doorn

                _____
                    Zhendong Jin

                _____
                    David L. Roman

                _____
                    Marc S. Wold

To my mom for her guidance
To my family for their support
To both for their unconditional love

ACKNOWLEDGMENTS

ABSTRACT

Fluoroquinolones, broad-spectrum bactericidal antibiotics, exert their effects by inhibiting type II topoisomerases through the formation of a fluoroquinolone-DNA-topoisomerase ternary complex. Recently, newer, structurally unique fluoroquinolones have been shown to kill bacteria by promoting chromosomal fragmentation in the presence and absence of protein synthesis, thus allowing fluoroquinolones to potentially be used in the treatment of microorganisms that go into a dormant state. There is a need to further understand the structure activity relationships (SAR) of fluoroquinolones to develop new antibiotics that can kill dormant bacteria and are active against current resistant strains. The hypothesis that structurally unique fluoroquinolones interact with the DNA- fluoroquinolone-topoisomerase ternary complex in a unique way that leads to different killing pathways is the basis of this work.

The first approach to understand SAR for fluoroquinolones to kill non-growing bacteria was to evaluate the effect of modifications at the C-8 and C-5 positions on lethality. Novel, synthetically-derived and commercially-available fluoroquinolones were evaluated for ability to kill *Escherichia coli* in the presence and absence of chloramphenicol, a known protein synthesis inhibitor used to simulate non-growing bacteria.

The second study was to understand SAR of fluoroquinolone-class agents necessary to maintain antibacterial activity against common fluoroquinolone resistance-causing bacterial mutations on topoisomerase IV. A panel of novel fluoroquinolones, 2,4-quinazoline diones, and fluoroquinolone-like analogues with unique substitution combinations at C-8 and C-7 was synthesized and evaluated for ability to poison wild-type and mutant *Bacillus anthracis* topoisomerase IV.

The third study to understand the contribution of SAR of fluoroquinolone-class agents to novel killing mechanisms was to evaluate the binding interaction of

fluoroquinolones to double-stranded and nicked DNA. Binding affinities of fluoroquinolones to DNA were determined; fluoroquinolones were found to bind different DNA types with varied affinities. The ability of a series of C-8 and C-7 modified fluoroquinolones to stabilize or destabilize DNA was assessed.

The results of these studies also add broadly to the understanding of SAR associated with fluoroquinolone-class antibiotics for killing in the presence and absence of protein synthesis, maintaining activity in the presence of resistance-causing mutations in the target enzymes, and increasing binding interactions with different types of DNA.

TABLE OF CONTENTS

LIST OF TABLES

LIST OF FIGURES

Figure

xvii

Scheme

CHAPTER 1 INTRODUCTION

1.1 <u>Antibiotics and Antibiotic Resistance</u>

Antibiotics are drugs, either of synthetic or natural origin, that are used to treat infections caused by bacteria and other microorganisms. The discovery of antibiotics beginning with sulfonamides and β-lactams in the mid-20th century enabled rapid treatment of bacterial infections that had previously proven to be fatal. Between 1930 and 1970 in the "golden age" of antibiotic research, many classes of antibiotics that are still in use today were discovered [1]. Since then, overuse and misuse of antibiotics has resulted in the emergence of antibiotic resistant microorganisms and has fueled the continuance of antibiotic development [2]. Increasingly, antibiotic resistance has become a major threat to public health [3].

The various classes of antibiotics are active against different types of bacteria and can have either intracellular or extracellular targets. Bacteria are generally classified into one of two groups based on the structural differences in their cell walls: Gram-positive or Gram-negative. Gram-positive bacteria have cell walls that are composed of a single peptidoglycan layer attached to an inner cytoplasmic membrane. Gram-positive bacteria retain crystal violet dye in the Gram staining protocol. In contrast, Gram-negative bacteria do not retain the dye. Gram-negative bacteria have an additional, second outer membrane, which acts as a permeability barrier and convers the peptidoglycan of the cell wall. Due to the additional cell membrane, it is more difficult for antibiotics to penetrate Gram-negative bacteria. Thus in many cases, classes of drugs that are useful against Gram-negative organisms are also useful against Gram-positive, but not vice versa. Narrow spectrum agents are active against only a specific type of bacteria, while broad spectrum agents are active against many different bacteria, often both Gram-positive and Gram-negative organisms. Some antibiotics have cellular targets that do not require the antibiotic to fully transverse into the bacterial cell or cytoplasm, such as vancomycin that

targets the peptidoglycan of Gram-positive bacteria, while others have cytoplasmic targets, such as sulfonamides and fluoroquinolones [1].

The activity of an antibiotic is commonly characterized by minimum inhibitory concentration (MIC). MIC is ascertained by a standard growth assay in which the concentration of the drug required to block visible growth of a bacterial population is determined. Lower MICs correspond to increased activity. MIC is a measure of bacterial growth and does not differentiate bactericidal and bacteriostatic antibiotics. Percent DNA cleavage is a measure of activity that is commonly used to evaluate activity of topoisomerase inhibitors, such as fluoroquinolone antibiotics. Higher percent DNA cleavage corresponds to increased activity. In the present work, both MIC and percent DNA cleavage are used as measures of fluoroquinolone-class antibiotic activity (Chapter 3).

Drug resistant microorganisms are responsible for an increasing number of community-acquired and hospital-acquired infections, including those from *Staphylococcus aereus*, *Pseudomonas aureginosa*, *Streptococcus pneumoniae*, and *Mycobacterium tuberculosis* [4-7]. These drug resistant microorganisms display reduced or nonexistent susceptibility to antibiotic drugs, thus allowing the infections to persist in patients and increase the numbers of fatalities. When first choice antibiotics do not work to treat an infection, a second or third, often more toxic "drug of last resort" is administered in an attempt to treat the drug resistant infection. Consequently, usage restrictions have been placed on these drugs of last resort in order to decrease the chance of selecting for microorganisms that are resistant to these agents [8].

There are three general mechanisms of resistance that are common to many classes of antibiotics: chemical modification or breakdown of the antibiotic, failure of penetration including efflux transporters, or specific changes to the target [1]. Common examples of chemical modification and antibiotic breakdown are the enzymatic addition of acyl functional groups to the aminoglycoside antibiotics, and the destruction of β-

lactam antibiotics by β-lactamases. Failure of the drug to penetrate the microorganism can occur by several methods: mutation or downregulation of the drug transporters that take in the drug, upregulation of efflux transports that actively pump the drug out of the bacterium once it is inside, or alteration of the cell wall composition so the drug can no longer penetrate the bacterium. Antibiotic targets can be altered through changes in expression levels or through spontaneous mutation in the genes encoding the target that cause alterations in target structure and prevent the antibiotic from interacting with the target. Alteration of the target through mutation is one of the main mechanisms of resistance to fluoroquinolones, the class of antibiotics that is the focus of this dissertation. Each of these mechanisms of resistance prevents the antibiotic from effectively acting on its bacterial target.

Resistance can exist, be selected for, and be promoted by using antibiotics [2]. In a large population of bacteria, it is likely that there are several cells that are inherently resistant to one or more antibiotic agents due to the genetic variation within the population. When an antibiotic is applied to the population of bacteria, all the susceptible cells die, leaving behind the resistant bacteria. The remaining bacteria can then reproduce to produce a large colony of drug resistant microorganisms over a short period of time. Thus, both the use of antibiotics and the rapid reproduction rate of microorganisms are attributed to the rapidly increasing resistance to antibiotics.

1.2 Fluoroquinolone Antibiotics

Fluoroquinolones are a class of broad spectrum antibiotics. Clinically, fluoroquinolone class agents have been used to treat a variety of infections due to their broad spectrum activity against Gram-positive and Gram-negative bacteria: respiratory infections, sexually transmitted diseases, and enteric infections among others. Fluoroquinolones are structurally based on nalidixic acid, an antibiotic of synthetic origin that was discovered in 1962 [9]. At low concentrations, nalidixic acid was found to be

bacteriostatic and inhibit bacterial cell growth, while at higher concentrations it is bactericidal, killing bacterial cells. However, at the time, the use of nalidixic acid was limited due to its narrow-spectrum activity against Gram-negative microorganisms [10]. Thus, there was a need for nalidixic acid to undergo structural modification in order to attempt to improve its activity against a broader spectrum of microorganisms and therefore improve its clinical usefulness.

Since the synthesis of nalidixic acid and discovery of its unique antimicrobial activity in the early 1960's, fluoroquinolone class antibiotics have undergone four generations of clinical development. As in most antibiotic taxonomies, each generation has both structural characteristics and activity profiles that set it apart from other
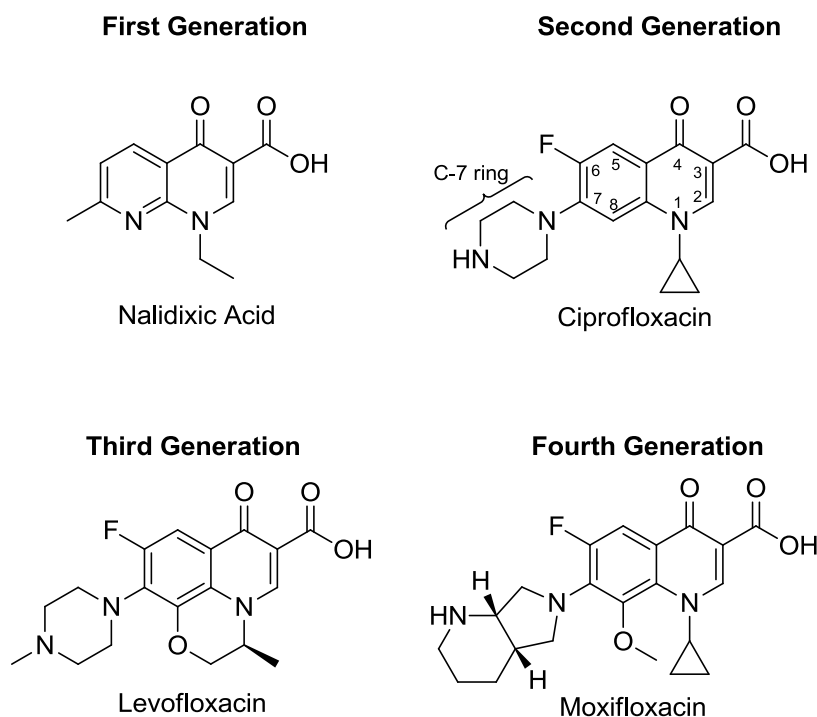
Figure 1. Fluoroquinolone structures by generation. Positions in the core ring structure are numbered for ciprofloxacin.

generations [11-13] (Figure 1). The structures of nalidixic acid and select fluoroquinolones from different generations of development are shown in Figure 1. Nalidixic acid and related acids were considered to be first generation quinolone-class agents. Structurally, nalidixic acid is a naphthyridone, not a quinolone, because its bicyclic core structure consists of two nitrogen atoms instead of one as in a quinolone core. The switch to the quinolone core and introduction of a fluorine atom at C-6 and piperazine at C-7 in second generation derivatives, such as ciprofloxacin and norfloxacin, lead to increased spectrum activity and thus a larger range of infections that these agents could be used to treat. Addition of the N-1 cyclopropyl group, such as that in ciprofloxacin, was also found to be an important modification in increasing antibacterial activity.

Further development of second generation derivatives with the introduction of new C-7 rings or chiral resolution of existing agents lead to third generation derivatives, such as levofloxacin. Third generation derivatives have demonstrated activity against Gram-positive bacteria and some penicillin resistant bacteria. The C-8 methoxy functionality was incorporated into the structures of current fourth generation fluoroquinolone agents, such as moxifloxacin and gatifloxacin. The C-8 methoxy functionality is thought to contribute to increased activity against Gram-positive microorganisms, as well as decreased phototoxicity, a problem that was seen with some earlier agents [14]. These agents demonstrate activity against anaerobic targets and some ciprofloxacin (a second generation fluoroquinolone) resistant targets.

When looking at the history of fluoroquinolone development, important trends are observed that make fluoroquinolones an important class of antibiotics for the future. First, researchers are able to modify the structure of the fluoroquinolone to improve effectiveness against different kinds of microorganisms. While early generation fluoroquinolones were effective against Gram-negative bacteria, the newer generation fluoroquinolones have been developed to be more effective against Gram-positive

bacteria. Additionally, researchers have successfully been able to modify the basic fluoroquinolone structure to gain antibiotic activity against bacterial mutants that arise and cause resistance. In the future, fluoroquinolones could continue to undergo structural modifications in order to overcome the challenges faced by the on-going emergence of resistant microorganisms.

<div align="center">1.3 Intracellular Targets of Fluoroquinolones</div>

Fluoroquinolones work by targeting and inhibiting DNA gyrase and/or Topoisomerase IV (Topo IV), both of which are type II bacterial topoisomerases involved in the DNA replication process. Type II topoisomerases function by breaking both strands of DNA, passing another segment of DNA through the break, and then religating the broken DNA [15]. Specifically, they relax positive supercoils so that the DNA can unwind and replicate. More specifically, Topo IV's primary role is that of a decatenase, while gyrase's primary function is to relax positive supercoils [15]. While DNA gyrase and Topo IV are similar in function, they are structurally distinct enzymes. Generally, DNA gyrase, composed of GyrA and GyrB subunits, is the primary target of fluoroquinolones in Gram-negative bacteria, while Topo IV, composed of ParC and ParE subunits that are sometimes referred to as GrlA (names as gyrase-like) and GrlB subunits, is the primary target in Gram-positive bacteria [16].

The ability of the fluoroquinolone class antibiotics to target type II topoisomerases offers several advantages over other antibiotic targets. First, type II topoisomerases are involved in DNA replication, an essential cell process that is universal to all bacteria. Second, type II topoisomerases are structurally unique enough from analogous human enzymes to allow for selectivity in targeting bacterial cells over human cells. Thirdly, the effect of target inhibition is bactericidal. Finally, fluoroquinolones have the ability to potentially inhibit two distinct bacterial enzymes, thus reducing the possibility of selecting resistant mutants [14, 17]. All of these

advantages demonstrate how fluoroquinolone class antibiotic agents have been, and will continue to be, attractive therapeutic options.
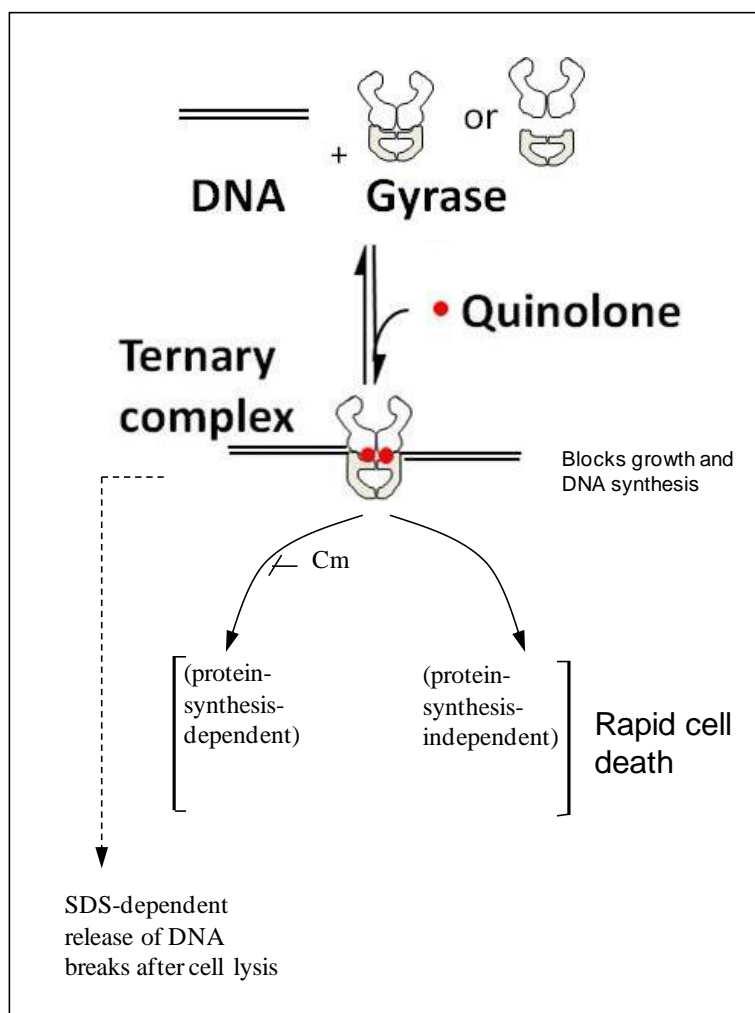
Figure 2. Mechanism of Fluoroquinolone Action. The quinolone binds the DNA-topoisomerase complex to form a ternary complex, which may lead to cell death by multiple pathways. Rapid cell death can occur via two different pathways: one requiring protein synthesis and one that does not. Cm = chloramphenicol, a known protein synthesis inhibitor. Adapted from [18, 19].

1.4 Fluoroquinolone Mechanism of Action

Fluoroquinolones form a ternary complex with the DNA and DNA gyrase/Topo IV, which then becomes trapped, disrupts replication, and triggers various cell death mechanisms [13, 18, 19]. As shown in Figure 2, topoisomerase binds and nicks each DNA strand in the replication process, with four DNA base pairs in between the nicked sites. The fluoroquinolone then binds the topoisomerase/nicked DNA complex in each of the nicked sites. However, it is not certain as to what the exact order of binding is.

Once the ternary complex is formed, different mechanisms of cell death are observed by different fluoroquinolones [18, 19]. With older generation fluoroquinolones, such as nalidixic acid and ciprofloxacin, slow cell death is observed. *In vitro* work with purified enzyme shows that ternary complex formation is fully reversible after the older generation drugs are removed because DNA religation is observed. However, with newer fluoroquinolones, such as moxifloxacin, rapid cell death is observed. With these agents in the *in vitro* purified enzyme assays, all of the DNA is not religated after the fluoroquinolone is removed. In cells, this effect is observed as chromosomal fragmentation. Rapid cell death also appears to be able to occur via two different mechanisms: one requiring protein synthesis and the other in the absence of protein synthesis (these two killing mechanisms are more thoroughly discussed in Chapter 3.1). For example, prior to MIC assays, chloramphenicol (Cm), a known protein synthesis inhibitor, can be added to stop protein synthesis. Some fluoroquinolones will kill in the presence of Cm, while others do not. The structural requirements for a fluoroquinolone to kill or not kill in the presence of Cm (absence of protein synthesis) are not known. Additionally, fluoroquinolone interactions with DNA may contribute to which mechanism of cell death are observed. A more detailed discussion of the interactions of fluoroquinolones with DNA follows in Chapter 4.

<p style="text-align:center">1.5 <u>Ternary Complex</u></p>

Due to the dynamic nature of the fluoroquinolone-DNA-DNA gyrase/Topo IV ternary complex, very little is understood about complex formation and what causes the different mechanistic cell death pathways to result once the complex is formed. While it is well-established that fluoroquinolones bind both DNA and the enzymes, crystal structures of the ternary complex have only recently been solved in the past 3 years. Solved ternary complex crystal structures with varying degrees of resolution consist of: moxifloxacin bound to *S. pneumoniae* Topo IV (4 Å) [20], GSK299423 bound to *S. aureus* GyrA (2.1 Å) and with ciprofloxacin superimposed (3.35 Å) [21], and moxifloxacin bound to *A. baumannii* Topo IV (2.2 A) [22].
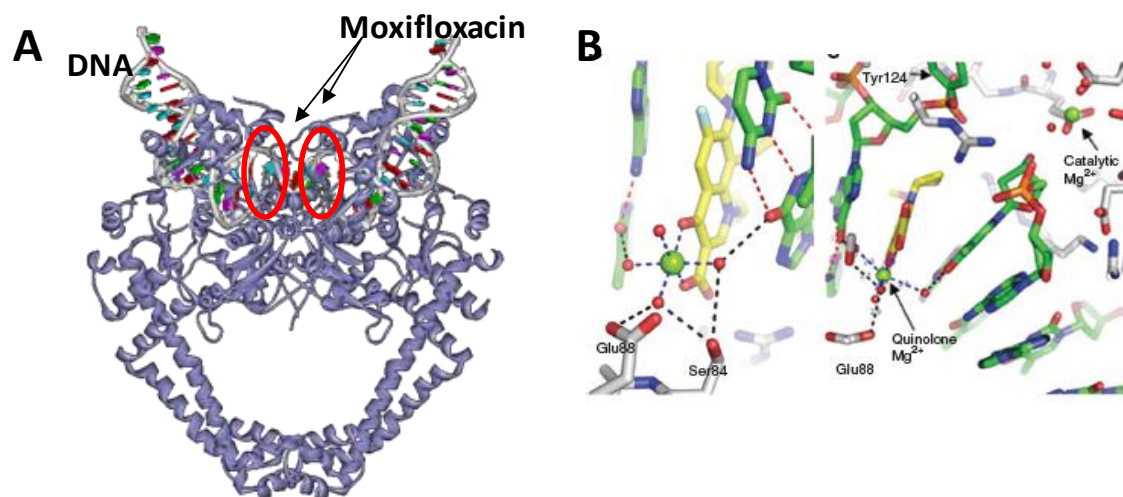
Figure 3. DNA-topoisomerase-fluoroquinolone ternary complex. **A**. Moxifloxacin bound to *S. pneumoniae* Topo IV. Adapted from 3FOF [20]. **B**. Moxifloxacin bound to *A. baumannii* Topo IV showing the binding interaction mediated by divalent magnesium cation. Adapted from [22].

All of the X-ray structures of ternary complexes show fluoroquinolones interacting with both the DNA and the topoisomerase (Figure 3A). Structure activity relationship studies have shown that the C-7 ring is responsible for the antibacterial activity against a broad spectrum of agents since it influences the cell permeability and DNA gyrase inhibition [11, 23, 24]. Surprisingly, none of the ternary complex structures show interaction between the C-7 ring of the fluoroquinolone and Topo IV, the binding interaction of the C-7 group is with DNA. Of the reported ternary complex structures, the Wolkonig structure most clearly shows a key binding interaction between helix-4 of Topo IV and the carboxylic acid and carbonyl of the fluoroquinolone that is mediated by a divalent magnesium cation (Figure 3B) [22]. This interaction through the magnesium ion is more thoroughly discussed in Chapter 3.2.

1.6 Resistance to Fluoroquinolones

While the advantages associated with fluoroquinolone class agents make them attractive therapeutic options, their development is not without the risk of resistance. Resistance to fluoroquinolones is a result of efflux transporters that prevent drug accumulation and mutations to the genes encoding the target enzymes, DNA gyrase and Topo IV [11, 12, 16].

Mutations to the genes encoding the target enzymes result in mutant forms of DNA gyrase and/or Topo IV having lower affinity for fluoroquinolone binding and decreased activity [25]. A vast majority of these mutations (amino acid substitutions) map to the region of the enzyme that interfaces with the DNA. This region is referred to as the Quinolone Resistance Determining Region (QRDR) [26]. Two common resistance mutations map to Ser83 and Asp87 on α-helix 4 of Gyrase A in the QRDR, the region close to the active site where DNA is bound [17] (Figure 4). Mutations in GyrB, such as Asp 426 and Lys 447, may also cause fluoroquinolone resistance and are found outside the QRDR [17, 25].

Fluoroquinolone resistance due to failure of penetration is a result of enhanced active expulsion or efflux of the drug from the bacterial cell by efflux transporters. This prevents the fluoroquinolone from reaching its intercellular target. The expression of a bacteria's endogenous efflux system, which in Gram-negative bacteria is made up of the efflux pump, an outer membrane protein, and a membrane fusion protein, is upregulated to contribute to fluoroquinolone resistance [16].
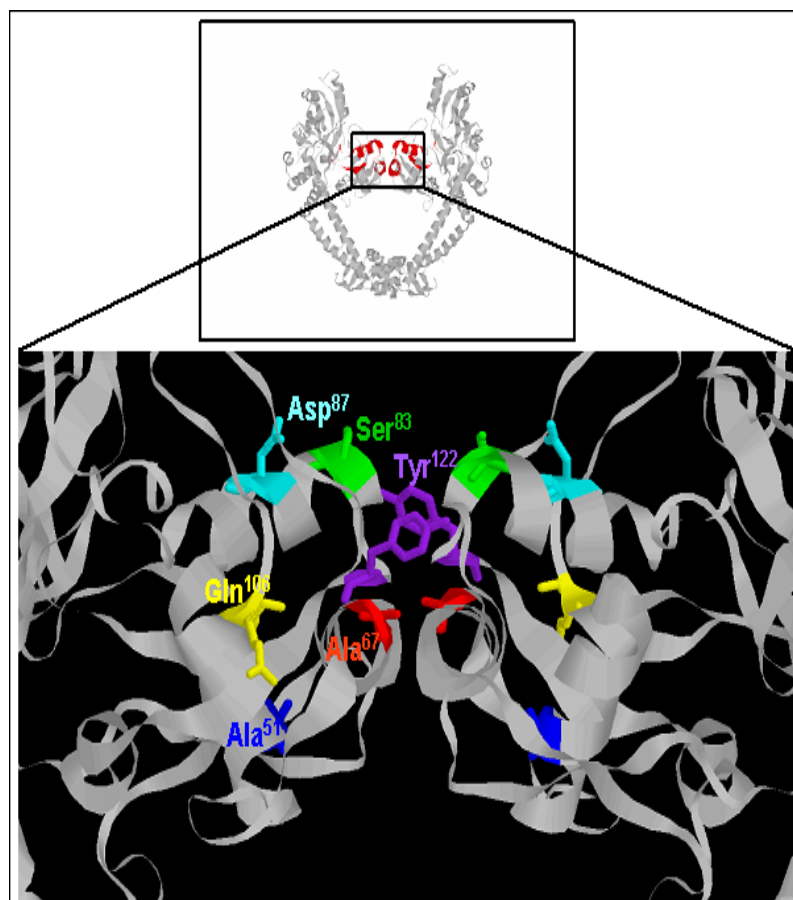
Figure 4. Quinolone Resistance Determining Region (QRDR) on GyrA with the important quinolone-resistance determining residues. Inset: GyrA dimer with QRDR highlighted in red. Adapted from [17, 27].

CHAPTER 2 STATEMENT OF THE PROBLEM

As the rate of resistance of bacteria to antibiotic agents continues to increase, affording single-drug, multi-drug, and extensively drug-resistant microorganisms, new antibiotics are needed. There have been only a few new classes of antibiotics introduced into clinical practice since the golden age of antibiotic research ended in the 1970's [1, 2]. The modification of existing antibiotic classes to overcome resistance may be ineffective if the newer agents have the same mechanism of action as the parent compounds. Furthermore, most current clinical agents are not effective against bacteria that enter latent or non-growing states, such as the tuberculosis-causing *Mycobacterium tuberculosis* and the persister cells of *Staphylococcus aureus* that result in lingering infections after a course of antibiotic treatment.

Like with other antibiotics, fluoroquinolone resistance emerged shortly after the drugs were introduced into clinical practice and became widespread in a relatively short period of time [28, 29]. Extensive use of this class of antibiotics has caused widespread resistance to fluoroquinolones. Specifically, resistance to ciprofloxacin, which has been frequently used in the clinical setting, continues to increase [6, 7, 30]. Consequently, there is a need to develop new fluoroquinolones that are active against non-growing bacterial cells and current resistant bacterial strains.

The first goal of this study was to understand the structural requirements necessary for fluoroquinolones to kill non-growing bacteria so that these structural features could be exploited in the development of more efficient fluoroquinolone antibiotics. To this end, fluoroquinolones with modifications at C-5 and C-8 were designed, synthesized, and evaluated for their ability to kill in the absence of protein synthesis.

The second goal of this study was to determine the structural requirements of fluoroquinolone-class agents to maintain activity against current fluoroquinolone-

resistant bacteria with mutations in the QRDR, in order to develop agents that would be active against current fluoroquinolone-resistant strains. This aim was accomplished by the design and synthesis of fluoroquinolones, 2,4-quinazoline diones, and fluoroquinolone-like analogues with unique substitution combinations at C-8 and C-7. Quinazoline diones are a class of compounds that act similarly to fluoroquinolones, but differ slightly in core structure with a different arrangement of carbonyl groups. CP-115,953 is a compound possessing a structural scaffold similar to fluoroquinolones, only differing by a C-7 carbon-carbon bond in place of a carbon-nitrogen bond, and the structure of the C-7 group. As a result of these modifications, CP-115,953 was found to have activity against human and bacterial topoisomerases. Human topoisomerase I is a target for many cancer agents. Thus, this compound has unique antibacterial and anticancer properties associated with it, making it an interesting scaffold for exploitation toward both antibacterial and anticancer agents. All of these fluoroquinolone-like derivatives were evaluated for their ability to maintain activity in the presence of mutation.

A third study evaluated the binding interaction of fluoroquinolones to different types of DNA present in the ternary complex, with a goal of better understanding the contribution of some structural features to novel killing mechanisms. By looking at these interactions, insights could be further gained on the unique mechanisms of fluoroquinolone action in order to optimize the development of more effective fluoroquinolone agents.

The overall hypothesis guiding this study is that novel killing mechanisms of fluoroquinolone-class topoisomerase inhibitors, such as the ability to kill in the absence of protein synthesis, are due to structural features not previously considered in the discovery and development of fluoroquinolone-class antibiotics. It is postulated that as a consequence of unique structural differences, certain fluoroquinolone-class agents form unique DNA-topoisomerase-fluoroquinolone ternary complexes that result in

fluoroquinolone release of fragmented DNA. Therefore, discrete structural differences in both the core and the substituents of the fluoroquinolone result in differences in ternary complex formation. The formation of different ternary complexes then creates differences in the activity profile of the fluoroquinolone-like compounds with regard to ability to kill in the presence and absence of protein synthesis and activity against topoisomerase mutants. Additionally, I set out to determine if these agents have different activity profiles due to the compounds binding differently to DNA based on intermolecular interactions that the structural changes have induced.

CHAPTER 3 SYNTHESIS AND STRUCTURE ACTIVITY

RELATIONSHIP STUDIES WITH FLUOROQUINOLONES

3.1 Effect of C-8/C-5 Substituents on the Ability to Kill in

the Presence and Absence of Protein Synthesis

Broad-spectrum fluoroquinolone antimicrobial agents have become an important

class of therapeutics that have undergone several generations of clinical development

since the initial discovery of nalidixic acid's antimicrobial activity in the early 1960's [9,

11, 12]. In fluoroquinolone development over the past fifty years, researchers have

successfully been able to modify the basic fluoroquinolone structure to improve the

spectrum of activity against microorganisms, as well as to gain activity against various

drug-resistant strains [13]. Important structural developments within this class of

antimicrobials include the introduction of a C-6 fluorine, C-7 piperazine, and N-1

cyclopropyl in second generation agents and incorporation of further C-7 structural

diversity and a critical C-8 methoxy functionality in third and fourth generation agents

[14].

Mechanistically, FQs inhibit type II topoisomerases, DNA gyrase and

Topoisomerase IV, by forming a ternary drug-topoisomerase-DNA complex that

becomes trapped, disrupts replication, and triggers various cell death mechanisms [13,

18, 19]. Different cell death mechanisms are observed by different fluoroquinolones. Of

particular interest are the cell death pathways that appear occur via two different lethal

mechanisms: one that requires protein synthesis and one that does not.

Structure-activity relationships (SAR) for fluoroquinolone activity in the presence

of protein synthesis are well established. For instance, the presence of a C-8 methoxy is a

structural requirement for the ability to kill growing bacteria, as observed with

Staphylococcus aureus [31] and various *Mycobacterium* sp. [32-34]. Older generation

fluoroquinolones, such as a ciprofloxacin, do not have a substituent at C-8, while newer

generation fluoroquinolones, such as moxifloxacin, have this C-8 methoxy and enhanced activity, especially against Gram-positive bacteria. A halogen at C-8, most particularly a chlorine, also contributes to the ability of the fluoroquinolone to have increased activity in the above microorganisms [32].

While SAR for fluoroquinolones killing in the presence of protein synthesis is well-established, SAR for fluoroquinolones killing in the absence of protein synthesis has only begun to emerge. The presence of a N-1 cyclopropyl group results in lethal activity against *Escherichia coli* in the absence of protein synthesis; ciprofloxacin was found to be lethal and norfloxacin (N-1 ethyl) was found not to be lethal [35] (see Figure 1 for the structure of ciprofloxacin). The C-6 fluorine is also required for improved activity against *Mycobacterium smegmatis* when protein synthesis is inhibited [36]. Like with killing in the presence of protein synthesis, a C-8 methoxy substituent is a structural requirement for killing in the absence of protein synthesis in *E. coli* [35, 37-39], *M. smegmatis* when protein synthesis is inhibited [36], and *Mycobacterium tuberculosis* [40]. When the C-8 methoxy substituent is tied up in a fused ring structure with N-1, like with levofloxacin, the fluoroquinolone loses its ability to kill *E. coli* in the absence of protein synthesis [41] (see Figure 1 for the structure of levofloxacin). Thus, unfused C-8 methoxy is required for killing *E. coli* in the absence of protein synthesis. Furthermore, C-7 substituents show species specific effects on lethality when protein synthesis is inhibited. In N-1-cyclopropyl-C-8-methoxy compounds, moxifloxacin and PD161144, which only differ in the C-7 substituent, moxifloxacin's C-7 diazabicyclo substituent affords insensitivity to ongoing protein synthesis in *M. tuberculosis* [40]; while PD161144's C-7 N-ethyl-piperazine has this effect in *E. coli* [19]. Despite these emerging structure-activity relationships, little is known about the specific role of C-8 or C-5 substituents and how these structures contribute to some fluoroquinolones being able to kill in the absence of protein synthesis.

3.1.1 Goals of this Study

To better understand the effects of fluoroquinolone substituents on killing non-replicating microorganisms, a series of FQ derivatives with structural variations at C-8, C-5, and N-1 was synthesized and lethal activity against *E. coli* was determined. MIC was measured, as well as the percent survival of *E. coli* at 10x MIC in the presence and absence of protein synthesis.

Commercially available fluoroquinolones (sarafloxacin, sparfloxacin, fleroxacin, orbifloxacin, sitafloxacin, gemifloxacin, grepafloxacin, besifloxacin, balofloxacin, clinafloxacin, tosufloxacin, lomefloxacin, ulifloxacin, 8-ethoxy moxifloxacin, and *N*-methyl gatifloxacin) were also included in the evaluation of lethal activity to further explore SAR of fluoroquinolones to kill. The ability of these compounds to kill in the absence of protein synthesis was unknown prior to this study because the pathway by which fluoroquinolones kill in the absence of protein synthesis has recently been discovered. As a result, the older generation agents and many of the newer generation agents have never been evaluated for lethal activity in the absence of protein synthesis.

3.1.2 Synthesis of C-8, C-5, and N-1 derivatives

The first series of C-8 substituted analogues containing a C-7 N-ethyl piperazine, *cis*-octahydropyrrolopyridine, or (*S*)-aminomethyl pyrrolidine was prepared through commercially available core structures or *de novo* synthesis. 2,4,5-trifluorobenzoic acid was methylated after conversion to the corresponding amide (Scheme 1) and two subsequent multi-step sequences (Scheme 2) yielded the desired C-8 methyl fluoroquinolone core **13**.
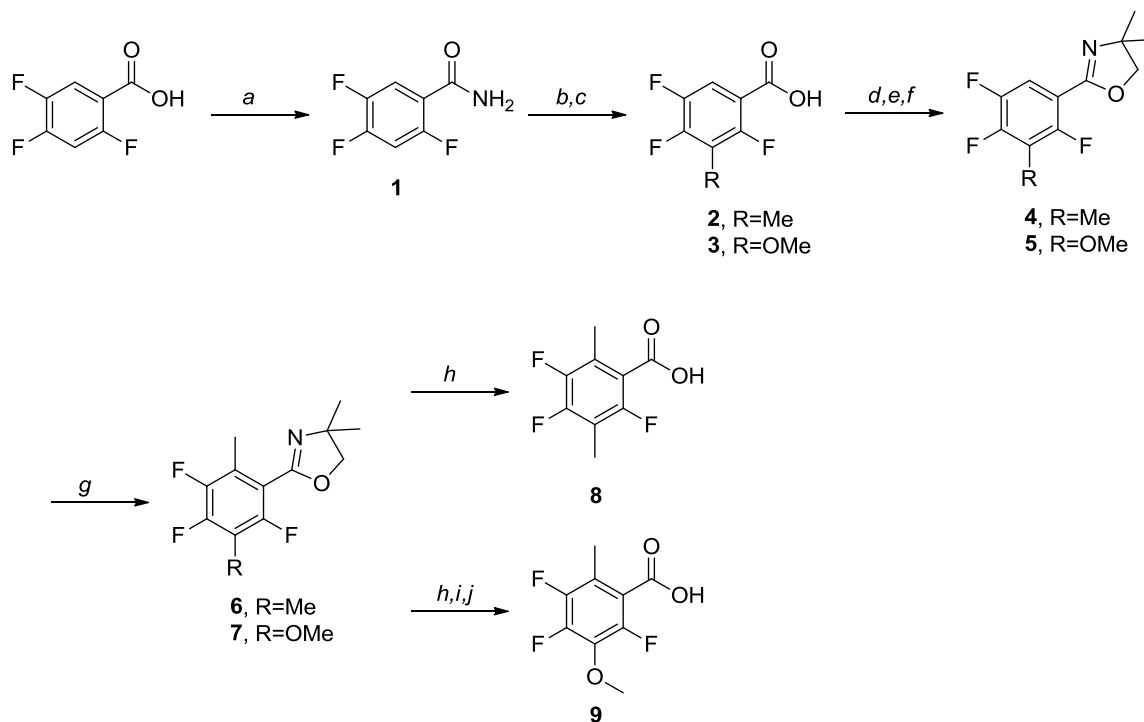
Scheme 1. *De novo* synthesis of fluoroquinolone intermediates **2**, **8**, and **9**. Reagents and conditions: (a) oxalyl chloride, DMF, NH$_4$OH, CH$_2$Cl$_2$, 1.5 hr (85%); (b) LiHMDS, methyl iodide, THF, -78 °C - rt, 6 hr (79%); (c) H$_2$SO$_4$, reflux, 3 hr (76%); (d) oxalyl chloride, DMF, CH$_2$Cl$_2$, 1.5 hr; (e) 2-amino-2-methyl-propan-1-ol, CH$_2$Cl$_2$, 20 hr; (f) thionyl chloride, 14 hr (**4**: 71% over 3 steps. **5**: 78% over 3 steps); (g) LDA, methyl iodide, -78 °C - rt, 14 hr (**6**: 81%. **7**: 86%); (h) 1N HCl, reflux, 7 hr (**8**: 87%); (i) Ac$_2$O, pyridine, 60 °C, 3 hr; (j) 1N NaOH, reflux, 3 hr (**9**: 63% over 3 steps).
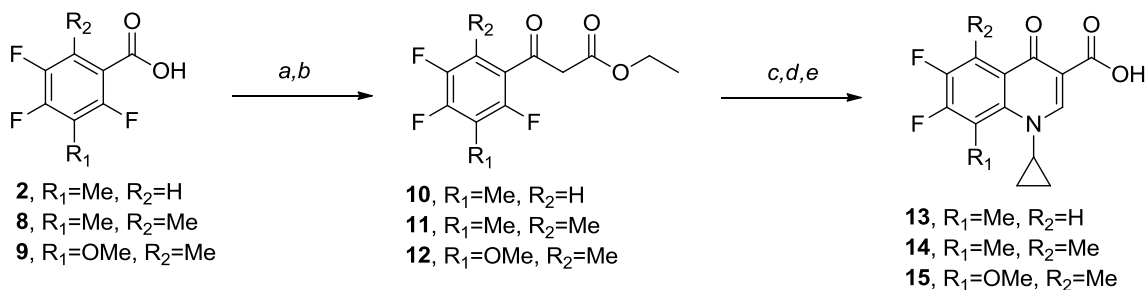
Scheme 2. Synthesis of fluoroquinolone cores **13**-**15**. Reagents and conditions: (a) oxalyl chloride, DMF, CH_2Cl_2, 1.5 hr; (b) ethyl potassium malonate, anhydrous magnesium chloride, ethyl acetate or acetonitrile, 20 hr (**10:** 79% over 2 steps, **11**: 88% over 2 steps, **12**: 81% over 2 steps); (c) triethyl orthoformate, Ac_2O, reflux, 4.5 hr; (d) cyclopropylamine, DMSO, potassium carbonate, 95-100 °C, 2 hr; (e) 10% KOH, rt, 1-2 d (**13**: 72% over 3 steps, **14**: 75% over 3 steps, **15**: 44% over 3 steps.

The second series of analogues with various C-5 substitutions was also prepared through commercially available core structures, *de novo* synthesis, or modifications to commercially available core structures. C-8-methyl-C-5-methyl core **14** was synthesized from intermediate **2** in the synthesis of **13**, while C-8-methoxy-C-5-methyl core **15** was synthesized in a parallel manner from the commercially available 2,4,5-trifluoro-3-methoxy-benzoic acid **3** (Scheme 1 and 2). Due to expected hydrolysis of oxazole **7** to a 2-amino-2-methylpropyl ester after acid reflux, two additional steps were required to obtain the desired acid **9** [42]. Additional cores **16**-**19** with C-5 modifications were obtained through the reductive nitration of 1-cyclopropyl-6,7-difluoro-8-methoxy-4-oxo-3-quinoline carboxylic acid [43] or *S*-(-)-9,10-difluoro-2,3-dihydro-3-methyl-7-oxo-7H-pyrido[1,2,3-de]-[1,4]-benzoxazine-6-carboxylic acid (Scheme 3).
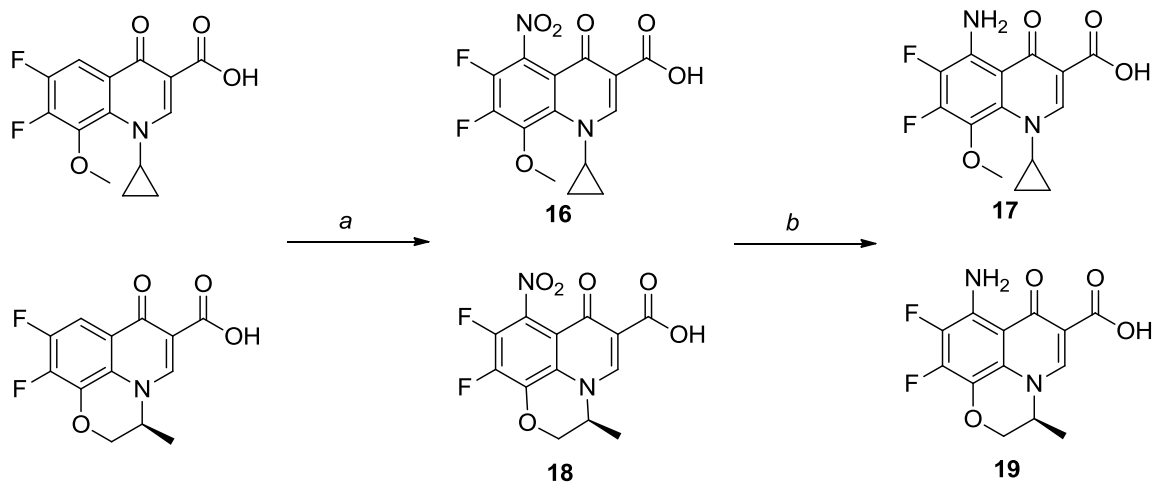
Scheme 3. Synthesis of fluoroquinolone cores **16-19**. Reagents and conditions: (a) potassium nitrate, H_2SO_4, 1 hr (**16**: 74%, **18**: 45%)(b) H_2, 1 atm, 10% Pd/C, 4:1 ethanol:DMF, 6 hr (**17**: 67%, **19**: 30%).

The third series of analogues containing modifications at N-1 was prepared from commercially available 9,10-difluoro-2,3-dihydro-3-methyl-7-oxo-7H-pyrido[1,2,3-de]-1,4-benzoxazine-6-carboxylic acid that underwent a base-induced ring opening that was previously observed as an unwanted side-product [44], further optimized to 95% yield, and converted to methyl ester **20** (Scheme 4). Methyl ester **20** was reduced under hydrogen to give both the major hydrogenation product **21** and minor hydrogenolysis product **22**, which was isolated and alkylated to yield the N-1 ethyl core **23**.

The C-7 substituents were added to all of the prepared or available fluoroquinolone cores through an SN aromatic addition of a secondary amine (Scheme 5, quinolone structures in Table 1). In some cases, as indicated in Table 1, the core structure was converted to the corresponding boronate ester to facilitate nucleophilic aromatic addition (SN_{ar}) at the C-7 position. A subsequent treatment with aqueous

Scheme 4. Synthesis of fluoroquinolone cores **20**, **21**, and **23**. Reagents and conditions: (a) LiHMDS, THF, -78 °C - rt, 20 hr (95%); (b) dimethylsulfate, potassium carbonate, acetone, reflux (95%), (c) H$_2$, 10% Pd/C, 60 psi, 3.33 mM KOH in EtOH (**21**: 50%, **22**: 25%); (d) ethyl iodide, potassium carbonate, DMF (95%).

Scheme 5. General synthetic scheme for the C-7 nucleophilic aromatic addition of secondary amines to the various fluoroquinolone cores to obtain compounds **24-46**. Reagents and conditions: (a) Triethylamine, DMSO, 80-100 °C, 1-6 hr (10-90%).

Table 1. Structures of fluoroquinolones synthesized as in Scheme 5 and used in this study.
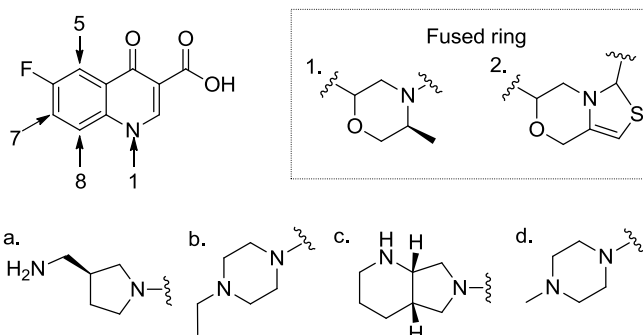
Compound	Substituent at position indicated in structure			
	C8	C5	C7	N1
24 (UIHS-IIIa-35)†	H	H	a*	Cyclopropyl
25 (UIHS-IIa-165)†	H	H	b	Cyclopropyl
26 (UIHS-IIa-161)†	H	H	b	Ethyl
27 (UIHS-IIIa-39)	F	H	a*	Fluoro-cyclopropyl
28 (UIHS-IIa-181)	F	H	b	Fluoro-cyclopropyl
29 (UIHS-I-303)†	Me	H	a*	Cyclopropyl
30 (UIHS-IIa-45)†	Me	H	c	Cyclopropyl
31 (UIHS-IIa-119)†	Me	H	b	Cyclopropyl
32 (UING5-249)	OMe	H	a*	Cyclopropyl
33 (PD161144)	OMe	H	b	Cyclopropyl
34 (UIHS-IIIa-41)	OMe	NH$_2$	a*	Cyclopropyl
35 (UIHS-IIa-141)	OMe	NH$_2$	b	Cyclopropyl
36 (UIHS-IIa-143)	OMe	NO$_2$	b	Cyclopropyl
37 (Antofloxacin)	Fused ring 1	NH$_2$	d	Fused ring 1
38 (UIHS-IIa-183)	Fused ring 2	H	b	Fused ring 2
39 (UIHS-IIa-215)	OMe	Me	a*	Cyclopropyl
40 (UIHS-IIa-213)	OMe	Me	b	Cyclopropyl
41 (UIHS-IIa-219)	Me	Me	a*	Cyclopropyl
42 (UIHS-IIa-221)†	Me	Me	b	Cyclopropyl
43 (UITT-II-111)‡	OMe	H	a*	Isopropene
44 (UITT-I-277)‡	OMe	H	b	Isopropene
45 (UITT-II-195) ‡	OMe	H	b	Isopropyl
46 (UITT-II-295)†‡	OMe	H	a*	Ethyl

†Core converted to borate ester in synthesis and cleaved with TFA or NaOH after secondary amine addition (Scheme 5).

‡Methyl ester core hydrolyzed prior to C-7 addition with acetic acid, HCl (Scheme 5).

*TFA added in synthesis after secondary amine addition to remove BOC(Scheme 5).

Table 2. MICs and percent survival at 10-times MIC of fluoroquinolones against DM4100 *E. coli* strain. *KD1397 strain with *tolC* mutation.

	Compound	MIC (µg/mL)	Percent Survival at 10x MIC			Compound	MIC (µg/mL)	Percent Survival at 10x MIC	
			-Cm	+Cm				-Cm	+Cm
24	UIHS-IIIa-35	0.156	0.24	50.6	**43**	UITT-II-111	0.6	0.1	18
25	UIHS-IIa-165	0.03	0.033	60	**44**	UITT-I-277*	0.242	0.73	103
26	UIHS-IIa-161	0.121	0.17	50	**45**	UITT-II-195*	0.6	0.17	14
27	UIHS-IIIa-39	0.078	3.32	66.27	**46**	UITT-II-295	0.25	0.33	8.03
28	UIHS-IIa-181	0.025	0.01	6		Sarafloxacin	0.086	0.022	15
29	UIHS-I-303	0.025	0.008	1.2		Sparfloxacin	0.125	0.035	41
30	UIHS-IIa-45	0.078	0.15	12.22		Fleroxacin	0.141	0.25	28
31	UIHS-IIa-119	0.055	0.003	2.3		Orbifloxacin	0.15	0.05	20
32	UING-5-249	0.065	0.022	0.58		Sitafloxacin	0.015	0.008	0.32
33	PD161144	0.096	0.001	1.7		Gemifloxacin	0.086	0.016	18
34	UIHS-IIIa-41	0.03	0.02	0.72		Grepafloxacin	0.016	0.073	50
35	UIHS-IIa-141	0.4	0.01	6		Besifloxacin	0.1	0.01	2.2
36	UIHS-IIa-143*	1.625	11	102		Balofloxacin	0.484	0.084	1.6
37	Antofloxacin	0.15	0.01	31		Clinafloxacin	0.0095	0.006	1.8
38	UIHS-IIa-183	0.038	0.06	41		Tosufloxacin	0.05	0.02	24
39	UIHS-IIa-215	0.045	0.01	4		Lomefloxacin	0.172	0.0052	48
40	UIHS-IIa-213	0.7	0.01	52		Ulifloxacin	0.022	0.13	18
41	UIHS-IIa-219	0.09	0.3	7		8-OEt Moxifloxacin*	0.2	10	50
42	UIHS-IIa-221	0.7	0.3	7		N-Me Gatifloxacin	0.065	0.005	2.8

sodium hydroxide (3%) cleaved the boronate ester to give the desired product. The methyl ester core of **20**, **22**, and **23** was hydrolyzed to the carboxylate with acetic acid and HCl prior to C-7 addition. Trifluoroacetic acid was used to remove the BOC protecting group after addition of the BOC protected (*S*)-aminomethyl pyrrolidine.

3.1.3 Bacteriostatic and Bactericidal Studies

The minimum inhibitory concentrations (MICs) of all synthesized and commercially available fluoroquinolones were determined *in vitro* with *E. coli* strain DM4100 [45] (Table 2). Four of the compounds exhibited activity levels that were too low to feasibly carry out lethality experiments with strain DM4100; instead, they were performed with strain KD1397 that contains a *tolC* knockout. Because *tolC* is knocked out, the bacterium has decreased ability to efflux fluoroquinolone so a higher concentration of fluoroquinolones can accumulate in the cytoplasm of this strain. One of the four fluoroquinolones evaluated against strain KD1397 was **36** UIHS-IIa-143, which had a MIC of 1.625 µg/mL. Otherwise, MIC in DM4100 varied over a range of 0.0095 to 0.7 µg/mL, with clinafloxacin being the most active and **40** UIHS-IIa-213 and **42** UIHS-IIa-221 being the least active. Survival was determined during treatment with various fluoroquinolones using an incubation of 2 hr. Data for two representative compounds are shown in Figure 5 (see Appendix B for all of the lethality data). From such curves, we determined percent survival at 10-times MIC with and without chloramphenicol (Cm), a known protein synthesis inhibitor (Table 2).
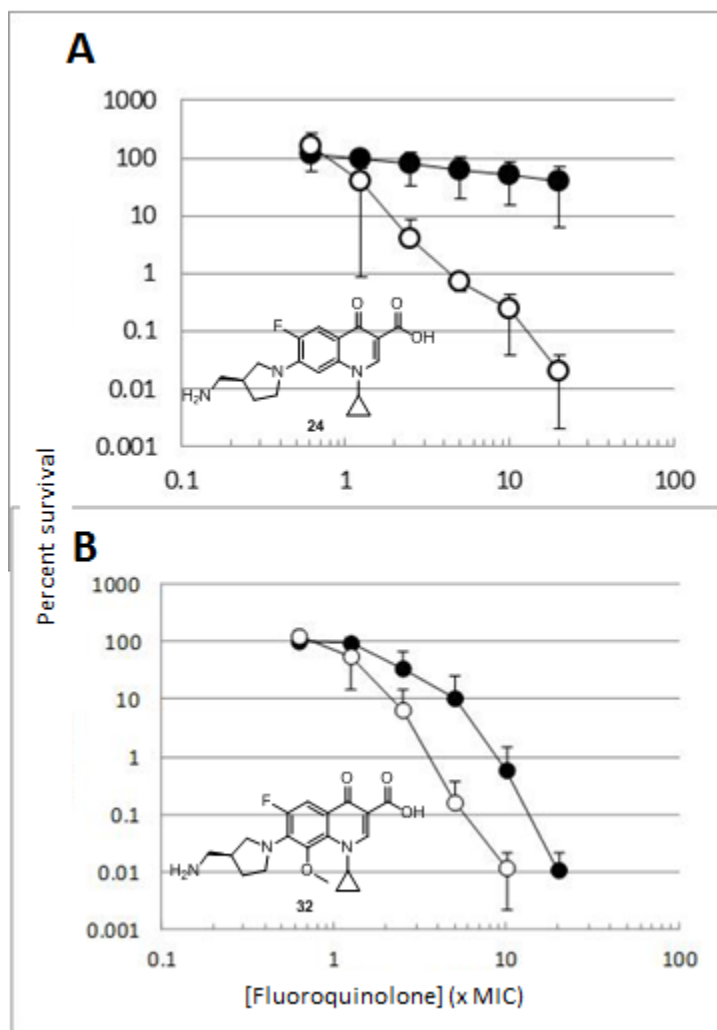
Figure 5. Representative lethal activity of fluoroquinolones with structural diversity at C-8 in the presence and absence of chloramphenicol. A. Percent survival of *E. coli* at various concentrations of **24** UIHS-IIIa-35. B. Percent survival of *E. coli* at various concentrations of **32** UING5-249. Survival of *E. coli* was measured as a function of the fluoroquinolone concentration expressed as a multiple of the MIC in the presence (filled symbols) or absence (open symbols) of chloramphenicol, an inhibitor of protein synthesis. The error bars represent standard deviation of the mean.

3.1.3.1 Effect of C-8 Substituent on Ability to Kill in the

Absence of Protein Synthesis

Since previous structure activity relationships in the presence of protein synthesis had suggested that a C-8 methoxy substituent contributed to higher lethal activity and very little was known about the structural requirements for killing by fluoroquinolones in the absence of protein synthesis, we prepared a series of fluoroquinolones with various C-8 substituents - hydrogen (no substituent), fluorine, methoxy, and methyl. Keeping the C-7 substituent constant as either aminomethyl pyrrolidine or N-ethyl piperazine, the effect of the C-8 substituent on killing was determined by measuring the percent survival of *E. coli* at 10-times the MIC (Table 2, Figure 6 Panel A). When there was no substituent at C-8 (*i.e.* **24** UIHS-IIIa-35 and **25** UIHS-IIa-165), percent survival was the highest and therefore the compounds were the least efficacious in the absence of protein synthesis. Likewise, when the C-8 substituent was fluorine (*i.e.* **27** UIHS-IIIa-39 and **28** UIHS-IIa-181), a bioisostere for hydrogen, a lesser effect was observed. However, when a larger substituent such as methyl or methoxy was placed at C-8 (**29** UIHS-I-303, **31** UIHS-IIa-119, **32** UING5-249 and **33** PD161144), there was a more pronounced ability to kill the cells. Of these compared, **32** UING5-249 was most efficacious in killing *E. coli* with a percent survival at 10-times MIC less than 1. With the exception of the two C-8 fluoro derivatives, compounds with a C-7 aminomethyl pyrrolidinyl substituent had the best activity in the absence of protein synthesis against the DM4100 strain of *E. coli*.

3.1.3.2 Effect of C-5 Substituent on Ability to Kill in the

Absence of Protein Synthesis

Two sets of compounds were used to evaluate the effect of the C-5 substituent on the ability of the fluoroquinolone to kill in the absence of protein synthesis (Table 2, Figure 6 Panel B and C). In each set, the C-8 substituent was held constant as either methyl or methoxy since those were found to be the C-8 groups that imparted the ability
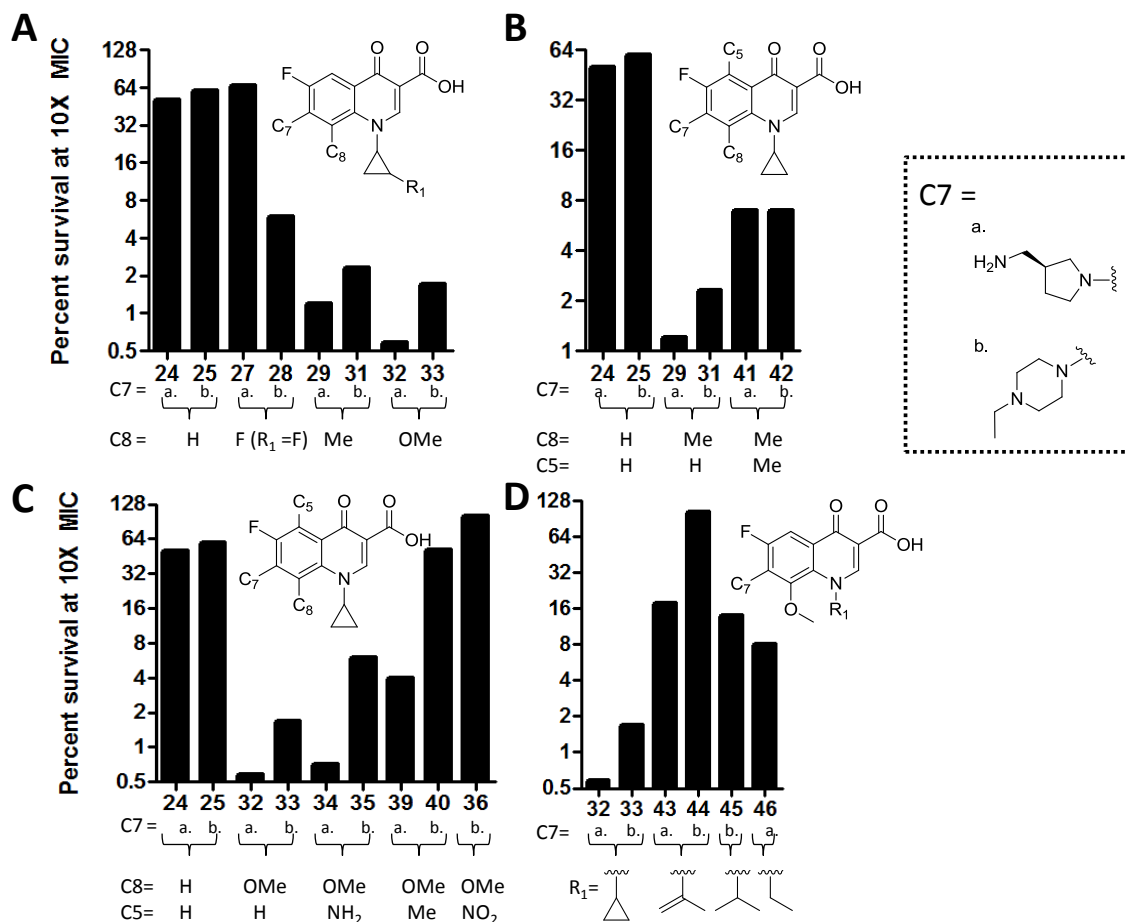
Figure 6. Effect of various substituents on the ability of the fluoroquinolone to kill in the absence of protein synthesis. A. Effect of C-8 substituents. B. Effect of C-5 substituents with the C-8 methyl core. C. Effect of C-5 substituents with the C-8 methoxy core. D. Effect of N-1 variants with the C-8 methoxy core. C-7 substituents are specified.

of the fluoroquinolones to kill in the absence of protein synthesis. Again, the effect of structure on killing in the absence of protein synthesis was determined by measuring the percent survival of *E. coli* at 10-times the MIC.

With C-8 methyl substituents, a C-5 methyl functionality was introduced (*i.e.* **41** UIHS-IIa-219 and **42** UIHS-IIa-221). As shown in Table 2 and Figure 6 Panel B, the C-5

methyl group was not tolerated; percent survival increased 3.5 to 7 fold over the C-5 unsubstituted derivatives (*i.e.* **29** UIHS-1-303 and **31** UIHS-IIa-119). However, C-5, C-8 dimethyl fluoroquinolone cores killed more effectively than the C-5, C-8 unsubstituted compounds. With a substitution only at C-5, as in grepafloxacin, percent survival was comparable to the unsubstituted fluoroquinolones. Thus, certain combinations of C-5, C-8 structural changes contribute to the ability to kill in the absence of protein synthesis with C-5 hydrogen, C-8 methyl being the most optimal combination.

Looking at the derivatives with a C-8 methoxy group and various C-5 substituents, unsubstituted C-5 derivatives (*i.e.* **32** UING5-249 and **33** PD161144 in Figure 6 Panel C) were in general ideal for killing in the absence of protein synthesis, and the inclusion of C-5 substituents led to decreased activity as seen by higher percent survival at 10-times MIC in the absence of protein synthesis (Table 2, Figure 6 Panel C). The same trend was observed for the C-8 methyl derivatives. The introduction of a nitro group at C-5 (**36** UIHS-IIa-143, Figure 6 Panel C) was not tolerated at all because essentially all the bacterial cells survived at 10-times MIC in the absence of protein synthesis. Like with the C-8 methyl compounds, C-5 methyl substitutions in the presence of a C-8 methoxy led to 6.5 to 30 fold increases in percent survival (Figure 6, Panel C). The C-5 methyl substitution was better tolerated on the compound with the aminomethyl pyrrolidine at C-7 (**39** UIHS-IIa-215) as seen by the lower percent survival in the absence of protein synthesis.

Of the functional groups introduced at C-5, the amine group was the best tolerated, although these derivatives were not as efficacious in the ability to kill in the absence of protein synthesis as the unsubstituted compounds. Most notably with these C-5 amine compounds, **34** UIHS-IIIa-41 with a C-7 aminomethyl pyrrolidinyl group had less than one percent survival at 10-times MIC. The only other compound tested that was able to cause a comparatively low percent survival against *E. coli* was **32** UING5-249 that was unsubstituted at C-5. When the C-5 amine was present in **37** (antofloxacin) and

sparfloxacin, high percent survivals in the absence of protein synthesis were observed. This was not surprising because compounds such as antofloxacin, with the fused ring core structure of levofloxacin, have been shown to be poor killers in the absence of protein synthesis compared to their open ring counterparts [41]. Again, with both sets of C-5 compounds in all instances, the C-7 aminomethyl pyrrolidinyl was found to be the best C-7 substituent of those tested to impart the ability to kill *E. coli* in the absence of protein synthesis.

3.1.3.3 Effect of N-1 Substituent on Ability to Kill in the Absence of Protein Synthesis

A few derivatives with N-1 groups that differ from the traditional fluoroquinolone N-1 cyclopropyl were prepared to further probe the structural requirements at N-1 for fluoroquinolones to kill in the absence of protein synthesis. When C-8 was held constant with a methoxy substituent and C-7 was either aminomethyl pyrrolidinyl or N-ethyl piperazinyl substituent, N-1 cyclopropyl derivatives (**32** UING5-249 and **33** PD161144) remained to be the most effective at killing in the absence of protein synthesis (Table 2, Figure 6 Panel D). The more rigid structure of the cyclopropyl group, instead of the more flexible, structurally similar isopropyl and isopropene groups, appears to be optimal of the N-1 groups tested.

3.1.3.4 Ability of Commercially Available Fluoroquinolones to Kill in the Absence of Protein Synthesis

A panel of 15 commercially available fluoroquinolones was obtained to evaluate structurally diverse fluoroquinolones and to determine which fluoroquinolones kill in the absence of protein synthesis (Table 2, Figure 7). To date, nalidixic acid, norfloxacin, ciprofloxacin, levofloxacin, moxifloxacin, gatifloxacin, garenoxacin, pazufloxacin,
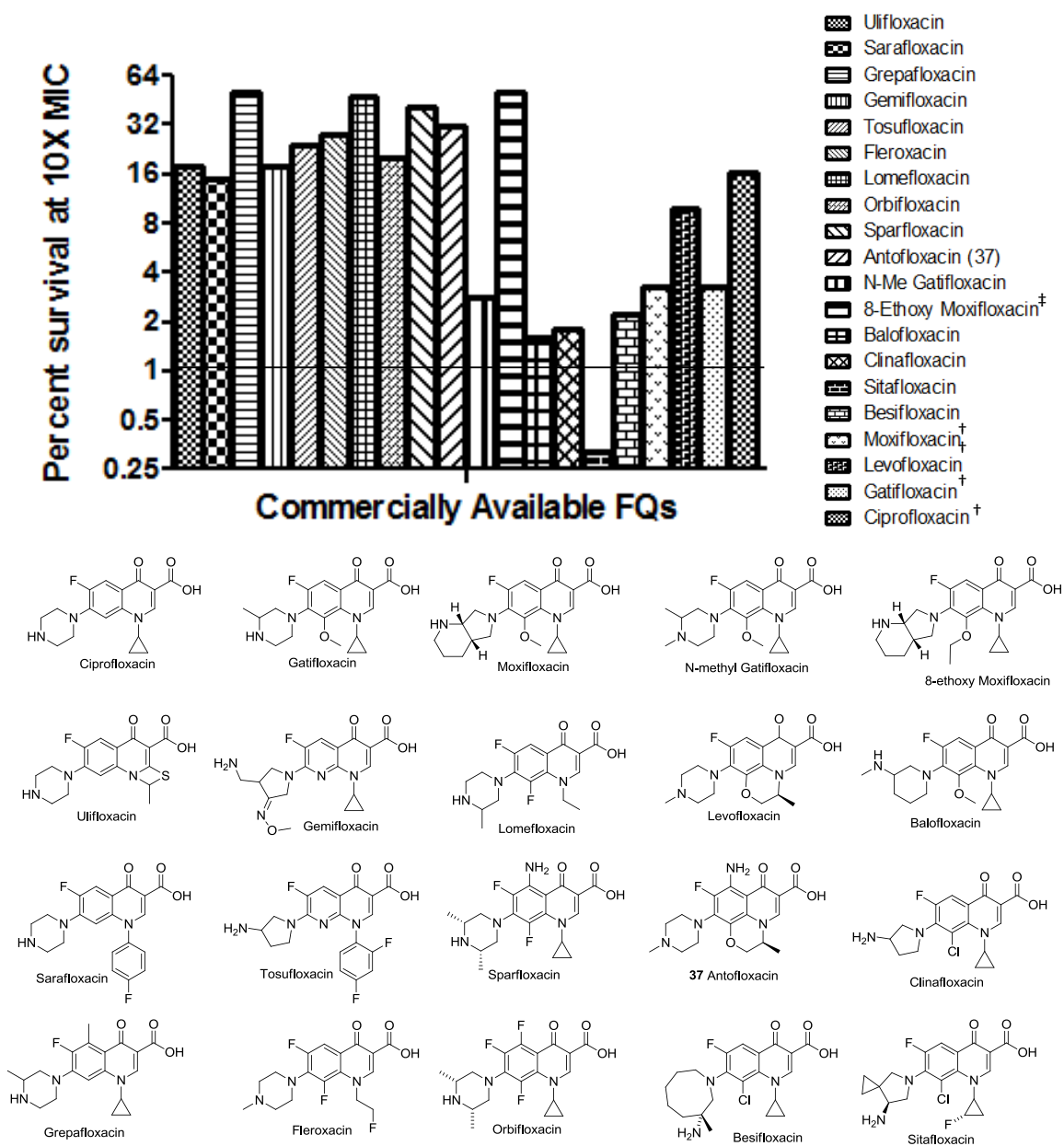
Figure 7. Lethal activity with *E. coli* DM4100 of commercially available
fluoroquinolones in the absence of protein synthesis. Percent survival is
shown at 10-times MIC. † Previously reported percent survival against *E. coli*
DM4100: moxifloxacin, levofloxacin, and gatifloxacin [41]; ciprofloxacin
[35]. ‡*E. coli* strain KD1397 with *tolC* mutation was used.

marbofloxacin, and rufloxacin are the only fluoroquinolone-class agents to have been screened in this manner against various bacterial species [34-36, 40, 41]. Sitafloxacin, clinafloxacin, balofloxacin, *N*-methyl gatifloxacin, and besifloxacin all induced less than 5 percent survival in *E. coli* at 10-times MIC in the absence of protein synthesis, with sitafloxacin being the most efficacious (Figure 7). These five were the only agents of those screened that contained either C-8 chlorine or C-8 methoxy. Thus, C-8 chlorine, along with C-8 methyl and methoxy, contributes to the agent's ability to kill in the absence of protein synthesis. The remainder of the agents had C-8 hydrogen, C-8 fluorine, a pyridine core, or a fused ring core structure.

The lack of many fluoroquinolones, including those that are commercially available, to be able to maintain their antimicrobial effect in the absence of ongoing protein synthesis implies that these agents should not be co-administered with protein synthesis inhibitors. It also implies that these agents should not be used to treat complex infections in which the microorganisms are capable of going into dormant or nongrowing stage in their lifecycles. Instead, agents such as moxifloxacin and sitafloxacin, should be administered.

3.1.4 Conclusions

Specific structural features contribute to both the ability of a fluoroquinolone to kill in the absence of protein synthesis and low MIC. Sitafloxacin, clinafloxacin, **29** UIHS-I-303 and **34** UIHS-IIIa-41 are the most effective fluoroquinolones with the lowest MIC's in our study that can kill both in the presence and absence of protein synthesis. All of these compounds contain common structural features that are concluded to be necessary for killing *E. coli* in the absence of protein synthesis: a C-7 substituted pyrrolidinyl group, C-8 chlorine, methoxy, or methyl, and N-1 cyclopropyl. Three out of the four of these most effective compounds have no substitution at C-5.

Deviations in structure from fluoroquinolones containing C-7-substituted pyrrolidinyl group, C-8 methoxy or methyl, and N-1 cyclopropyl generally result in the inability of the fluoroquinolone to kill in the absence of protein synthesis. Two close structural derivatives of moxifloxacin, C-8 ethoxy moxifloxacin and **30** UIHS-IIa-45 (C-8 methyl), were less able to kill in the absence of protein synthesis when C-8 deviated from the methoxy functionality of moxifloxacin. Deviations from N-1 cyclopropyl in **43-46** led to decreased ability to kill in the absence of protein synthesis. With the exception of **34** UIHS-IIIa-41 containing at C-5 amine, the introduction of substituents at C-5 had a negative impact on the ability to kill in the absence of protein synthesis, especially the introduction of a nitro group as in **36** UIHS-IIa-143.

The species specific effect of C-7 substituent in the absence of protein synthesis is clearly demonstrated with **32** UING5-249, a C-8 methoxy fluoroquinolone with a C-7 chiral aminomethyl pyrrolidinyl substituent; against *M. smegmatis* it is unable to kill in the absence of protein synthesis [34], while it can effectively kill against *E. coli*.

3.2 Effect of fluoroquinolone and quinazoline dione core structure on magnesium bridge formation

Due to its ability to produce stable spores and cause anthrax, *Bacillus anthracis* is considered a serious threat as a bioweapon [46, 47]. Ciprofloxacin, a broad spectrum fluoroquinolone antibiotic, is the most effective first line treatment for anthrax [48, 49]. As with all fluoroquinolone agents, ciprofloxacin targets and inhibits *B. anthracis*'s type II topoisomerases, DNA gyrase and topoisomerase IV (Topo IV), that are discussed more thoroughly in Chapter 1.3 on page 6. Bacterial cell death is caused by the fluoroquinolones increasing the levels of chromosomal fragmentation or DNA cleavage generated by the enzymes after the ternary complex is formed. The different mechanisms of cell death that are caused by different fluoroquinolones after ternary complex formation are described more thoroughly in Chapter 1.4 beginning on page 8.
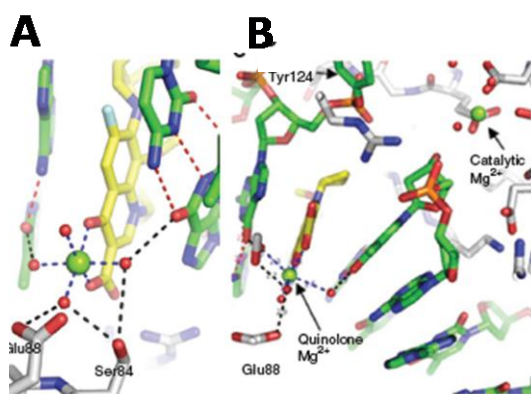
Figure 8. Moxifloxacin bound to *A. baumannii* Topo IV showing the binding interaction mediated by divalent magnesium cation in both panel A and B. Ser84, the "Ser83 equivalent" in *A. baumannii*, is involved in forming a magnesium ion-mediated bridge between moxifloxacin and Topo IV. Adapted from [22].

Resistance to fluoroquinolones, which is discussed in more depth in Chapter 1.6, is a result of efflux mechanisms to prevent drug accumulation in the cell and mutations to the genes encoding the target enzymes, DNA gyrase and Topo IV [11, 12, 16]. These mutations result in lower affinity for fluoroquinolone binding and decreased activity [25], with a vast majority mapping to the Quinolone Resistance Determining Region (QRDR) in the region of the enzyme that interfaces with the DNA [26]. A common resistance mutation maps to Ser83 of Gyrase A in the QRDR in *E. coli* [17] (Figure 4). The homologous residue on GrlA of Topo IV in *B. anthracis* is Ser81 [50]. Ser81 is also analogous to Ser84 in *Acinetobacter baumannii*. In a recent crystal structure of the *A. baumannii* TopoIV-DNA-moxifloxacin ternary complex, Ser84 is seen to be responsible for forming the magnesium ion bridge between the enzyme, fluoroquinolone, and DNA (Figure 8) [22]. Because extensive research has been done with the QRDR in *E. coli* and the resistance mutation mapping to Ser83, the analogous Ser84 in *A. baumannii* and Ser81 in *B. anthracis* are "Ser83 equivalent" residues. The ability of *B. anthracis* to

develop resistance to fluoroquinolones, such as ciprofloxacin, that are used to treat anthrax infection is a major concern due to the potential use of the fluoroquinolone-resistant *B. anthracis* as a bioweapon [51-54]. Thus, there is a need to develop more effective drugs that display activity against the fluoroquinolone-resistant strains.

In previous work to better understand the basis for fluoroquinolone action and resistance in *B. anthracis*, wild-type *B. anthracis* Topo IV, the GrlA^{S81F} and GrlA^{S81Y} fluoroquinolone-resistant mutants were characterized, and the effects of fluoroquinolones and fluoroquinolone-like compounds on these enzymes were determined [50]. Ciprofloxacin, moxifloxacin, levofloxacin, norfloxacin, sparfloxacin were the clinically relevant fluoroquinolones tested, while 3-amino-7-(3*S*)-3-(aminomethyl)-1-pyrrolidinyl]-1-cyclopropyl-6-fluoro-8-methyl-2,4(1*H*,3*H*)-quinazoline-dione (8-methyl-2,4-quinazoline dione) and CP-115,953 were the two synthetic FQ-like compounds tested
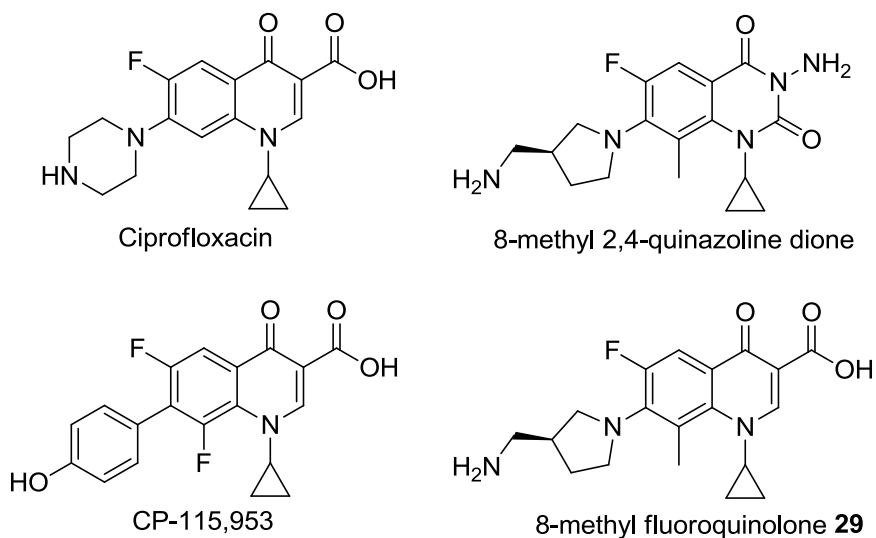
Figure 9. Structures of ciprofloxacin, 8-methyl-2,4-quinazoline dione, CP-115,953, and the 8-methyl fluoroquinolone **29**.

(Figure 9). The 8-methyl-2,4-quinazoline dione is a fluoroquinolone class gyrase inhibitor that was found to have activity against bacteria gyrase mutations [55]. Structurally, it has a different arrangement of the carbonyls in the second ring, allowing it to pick up additional binding contacts and giving it a DNA base-like appearance. CP-115,953 is an experimental fluoroquinolone that contains a C-7 carbon-carbon bond instead of the traditional carbon-nitrogen bond, as well as a C-7 phenol group. To date, it is the only topoisomerase II poison that displays high activity against both bacterial and eukaryotic type II topoisomerases [56-58].

When the percent DNA cleavage was determined for all of the compounds, the clinically relevant fluoroquinolones and CP-115,953 were found to display decreased activity against GrlA^{S81F} and GrlA^{S81Y}. This was expected since mutations in the *B. anthracis* Ser81 equivalent residue in past resistance studies with *E. coli*'s Ser83 had resulted in decreased activity [55, 59-62]. Thus, it was concluded that formation of the magnesium ion-mediated bridge through the "Ser83 equivalent" residue (as seen with Ser84 in *A. baumannii* in Figure 8) that allowed the fluoroquinolone to interact with Topo IV is an important interaction for fluoroquinolone ability to cause chromosomal fragmentation. However, with the quinazolinedione, it was observed that the dione was able to maintain cleavage activity in the presence of the "Ser83 equivalent" mutation in Topo IV. This result suggested that the quinazolinedione does not require the magnesium -mediated bridge interaction to interact with Topo IV and exert its bacteriostatic effects.

3.2.1 Goals of this Study

In preliminary data with a C-8 methyl fluoroquinolone **29** UIHS-I-303 (synthesis described in Chapter 3.1.2), the ability of the fluoroquinolone **29** was found to maintain or enhance DNA cleavage activity against the *B. anthracis* Ser81 mutants like the 8-methyl-2,4-quinazoline dione did. Fluoroquinolone **29** is structurally similar to ciprofloxacin, but has a C-8 methyl and C-7 aminomethyl pyrrolidinyl group instead of

C-7 piperazinyl (Figure 9). Thus something unique about the structure of

fluoroquinolone **29** allowed it to maintain activity in the absence of a magnesium ion-

mediated bridge between the drug and Topo IV while other fluoroquinolones lost

activity.

   We hypothesized that unique structural features at C-8 and C-7 allow the

fluoroquinolone **29** to maintain activity against Ser81 mutants in *B. anthracis* TopoIV.

To better understand the importance of the ability to form the magnesium ion-mediated

bridge, the effects of fluoroquinolone and 2,4-quinazoline dione core structure on DNA

cleavage activity were assessed. A panel of fluoroquinolones and diones with distinct

structural changes at C-7 and C-8 was synthesized for direct comparison to the parent

compounds used in the original report: ciprofloxacin, moxifloxacin, 8-methyl-2,4-

quinazoline dione, and CP-115,953.

3.2.2 Synthesis of C-8 and C-7 fluoroquinolone and 2,4-
quinazoline dione derivatives

   The panel of C-8 substituted fluoroquinolone and quinazolinedione analogues

having a C-7 *cis*-octahydropyrrolopyridine, (*S*)-aminomethyl pyrrolidine, or piperazine

was prepared through commercially available core structures or *de novo* synthesis. Of

the core structures requiring *de novo* synthesis, the C-8 methyl fluoroquinolone core **13**

was prepared as described in Chapter 3.1.2 (Schemes 1 and 2), while all three 2,4-

quinazoline dione cores were available in the Kerns laboratory.

   The C-7 substituents were added to each of the prepared or available

fluoroquinolone or 2,4-quinazoline dione cores through nucleophilic aromatic

substitution by a secondary amine (Scheme 6, final structures in Table 3). In some cases

with the fluoroquinolone cores, as indicated in Table 3, the core structure was converted

to the corresponding boronate ester to facilitate addition of the C-7 group. A subsequent

treatment with aqueous sodium hydroxide (3%) cleaved the boronate ester to give the
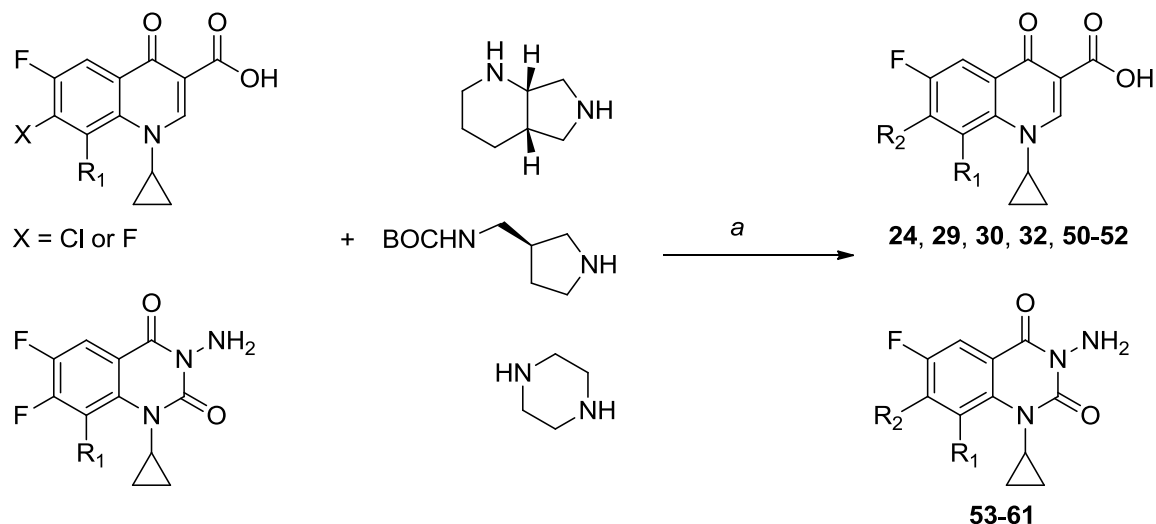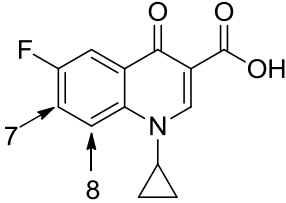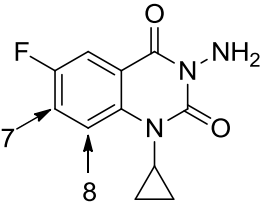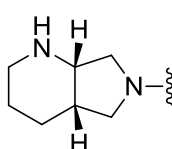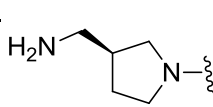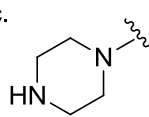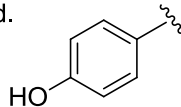
Scheme 6. General synthetic scheme for the C-7 SN aromatic addition of secondary amines to the various fluoroquinolone cores to obtain compounds **24**, **29**, **30**, **32**, **50-52** and various quinazolinedione cores to obtain compounds **53-61**. Reagents and conditions: (a) Triethylamine, DMSO, 60-80 °C, 1-6 hr (22-80%).

desired carboxylate. Trifluoroacetic acid was used to remove the BOC protecting group after addition of the BOC protected aminomethyl pyrrolidine.

The CP-115,953 derivatives were synthesized from either the 8-methyl fluoroquinolone core **13**, which was *de novo* synthesized as described in Chapter 3.1.2 on page 18, or 1-cyclopropyl-6,7-difluoro-1,4-dihydro-8-methoxy-4-oxo-quinoline-3-carboxylic acid **62** that was purchased from 3B Scientific. As shown in Scheme 7, the core structures were converted to the boronate esters to facilitate substitution of the 4-methoxybenzylamine at the C-7 position. After cleavage of the boronate ester, the 4-methoxybenzyl functionality was removed with trifluoroacetic acid to give the resulting compounds **63** and **64** with a primary amine at C-7. The primary amine was then functionalized with t-butyl nitrite and displaced with bromine to yield the brominated fluoroquinolone cores **65** and **66**. The protected phenol was added in a modified Suzuki

Table 3. Structures of fluoroquinolone and quinazolinedione derivatives **24**, **29**, **30**, **32**, **50**-**61**, and **67**-**71**.

fluoroquinolone

quinazolinedione

a.   b.   c.   d.

Compound	Core	C8	C7	Compound	Core	C8	C7
50 UIHS-IIa-239	fq	H	a	**53** UIHS-IIa-247	qd	H	a
24 UIHS-IIIa-35†	fq	H	b*	**54** UIHS-IIa-245	qd	H	b*
Ciprofloxacin	fq	H	c	**55** UIHS-IIa-249	qd	H	c
CP-115,953	fq	F	d	**69** UILI-II-61	qd	H	d
30 UIHS-IIa-45†	fq	Me	a	**56** UILI-II-81	qd	Me	a
29 UIHS-I-303†	fq	Me	b*	**57** UIJR-I-048	qd	Me	b*
51 UILI-II-89	fq	Me	c	**58** UILI-II-87	qd	Me	c
67 UIHS-IIIa-23	fq	Me	d	**70** UILI-II-297	qd	Me	d
Moxifloxacin	fq	OMe	a	**59** UIHS-IIa-251	qd	OMe	a
32 UING-5-249	fq	OMe	b*	**60** UING-5-207	qd	OMe	b*
52 UIHS-IIa-101	fq	OMe	c	**61** UIHS-IIa-253	qd	OMe	c
68 UIHS-IIIa-27	fq	OMe	d	**71** UILI-III-11	qd	OMe	d

†Core converted to borate ester in synthesis and cleaved with TFA or NaOH after secondary amine addition (Scheme 6).

*TFA added in synthesis after secondary amine addition to remove BOC (Scheme 6).
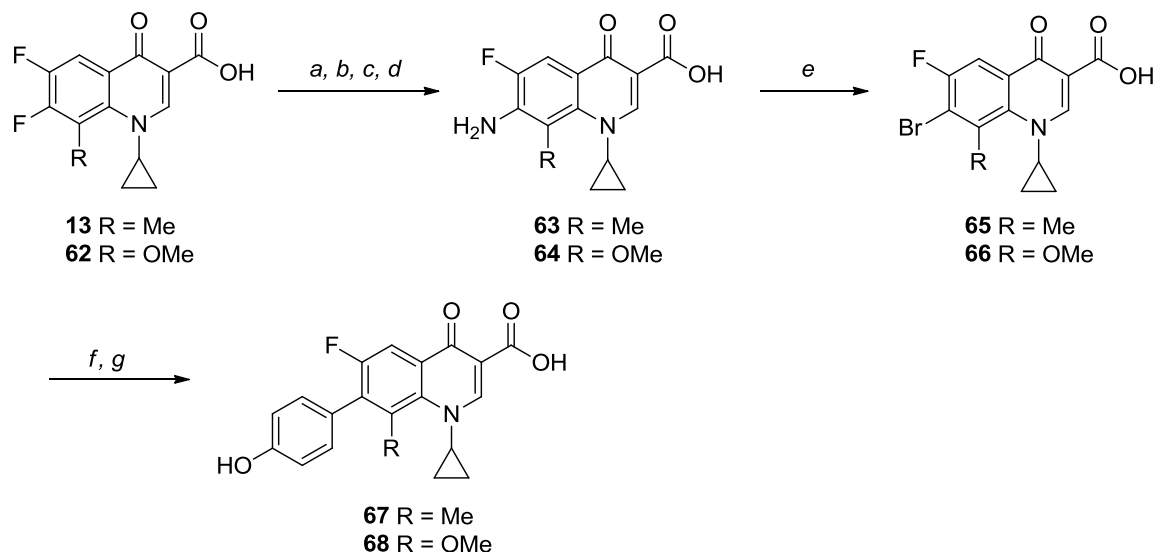
Scheme 7. Synthesis of CP-115,953 derivatives **67** and **68**. (a) B$_2$O$_3$, Ac$_2$O, 100 °C for 1 hr; (b) 4-methoxybenzylamine, triethylamine, acetonitrile, 24 hrs at rt; (c) 3% NaOH, 4 hrs at rt; (d) TFA:CH$_2$Cl$_2$ 1:4, 10 hrs at rt; (e) Cu(II)Br$_2$, *t*BuONO, acetonitrile, 67 °C for 15 min (**65**: 36% over 5 steps, **66**: 55% over 5 steps); (f) 4,4,5,5-tetramethyl-2-[4-[[tris(1-methylethyl)silyl]oxy]phenyl]-1,3,2-dioxaboranolane, potassium carbonate, Pd(Ph$_3$)$_4$, 85 °C for 18 hrs; (g) concentrated HCl, dioxane (**67**: 5% over 2 steps, **68**: 15% over 2 steps).

coupling procedure with a boronate, 4,4,5,5-tetramethyl-2-[4-[[tris(1-methylethyl)silyl]oxy]phenyl] -1,3,2-dioxaboranolane which was prepared as described [63], that was coupled to the brominated fluoroquinolone cores. The TIPS group was removed with concentrated hydrochloric acid to yield compounds **67** and **68**. Despite the addition of the dioxane to help solubilize, the removal of TIPS and subsequent purification by semi-preparative HPLC was quite difficult as reflected by the low yields.

For SAR comparison, the 2,4,-quinazoline dione derivatives of CP-115,953 (**69-71**) were prepared in a manner similar to the one described above for the fluoroquinolone derivatives **67** and **68** (completed in a collaborative manner by Gangqin Li). Similar problems with the loss of product in the final deprotection and purification steps were encountered.

3.2.3 DNA Cleavage Studies in wild-type and mutant *B.*

anthracis TopoIV

Wild-type and mutant *B. anthracis* GrlA and GrlB enzymes were cloned, expressed, and purified as previously described [50]. DNA cleavage reactions were carried out using the procedure of Fortune and Osheroff [64]. DNA bands were visualized and quantified as described and DNA cleavage was monitored by the conversion of supercoiled plasmid to linear molecules. Assays that assessed the DNA cleavage activities of the wild-type and mutant enzymes in the presence of drugs contained 0-100 μM compound. DNA cleavage activity was compared at 20 μM for all compounds.

The effect of the C-8 group on DNA cleavage activity for compounds with fluoroquinolone and 2,4-quinazoline dione core structures was determined by comparing activity of the compounds where the C-7 group was held constant. When the C-7 group was a *cis*-octahydropyrrolopyridine, as in compounds **50**, **53**, **54**, **56**, **59**, and moxifloxacin (Figure 10), the fluoroquinolones with either a C-8 hydrogen (**50**) or C-8 methoxy (moxifloxacin) lost DNA cleavage activity in the presence of Ser81 mutations. When a C-8 methyl was present (**54**), activity against the Ser81 mutants was maintained. The 2,4-quinazoline dione derivatives **53**, **56**, and **59** all maintained DNA cleavage activity against enzymes with the Ser81 mutations.

When the C-7 group was an aminomethyl pyrrolidine, as in compounds **24**, **29**, **32**, **54**, **57**, and **60**, all three fluoroquinolones (**24**, **29**, and **32**) either displayed similar or improved DNA cleavage activity against Ser81 mutations in *B. anthracis* TopoIV (Figure 11); it didn't matter if C-8 had a hydrogen, methyl, or methoxy substituent. All three compounds showed improved cleavage activity against the Ser81Phe mutation. Again, the 2,4-quinazoline dione derivatives (**54**, **57**, and **60**) maintained DNA cleavage activity in the presence of Ser81 mutations.
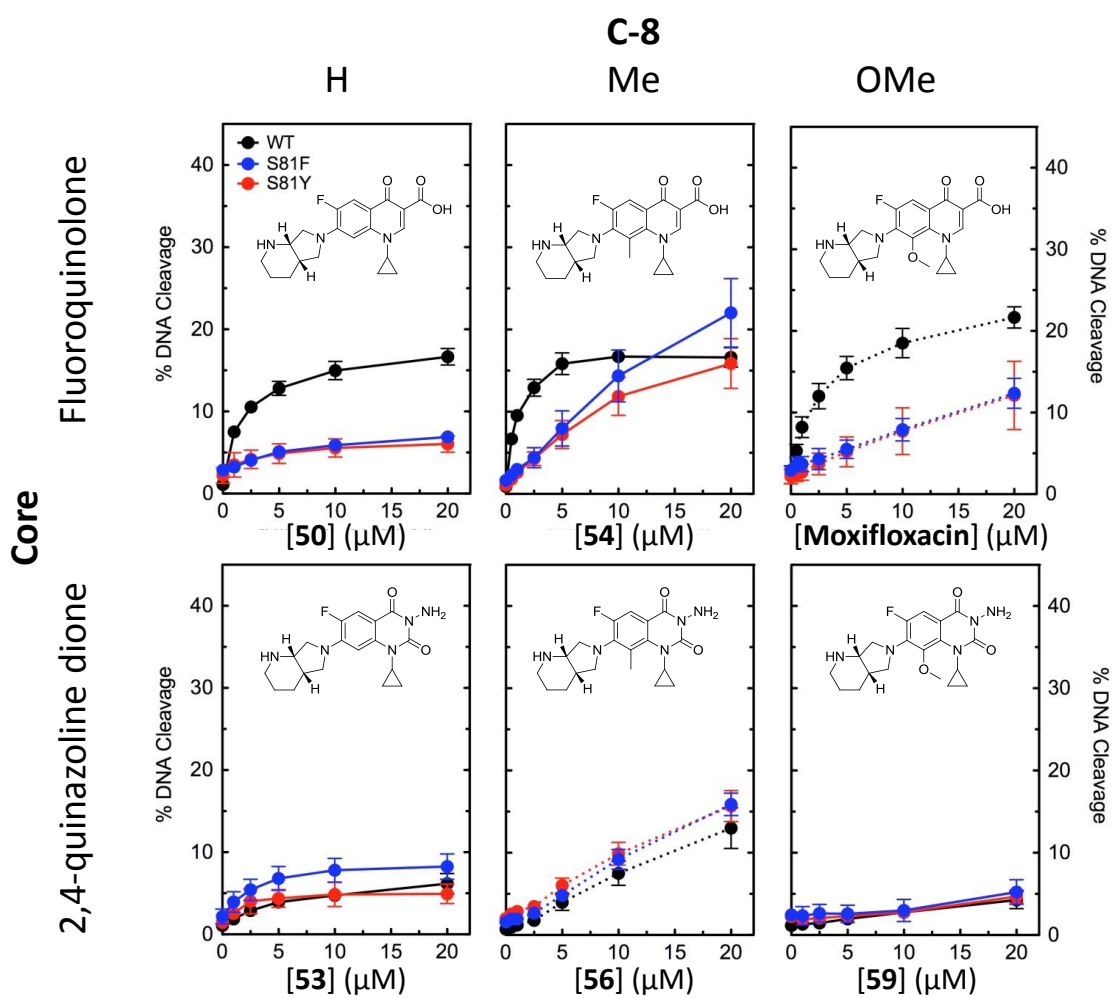
Figure 10. Effects of fluoroquinolones and 2,4-quinazoline diones with C-7 octahydropyrrolopyridine on the DNA cleavage activities of wild-type (black), GrlA[S81F] (blue), and GrlA[S81Y] (red) topoisomerase IV.
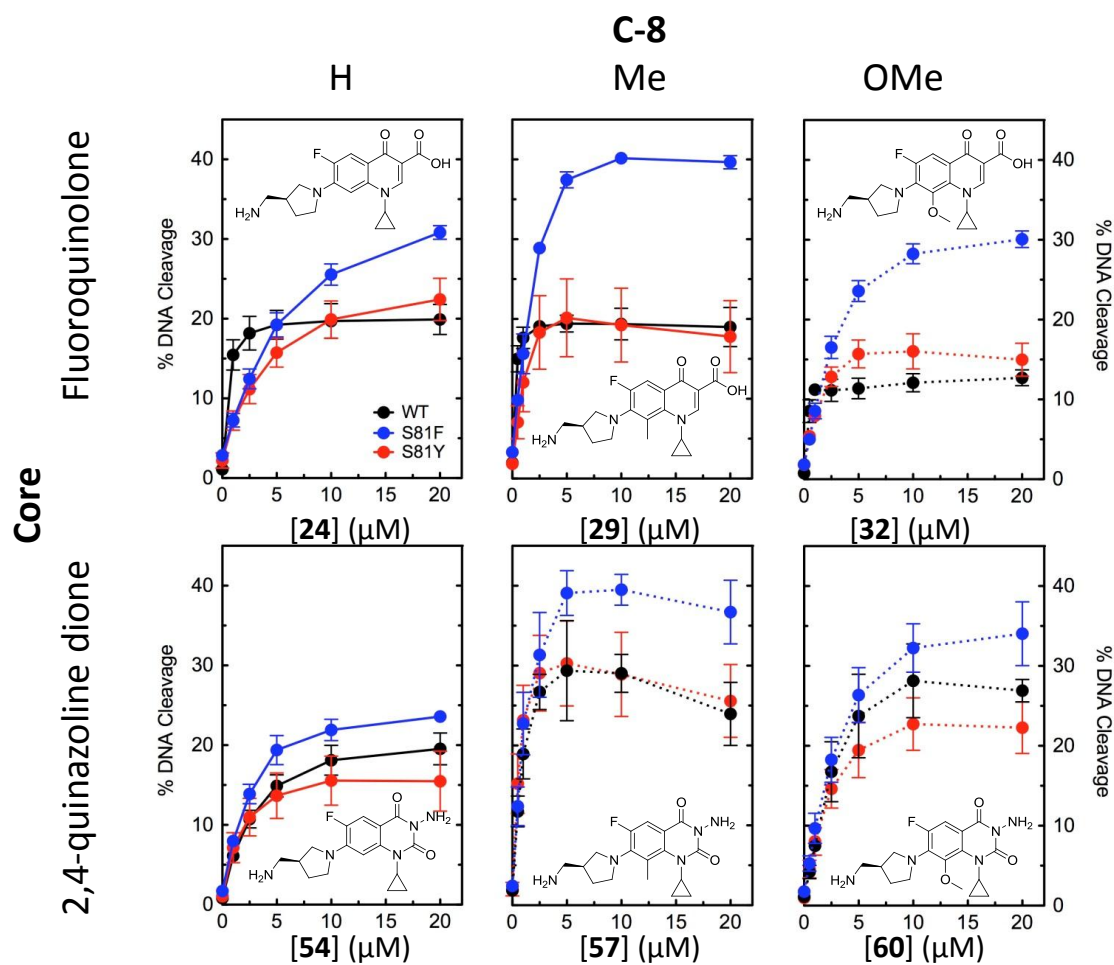
Figure 11. Effects of fluoroquinolones and 2,4-quinazoline diones with C-7 aminomethyl pyrrolidine on the DNA cleavage activities of wild-type (black), GrlA[S81F] (blue), and GrlA[S81Y] (red) topoisomerase IV.
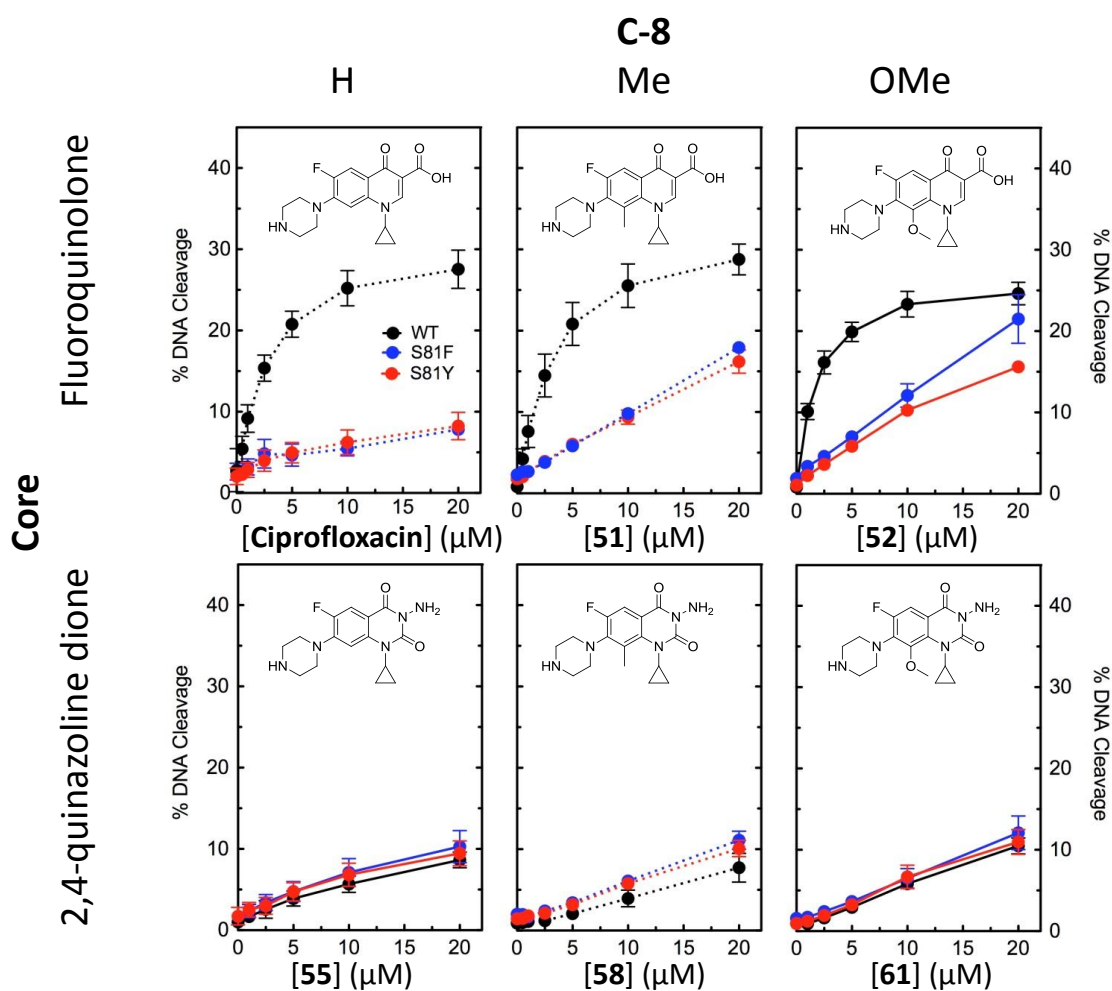
Figure 12. Effects of fluoroquinolones and 2,4-quinazoline diones with C-7 piperazine on the DNA cleavage activities of wild-type (black), GrlA[S81F] (blue), and GrlA[S81Y] (red) topoisomerase IV.

C-8

H* Me OMe

Core

Fluoroquinolone

2,4-quinazoline dione

Figure 13. Effects of fluoroquinolones and 2,4-quinazoline diones with C-7 phenol on the DNA cleavage activities of wild-type (black), GrlA[S81F] (blue), and GrlA[S81Y] (red) topoisomerase IV.

When the C-7 group was an unsubstituted piperazine, as in compounds **51**, **52**, **55**, **58**, **61**, and ciprofloxacin (Figure 12), all of the fluoroquinolones displayed decreased DNA cleavage activity in the presence of Ser81 mutation. As seen with the other C-7 substituents, the 2,4-quinazoline dione derivatives **55**, **58**, and **61** continued to maintain activity against enzymes with the Ser81 mutations.

Finally, when a phenol moiety was introduced at C-7, as in CP-115,953 (Figure 13), like CP-115,953 the fluoroquinolone derivatives with C-8 methyl (**67**) and methoxy (**68**) both had lower DNA cleavage activity against the Ser81 mutations. Although not as active as with the wild-type enzyme, both compounds had better activity against the Ser81Tyr mutation than the Ser81Phe mutation. The dione derivatives **69**-**71** maintained activity against the Ser81 mutations, even though the activity levels were quite low when compared to the DNA cleavage activity level of the fluoroquinolone derivatives. Of the dione cores, the C-8 methyl dione **70** had the best activity against the enzymes.

3.2.4 Conclusions

The 2,4-quinazoline diones, regardless of their structure at C-7 or C-8, showed no difference in activity against the Ser81 mutations. This was expected if diones do not require magnesium bridging with Ser81 for activity. The C-7 substituent appeared to affect the degree of DNA cleavage with the 2,4-quinazoline dione derivatives.

When the aminomethyl pyrrolidine was present at C-7 (Figure 11), the dione displayed higher DNA cleavage than when C-7 was piperazine (Figure 12) or *cis*-octahydropyrrolopyridine (Figure 13). It is not surprising that C-7 is important for 2,4-quinazoline dione activity against *B. anthracis*, because C-7 is known to contribute to species specific killing effects, which are described earlier in Chapter 3 on page 16. With the exception of **70**, the structure at C-8 did not affect the degree of DNA cleavage of 2,4-quinazoline dione derivatives against Ser81 mutations.

As observed in a previous study [50], structures with the fluoroquinolone core generally displayed DNA cleavage activity against Ser81 mutations that was less than the DNA cleavage observed in the presence of the wild-type enzyme. However, interestingly, with some fluoroquinolone derivatives, activity was maintained or improved by removing the magnesium bridge through Ser81 mutation. In particular, fluoroquinolone derivatives with C-8 methyl substituents or C-7 aminomethyl pyrrolidine substituents displayed this ability to maintain or have improved activity. Thus, it possible that other binding contacts, such as those between the C-7 group and DNA, are more important for these compounds, or that the interaction of the other fluoroquinolones with magnesium prevents an ideal carboxylate interaction that these compounds are able to obtain with the enzyme. The C-7 substituent may have a critical role in orientating the fluoroquinolone so that an optimal binding interaction may occur. For instance, while both the aminomethyl pyrrolidine and the *cis*-octahydropyrrolopyridine substituents contain an amine attached to a pyrrolidinyl group, the amine in the *cis*-octahydropyrrolopyridine is less flexible and has more bulk associated with it due to it being part of the pyridine ring system; thus, it is does not have the freedom to interact optimally with the enzyme, while the primary amine in the aminomethyl pyrrolidine is able to be more flexible to better fit and gain enzyme interactions. Therefore, derivatives with the aminomethyl pyrrolidine substituent were found to display the maintained or improved DNA cleavage activity against the Ser81 mutations. In summary, the combination of both the C-7 and C-8 substituents on fluoroquinolone derivatives is important for optimal DNA cleavage against Ser81 mutations.

CHAPTER 4 DNA-FLUOROQUINOLONE INTERACTIONS

4.1 Fluoroquinolones and DNA Interactions

Fluoroquinolones, broad spectrum antibiotic agents, target and inhibit type II topoisomerases, DNA gyrase and/or Topoisomerase IV (Topo IV), in bacteria by forming a ternary complex with the DNA and topoisomerase that then becomes trapped, disrupts replication, and triggers various cell death mechanisms [13, 18, 19]. Recently resolved crystal structures of the fluoroquinolone-DNA-topoisomerase ternary complex show fluoroquinolones interacting with both the DNA and the enzyme, with the fluoroquinolone positioned partially into a topoisomerase-induced nick site on the DNA [20, 22].

Once the ternary complex is formed, different mechanisms of cell death are observed by different fluoroquinolones [18, 19]. With older generation fluoroquinolones, such as nalidixic acid and ciprofloxacin **72**, slow cell death is observed. However, with newer fluoroquinolones, such as moxifloxacin **73**, rapid cell death and chromosomal fragmentation are observed. Chromosomal fragmentation occurs via two different mechanisms: one requiring protein synthesis and the other in the absence of protein synthesis (see Chapter 3.1 for more in-depth discussion). Moxifloxacin **73** kills in the
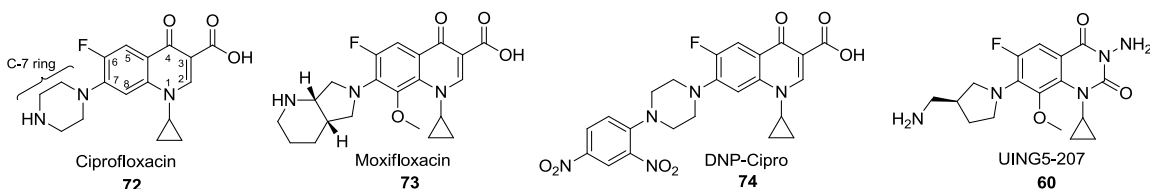
Figure 14. Structures of quinolone-class gyrase inhibitors: clinically relevant fluoroquinolones ciprofloxacin and moxifloxacin, C-7 aryl ciprofloxacin derivative, and a 2,4-quinazoline dione.
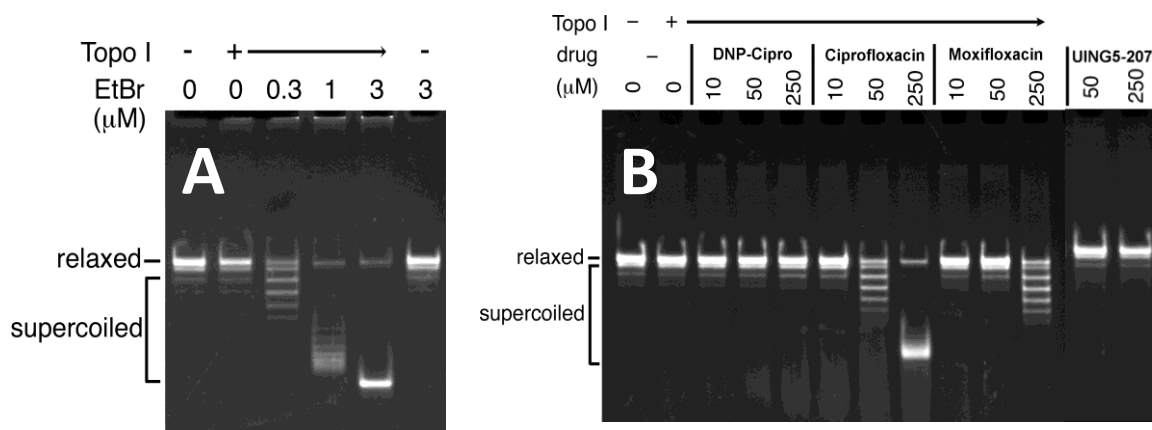
Figure 15. *In vitro* DNA unwinding assay measuring the extent of intercalation into plasmid DNA.

presence and absence of protein synthesis [40], while ciprofloxacin **72** and other older generation fluoroquinolones either kill at high concentrations or do not [33, 35]. Theintroduction of a C-8 methoxy functionality, the major core structural difference between **72** and **73** (Figure 14), is thought to be one of the contributing factors that allow **73** to have unique killing mechanisms [33].

While it is clear that fluoroquinolones interact with gyrase subunits, there is also evidence that they bind to DNA. Binding of older generations of fluoroquinolones, such as norfloxacin and ciprofloxacin **72**, to DNA has been investigated and a majority of the models imply that there is a direct interaction between drug and either single-stranded or double-stranded DNA [65-75]. However, the binding of newer C-8 methoxy fluoroquinolones (*i.e.* moxifloxacin **73**) to DNA has not been investigated. Likewise, the binding of the fluoroquinolone to nicked DNA, the type of DNA found in the ternary complex, has not been investigated.

In some previous unpublished work investigating C-7 aryl fluoroquinolones, such as 2,4-dinitrophenyl ciprofloxacin (**74**, DNP-cipro), and 2,4-quinazoline diones with a collaborator at the University of Minnesota, an *in vitro* DNA unwinding assay was

performed to measure the ability of ciprofloxacin **72**, moxifloxacin **73**, DNP-cipro **74**, and 8-methoxy-2,4-quinazoline dione **60** to intercalate into DNA (Figure 15). The ability of a C-7 aryl fluoroquinolone **74** and a 2,4-quinazoline dione **60** to intercalate into DNA was investigated due to interesting microbiological activities seen with these compounds; both of these compounds have activity against gyrase A and B mutants [55] (unpublished for **74**). We hypothesized that their unique activity was due to decreased binding contacts with gyrase and increased binding interactions with DNA. Due to the more planar structure of the C-7 aryl fluoroquinolone **74**, compared to the parent compound **72**, we expected an increased ability to intercalate to be the reason for **74**'s activity against gyrase mutants.

In the DNA unwinding assay, the extent of intercalation of the drug is related to the conversion of relaxed to supercoiled DNA after the drug is removed. Topoisomerase I was incubated with DNA and increasing concentrations of fluoroquinolone. Ethidium bromide (EtBr), a known intercalator, was used as a control and showed concentration dependent ability to block Topo I's ability to relax supercoiled DNA. Ciprofloxacin **72** and moxifloxacin **73** both showed concentration dependent ability to block Topo I's function, but they differ in their extent of intercalation as expected because fluoroquinolones are known partial intercalators. Contrary to expectations, neither the C-7 aryl fluoroquinolone **74** nor dione **60** alters super helicity, suggesting that they are much weaker intercalators or that they do not intercalate.

The unwinding assay results raised questions about how **74** and **60** interact with DNA, and if unique interactions with DS or nicked DNA play a role in their ability to maintain activity against gyrase mutants. The DNA unwinding assay results are interesting because structural studies have revealed that both fluoroquinolones and a quinazoline-2,4-dione intercalate at DNA cleavage sites [20-22, 76]. However, the DNA intercalation assay has shown that fluoroquinolones **72** and **73**, but not the C-7 aryl

fluoroquinolone **74** or quinazoline-2,4-dione **60**, intercalate into DS DNA and promote DNA unwinding [62].

4.2 Fluorescence-based DNA Binding Studies

4.2.1 Goals of this Study

While binding of ciprofloxacin, an older generation fluoroquinolone, to DNA is well investigated, the ability of newer C-8 methoxy fluoroquinolones that have been shown to kill microorganisms through novel mechanistic pathways has not been investigated. To better understand the role of the C-8 methoxy substituent and its contribution to rapid lethality, we assessed the ability of the two different fluoroquinolones to bind single-stranded (SS), double-stranded (DS), and nicked DNA – all types of DNA present in the ternary complex – by utilizing the innate fluorescence of the fluoroquinolones to determine binding affinities and then determining if affinity discrepancies would account for the mechanistic and activity differences observed between ciprofloxacin **72** and moxifloxacin **73**.

Also, due to the interesting observations in the DNA unwinding assay with the C-7 aryl fluoroquinolone **74** and the 8-methoxy-2,4-quinazoline dione **60**, we aimed to investigate more thoroughly how **74** and **60** interact with DNA to determine and if the affinity of the compounds with different types of DNA would lead to further insights into the DNA unwinding assay results or reflect on the ability of these two compounds to maintain activity against gyrase mutants.

4.2.2 Assembly and Characterization of 16-mer DNA oligonucleotides

The DNA sequence from the Laponagov crystal structure of a ternary complex [20] was used to assemble short 16mer oligonucleotides (Figure 16). The DNA sequences were intentionally kept short in order to minimize fluoroquinolone binding
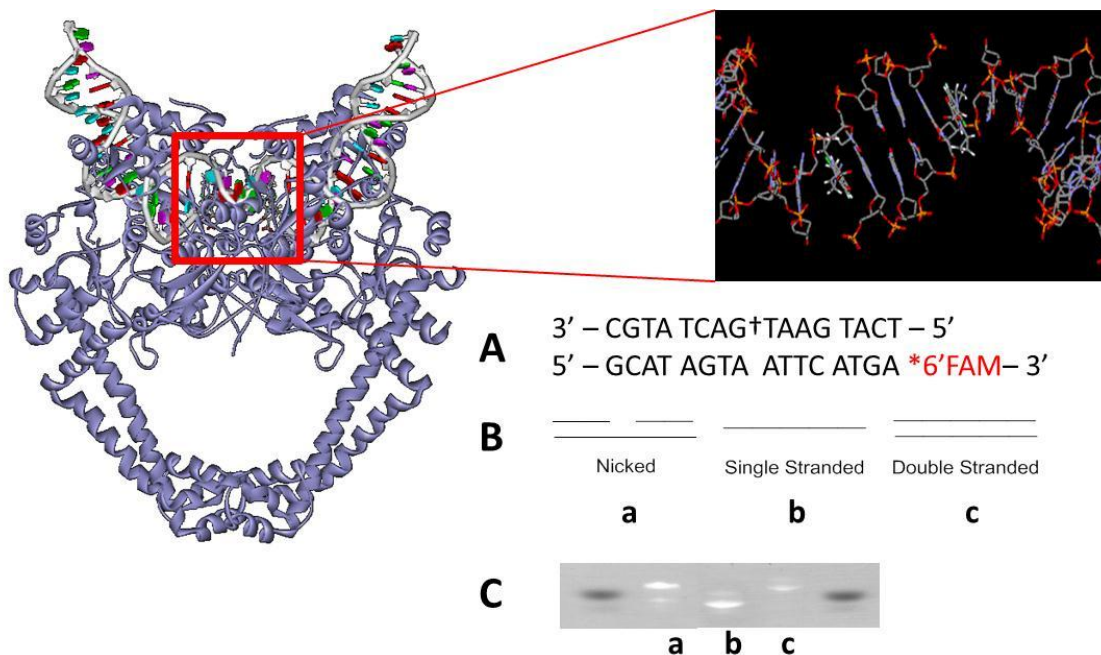
Figure 16. DNA sequence of 16-mer oligonucleotide from the Laponogov ternary complex crystal structure and types of DNA assayed. A. Sequence of labeled 16-mer oligonucleotides. † nicked site in the nicked DNA. B. Types of DNA assembled and assayed: (a) nicked, (b) single-stranded, and (c) double-stranded. C. Visualization of 16-mer DNA oligonucleotides on a 20% polyacrylamide gel: (a) nicked, (b) single-stranded, and (c) double-stranded.

Figure 17. DNA Stability Assay. Fluoroquinolone concentration (nmol) was increased and the DNA oligonucleotide complex of (a) nicked DNA and (b) double-stranded DNA was assessed on a 20% polyacrylamide gel. 1 nmol of fluorescently labeled DNA was used in each lane. *SS DNA was loaded with no fluoroquinolone as a control.

contacts on the DNA in order to distinguish DS-fluoroquinolone binding from binding to DS DNA with one nick site (*i.e.* nicked DNA). To verify oligonucleotide assembly, the fluorescein-like fluorophore 6-FAM was attached to the 3' end of the DNA oligonucleotide. Both DS and nicked DNA were annealed, as indicated by the visualization of appropriate fluorescent bands on a 20% PAGE gel (Figure 16, Panel C). Non-labeled DNA was annealed in parallel with the labeled DNA.

4.2.3 Control Studies

Control studies with the assembled DNA oligonucleotides were performed in order to verify that the DNA complexes were stable and intact at high concentrations of fluoroquinolone. Fluoroquinolones – ciprofloxacin **72**, moxifloxacin **73**, and DNP-cipro **74** - were incubated with 1 μM DNA up to 30-100 times the concentration of the DNA. The stability of each fluorescently labeled DNA type (nicked and DS) was verified with each fluoroquinolone on a 20% PAGE gel (Figure 17).

An additional control study, based on a previous investigation of fluoroquinolone aggregation [23], was performed in order to establish that aggregation of the compounds was not occurring. The absorbance of fluoroquinolones **72** and **74** and the 2,4-quinazoline dione **60** was measured from 0.25-64 μM in the presence and absence of 5.0 mM $MgCl_2$ in phosphate buffered saline (PBS). When the absorbance was plotted versus the fluoroquinolone concentration, straight lines were obtained (Figure 18) indicating that simple aggregation and stacking do not account for the observed differences in fluoroquinolone-class agents that demonstrate different microbiological activities.

4.2.4 DNA Binding Affinities in the presence and absence
of magnesium ions

The annealed, stable 16-mer oligonucleotides were used in fluorescence-based DNA binding assay, in which the innate fluorescence of the fluoroquinolone was used to evaluate the direct binding to DNA. The 2,4-quinazoline dione **60** was not evaluated
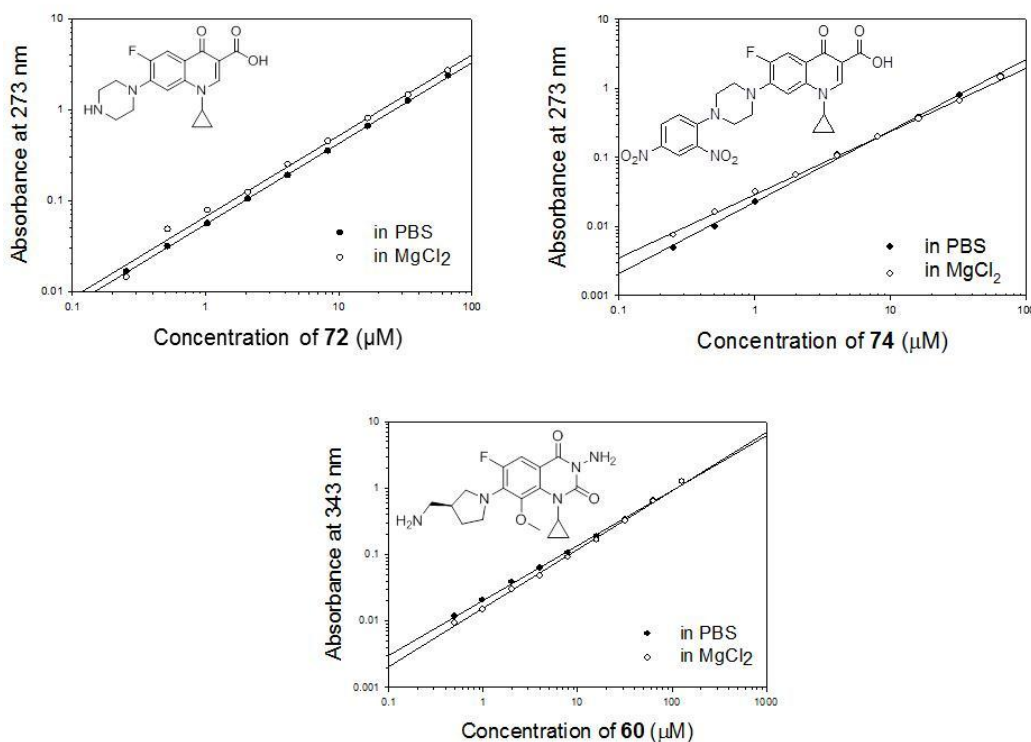
Figure 18. UV-based aggregation studies in which the concentration of the fluoroquinolone or quinazoline dione was increased while the absorbance was monitored in both the presence (open circles) and absence (solid circles) of 5.0 mM MgCl$_2$ buffer.

because it is not innately fluorescent. In the past, fluoroquinolone binding had been investigated in the presence and absence of magnesium [68, 72]. Recent work has indicated that fluoroquinolones bind DNA in a magnesium dependent manner [65]. Thus the binding was evaluated both in the presence and absence of magnesium.

In the experiment, MgCl$_2$ was present or absent in the buffer, the concentration of the fluoroquinolone was constant at 1μM, DNA was titrated in, and the fluoroquinolone fluorescence was measured at the appropriate wavelength (ciprofloxacin **72** and DNP cipro **74**: λ_{ex} = 275 nm, λ_{em} = 550 nm, moxifloxacin **73** : λ_{ex} = 289 nm, λ_{em} = 579 nm). The concentration of DNA was plotted against the change in fluoroquinolone
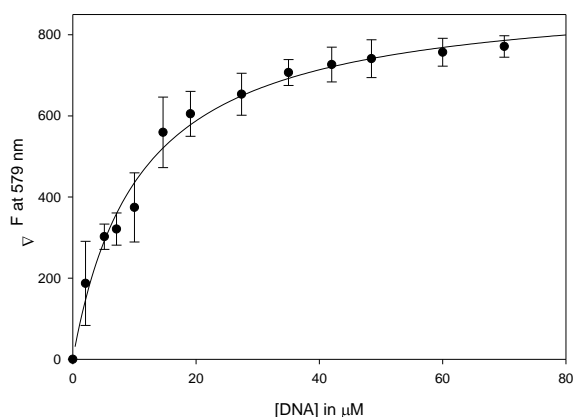
Figure 19. Representative binding curve of moxifloxacin **73** to DS DNA in 5 mM MgCl$_2$.

fluorescence (Figure 19; Appendix C). A one binding site model was used to determine K_d in µM to assess affinity. Binding affinities were determined for SS, DS, and nicked DNA (Table 4).

When comparing the affinity of the fluoroquinolones to DNA in the absence of magnesium, both ciprofloxacin **72** and moxifloxacin **73** bound tighter to DS DNA than to SS DNA. This was surprising because previous studies with norfloxacin concluded the norfloxacin bound strongest to SS DNA [23, 71]. When comparing the binding of the compounds to nicked DNA, moxifloxacin **73** bound tighter than ciprofloxacin **72**. However, when the affinity of the fluoroquinolones to DNA in the presence of magnesium was evaluated, significant changes in the affinity of the compounds to the different DNA types were observed. Both ciprofloxacin **72** and moxifloxacin **73** had a six-fold decrease in affinity to nicked DNA and two to five fold increase in affinity to SS DNA. Ciprofloxacin **72** had increased affinity to both DS and SS DNA in the presence of magnesium, while moxifloxacin **73** retained affinity for DS DNA and increased

Table 4. DNA Binding affinity (K_{app}) in the absence and presence of Mg^{2++} (in μM).

DNA	No Mg^{2++}			Mg^{2++}		
Type	Ciprofloxacin **72**	Moxifloxacin **73**	DNP-Cipro **74**	Ciprofloxacin **72**	Moxifloxacin **73**	DNP-Cipro **74**
SS	36.78 ± 8.1	40.25 ± 11.1	17.67 ± 4.5	6.79 ± 1.1	22.17 ± 3.7	11.93 ± 1.8
DS	11.59 ± 4.0	9.17 ± 1.7	30.28 ± 3.8	2.51 ± 0.3	10.71 ± 2.3	6.89 ± 0.6
Nicked	12.13 ± 1.8	8.24 ± 1.6	47.6 ± 27.6	76.67 ± 18.2	24.55 ± 4.0	3.08 ± 0.6

affinity to SS DNA. Thus, moxifloxacin **73**, a rapid killer, had a stronger affinity for DS and nicked DNA than ciprofloxacin **72**, both in the presence and absence of magnesium.

Like with ciprofloxacin **72** and moxifloxacin **73**, we assessed the ability of the C7-aryl fluoroquinolone **74** to directly bind DNA through the described fluorescence assays (Table 2). In the absence of magnesium, DNP-cipro **74** had the lowest affinity to nicked and DS DNA. This is not surprising since the DNA unwinding assay showed that DNP-cipro **74** does not intercalate into DNA like ciprofloxacin **72** and moxifloxacin **73**. DNP-cipro **74** has the highest affinity to SS DNA. Interestingly, in the presence of magnesium, DNP-cipro **74** bound DS DNA at least as tightly as moxifloxacin **73**; however, in the unwinding assay DNP-cipro **74** was found to not intercalate. Furthermore, DNP-cipro **74** bound nicked DNA with five times higher affinity than moxifloxacin **73** and with 20 times higher affinity than ciprofloxacin **72**. When comparing affinity to DS DNA and nicked DNA, both ciprofloxacin **72** and moxifloxacin **73** lose affinity by thirty-fold and two-fold respectively, while DNP-cipro **74** doubles its affinity to the nicked DNA.

4.2.5 Conclusions

In conclusion, ciprofloxacin **72** and moxifloxacin **73** kill via different pathways after inhibiting topoisomerase and forming a ternary complex, but bind DNA differently. In the absence of magnesium, there is essentially no difference in the way that they bind DNA, but in the presence of magnesium, a difference is observed: ciprofloxacin **72** binds DS DNA tighter than moxifloxacin **73**, while moxifloxacin **73** binds nicked DNA tighter than ciprofloxacin **72**. These observations lead us to hypothesize that either the tight binding of ciprofloxacin **72** to DS DNA with intercalative character promotes a more stable ternary complex so DNA cannot fall off the complex, or moxifloxacin's (**73**) higher affinity to nicked DNA destabilizes the complex and thus promotes release of DNA from the complex and chromosomal fragmentation. While DNP-cipro **74**, does not intercalate into DNA, it binds nicked DNA with the highest affinity of the fluoroquinolones. Perhaps the higher affinity to nicked DNA results in increased binding contacts with this type of DNA in the ternary complex and fewer binding contacts with the gyrase enzyme. Thus mutations on gyrase have minimal effect on the activity of DNP-cipro **74**. The direct DNA binding of the 2,4-quinazoline dione **60** to the different types of DNA was not assessed and compared to the fluoroquinolones due to its poor ability to absorb UV light and lack of innate fluorescence. Our group is currently pursuing ways to assess the direct binding of the quinazoline dione to DNA.

Furthermore, it is apparent that past observations for how fluoroquinolone-class topoisomerase inhibitors interact with DNA cannot be applied across this class of compounds. Newer generation inhibitors have demonstrated improved microbiological activity, as well as different affinity to DNA as shown here. Thus, it is evident that each new compound in the fluoroquinolone-class of topoisomerase inhibitors needs to be individually evaluated for how it interacts with DNA if DNA binding is expected to play a role in antimicrobial activity.

4.3 Assessment of the effect of the fluoroquinolone on the
stability of DNA

4.3.1 Goals of this Study

Due to the unique affinities seen between fluoroquinolones and nicked DNA (Chapter 4.2), we questioned whether any of the compounds had the ability to stabilize or destabilize DNA, particularly nicked DNA because the crystal structure shows fluoroquinolones binding in the nicked sites (see Figure 3 and Figure 16) . In order to answer this question, we performed DNA denaturation studies to determine the melting temperature (T_m) and the following investigation ensued.

A series of control studies were performed in order to identify the conditions, reagents, and materials that were optimal for performing the melting temperature experiments with DNA. 16-mer oligonucleotides (see Section 4.2.2) were used in the first studies, but were determined to be too short, not stable enough at the low temperature range of the UV-Vis equipped instrumentation that was available at the time of the study, and produced a larger range of error. Therefore, the oligonucleotides were redesigned and longer, more stable 27-mer oligonucleotides were used. The 27-mer oligonucleotides allowed the optimization of the procedure that was eventually used in this study, but were slightly too stable for the high end temperature range of the temperature controller associated with the UV-Vis equipped instrumentation. Thus, 25-mer oligonucleotides were designed. Due to the desire to compare consistent data across the same type of oligonucleotides, all data reported and discussed hereafter is with a set of 25-mer oligonucleotides and conditions that have been optimized for obtaining quantitative results.

By assessing the stability of DS and nicked DNA in the presence of a fluoroquinolone, we set out to accomplish two goals. The first objective was to determine the effect that structural differences at C-7 and C-8 of the fluoroquinolone core

structure have on the ability of a compound to stabilize or destabilize DS and nicked DNA. In order to accomplish this goal, we assayed a set of 4 compounds that had specific structural combinations at C-7 and C-8: ciprofloxacin **72**, moxifloxacin **73**, UIHS-IIa-101 **52**, and UIHS-IIa-239 **50**. The second objective was to determine the effect of the core structure on the ability of a fluoroquinolone-like compound to stabilize or destabilize DS or nicked DNA. A structurally related fluoroquinolone, UIHS-I-303 **29**, and 2,4-quinazoline dione, UIJR-1-048 **57**, were assayed.

4.3.2 Melting Temperature Experiments

25-mer oligonucleotides were designed based on the DNA sequence in the Wohlkonig crystal structure [22]. Like with the 16-mer oligonucleotides, they were designed to be short in order to minimize the net number of fluoroquinolone binding contacts so a difference would likely be detected in the melting temperature (T_m) for the DS DNA or DNA with one nick site (*i.e.* nicked DNA) with the drug. Two different nicked oligonucleotides were used (Table 5). The oligonucleotides had the same sequence with the nick at different site. The original sequence in the Wohlkonig crystal structure had a nick between the bases adenine and thymine [22], while the additional

Table 5. DNA sequences of the 25-mer oligonucleotides. Partially adapted from [22]. † indicates nicked site.

DNA	Sequence
DS	3'-GCCATACTTACTGATACGTGATTCC-5'
	5'-CGGTATGAATGACTATGCACTAAGG-3'
Nicked 1 (N_1)	3'-GCCATACTTACTGA†TACGTGATTCC-5'
	5'-CGGTATGAATGACTATGCACTAAGG-3'
Nicked 2 (N_2)	3'-GCCATACTTACT†GATACGTGATTCC-5'
	5'-CGGTATGAATGACTATGCACTAAGG-3'

nicked DNA that was designed contained a nick between bases guanine and thymine. The design of a nick between guanine and thymine was chosen based on past work that had determined that the topoisomerase enzyme prefers to cleave, or nick, the DNA between these two bases [77, 78].

Additionally, two different ratios of drug:DNA were assayed. A ratio of 20:1 DNA:drug was evaluated because in the fluorescence-based DNA binding, the binding curves were saturated at 20 µM DNA: 1 µM fluoroquinolone (Chapter 4.2.4). A ratio of 1:1 DNA:drug was used because all reported crystal structures show one fluoroquinolone binding per nick site [20-22], and the nicked DNA we used in the assay contained only one nick site.

Well-established, previously reported procedures for the analysis of melting temperature curves were followed and incorporated into the experimental design [79]. A Shimadzu UV-2101PC UV-Vis scanning spectrophotometer connected to a temperature controller was used to measure the absorbance of DNA at 280 nm from 20 °C to 60 °C
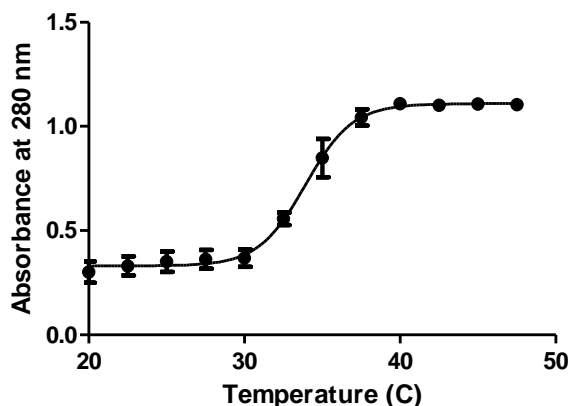
Figure 20. Representative melting curve of DS DNA with HS-IIa-239 **50** at the 20:1 DNA:fluoroquinolone ratio (n = 3). The inflection point is the melting temperature (T_m) of the DNA.

when it was incubated with drug. As temperature was increased, the absorbance was recorded and plotted versus temperature, with the T_m being the inflection point (Figure 20, Appendix D). The T_m of the DNA without the drug was used as a control.

In the experiments, ethidium bromide (EtBr) was used as a control; it is a known intercalator. Thus from the EtBr assays, we controlled for how an intercalator affects the destabilization or stabilization of DS DNA and each individual nicked DNA, thus providing a basis of comparison for the other assays.

4.3.3 Quantitative Comparison of Melting Temperature Experiments

First, the T_m of each DNA was determined. The T_m for each DNA in the presence of test compounds was then determined, and the ratio of the T_m in the presence of test compound to the T_m in the absence of test compound was calculated (Table 6). When the DNA:compound ratio was equal to 1, the test compound had no effect on the T_m of the DNA. If the ratio was greater than 1, the test compound had a stabilizing effect on the DNA. Conversely, if the ratio was less than 1, the test compound had a destabilizing effect on the DNA. While also reported in Table 6, Figure 21 better illustrates the ratios and T_m values that were obtained.

When comparing the effect of test compound at the 20:1 ratio to the effect of test compound at the 1:1 ratio of DNA:drug, a larger stabilizing effect was seen at the 1:1 ratio with DS DNA for all compounds except HS-IIa-101 **52**. With both types of nicked DNA, there was little difference between T_m's observed with the 1:1 ratio and then 20:1 ratio.

In general, there was little difference with test compounds between the T_m of the DNA with one nick site between adenine and thymine (N_1) and the T_m of the DNA with the other nick site between guanine and thymine (N_2). When a difference was observed, such as with moxifloxacin, the T_m of the DNA with the nick site in between guanine and
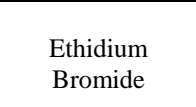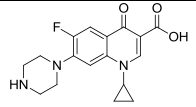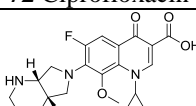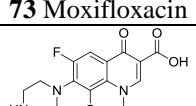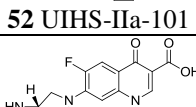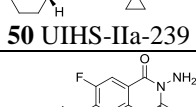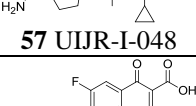
thymine (N_2) was higher and therefore the drug had a higher stabilization effect on this nicked DNA.

When looking at which compound had a stabilizing effect most like the intercalator EtBr, HS-IIa-239 **50** was found to be the most similar. Of the two commercially available fluoroquinolones, moxifloxacin **73** interacted with DNA more like the intercalator EtBr than ciprofloxacin **72** did. This was surprising because in the DNA unwinding assay (Figure 15), ciprofloxacin **72** behaved more like EtBr than moxifloxacin **73** did.

The unique combination of the C-8 methoxy and C-7 substituent both contribute to the ability of moxifloxacin **73** to stabilize DNA. Of the two, the C-7 substituent appears to be important for interacting with DNA. When comparing HS-IIa-101 **52** and moxifloxacin **73**, in which only the C-7 substituent is different, HS-IIa-101 **52** has a slight destabilizing or no effect on DNA stability. Likewise when comparing ciprofloxacin **72** and HS-IIa-239 **50**, HS-IIa-239 **50** (the compound with the same C-7 substituent as moxifloxacin **73**) has a higher stabilizing effect. The presence of the C-8 methoxy has a lesser effect. When the C-8 methoxy group is present, as in HS-IIa-101 **52** and moxifloxacin **73**, it has no or a slight effect as compared to when it is absent in ciprofloxacin **72** or HS-IIa-239 **50**.

The effect of the different core structures on the stability of the DS DNA and each of the nicked DNAs varied. There was not much difference between the fluoroquinolone HS-I-303 **29** and the 2,4-quinazoline dione JR-I-048 **57**. At the 20:1 DNA: fluoroquinolone ratio, HS-I-303 **29** had no effect on DS DNA, while the JR-I-048 **57** showed no effect on DS DNA at the 1:1 ratio. While the C-7 and C-8 substituents were the same in both structures, changing the core structure resulted in too many structural changes and thus the ability to determine correlations with the ability of the compounds to stabilize or destabilize DNA to structure were unable to be definitively made.

Table 6. Results of the melting temperature (T_m) experiments. T_m values in °C were reported by calculating the average of three individual denaturation experiments and are listed first. The ratio of (Tm of the DNA in the presence of the drug)/(Tm of the DNA in the absence of the drug) is listed underneath the calculated Tm. In the one way ANOVA, comparisons were within DNA type: DS, N_1, or N_2 and significance was indicated as: *$p<0.5$; ** $p<0.0001$. In the far right columns, the Tukey post analysis pairwise comparisons with alpha = 0.05; significance between the T_m's for the 20:1 and 1:1 was indicated as yes or no.

Drug (DNA:Drug)		DS	N_1 (A-T)	N_2 (G-T)	DS	N_1	N_2
No Drug		35.3 ± 1.0	33.9 ± 0.9	35.9 ± 0.8	Pairwise comparisons between 20:1 and 1:1		
Ethidium Bromide	20:1	37.7 ± 1.1* 1.07	41.6 ± 0.3** 1.23	44.6 ±0.1** 1.24	Yes	No	Yes*
	1:1	43.0 ± 0.9** 1.22	42.5 ± 0.5** 1.25	42.0 ± 0.6** 1.17			
72 Ciprofloxacin	20:1	35.7 ± 0.3 1.01	34.1 ± 0.5 1.01	38.3 ± 1.2 1.09	Yes	Yes *	No
	1:1	43.5 ± 1.6** 1.23	37.5 ± 1.3** 1.11	38.9 ± 1.4* 1.08			
73 Moxifloxacin	20:1	41.0 ± 0.2** 1.16	41.9 ± 0.4** 1.24	49.5 ± 0.5** 1.38	No	No	No
	1:1	42.9 ± 0.7** 1.22	42.6 ± 1.5** 1.26	48.4 ± 0.9** 1.35			
52 UIHS-IIa-101	20:1	35.9 ± 0.2 1.02	33.8 ±0.7 1.00	33.6 ± 0.4 0.94	Yes	No	No
	1:1	30.3 ± 0.5** 0.86	32.6 ± 1.0 0.96	33.3 ± 0.5* 0.93			
50 UIHS-IIa-239	20:1	33.9 ± 0.5 0.96	39.7 ± 0.8** 1.17	40.2 ± 1.2** 1.12	Yes	No	No
	1:1	41.6 ± 0.8** 1.24	41.7 ± 1.2** 1.23	41.9 ± 0.5** 1.17			
57 UIJR-I-048	20:1	39.7 ± 1.3** 1.12	41.3 ± 0.8** 1.22	41.5 ±0.7** 1.16	Yes	No	Yes
	1:1	34.1 ± 0.9 0.97	39.7 ± 1.0** 1.17	44.8 ± 0.2** 1.25			
29 UIHS-I-303	20:1	35.0 ± 0.4 0.99	40.5 ± 0.7** 1.19	38.9 ± 0.3** 1.08	Yes	Yes*	Yes
	1:1	41.9 ± 1.0** 1.19	44.0 ± 1.2 ** 1.30	46.1 ± 0.3** 1.28			
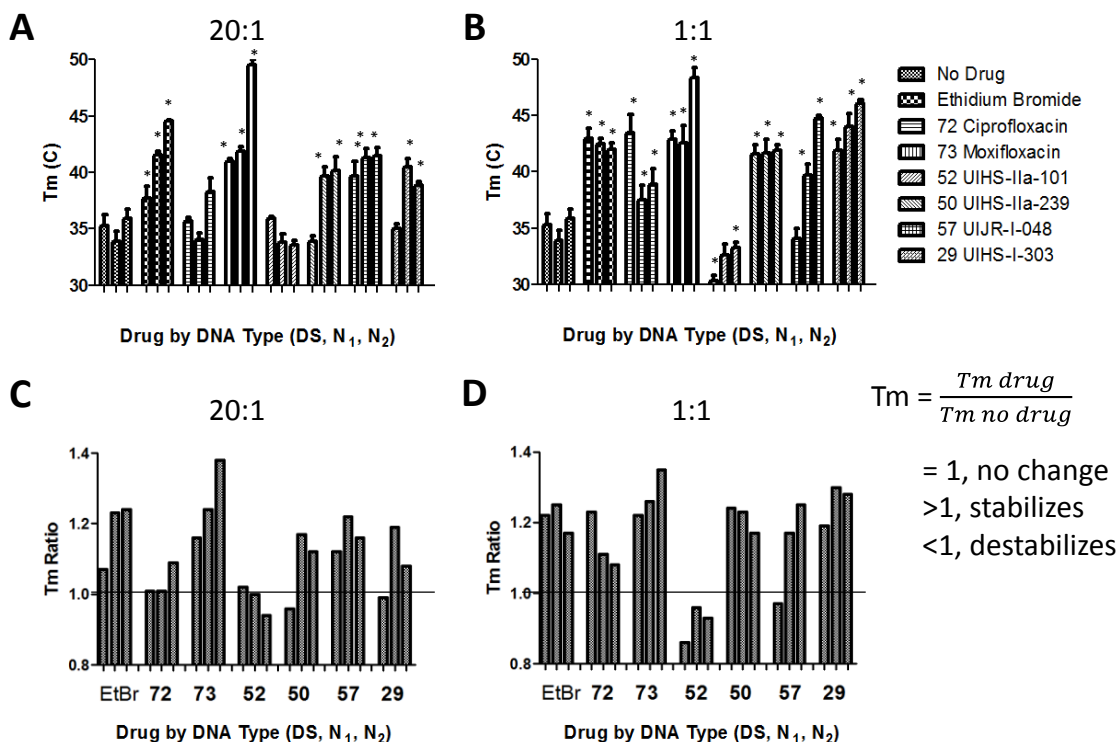
Figure 21.   Results of the melting temperature (T_m) experiments. T_m values in °C for DS, nicked A-T (N_1), and nicked G-T (N_2) for A. 20:1 DNA:drug ratio and B. 1:1 DNA:drug ratio (n = 3). The drugs used are listed in the key to the right. *significantly different from T_m with no drug. p<0.5, alpha = 0.05. The ratio of (Tm of the DNA in the presence of the drug)/(T_m of the DNA in the absence of the drug) for DS, nicked A-T (N_1), and nicked G-T (N_2) for C.20:1 DNA:drug ratio and D. 1:1 DNA:drug ratio.

4.3.4 Conclusions

The unique combination of C-8 methoxy and the C-7 *cis*-octahydropyrrolopyridine substituents in moxifloxacin **73** both contribute to the stabilizing effect that moxifloxacin has on DNA. Additionally, of the two different nicked sites examined, moxifloxacin stabilized the guanine-thymine (G-T nick site on N_2 DNA) more than the adenine-thymine (A-T nick site on N_1 DNA). This was most likely due to the expected preferential binding to the guanine base at the nick site that had been

previously reported [77, 78]. As a result, we hypothesized that moxifloxacin might act to better stabilize one nicked site in the ternary complex and thus cause subsequent destabilization with the whole complex, which prevents DNA religation and results in the observed chromosomal fragmentation. *In vitro* enzymatic work with the ternary complex looking at moxifloxacin and the other fluoroquinolones is currently being investigated by our collaborator at the University of Minnesota to further prove or disprove this hypothesis.

With regards to the effect of the different fluoroquinolone and 2,4-quinazoline dione core structures on the ability to stabilize or destabilize DNA, the results were not conclusive. Thus, future work with developing more effective methods to analyze the interactions between 2,4-quinazoline diones and DNA, as well as enzymatic work with the whole ternary complex, is necessary to understand the importance of core structure. While we had hypothesized that the ability of a fluoroquinolone to stabilize or destabilize nicked DNA would correlate to the ability of a compound to block religation, it is possible that interactions with DNA only, separate from the ternary complex, will not correlate to effects with the ternary complex.

CHAPTER 5 EXPERIMENTAL SECTION

5.1 General Methods and Equipment

5.1.1 Synthesis and Structure Activity Studies (Chapter 3)

5.1.1.1 Bacterial cells, culture conditions and susceptibility

testing (Chapter 3.1)

E. coli K-12 strain DM4100 [45] and *E. coli tolC* mutant strain was grown on LB

agar or in LB liquid medium [80]. Test compounds were dissolved in dimethylsulfoxide

(DMSO) to a concentration of 10 mg/mL, and further diluted to 1 mg/mL and 0.1 mg/mL

in DMSO. The MIC was measured by incubation of 10^4 to 10^5 cells/mL in LB liquid

medium containing serial 2-fold dilutions of quinolone at 37 °C. To measure lethal

action, cells were grown aerobically at 37 °C in liquid medium to mid-log phase.

Solutions of fluoroquinolone were added and incubation was continued for 2 hr. The

cells were diluted in liquid growth medium, applied to agar plates lacking the drug, and

incubated overnight at 37 °C to determine the colony forming units (CFU). Percent

survival was determined relative to CFU numbers at the time of fluoroquinolone addition.

Chloramphenicol (MIC = 2 µg/mL) was added to 20 µg/mL 10 min prior to the addition

of fluoroquinolone for measurement of killing in the absence of protein synthesis. Cell-

based MIC and killing data were obtained in the Drlica lab at the University of Medicine

and Dentistry of New Jersey.

5.1.1.2 Antimicrobial agents (Chapter 3.1)

Sarafloxacin, sparfloxacin, fleroxacin, and orbifloxacin were obtained from AK

Scientific (Union City, CA); sitafloxacin sesquihydrate, N-methyl gatifloxacin, and

gemifloxacin mesilate were obtained from Toronto Research Chemicals, Inc. (North

York, Ontario, Canada); grepafloxacin, besifloxacin, and balofloxacin were obtained

from Sequoia Research Products, Ltd. (Pangbourne, United Kingdom); clinafloxacin and

tosufloxacin were obtained from LKT Laboratories, Inc. (St. Paul, MN); lomefloxacin and chloramphenicol were obtained from Sigma-Aldrich (St. Louis, MO); 8-ethoxy moxifloxacin was obtained from Santa Cruz Biotechnology, Inc. (Santa Cruz, CA); ulifloxacin was obtained from Bosche Scientific, LLC. (New Brunswick, NJ). All other reagents were purchased from commercial sources and used without further purification.

5.1.1.3 Enzymes and Materials (Chapter 3.2)

Genes encoding wild-type *Bacillus anthracis* GrlA and GrlB and drug-resistant GrlA[S81F] and GrlA[S81Y] (generated by site-directed mutagenesis) were individually cloned, N-terminally His-tagged, and expressed in *E. coli*. The resulting proteins were purified by affinity chromatography, dialyzed into Tris-HCL (pH 7.5), 200 mM NaCl, and 20% glycerol, and stored at -20 °C. In all assays, topoisomerase IV (Topo IV) was used as a 1:1 GrlA:GrlB mixture.

Negatively supercoiled pBR322 plasmid DNA was prepared from *E. coli* using a Plasmid Mega Kit (Qiagen) as described by the manufacturer.

All drugs were stored at 4 °C as 20 mM stock solutions in 100% DMSO.

Experiments were performed in the Osheroff lab at Vanderbilt University.

5.1.1.4 Plasmid DNA Cleavage (Chapter 3.2)

DNA cleavage reactions were carried out using the procedure of Fortune and Osheroff [64]. Reaction mixtures contained 200 nM wild-type or mutant Topo IV and 10 nM negatively supercoiled pBR322 in a total of 20 µL of cleavage buffer [40 mM Tris-HCl (pH 7.9), 10 mM $MgCl_2$, 50 mM NaCl, and 2.5% (v/v) glycerol]. Reaction mixtures were incubated at 37 °C for 10 min, and enzyme-DNA cleavage complexes were trapped by the addition of 2 µL of 5% SDS followed by 1 µL of 250 mM EDTA (pH 8.0), Proteinase K (2 µL of a 0.8 mg/mL solution) was added, and samples were incubated at 45 °C for 45 min to digest the enzyme. Samples were mixed with 2 µL of agarose gel loading buffer, heated at 45 °C for 5 min, and subjected to electrophoresis in 1% agarose

gels in 40 mM Tris-acetate (pH 8.3) and 2 mM EDTA containing 0.5 μg/mL ethidium bromide. DNA bands were visualized with medium-range ultraviolet light and quantified using an Alpha Innotech digital imaging system. DNA cleavage was monitored by the conversion of supercoiled plasmid to linear molecules. DNA cleavage assays were performed in the Osheroff lab at Vanderbilt University.

<u>5.1.1.5 General Chemistry</u>

All reagents were purchased from commercial sources and used without further purification. Semi-preparative HPLC separations to purify final compounds were carried out with a Phenomenox-Luna 5u PFP (150 mm × 21.2 mm) column connected to a Shimadzu system that was equipped with two LC-10AT pumps (one for solvent A and one for solvent B), SPD-M10Avp photodiode array detector, and SCL-10Avp system controller. The system was connected to a Dell Optiplex 755 and controlled by Shimadzu EZStart Version 7.4 software. All synthetic derivatives were characterized by nuclear magnetic resonance (NMR) and mass spectrometry. Routine NMR spectra were obtained for ^{1}H and ^{19}F using a Bruker Ultrashield 300 MHz instrument. ^{13}C spectra were obtained by a Bruker Ultrashield 600 MHz instrument at ambient temperature. Chemical shifts are reported in parts per million from lot to high field and referenced to residual solvent. Standard abbreviations indicating multiplicity are used as follows: br s = broad, d = doublet, m = multiplet, s = singlet, and t = triplet. In many cases either DMSO or CDCl$_3$ were used as the solvent (DMSO-δ_6 – 2.50, CDCl$_3$ – 7.26). Low resolution mass spectrometry (LRMS) was determined using a Thermo LCQ Deca mass spectrometer with electrospray ionization (ESI) and quadrupole ion trap mass analyzer.

All final compounds were purified >95%, as determined by analytical high-performance liquid chromatography (HPLC). The analytical HPLC analysis was determined using a Shimadzu system equipped with LC-20AT pump, DGU-14A degasser, CBM-20A system controller, and SPD-M10A vp photodiode array detector.

The system was connected to a Dell Optiplex GX400 PC and controlled by Shimadzu Client/Server Version 7.4 software. A Restek Allure PFP Propyl (150 mm x 4.6 mm) 5u column was used as stationary phase, while mobile phase consisted of solvent A (water, buffered 0.1% TFA) and solvent B (acetonitrile, buffered 0.1% TFA). Gradient elution used the following program: from t = 0 min [solvent A (0.95 mL/min), solvent B (0.05 mL/min)] to t = 30 min [solvent A (0.05 mL/min), solvent B (0.95 mL/min)], to t = 35 min [solvent A (0.05 mL/min), solvent B (0.95 mL/min)], to t = 40 [solvent A (0.95 mL/min), solvent B (0.05 mL/min)]. Analytical HPLC was used to monitor reactions, as well as to prove the >95% purity for final products.

5.1.2 DNA Assays (Chapter 4)

5.1.2.1 DNA Assembly (Chapter 4.2)

DNA oligonucleotides were purchased from Integrated DNA Technologies (Coralville, IA). A bottom strand oligonucleotide, which was present in each duplex DNA assembled, contained a 6-FAM on the 3'end; 6-FAM is a fluorescein-type fluorophore and was necessary for gel visualization purposes since the duplexed oligonucleotides were so small. Non-labeled DNA was annealed in parallel with the labeled DNA and was used for all the experiments. Duplex buffer (Integrated DNA Technologies) was added so that the resulting concentration of the each oligonucleotide was 2100 μM. Equal molar equivalents of DNA oligonucleotides were mixed together with their complementary strand to form each respective 16-mer. Nicked DNA was formed by combining two different top strands with the complimentary bottom strand, while the DS DNA was formed by combing the full length top strand with the complimentary bottom strand. An Eppendorf Mastercycler pro was used to anneal the oligonucleotides over a temperature gradient: 95 °C for 5 min, 50 °C for 15 min, 37 °C for 15 min, 10 °C for 5 min, and finally 4 °C for 2 min.

A standard ethanol precipitation procedure was used to precipitate the DNA from the duplex buffer. Everything was carried out in a cold room (~4 °C). An equal volume of 5 M ammonium acetate was added to the DNA solution and mixed. 2.5 volumes of ice cold 100% ethanol (Fisher) was added, mixed well, and placed on ice. After 20 minutes, the samples were placed in Savant SFA13K microcentruge and spun at 13,000 g for 15 min. The supernatant was decanted and 1 mL of 70% ethanol was added and mixed. Samples were briefly spun, supernatant was decanted, and the resulting pellet was allowed to air dry at 4 °C for 4-12 hours. The DNA pellet was resuspended in PBS to a final concentration of 1000 μM.

Polyacrylamide gel electrophoresis (PAGE) was used to help visualize the DNA to confirm that it was annealed. DNA was combined with glycerol and loaded onto the gel. A blank lane containing a standard blue running dye was used to track the progress of the DNA down the gel. On a 20% polyacrylamide gel, DS DNA and nicked DNA ran higher than SS DNA. After the gel electrophoresis was complete, it was imaged with a Biospectrum UVP imager equipped with VisionWorksLS6 software. A UVP VISI Blue converter plate was placed over the gel and used in conjunction with the built-in Syber Safe (485-655 nm) filter and UV transilluminator to visualize the DNA on the gel.

5.1.2.2 Gel-based Stability Assays (Chapter 4.2)

Both types of assembled DNA, nicked and DS, were used. Ciprofloxacin **72**, moxifloxacin **73**, and DNP-cipro **74** were the agents used to assess DNA stability. 1 nmol of 6-FAM labeled DNA was incubated with increasing concentrations of drug (0, 0.1, 1, 10, max nmol). The maximum concentration of the drug used was determined by the highest stock concentration of the drug in solution and was 33.3 nmol for ciprofloxacin **72**, 100 nmol for moxifloxacin **73**, and 41.4 nmol for DNP-cipro **74**. The DNA was mixed with the different concentrations of drug and allowed to equilibrate for several minutes before it was loaded until a 20% polyacrylamide gel for gel

electrophoresis. 20% polyacrylamide gels were run and visualized as described above. SS DNA was run on the gel as a control to monitor for the presence of SS DNA if the complexes fell apart.

5.1.2.3 UV-based Aggregation Studies (Chapter 4.2)

A procedure similar to one that examined drug-drug interactions in dilute norfloxacin solution was used [23]. A double beam Shimadzu UV-2101PC UV-Vis scanning spectrophotometer was used with two matched quartz cuvettes to measure the absorbance and determine λ_{max} of ciprofloxacin **72**, 2,4-dinitrophenyl ciprofloxacin **74**, and 8-methoxy-2,4-quinazoline dione **60**. Each quinolone-class agent was dissolved in 0.1N NaOH and diluted with PBS. The cuvettes contained either PBS (pH 7.4) or 5 mM $MgCl_2$ in PBS (total cuvette volume was 3 mL). Appropriate amounts were titrated into the cuvettes as the concentration was increased from 0.25 μM to 64 μM. After addition, the samples were mixed and allowed to equilibrate for 2 min. A scan was taken from 200-400 nm (slit width = 1 nm) and the absorbance at the λ_{max} was recorded. A double log plot was obtained to determine if UV absorbance at the maximum showed either a hyper- or hypochromatic effect. Since it did not and linear plots were observed, the results suggested that the molecular species of the quinolone-class agents at all concentrations were monomers.

5.1.2.4 Fluorescence-based DNA Binding (Chapter 4.2)

The binding affinities of ciprofloxacin **72**, moxifloxacin **73**, and DNP-cipro **74** to SS, DS, and nicked DNA were determined by using the innate fluorescence of the fluoroquinolones. Fluorescence of ciprofloxacin **72** (λ_{ex}: 275 nm, λ_{em}: 550 nm), moxifloxacin **73** (λ_{ex}: 289 nm, λ_{em}: 579 nm), and DNP-cipro **74** (λ_{ex}: 275 nm, λ_{em}: 550 nm) was detected using a Perkin Elmer LS-55 spectrofluorimeter (slits ex/em: 3.0/3.0). 1.26 μM stock solutions of fluoroquinolone in PBS or 5 mM $MgCl_2$ PBS were used and 200 μL of 1 μM fluoroquinolone was placed in a 400 μL cuvette to begin the studies. An

initial fluorescence intensity of the fluoroquinolone was determined. DNA was titrated in, thoroughly mixed, and allowed to equilibrate before fluorescence measurements were taken. Additions were continued until the DNA concentration reached 90 μM. In order to keep the fluoroquinolone concentration in the cuvette constant at 1 μM throughout the titrations, the DNA added was a mixture of the respective fluoroquinolone and DNA required to attain the desired concentrations after titration. Data were recorded as the change in fluorescence (ΔF), or the difference in the fluorescence observed at each DNA concentration from the initial fluorescence of the drug and plotted as the concentration of DNA in μM versus the ΔF at the emission wavelength. Data was plotted and analyzed with Sigma Plot software. In a one-binding site model, the Hill equation $[f = (B_{max} \times X^n)/(K_{app} + X^n)]$ where X is the concentration of the DNA, f is ΔF, n is the cooperativity, and K_{app} is the binding constant in μM, was used to determine the K_{app}.

5.1.2.5 Melting Temperature (T_m) Studies (Chapter 4.3)

25-mer oligonucleotides were designed based on the DNA sequence in the Wohlkonig crystal structure (protein data bank 2xkk) [22]. The longer oligonucleotides were chosen in place of the 16-mer oligonucleotides because they had added stability due to their length. The A/T nucleotides at the ends of the DNA sequence in the crystal structure were replaced with G/C nucleotides for better annealing and additional stability. An additional nicked DNA (G-T nick) oligonucleotide was designed in order to evaluate if there was a nick-site specific effect that would be observed. The duplexed DNA (nicked DNA with A-T nick site, nicked DNA with G-T nick site, and DS DNA) was purchased and assembled by Integrated DNA Technologies (Coralville, IA).

General, previously reported procedure insights on the analysis of melting temperature curves were incorporated into experimental design [79]. A double beam Shimadzu UV-2101PC UV-Vis scanning spectrophotometer (slit width 0.8 nm) connected to a Shimadzu CPS temperature controller was used with two matched 600 μL

quartz cuvettes to measure the absorbance of DNA at 280 nm. 280 nm was chosen instead of 260 nm because it showed the largest change in absorbance for the small 25-mer oligonucleotides. The reference cuvette contained a 1 μM solution of drug, while the sample cuvette contained a solution of 1 μM drug and either 20 μM DNA or 1 μM DNA. The cuvettes were zeroed when they each contained the 1 μM solution of drug so that only the absorbance of the DNA would be read by the instrument. Drugs used were with obtained through commercial sources (ciprofloxacin and moxifloxacin) or synthesized as described (**29** HS-I-303, **50** HS-IIa-239, **52** HS-IIa-101, and **57** UIJR-1-048). All drugs were incubated with all DNA types (two nicked DNAs and DS DNA). Temperature was increased 2.5 °C over a temperature range of 20-60°C and held constant for 7 min before absorbance readings were taken. Each experiment was run in triplicate. Data was plotted and analyzed with GraphPad Prism5 software to determine the inflection point of the denaturation curve or melting temperature (T_m). GraphPad Prism5 was also used to run statistical analysis that consisted of one way ANOVAs with Tukey post analysis pairwise comparisons within DNA types.

5.2 Synthesis of C-8/C-5 fluoroquinolone derivatives for lethality studies (Chapter 3.1)

5.2.1 Preparation of 2,4,5-trifluorobenzamide (**1**, HS-I-277)

Oxalyl chloride (Alfa-Aesar, 5.8 mL, 68.2 mmol) was added to a stirred solution of 2,4,5-trifluorobenzoic acid (Oakwood Products, Inc, 10 gm 56.8 mmol) in dichloromethane (100 mL) at room temperature, followed by a dropwise addition of *N,N*-dimethylformamide (Acros, 0.45 mL, 5.7 mmol). After 90 minutes, the reaction mixture was concentrated *in vacuo*, dissolved in dichloromethane (100 mL), and cooled to 0 °C. Ammonium hydroxide (Fisher, 40 mL, 600 mmol) was added and the reaction was stirred for two hours. The product was extracted in the organic layer, washed with dichloromethane (100 mL), ethyl acetate (150 mL), and water (100 mL), dried over

sodium sulfate, and concentrated *in vacuo*. The resulting solid collected via filtration after recrystallization with hexanes:ethyl acetate (9:1, 50 mL) to yield **1** (8.41 mg, 85%). Spectral data were consistent with published literature values [81].

5.2.2 Preparation of 2,4,5-trifluoro-3-methylbenzamide

(**1 m.a.**, HS-I-101)

Benzamide **1** (0.724 g, 4.19 mmol) was added to dry THF (15 mL) and cooled to -78 °C while stirring. Lithium bis(trimethylsilyl)amide (Aldrich, 1.0M/THF, 20 mL) was added dropwise over 20 min. After stirring at 0 °C for 3.5 hours, iodomethane (Acros, 0.6 mL, 9.6 mmol) was added. The reaction mixture was stirred for three hours and quenched with aqueous hydrochloric acid (1 N, 30 mL). The product was extracted with ethyl acetate (30 mL), washed with sodium bisulfite (625 mg/10 mL, 2 x 30 mL) and water (30 mL), dried over sodium sulfate, and concentrated *in vacuo*. Recrystallization (hexanes:ethyl acetate 9:1) afforded **1 m.a.** (0.44 g, 78.7%). Spectral data were consistent with published literature values [82].

5.2.3 Preparation of 2,4,5-trifluoro-3-methyl benzoic acid

(**2**, HS-I-229)

A mixture of **1 m.a.** (1.275 g, 6.741 mmol) in sulfuric acid (10 mL, 18N) was heated to 100-110 °C while stirring for three hours. After cooling, ice-water (10 mL) was added to the reaction mixture and the resulting precipitate was collected via filtration. The collected solid was recrystallized from hot hexanes to afford **2** (76%). Spectral data were consistent with published literature [82, 83].

5.2.4 Preparation of 3-oxo-3-(2,4,5-trifluoro-3-methyl-
phenyl)-propionic acid ethyl ester (**10**, HS-I-143)

A procedure similar to that for the preparation of 3-oxo-3-(2,4,5-trifluorophenyl)-propionic acid ethyl ester was used [84]. Oxalyl chloride (Alfa Aesar, 0.4 mL, 4.8 mmol)

and *N,N*-dimethyl formamide (Acros, 0.03 mL, 0.4 mmol) were added to a stirring

mixture of **2** (0.76 g, 4 mmol) and dichloromethane (20 mL, dry) under argon atmosphere

for 90 minutes. The solution was concentrated *in vacuo*. The resulting acid chloride was

twice dissolved in dichloromethane and concentrated *in vacuo*.

Ethyl potassium malonate (Acros, 1.40g, 8.216 mmol) and anhydrous magnesium

chloride (Aldrich, 1.03 g, 10.8 mmol) were stirred at 0 °C for 15 minutes in anhydrous

acetonitrile (Aldrich, 20 mL), followed by the addition of triethylamine (Aldrich, 1.12

mL, 8.06 mmol) and continued stirring at room temperature for three hours. It was

cooled to 0 °C. The previously generated acid chloride was dissolved in dichloromethane

(1.5 mL) and added dropwise to the stirring malonate solution. The reaction was warmed

to room temperature and allowed to age for 20 hours, upon which time it was

concentrated *in vacuo*. It was dissolved in toluene (40 mL), concentrated *in vacuo*, re-

dissolved in toluene (20 mL), and stirred at 0 °C while aqueous hydrochloric acid (4M,

24 mL) was added dropwise. The organic layer was extracted, washed with aqueous HCl

(4 M, 2 x 24 mL) and water (2 x 20 mL), dried over sodium sulfate, and concentrated *in

vacuo* to give a mixture of keto and enol tautomers (4:1) of **10** as a pale yellow oil

(79.4%). ^{1}H NMR (300 MHz, CDCl$_3$) keto tautomer δ = 7.64 (m, 1H), 4.23 (q, *J* = 7.1

Hz, 2H), 3.96 (d, *J* = 4 Hz, 2H), 2.29 (m, 3H), 1.28 (t, *J* = 7.1 Hz, 3H); enol tautomer δ =

12.71 (s, 1H), 7.61 (m, 1H), 5.84 (s, 1H), 4.28 (q, *J* = 7.1 Hz, 2H), 2.27 (m, 3H), 1.35 (t,

J = 7.1 Hz, 3H). ^{19}F NMR (282 MHz CDCl$_3$) keto tautomer δ = -114.48, -127.00, -

140.66; enol tautomer δ = -115.47, -132.57, -141.98.

5.2.5 Preparation of 1-cyclopropyl-6,7-difluoro-8-methyl-

4-oxo-1,4-dihydro-quinoline-3-carboxylic acid ethyl ester

(**13 e.**, HS-I-147)

Previously prepared **10** (2 mmol), acetic anhydride (Fisher, 0.54 mL, 5.712

mmol), and triethyl orthoformate (Aldrich, 0.48 mL, 2.88 mmol) were heated to 115 °C

and refluxed for 4.5 hours, cooled, concentrated *in vacuo*, and re-dissolved in DMSO (5 mL). Cyclopropylamine (Acros, 0.35 mL, 4.96 mmol) was added dropwise as the reaction mixture was cooled to 10 °C. An additional portion of DMSO (5 mL) was added and the reaction mixture was stirred at room temperature for 20 hours. The mixture was treated with potassium carbonate (Acros, 1.13 g, 8.22 mmol) and heated to 95-100 °C for 2 hours. After cooling, water (40 mL) was added. The resulting precipitate was filtered and dried to yield **13 e.** (76.6%). Spectral data were consistent with published literature values [85].

<div align="center">

5.2.6 Preparation of 1-cyclopropyl-6,7-difluoro-8-methyl-

4-oxo-1,4-dihydro-quinoline-3-carboxylic acid (**13**,

HS-I-297)

</div>

A mixture of aqueous potassium hydroxide (10%, 150 mL) and **13 e.** (1.5 g, 4.88 mmol) were stirred at room temperature for 26 hours. The mixture was chilled on ice as concentrated hydrochloric acid was added dropwise until the pH became acidic and the product precipitated. The product precipitate was collected and dried to yield **13** (93%). Spectral data were consistent with published literature values [85].

<div align="center">

5.2.7 Preparation of 1-cyclopropyl-6,7-difluoro-1,4-

dihydro-8-methyl-4-oxo-quinoline-3-carboxylic acid

B(OCOCH$_3$)$_2$ chelate (**13 b.e.**, HS-I-301)

</div>

Boric acid (Fisher, 0.34 g, 5.34 mmol) was added portionwise to acetic anhydride (Aldrich, 12.14 mL) at 100 °C during one hour. **13** (1.25 g, 4.47 mmol) was added to the clear solution, and the mixture was heated to 100 °C for one hour. The reaction mixture was concentrated *in vacuo*, diisopropyl ether (Fisher, 25 mL) was added, and a whitish tan precipitate formed. The precipitate was collected and dried to yield the borate ester **13 b.e.** (95%). Spectral data were consistent with published literature values [85].

5.2.8 Preparation of 5-nitro-1-cyclopropyl-6,7-difluoro-8-

methoxy-4-oxo-1,4-dihydroquinoline carboxylic acid (**16**,

HS-IIa-127)

Potassium nitrate (Acros, 24.1 mg, 2.38 mmol) was added to a chilled mixture of

1-cyclopropyl-6,7-difluoro-8-methoxy-4-oxo-3-quinoline carboxylic acid (3B Scientific,

500 mg, 1.69 mmol) and sulfuric acid (Fisher, concentrated, 5 mL). After one hour, the

reaction mixture was added to water (25 mL), a precipitate formed and was collected via

filtration. After recrystallization from dichloromethane:methanol (1:1), the desired

product **16** was obtained (74%). Spectral data were consistent with published literature

values [43].

5.2.9 Preparation of 5-amino-1-cyclopropyl-6,7,-difluoro-

8-methoxy-4-oxo-1,4-dihydroquinoline carboxylic acid

(**17**, HS-IIa-129)

A mixture of **16** (300 mg, 0.88 mmol) and a catalytic amount of palladium on

carbon (Aldrich, 10%) was stirred in a mixture of ethanol and *N,N*-dimethyl formamide

(4:1, 8 mL) under hydrogen gas for 6 hours. The palladium on carbon was filtered off.

The filtrate was washed with chloroform:methanol:ammonium hydroxide (10:10:3),

concentrated *in vacuo*, and recrystallized from chloroform:methanol:ammonium

hydroxide (20:6:1) to yield **17** (67%). Spectral data were consistent with published

literature values [43].

5.2.10 Preparation of (*S*)-9,10-difluoro-3-methyl-8-nitro-7-

oxo-3,7-dihydro-2*H*-[1,4]oxazino[2,3,4-*ij*]quinolone-6-

carboxylic acid (**18**, HS-IIa-187)

A procedure similar to that for the synthesis of **16** was used [43]. Potassium

nitrate (Acros, 51 mg, 0.501 mmol) was added to a chilled mixture of (*S*)-(-)-9,10-

difluoro-2,3-dihydro-3-methyl-7-oxo-7H-pyrido[1,2,3-de]-[1.4]benzoxazine-6-carboxylic

acid (Aldrich, 96.4 mg, 0.3556 mmol) and sulfuric acid (Fisher, concentrated, 1 mL).
After one hour, the reaction mixture was added to water (5 mL), a precipitate formed and
was collected via filtration. After recrystallization from dichloromethane:methanol (1:1),
the desired product **18** was obtained (45%). While previously reported, spectral data
were not provided [86, 87]. ^{1}H NMR (300 MHz, DMSO-d_6) δ = 9.16 (s, 1H), 5.08 (m,
1H), 4.77 d, J = 11.2 Hz, 1H), 4.51 (d, J = 11.2 Hz, 1H), 1.46 (d, J = 5.5 Hz, 3H). ^{19}F
NMR (282 MHz, DMSO-d_6) δ = -149.7 (m, 1F), -148.2 (m, 1F). LRMS (ESI) calcd for
(M+H$^+$) 327.05, found 326.98.

<div style="text-align:center">

5.2.11 Preparation of (*S*)-8-amino-9,10-difluoro-3-methyl-

7-oxo-3,7-dihydro-2*H*-[1,4]oxazino[2,3,4-*ij*]quinolone-6-

carboxylic acid (**19**, HS-IIa-189)

</div>

A mixture of **18** (50 mg, 0.153 mmol) and a catalytic amount of palladium on
carbon (Aldrich, 10%) was stirred in a mixture of ethanol and *N,N*-dimethyl formamide
(4:1, 1 mL) under hydrogen gas for 6 hours. The palladium on carbon was filtered off.
The filtrate was washed with chloroform:methanol:ammonium hydroxide (10:10:3),
concentrated *in vacuo*, and recrystallized from chloroform:methanol:ammonium
hydroxide (20:6:1) to yield **19** (30%). While previously reported, spectral data were not
provided [86]. ^{1}H NMR (300 MHz, DMSO-d_6) δ = 8.90 (s, 1H), 4.88 (m, 1H), 4.45 (d, J
= 10.6 Hz, 1H), 4.21 (d, J = 1.6 Hz, 1H), 1.40 (d, J = 6.4 Hz, 3H). ^{19}F NMR (282 MHz,
DMSO-d_6) δ = -162.75 (m, 1F), -149.85 (m, 1F). LRMS (ESI) calcd for (M+H$^+$) 297.07,
found 297.04.

<div style="text-align:center">

5.2.12 Preparation of (*S*)-7-(3-aminomethyl-pyrrolidin-1-

yl)-1-cyclopropyl-6-fluoro-8-4-oxo-1,4-dihydro-quinoline-

3-carboxylic acid (**24**, HS-IIIa-35)

</div>

A mixture of 1-cyclopropyl-6,7-difluoro-1,4-dihydro-4-oxo-quinoline-3-
carboxylic acid B(OCOCH$_3$)$_2$ chelate (synthesized by another researcher utilizing

methods similar to the synthesis of **13 b.e.**) (15 mg, 0.0366 mmol), (*R*)-3-N-Boc-aminomethyl pyrrolidine (Asta Tech, Inc., 22 mg, 0.1099 mmol), and triethylamine (Fisher, 20 μL) in DMSO (anhydrous, 0.3 mL) was heated to 90 °C and stirred for one hour. Aqueous sodium hydroxide (3%, 1 mL) was added and allowed to stir for two hours. The resulting product was purified as the di-trifluoroacetate salt by semipreparative HPLC. Fractions of **24** were combined and concentrated *in vacuo* to remove acetonitrile and trifluoroacetic acid, followed by lyophilization (92%). While it was previously reported in literature [88], no spectral data were provided. ^{1}H NMR (300 MHz, DMSO-d$_6$) δ = 15.506 (s, 1H), 8.58 (s, 1H), 7.93 (br m, 3H), 7.81 (d, *J* = 14.2 Hz, 1H), 7.06 (d, *J* = 5.8 Hz, 1H), 3.81-3.59 (m, 4H), 3.44 (m, 1H), 2.99 (m, 2H), 2.60 (m, 1H), 2.18 (m, 1H), 1.82 (m, 1H), 1.30 (m, 2H), 1.16 (m, 2H). ^{19}F NMR (282 MHz, DMSO-d$_6$) δ = -127.09. LRMS (ESI) calcd for (M+H$^+$) 346.16, found 346.21.

5.2.13 Preparation of 1-cyclopropyl-7-(4-ethylpiperazin-1-yl)-6-fluoro-4-oxo-1,4-dihydroquinoline-3-carboxylic acid (**25**, HS-IIa-165)

25 was prepared similarly as **26** with N-ethyl piperazine (TCI America, 0.04 mL, 0.305 mmol), substituting 1-cyclopropyl-6,7-difluoro-1,4-dihydro-4-oxo-quinoline-3-carboxylic acid B(OCOCH$_3$)$_2$ chelate (synthesized by another researcher utilizing methods similar to the synthesis of **13 b.e.**) (50 mg, 0.122 mmol) for 1-ethyl-6,7-difluoro-1,4-dihydro-4-oxo-quinoline-3-carboxylic acid B(OCOCH$_3$)$_2$ chelate. **25** was purified as the di-trifluoroacetate salt by semi-preparative HPLC (74%). While it was previously reported [89], no spectral data were provided. ^{1}H NMR (300 MHz, DMSO-d$_6$) δ = 15.13 (s, 1H), 10.11 (br s, 1H), 8.69 (s, 1H), 7.98 (d, J = 12.8 Hz, 1H), 7.62 (d, J = 7.7 Hz, 1H), 3.86 (m, 3H), 3.64 (m, 2H), 3.27 (m, 6H), 1.26 (m, 7H). ^{19}F NMR (282 MHz, DMSO-d$_6$) δ = -121.85. LRMS (ESI) calcd for (M+H$^+$) 360.17, found 360.15.

5.2.14 Preparation of 1-ethyl-7-(4ethylpiperazin-1-yl)-6-fluoro-4-oxo-1,4-dihydroquinoline-3-carboxylic acid (**26**, HS-IIa-161)

N-ethyl piperazine (TCI America, 0.03 mL, 0.2323 mmol) and 1-ethyl-6,7-difluoro-1,4-dihydro-4-oxo-quinoline-3-carboxylic acid $B(OCOCH_3)_2$ chelate (synthesized by another researcher utilizing methods similar to the synthesis of **13 b.e.**) (36.9 mg, 0.0929 mmol) were added to DMSO (0.2 mL), stirred at room temperature for one hour, and heated to 60 °C for one hour. Aqueous sodium hydroxide (1 mL, 3%) was added and the mixture was stirred for an additional hour. **26** was purified as the di-trifluoroacetate salt by semi-preparative HPLC (37%). While it was previously reported [90], no spectral data were provided. ^{1}H NMR (300 MHz, DMSO-d_6) δ = 15.27 (s, 1H), 9.77 (br s, 1H), 9.00 (s, 1H), 8.00 (d, J = 13 Hz, 1H), 7.27 (d, J = 6.8 Hz, 1H), 4.68 (q, J = 6.8 Hz, 2H), 3.90 (m, 2H), 3.63 (m, 2H), 3.27 (m, 6H), 1.42 (t, J = 6.8 Hz, 3H), 1.26 (t, J = 6.8 Hz, 3H). ^{19}F NMR (282 MHz, DMSO-d_6) δ = -121.68. LRMS (ESI) calcd for (M+H$^+$) 348.17, found 348.18.

5.2.15 Preparation of 7-((*S*)-3-(aminomethyl)pyrrolidin-1-yl)-6,8-difluoro-1-(2-fluorocyclopropyl)-4-oxo-1,4-dihydroquinoline-3-carboxylic acid (**27**, HS-IIIa-39)

27 was prepared similarly as **28**, substituting (*R*)-3-N-Boc-aminomethyl pyrrolidine (AstaTech Inc., 24.9 mg, 0.1245 mmol) for N-ethyl piperazine and adding concentrated trifluoroacetic acid (1 mL) and allowing the reaction to age for one hour at room temperature after heating. **27** was purified as the trifluoroacetate salt by semi-preparative HPLC (80%). ^{1}H NMR (300 MHz, DMSO-d_6) δ = 14.87 (s, 1H), 8.67 (m, 1H), 7.93 (br s, 3H), 7.73 (d, J = 13.7 Hz, 1H), 5.07 (d, J = 65 Hz, 1H), 4.07 (m, 1H), 3.79 (m, 3H), 3.58 (m, 1H), 2.97 (m, 2H), 2.11 (m, 1H), 1.94-1.56 (m, 3H). ^{19}F NMR

(282 MHz, DMSO-d$_6$) δ = -120.35, -133.11, -219.56. LRMS (ESI) calcd for (M+H$^+$) 382.14, found 382.19.

5.2.16 Preparation of 7-(4-ethylpiperazin-1-yl)-6,8-difluoro-1-(2-fluorocyclopropyl)-4-oxo-1,4,-dihydroquinoline-3-carboxylic acid (**28**, HS-IIa-181)

N-ethyl piperazine (TCI America, 0.04 mL, 0.332 mmol), triethylamine (Fisher, 0.020 mL), and 6,7,8-trifluoro-1-(2-fluoro-cyclopropyl)-4-oxo-1,4-dihydroquinoline-3-carboxylic acid (Chem Collect, 40 mg, 0.132 mmol) were added to DMSO (0.4 mL), stirred and heated to 90 °C for one hour. **28** was purified as the di-trifluoroacetate salt by semi-preparative HPLC (98%). ^{1}H NMR (300 MHz, DMSO-d$_6$) δ = 14.54 (br s, 1H), 9.92 (br s, 1H), 8.77 (s, 1H), 7.90 (dd, J = 11.8 Hz, J = 1.8 Hz, 1H), 5.11 (dm, J = 3.1 Hz, J = 65 Hz, 1H), 4.12 (m, 1H), 3.63 (m, 6H), 3.20 (m, 4H), 1.94 (dm, J = 26.5 Hz, 1H), 1.73 (dm, 1H), 1.31 (t, J = 7.1 Hz, 3H). ^{19}F NMR (282 MHz, DMSO-d$_6$) δ = -119.32 (1F), -126.20 (1F), -220.01 (1F). LRMS (ESI) calcd for (M+H$^+$) 396.16, found 396.13.

5.2.17 Preparation of (*S*)-7-(3-aminomethyl-pyrrolidin-1-yl)-1-cyclopropyl-6-fluoro-8-methyl-4-oxo-1,4-dihydro-quinoline-3-carboxylic acid (**29**, HS-I-303)

A mixture of **13 b.e.** (50 mg, 0.1225 mmol) and (*R*)-3-N-Boc-aminomethyl pyrrolidine (AstaTech Inc., 44.1 mg, 0.3675 mmol) in DMSO (anhydrous, 0.5 mL) was stirred at 100°C for 21 hours. Aqueous sodium hydroxide (3%, 0.8 mL) was added after the mixture was removed from heat and stirred for three hours. After three hours, trifluoroacetic acid (conc., 1 mL) was added and stirred overnight. The product was purified as the di-trifluoroacetate salt by semi-preparative HPLC. Fractions of **29** were combined and concentrated *in vacuo* to remove acetonitrile and trifluoroacetic acid, followed by lyophilization (31% yield). Previous synthesis of **29** does not contain spectral data [85]. ^{1}H NMR (300 MHz, DMSO-d$_6$) δ = 15.10 (s, 1H), 8.80 (s, 1H), 7.88

(br s, 3H), 7.73 (d, 1H), 4.33 (m, 1H), 3.56 (m, 4H), 3.39 (m, 1H), 2.97 (m, 2H), 2.57 (s, 3H), 2.15 (m, 1H), 1.75 (m, 1H), 1.19 (m, 2H), 0.88 (m, 2H). ^{19}F NMR (282 MHz, DMSO-d$_6$) δ = -122.2. LRMS (ESI) calcd for (M+H$^+$) 360.17, found 360.10.

5.2.18 Preparation of 1-cyclopropyl-6-fluoro-8-methyl-7-
(octahydro-pyrrolo[3,4-*b*]pyridine-6-yl)-4-oxo-1,4-dihydro-
quinoline-3-carboxylic acid (**30**, HS-IIa-45)

30 was prepared similarly as **29** from **13 b.e.**, substituting *cis*-octahydropyrrolo[3,4b]pyridine (3B Scientific, 27.8 mg, 0.3675 mmol) for (*R*)-3-N-Boc-aminomethyl pyrrolidine. Consequently, trifluoroacetic acid was not added to remove the Boc protecting group. **30** was purified as the di-trifluoroacetate salt by semi-preparative HPLC (16%). While it was previously reported in a patent [91], no spectral data were provided. ^{1}H NMR (300 MHz, DMSO-d$_6$) δ = 15.11 (br s, 1H), 9.34 (m, 1H), 8.79 (s, 1H), 8.56 (m, 1H), 7.72 (d, *J* = 13.4 Hz, 1H), 4.33 (m, 1H), 4.07 (m, 1H), 3.93 (m, 1H), 3.72 (m, 1H), 3.51 (m, 2H), 3.25 (m, 1H), 2.91 (m, 1H), 2.71 (m, 1H), 2.62 (s, 3H), 1.73 (m, 4H), 1.20 (m, 1H), 0.94 (m, 1H), 0.81 (m, 1H). ^{19}F NMR (282 MHz, DMSO-d$_6$) δ = -121.67. LRMS (ESI) calcd for (M+H$^+$) 386.19, found 386.21.

5.2.19 Preparation of 1-cyclopropyl-7-(4-ethylpiperazin-1-
yl)-6-fluoro-8-methyl-4-oxo-1,4-dihydroquinoline-3-
carboxylic acid (**31**, HS-IIa-119)

31 was prepared similarly as **29** from **13 b.e.**, substituting N-ethyl piperazine (TCI America, 0.047 mL, 0.3675 mmol) for (*R*)-3-N-Boc-aminomethyl pyrrolidine. Consequently, trifluoroacetic acid was not added to remove the Boc protecting group. **31** was purified as the di-trifluoroacetate salt by semi-preparative HPLC (10%). While it was previously reported in a patent [92], no spectral data were provided. ^{1}H NMR (300 MHz, DMSO-d$_6$) δ = 14.84 (br s, 1H), 9.60 (br s, 1H), 8.86 (s, 1H), 7.86 (d, *J* = 12.6 Hz, 1H), 6.57 (br s, 1H), 4.39 (m, 1H), 3.54 (m, 4H), 3.25 (m, 6H), 2.80 (s, 3H), 1.27 (t, *J* =

7.5 Hz, 3H), 1.19 (m, 2H), 0.91 (m, 2H). ^{19}F NMR (282 MHz, DMSO-d$_6$) δ = -121.74. LRMS (ESI) calcd for (M+H$^+$) 374.19, found 374.17.

5.2.20 Preparation of (*S*)-5-amino-7-(3-

(aminomethyl)pyrrolidin-1-yl)-1-cyclopropyl-6-fluoro-8-

methoxy-4-oxo-1,4-dihydroquinoline-3-carboxylic acid

(**34**, HS-IIIa-41)

34 was prepared similarly as **35** from **17** (10 mg, 0.032 mmol), substituting (*R*)-3-N-Boc-aminomethyl pyrrolidine (AstaTech Inc., 16 mg, 0.08 mmol) for N-ethyl piperazine and adding concentrated trifluoroacetic acid (1 mL) and allowing the reaction to age for one hour at room temperature after heating. **34** was purified as the trifluoroacetate salt by semi-preparative HPLC (74%). ^{1}H NMR (300 MHz, DMSO-d$_6$) δ = 15.05 (br s, 1H), 8.51 (s, 1H), 7.89 (br s, 3H), 7.10 (br s, 2H), 4.02 (m, 1H), 3.65 (m, 3H), 3.46 (m, 1H), 3.41 (s, 3H), 2.96 (m, 2H), 2.45 (m, 1H), 2.09 (m, 1H), 1.72 (m, 1H), 1.11-0.77 (m, 4H). ^{19}F NMR (282 MHz, DMSO-d$_6$) δ = -150.34. LRMS (ESI) calcd for (M+H$^+$) 391.18, found 391.22.

5.2.21 Preparation of 5-amino-1-cyclopropyl-7-(4-

ethylpiperazin-1-yl)-6-fluoro-8-methoxy-4-oxo-1,4-

dihydroquinoline-3-carboxylic acid (**35**, HS-IIa-141)

35 was prepared similarly as **36** with N-ethyl piperazine (TCI America, 0.01 mL, 0.806 mmol), substituting **17** (10 mg, 0.032 mmol) for **16**. **35** was purified as the di-trifluoroacetate salt by semi-preparative HPLC (80%). ^{1}H NMR (300 MHz, DMSO-d$_6$) δ = 14.77 (s, 1H), 9.67 (br s, 1H). 8.57 (s, 1H), 7.29 (m, 2H), 4.07 (m, 1H), 3.61 (s, 3H), 3.55 (m, 4H), 3.36 (m, 2H), 3.09 (m, 4H), 1.27 (t, *J* = 7.3 Hz, 3H), 1.04 (m, 2H), 0.89 (m, 2H). ^{19}F NMR (282 MHz, DMSO-d$_6$) δ = -147.8. LRMS (ESI) calcd for (M+H$^+$) 405.20, found 405.19.

5.2.22 Preparation of 5-nitro-1-cyclopropyl-7-(4-

ethylpiperazin-1-yl)-6-fluoro-8-methoxy-4-oxo-1,4-

dihydroquinoline-3-carboxylic acid (**36**, HS-IIa-143)

N-ethyl piperazine (TCI America, 0.01 mL, 0.0735 mmol) and **16** (10 mg, 0.029 mmol) were added to DMSO (0.2 mL), stirred at room temperature for one hour, and heated to 60 °C for one hour. **36** was purified as the di-trifluoroacetate salt by semi-preparative HPLC (54%). ^{1}H NMR (300 MHz, DMSO-d$_6$) δ = 13.84 (s, 1H), 9.81 (br s, 1H), 8.76 (s, 1H), 4.19 (m, 1H), 3.80 (s, 3H), 3.72 (m, 2H), 3.57 (m, 4H), 3.21 (m, 4H), 1.25 (t, J = 7.3 Hz, 3H), 1.05 (m, 4H). ^{19}F NMR (282 MHz, DMSO-d$_6$) δ = -136.59. LRMS (ESI) calcd for (M+H$^+$) 435.17, found 435.15.

5.2.23 Preparation of (*S*)-8-amino-9-fluoro-3-methyl-10-(4-

methylpiperazin-1-yl)-7-oxo-3,7-dihydro-2*H*-

[1,4]oxazino[2,3,4-*ij*]quinolone-6-carboxylic acid (**37**,

HS-IIa-191, Antofloxacin)

1-methyl piperazine (Acros, 0.01 mL, 0.0844 mmol) and **19** (10 mg, 0.034 mmol) were added to DMSO (0.2 mL) and heated to 90 °C while stirring for three hours. **37** was purified as the di-trifluoroacetate salt by semi-preparative HPLC (80%). While previously reported, spectral data were not provided [86]. ^{1}H NMR (300 MHz, DMSO-d$_6$) δ = 14.96 (br s, 1H), 10.41 (br s, 1H), 8.79 (s, 1H), 6.98 (br s, 2H), 4.80 (m, 1H), 4.42 (d, J = 10.6 Hz, 1H), 4.14 (d, J = 10.6 Hz, 1H), 3.53 (m, 8H), 2.87 (s, 3H), 1.39 (d, J = 6.1, 3H). ^{19}F NMR (282 MHz, DMSO-d$_6$) δ = -148.07. LRMS (ESI) calcd for (M+H$^+$) 377.16, found 377.20.

5.2.24 Preparation of 5-(4-ethylpiperazin-1-yl)-6-fluoro-8-

oxo-3,8-dihydro-4-oxa-1-thia-2a^1-

azacyclopenta[*cd*]phenalene-9-carboxylic acid (**38**,

HS-IIa-183)

38 was prepared similarly as **28**, substituting 5-6-difluoro-8-oxo-3,8-dihydro-4-

oxa-1-thia-2a^1-azacyclopenta[*cd*]phenaliene-9-carboxylic acid (Chem Collect, 40 mg,

0.129 mmol) for 6,7,8-trifluoro-1-(2-fluoro-cyclopropyl)-4-oxo-1,4-dihydroquinoline-3-

carboxylic acid. **38** was purified as the di-trifluoroacetate salt by semi-preparative HPLC

(63%). ^{1}H NMR (300 MHz, DMSO-d$_6$) δ = 15.59 (s, 1H), 9.83 (br s, 1H), 7.67 (m, 1H),

7.64 (d, *J* = 12.8 Hz, 1H), 5.61 (m, 2H), 3.57 (m, 6H), 3.19 (m, 4H), 1.27 (m, 3H). ^{19}F

NMR (282 MHz, DMSO-d$_6$) δ = -119.10. LRMS (ESI) calcd for (M+H$^+$) 404.11, found

404.06.

5.2.25 Preparation of (*S*)-7-(3-(aminomethyl)pyrrolidin-1-

yl)-1-cyclopropyl-6-fluoro-8-methoxy-5-methyl-4-oxo-1,4-

dihydroquinoline-3-carboxylic acid (**39**, HS-IIa-215)

39 was prepared similarly as **40**, substituting (*R*)-3-N-Boc-aminomethyl

pyrrolidine (AstaTech Inc., 30.2 mg, 0.1615 mmol) for N-ethyl piperazine and adding

concentrated trifluoroacetic acid (1 mL) and allowing the reaction to age for one hour at

room temperature after heating. **39** was purified as the trifluoroacetate salt by semi-

preparative HPLC (69%). ^{1}H NMR (300 MHz, DMSO-d$_6$) δ = 15.63 (s, 1H), 8.65 (s,

1H), 7.89 (br s, 3H), 4.13 (m, 1H), 3.67 (m, 3H), 3.48 (m, 3H), 3.46 (m, 2H), 2.96 (m,

2H), 2.68 (d, *J* = 3.4 Hz, 3H), 2.14 (m, 1H), 1.74 (m, 1H), 0.98 (m, 4H). ^{19}F NMR (282

MHz, DMSO-d$_6$) δ = -125.12. LRMS (ESI) calcd for (M+H$^+$) 390.19, found 390.13.

5.2.26 Preparation of 1-cyclopropyl-7-(4-ethylpiperazin-1-yl)-6-fluoro-8-methoxy-5-methyl-4-oxo-1,4-dihydroquinoline-3-carboxylic acid (**40**, HS-IIa-213)

40 was prepared similarly as **28**, substituting 1-cyclopropyl-6-7-difluoro-8-methoxy-5-methyl-4-oxo-1,4-dihydroquinoline-3-carboxylic acid (**15**, 10 mg, 0.0323 mmol) for 6,7,8-trifluoro-1-(2-fluoro-cyclopropyl)-4-oxo-1,4-dihydroquinoline-3-carboxylic acid. **40** was purified as the di-trifluoroacetate salt by semi-preparative HPLC (60%). ^{1}H NMR (300 MHz, DMSO-d$_6$) δ = 15.27 (br s, 1H), 9.23 (br s, 1H), 8.71 (s, 1H), 4.16 (m, 1H), 3.70 (s, 1H), 3.60 (m, 6H), 3.20 (m, 4H), 2.71 (d, J = 2.9 Hz, 3H), 1.27 (t, J = 7.2 Hz, 3H), 1.05 (m, 2H), 0.89 (m, 2H). ^{19}F NMR (282 MHz, DMSO-d$_6$) δ = -124.8. LRMS (ESI) calcd for (M+H$^+$) 404.20, found 404.21.

5.2.27 Preparation of (*S*)-7-(3-(aminomethyl)pyrrolidin-1-yl)-1-cyclopropyl-6-fluoro-5,8-dimethyl-4-oxo-1,4-dihydroquinoline-3-carboxylic acid (**41**, HS-IIa-219)

41 was prepared similarly as **39**, substituting 1-cyclopropyl-6-7-difluoro-8-methyl-5-methyl-4-oxo-1,4-dihydroquinoline-3-carboxylic acid (**14**, 10 mg, 0.034 mmol) for **15** and heating for six hours instead of one hour. **41** was purified as the trifluoroacetate salt by semi-preparative HPLC (76%). ^{1}H NMR (300 MHz, DMSO-d$_6$) δ = 15.56 (br s, 1H), 8.74 (s, 1H), 7.90 (br s, 3H), 4.27 (m, 1H), 3.57 (m, 3H), 3.39 (m, 1H), 2.97 (m, 2H), 2.65 (d, 3H), 2.56 (m, 1H), 2.47 (s, 3H), 2.16 (m, 1H), 1.77 (m, 1H), 1.13 (m, 2H), 0.77 (m, 2H). ^{19}F NMR (282 MHz, DMSO-d$_6$) δ = -126.51. LRMS (ESI) calcd for (M+H$^+$) 374.19, found 374.16.

5.2.28 Preparation of 1-cyclopropyl-7-(4-ethylpiperazin-1-

yl)-6-fluoro-5,8-dimethyl-4-oxo-1,4-dihydroquinoline-3-

carboxylic acid (**42**, HS-IIa-221)

42 was prepared similarly as **40**, substituting **14** (10 mg, 0.034 mmol) for **15** and heating to 100 °C for 24 hours. **42** was purified as the di-trifluoroacetate salt by semi-preparative HPLC (17%). ^{1}H NMR (300 MHz, DMSO-d$_6$) δ = 15.26 (br s, 1H), 10.24 (br s, 1H), 8.78 (s, 1H), 4.32 (m, 1H), 3.58 (m, 4H), 3.44 (m, 2H), 3.28-3.17 (m, 4H), 2.68 (m, 6H), 1.28 (t, J = 7.1 Hz, 3H), 1.15 (m, 2H), 0.76 (m, 2H). ^{19}F NMR (282 MHz, DMSO-d$_6$) δ = -126.49. LRMS (ESI) calcd for (M+H$^+$) 388.21, found 388.24.

5.2.29 Preparation of 1-cyclopropyl-6,7-difluoro-1,4-

dihydro-8-methoxy-4-oxo-quinoline-3-carboxylic acid

B(OCOCH$_3$)$_2$ chelate (**62 b.e.**, HS-IIa-89)

62 b.e. was made similarly to **13 b.e.**, substituting 1-cyclo-propyl-6,7-difluoro-1,4-dihydro-8-methoxy-4-oxo-quinoline-3-carboxylic acid (3B Scientific) for **13**. **62 b.e.** was obtained in >95% yield. ^{1}H NMR (300 MHz, CDCl$_3$) δ = 9.24 (s, 1H), 8.13 (t, 1H), 4.40 (m, 1H), 4.22 (d, 3H), 2.06 (s, 6H), 1.40 (m, 4H).

5.2.30 Preparation of Previously Synthesized Compounds

The synthesis of **32** (NG-5-249) and **33** (PD161144), which were included in Chapter 3.1, is described in Chapter 5.4. The remaining compounds included in this study whose synthesis and characterization are not described were synthesized by other researchers in a collaborative effort.

5.3 Synthesis of fluoroquinolones and 2,4-quinazoline

diones for magnesium bridge studies (Chapter 3.2)

5.3.1 Preparation of 1-cyclopropl-6-fluoro-7-(octahydro-

pyrrolo[3,4-*b*]pyridine-6-yl)-4-oxo-1,4-dihydroquinoline-3-

carboxylic acid (**50**, HS-IIa-239)

A mixture of 1-cyclopropyl-6,7-difluoro-1,4-dihydro-4-oxo-quinoline-3-carboxylic acid $B(OCOCH_3)_2$ chelate (synthesized by another researcher utilizing methods similar to the synthesis of **13 b.e.**) (15 mg, 0.0366 mmol), *cis*-octahydropyrrolo[3,4*b*]-pyridine (3B Scientific, 13.9 mg, 0.1099 mmol), and triethylamine (Fisher, 20 µL) in DMSO (anhydrous, 0.4 mL) was heated to 90 °C and stirred for one hour. Aqueous sodium hydroxide (3%, 1 mL) was added and allowed to stir for two hours. The resulting product was purified as the di-trifluoroacetate salt by semipreparative HPLC. Fractions of **50** were combined and concentrated *in vacuo* to remove acetonitrile and trifluoroacetic acid, followed by lyophilization (78%). While it was previously reported in a patent [93], no spectral data were provided. ^{1}H NMR (300 MHz, DMSO-d$_6$) δ = 15.48 (br s, 1H), 9.13 (br m, 1H), 8.61 (s, 1H), 7.86 (d, J = 14.5 Hz, 1H), 7.18 (d, J = 7.2 Hz, 1H), 3.90-4.07 (m, 2H), 3.59-3.81 (m, 4H), 3.24 (m, 1H), 2.96 (m, 1H), 2.75 (m, 1H), 1.66-1.84 (m, 4H), 1.32 (m, 1H), 1.15 (m, 1H). ^{19}F NMR (282 MHz, DMSO-d$_6$) δ = -127.71. LRMS (ESI) calcd for (M+H$^+$) 372.17, found 372.21.

5.3.2 Preparation of 1-cyclopropyl-6-fluoro-8-methoxy-4-

oxo-7-(piperazine-1-yl)-1,4-dihydroquinoline-3-carboxylic

acid (**52**, HS-IIa-101)

A mixture of **62 b.e.** (28.55 mg, 0.0675 mmol) and piperazine (Acros, 14.5 mg, 0.1685 mmol) in DMSO (anhydrous, 0.3 mL) was stirred at room temperature for four hours. Aqueous sodium hydroxide (3%, 0.5 mL) was added and allowed to stir for two hours. The resulting product was purified as the trifluoroacetate salt by semi-preparative

HPLC. Fractions of **52** were combined and concentrated *in vacuo* to remove acetonitrile and trifluoroacetic acid, followed by lyophilization (96%). While it was previously reported in a patent [43], no spectral data were provided. ^{1}H NMR (300 MHz, DMSO-d$_6$) δ = 14.87 (br s, 1H), 8.87 (br s, 1H), 8.74 (s, 1H), 7.82 (d, J = 12 Hz, 1H), 4.17 (m, 1H), 3.81 (s, 3H), 3.51 (m, 4H), 3.28 (m, 4H), 0.98-1.18 (m, 4H). ^{19}F NMR (282 MHz, DMSO-d$_6$) δ = -120.23. LRMS (ESI) calcd for (M+H$^+$) 362.15, found 362.13.

5.3.3 Preparation of 3-amino-1-cyclopropyl-6-fluoro-7-(octahydro-pyrrolo[3,4-*b*]pyridine-6-yl)-quinazoline-2,4(1*H*,3*H*)-dione (**53**, HS-IIa-247)

53 was prepared similarly as **54** from 3-amino-1-cyclopropyl-6,7-difluoro-2,4(1*H*,3*H*)-quinazolinedione (Li-I-195), substituting *cis*-octahydropyrrolo[3,4*b*]pyridine (3B Scientific, 24.9 mg, 0.1975 mmol) for (*R*)-3-N-Boc-aminomethyl pyrrolidine. Consequently, trifluoroacetic acid was not added to remove the Boc protecting group. **53** was purified as the di-trifluoroacetate salt by semi-preparative HPLC (69%). ^{1}H NMR (300 MHz, DMSO-d$_6$) δ = 9.13 (br m, 1H), 8.58 (br m, 1H), 7.54 (d, J = 13.9 Hz, 1H), 6.71 (d, J = 7.5 Hz, 1H), 3.93 (m, 2H), 3.66 (m, 3H), 3.23 (m, 1H), 2.92 (m, 2H), 2.72 (m, 1H), 1.75 (m, 4H), 1.25 (m, 2H), 0.81 (m, 2H). ^{19}F NMR (282 MHz, DMSO-d$_6$) δ = -135.16. LRMS (ESI) calcd for (M+H$^+$) 360.19, found 360.29.

5.3.4 Preparation of (*S*)-3-amino-7-(3-aminomethyl-pyrrolidin-1-yl)-1-cyclopropyl-6-fluoroquinazoline-2,4(1*H*,3*H*)-dione (**54**, HS-IIa-245)

3-amino-1-cyclopropyl-6,7-difluoro-2,4(1*H*,3*H*)-quinazolinedione (Li-II-195, 20 mg, 0.079 mmol), (*R*)-3-N-Boc-aminomethyl pyrrolidine (Asta Tech, Inc., 39.6 mg, 0.1975 mmol), and triethylamine (Fisher, 20 µL) in DMSO (anhydrous, 0.3 mL) were combined and stirred at 80 °C for three hours. Trifluoroacetic acid (concentrated, 1 mL) was added and stirred for one hour. The resulting product was purified as the di-

trifluoroacetate salt by semipreparative HPLC. Fractions of **54** were combined and concentrated *in vacuo* to remove acetonitrile and trifluoroacetic acid, followed by lyophilization (28%). While it was previously reported in literature [94], no spectral data were provided. ^{1}H NMR (300 MHz, DMSO-d$_6$) δ = 7.92 (br s, 3H), 7.52 (d, J = 13.8 Hz, 1H), 6.72 (d, J = 7.5 Hz, 1H), 3.49 (m, 4H), 3.35 (m, 1H), 2.97 (m, 2H), 2.87 (m, 1H), 2.15 (m, 1H), 1.78 (m, 1H), 1.24 (m, 2H), 0.83 (m, 2H). ^{19}F NMR (282 MHz, DMSO-d$_6$) δ = -134.52. LRMS (ESI) calcd for (M+H$^+$) 334.17, found 334.26.

5.3.5 Preparation of 3-amino-1-cyclopropyl-6-fluoro-7-(piperazine-1-yl)-2,4(1*H*,3*H*)-dione (**55**, HS-IIa-249)

55 was prepared similarly as **54** from 3-amino-1-cyclopropyl-6,7-difluoro-2,4(1*H*,3*H*)-quinazolinedione (Li-I-195), substituting piperazine (Acros, 17.0 mg, 0.1975 mmol) for (*R*)-3-N-Boc-aminomethyl pyrrolidine. Consequently, trifluoroacetic acid was not added to remove the Boc protecting group. **55** was purified as the di-trifluoroacetate salt by semi-preparative HPLC (22%). ^{1}H NMR (300 MHz, DMSO-d$_6$) δ = 8.96 (br s, 2H), 7.67 (d, J = 12.5 Hz, 1H), 7.18 (d, J = 7.1 Hz, 1H), 3.43 (m, 4H), 3.32 (m, 4H), 2.97 (m, 1H), 1.25 (m, 2H), 0.84 (m, 2H). ^{19}F NMR (282 MHz, DMSO-d$_6$) δ = -128.47. LRMS (ESI) calcd for (M+H$^+$) 320.15, found 320.14.

5.3.6 Preparation of 3-amino-1-cyclopropyl-6-fluoro-7-(octahydro-pyrrolo[3,4-*b*]pyridine-6-yl)-8-methoxyquinazoline-2,4(1*H*,3*H*)-dione (**59**, HS-IIa-251)

3-amino-1-cyclopropyl-6,7-difluoro-8-methoxy-2,4(1*H*,3*H*)-quinazolinedione (Li-II-209, 20 mg, 0.0706 mmol), *cis*-octahydropyrrolo[3,4*b*]pyridine (3B Scientific, 22.4 mg, 0.1776 mmol), and triethylamine (Fisher, 20 μL) in DMSO (anhydrous, 0.3 mL) were combined and stirred at 80 °C for three hours. The product was purified as the di-trifluoroacetate salt by semi-preparative HPLC. Fractions of **59** were combined and

concentrated *in vacuo* to remove acetonitrile and trifluoroacetic acid, followed by lyophilization (54%). Spectral data were consistent with literature values [95].

5.3.7 Preparation of 3-amino-1-cyclopropyl-6-fluoro-8-methoxy-7-(piperazine-1-yl)-quinazoline-2,4(1*H*,3*H*)-dione (**61**, HS-IIa-253)

61 was prepared similarly as **59** from 3-amino-1-cyclopropyl-6,7-difluoro-8-methoxy-2,4(1*H*,3*H*)-quinazolinedione (Li-II-209), substituting piperazine (Acros, 15.2 mg, 0.1776 mmol) for *cis*-octahydropyrrolo[3,4*b*]pyridine. **61** was purified as the di-trifluoroacetate salt by semi-preparative HPLC (25%). ^{1}H NMR (300 MHz, DMSO-d$_6$) δ = 8.933 (br s, 2H), 7.47 (d, *J* = 11.8 Hz, 1H), 3.69 (s, 3H), 3.46 (m, 4H), 3.27 (m, 5H), 0.96 (m, 2H), 0.58 (m, 2H). ^{19}F NMR (282 MHz, DMSO-d$_6$) δ = -126.29. LRMS (ESI) calcd for (M+H$^+$) 350.16, found 350.24.

5.3.8 Preparation of 1-cyclopropyl-6-fluoro-7-(4-hydroxyphenyl)-8-methyl-4-oxo-1,4-dihydroquinoline-3-carboxylic acid (**67**, HS-IIIa-23)

13 b.e. (300 mg, 0.737 mmol), 4-methoxybenzylamine (Acros, 0.19 mL, 1.4737 mmol), and triethylamine (Fisher, 50 μL) were added to acetonitrile (1.5 mL) and stirred at room temperature for 24 hours. The boric acid anhydride was removed with aqueous sodium hydroxide (3%, 1.5 mL) at room temperature for 4 hours. The reaction mixture was then added to ethyl acetate (20 mL), washed with hydrochloric acid (1N, 3 mL x2) and brine (3 mL x2), dried over sodium sulfate, and concentrated *in vacuo* to yield crude 1-cyclopropyl-6-fluoro-1,4-dihydro-8-methyl-7-[[(4-methoxyphenl)methyl]amino]-4-oxo-3-quinolinecarboxylic acid.

A mixture of trifluoroacetic acid and dichloromethane (5 mL, 1:4) was added to the crude 1-cyclopropyl-6-fluoro-1,4-dihydro-8-methyl-7-[[(4-methoxyphenyl)methyl]amino]-4-oxo-3-quinolinecarboxylic acid and stirred at room

temperature. After 10 hours, the solvent was removed *in vacuo* and washed with dichloromethane to yield crude 7-amino-1-cyclopropyl-6-fluoro-1,4-dihydro-8-methyl-4-oxo-3-quinolinecarboxylic acid (**63**).

A mixture of *t*-butyl nitrite (Alfa Aesar, 392 mg, 3.803 mmol) and copper (II) bromide (Acros, 1.04 g, 4.67 mmol) was heated to 67 $^{\circ}$C prior to the addition of the crude **63** and acetonitrile (1mL). The reaction mixture continued to heat at 67 $^{\circ}$C for 15 minutes. It was extracted with ethyl acetate (20 mL), washed with ammonium chloride (1N, 5 mL x2), hydrochloric acid (1N, 5 mL x2), and brine (5 mL x2), dried over sodium sulfate, and recrystallized with ethyl acetate to yield 7-bromo-1-cyclopropyl-6-fluoro-1,4-dihydro-8-methyl-4-oxo-3-quinolinecarboxylic acid (**65**) (36% yield over five steps).

In a sealed argon-filled flask, potassium carbonate (Acros, 552 mg, 1N), **65** (45 mg, 0.1323 mmol), tetrakis(triphenyl-phosphine) palladium(0) (Aldrich, 15.3 mg, 0.0132 mmol), 4,4,5,5-tetramethyl-2-[4-[[tris(1-methylethyl)silyl]oxy]phenyl-1,3,2-dioxaborolane (synthesized by another researcher, 99.5 mg, 0.2646 mmol), and a mixture of water and dioxane (1:3, degassed, 4mL) were combined and heated to 85 $^{\circ}$C under argon for 18 hours. The product was extracted with ethyl acetate (30 mL), washed with hydrochloric acid (1N, 5 mL x1), water (5 mL x2), and brine (5 mL x2), and dried over sodium sulfate. The protecting group was then hydrolyzed with concentrated hydrochloric acid at room temperature over 36 hours, purified with semi-prep HPLC, and recrystallized from dichloromethane and methanol to yield **67** (5%). ^{1}H NMR (300 MHz, DMSO-d$_6$) δ = 14.76 (s, 1H), 9.80 (s, 1H), 8.88 (s, 1H), 7.91 (d, J = 9.1 Hz, 1H), 7.21 (d, J = 7.8 Hz, 2H), 6.92 (d, J = 8.4, 2H), 4.37 (m, 1H), 2.60 (s, 3H), 1.22 (m, 2H), 1.03 (m, 2H). ^{19}F NMR (282 MHz, DMSO-d$_6$) δ = -113.79. HRMS (ESI) calcd for (M-H$^+$) 352.0989, found 352.0985.

5.3.9 Preparation of 1-cyclopropyl-6-fluoro-7-(4-

hydroxypenyl)-8-methoxy-4-oxo-1,4-dihydroquinoline-3-

carboxylic acid (**68**, HS-IIIa-27)

68 was prepared similarly as HS-IIIa-23, substituting **62 b.e.** for **13 b.e**. 7-bromo-

1-cyclopropyl-6-fluoro-1,4-dihydro-8-methyl-4-oxo-3-quinolinecarboxylic acid (**66**) was

isolated as an intermediate (55% yield over five steps) and **68** was obtained after

undergoing Suzuki coupling with 4,4,5,5-tetramethyl-2-[4-[[tris(1-

methylethyl)silyl]oxy]phenyl-1,3,2-dioxaborolane, deprotection, and recrystallization

(15%). ^{1}H NMR (300 MHz, DMSO-d$_6$) δ = 14.76 (s, 1H), 9.87 (s, 1H), 8.79 (s, 1H), 7.89

(d, J = 9.2 Hz, 1H), 7.37 (d, J = 8.4 Hz, 2H), 6.94 (d, J = 8.4 Hz, 2H), 4.21 (m, 1H), 3.36

(s, 3H), 1.15 (m, 4H). ^{19}F NMR (282 MHz, DMSO-d$_6$) δ = -133.71. HRMS (ESI) calcd

for (M+H$^+$) 370.1087, found 370.1091.

5.3.10 Previously synthesized compounds

The synthesis of several compounds included in Chapter 3.2 was described earlier

in Chapter 3.1 or later in Chapter 5.4. **24** (HS-IIIa-35), **29 (**HS-I-303), and **30 (**HS-IIa-

45) are described in 5.2, while **32 (**NG-5-249) and **60 (**NG-5-207) are described in 5.5.

The remaining compounds included in this study whose synthesis and characterization

are not described were synthesized by other researchers in a collaborative effort.

5.4 Remakes of Previously Reported Compounds

Several compounds were re-synthesized as previously described: **60 (**UING-5-

207, lot HS-IIa-229) [95], **32 (**UING-5-249, lot HS-IIa-77) [95], and **33** (PD161144, lot

HS-IIa-163) [96]. Spectral data on re-made compounds matches the literature reports.

CHAPTER 6 CONCLUSIONS AND FUTURE DIRECTIONS

In order to combat the constant emergence of drug-resistant microorganisms, continued research efforts to develop new fluoroquinolone-class antibiotics are necessary. Improved agents that can effectively and quickly clear drug-resistant infections are vital to patient treatment and public health, but are also important in restricting the emergence of resistance.

The ability of clinically relevant fluoroquinolones and a large panel of fluoroquinolone derivatives with specific modifications at C-8 and C-5 to kill *E. coli* in the presence and absence of ongoing protein synthesis was evaluated. The ability to kill non-growing microorganisms is important with pathogens that are able to enter dormant growth states in their life cycles, such as the causative agents of tuberculosis. In general, the introduction of substituents at C-5 had a negative impact on the ability of the fluoroquinolone to kill in the absence of protein synthesis. However, a set of specific structural features contributed to both the ability of the fluoroquinolone to kill in the absence of protein synthesis and maintain low MIC: a C-7 substituted pyrrolidinyl group, a C-8 chlorine, methoxy, or methyl substituent, and an N-1 cyclopropyl.

Perhaps one of the most interesting findings was that some of clinically relevant fluoroquinolones, *i.e.*moxifloxacin and sitafloxacin, were able to maintain their antimicrobial effect in the absence of ongoing protein synthesis. Thus, these agents could be co-administered with protein synthesis inhibitors in the clinic or be used to treat complex infections in which the pathogens are capable of going into dormant or nongrowing stages in their lifecycles.

Important additions to this study would involve the use of molecular modeling with published ternary complex crystal structures to look for correlations between how a compound interacts with the binding pocket and observed microbiological activity. However, since a crystal structure of a ternary complex consisting of *E. coli* gyrase,

DNA, and fluoroquinolone is not yet available, the select compounds could be evaluated against a species of bacteria in which there is a known DNA-fluoroquinolone-gyrase ternary complex structure and then correlations could be looked for. Alternatively, fluoroquinolones could effectively be docked into the nicked DNA sites in the known crystal structures of *E. coli* gyrase with DNA bound and correlations with the ability of the fluoroquinolone to kill in the absence of protein synthesis could be made.

With regards to structure activity, there is potential for further exploration of the structural requirements for killing in the absence of protein synthesis. While fluoroquinolones with C-5 substituents were generally poor killers, **34**, a compound with a C-5 amine, a C-8 methoxy, and a C-7 aminomethyl pyrrolidinyl substituent, was identified as a lead compound. It is most likely that the specific combination of the C-5 and C-8 substituents were responsible for **34**'s good microbiological activity. A series of compounds with a C-5 amine and different substituents at C-8 would confirm this. Since compounds with either a C-8 methyl, fluorine or chlorine were found to have good killing activity in the absence of protein synthesis, it would be interesting to see if a derivative with C-5 amine in combination with one of these at C-8 would have comparable activity to **34**. Also, perhaps the ability of the C-5 amine to contribute to hydrogen-bonding interactions in the binding pocket was important for the observed microbiological activity. This could be further probed to see if derivatives with other hydrogen bond donating groups at C-5 have different or identical activity profiles. The introduction of a formal positive charge through the placement of a guanidinyl group at C-5 would provide more insights.

As a result of this study, the next steps in order to determine if the identified lead compounds **29** and **34** would make good candidates for novel antibiotics and clinical development would consist of *in vitro* toxicity testing and evaluation of pharmacodynamic profiles. Toxicity testing is important early in fluoroquinolone

development because high toxicity seems to be one of the major deterrents for the continued development of fluoroquinolones showing promising microbiological results.

In the work presented in the second part of Chapter 3, substitutions at C-8 and C-7 in combination with core structure diversification were investigated to determine the specific structural features that allowed 2,4-quinazoline diones and some fluoroquinolones to maintain activity against Ser81 mutants in *B. anthracis* Topo IV. Ser81 of Topo IV is important in forming a magnesium ion-mediated bridge between the fluoroquinolone and the enzyme. The investigation was based on prior work that showing that an 8-methyl-2,4-quinazoline dione was able to maintain DNA cleavage activity against Ser81 mutants, while several clinically relevant fluoroquinolones were not able to [50]. By synthesizing these derivatives and evaluating them against Ser81 mutants, we sought to gain some mechanistic insight into the importance of the magnesium ion-mediated bridge.

2,4-quinazoline diones, regardless of their structure at C-7 or C-8, showed no difference in DNA cleavage activity against the Ser81 mutants. This was expected since the structure of the 2,4-quinazoline diones prevents them from being able to form a magnesium-mediated bridge interaction with the enzyme. The fluoroquinolone derivatives generally lost DNA cleavage activity in the presence of Ser81 mutants, as was previously observed. However, some fluoroquinolones, specifically with C-8 methyl and/or C-7 aminomethyl pyrrolidinyl substituents, maintained or improved DNA cleavage activity against *B. anthracis* Topo IV containing Ser81 mutations.

There are a number of possibilities for why C-8 methyl fluoroquinolones were able to maintain DNA cleavage activity in the presence of a mutation that would eliminate magnesium ion-mediated binding interactions between the drug and enzyme. It is possible that binding contacts other than the magnesium ion-mediated bridge between the drug and the enzyme are important for the binding interactions of the C-8 methyl

fluoroquinolone. It is also possible that the interaction of other fluoroquinolones with magnesium ion prevents the drugs from obtaining an ideal interaction with the enzyme.

Further work in understanding what interactions occur and allows the C-8 methyl fluoroquinolones to be able to uniquely maintain activity against Ser81 mutants needs to be addressed. Molecular modeling and docking may help show different interactions that are occurring with these fluoroquinolones. As investigated in Chapter 4, fluoroquinolone-DNA interactions are another essential component of the ternary complex that forms prior to the observation of microbiological effects. It is important to determine what is unique about the ternary complex formed with the C-8 methyl fluoroquinolones because then other agents that exploit the same binding contacts that allow the drugs to maintain activity against drug resistant mutants can be developed.

Unique CP-115,953 derivatives that were synthesized (**67**-**71**) need to be evaluated for their ability to inhibit both bacterial and eukaryotic type II topoisomerases. To date, CP-115,953 is the only topoisomerase II poison that displays high activity against both of these topoisomerases. **67**-**71** are novel compounds that have never been synthesized before. **67** and **68**, both with larger substituents at C-8 that were found to be ideal structural features for the ability of fluoroquinolones to effectively kill in the absence of protein synthesis and maintain low MIC, may offer similar activity improvements when compared to the parent compound CP-115,953 against the bacterial and eukaryotic type II topoisomerases. **69**-**71** are CP-115,953 analogues that incorporate the 2,4-quinazoline dione core structure instead of the fluoroquinolone core structure and may display novel activity since compounds with the 2,4-quinazoline dione core structure have been shown to have activity against drug-resistant mutations. If this is the case, a new class of topoisomerase II poisons could emerge and result in the development of novel agents that are active against drug-resistant microorganisms.

In the final chapter, interactions between fluoroquinolones and DNA were investigated. Newer generation fluoroquinolones have demonstrated improved

microbiological activity. These structurally unique fluoroquinolones with novel killing mechanisms fluoroquinolones were found to interact with DNA differently than older generation fluoroquinolones. Thus, it is apparent that past observations of how fluoroquinolones interact with DNA cannot be applied to all fluoroquinolones and that each new compound needs to be individually evaluated for how it interacts with DNA.

Further investigations into interactions between fluoroquinolone-class agents and DNA proved to be more problematic than expected, especially those with the 2,4-quinazoline dione. The dione had to be excluded from the direct binding studies because it was not innately fluorescent like the fluoroquinolones. When UV-based binding studies with the dione were attempted, they were unsuccessful because the dione had a weak UV absorbance.

Additionally, as mentioned in Chapter 4, several rounds of optimazations went into the development of the melting temperature studies, both with regard to the size of the DNA oligonucleotide and the instrumentation that would be used for the assay. Several attempts were made to turn the UV-based cuvette assay with the dual beam spectrophotometer into a higher throughput assay. However, either the available plate readers were unable to read UV or unable to control the temperature in the range required to denature the oligonucleotides. Thus, the experiments in Chapter 4.3 focused on answering two distinct questions with the instrumentation that was available even though the experimental process was time consuming.

Since recent ternary complex crystal structures show that fluoroquinolone-DNA interactions are prevalent, future work needs to continue to further probe these interactions. My work has just begun to scratch the surface. A large amount of work published does not present a consistent representation of fluoroquinolone-DNA interactions. Future work could include the investigation of fluoroquinolones and 2,4-quinazoline diones with nicked DNA by ^{1}H or ^{31}P NMR and molecular docking of the compounds to DNA. A large benefit of using ^{1}H NMR is that the 2,4-quinazoline dione

could be included in the assay. Alternatively, circular dichroism could also be used to analyze interactions between fluoroquinolones and diones with nicked DNA, since it is a method that has commonly been used to analyze these interactions. It would also be useful to conduct a more thorough investigation into sequence dependent binding with different types of nicked DNA.

While much of my work focused on fluoroquinolone-DNA interactions, the topoisomerase is a vital component of the ternary complex that needs to be investigated. It is the formation of fluoroquinolone-DNA-topoisomerase ternary complex that causes the ultimate death of microorganisms. Thus, all three components of the ternary complex need to be investigated together to better understand the microbiology that is observed with fluoroquinolones. Enzymatic studies that incorporate all three components, in conjunction with microbiological testing, will be able to provide a more complete perspective on how fluoroquinolones with discrete structural changes affect enzymatic activity.

APPENDIX A. SPECTRAL DATA
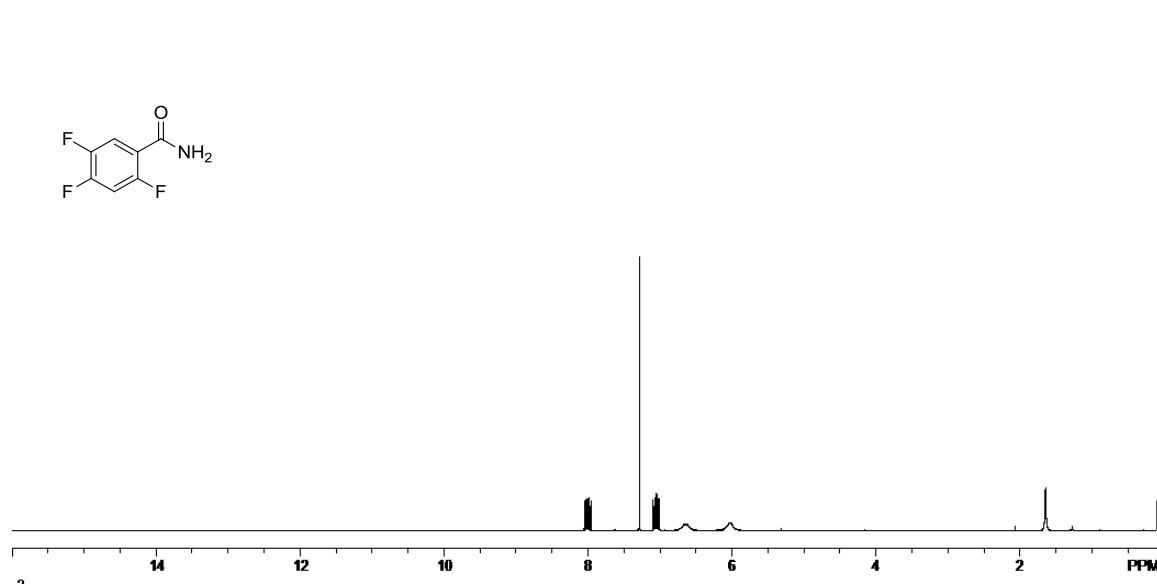
Figure A 1. ^{1}H NMR of **1** (HS-I-277) in CDCl$_3$.
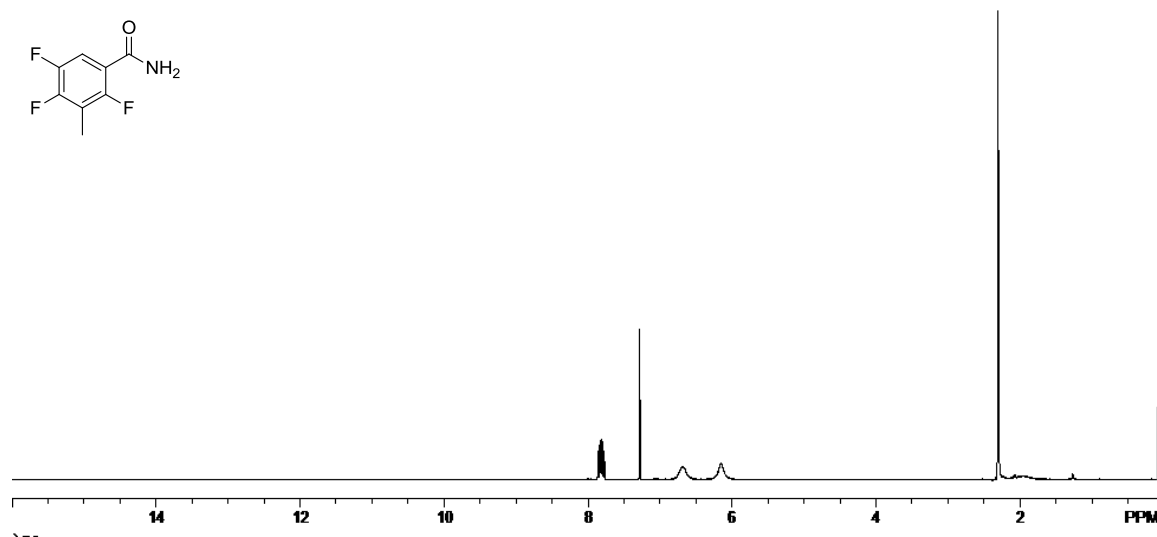
Figure A 2. ^{1}H NMR of **1 m.a.** (HS-I-101) in CDCl$_3$.
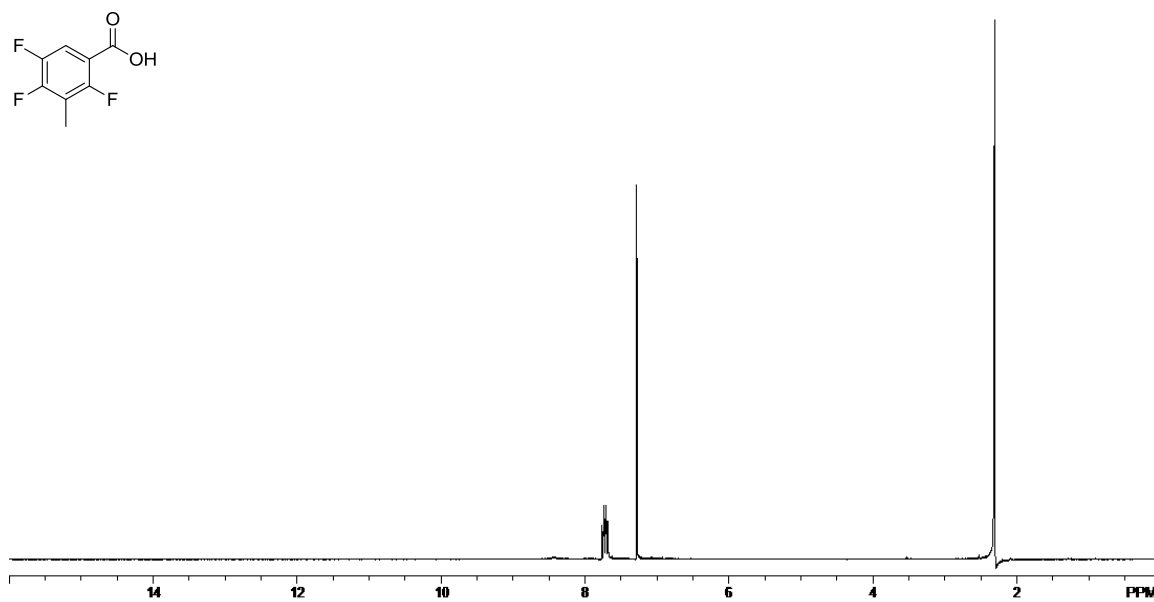
Figure A 3. ^{1}H NMR of **2** (HS-I-229) in CDCl$_3$.
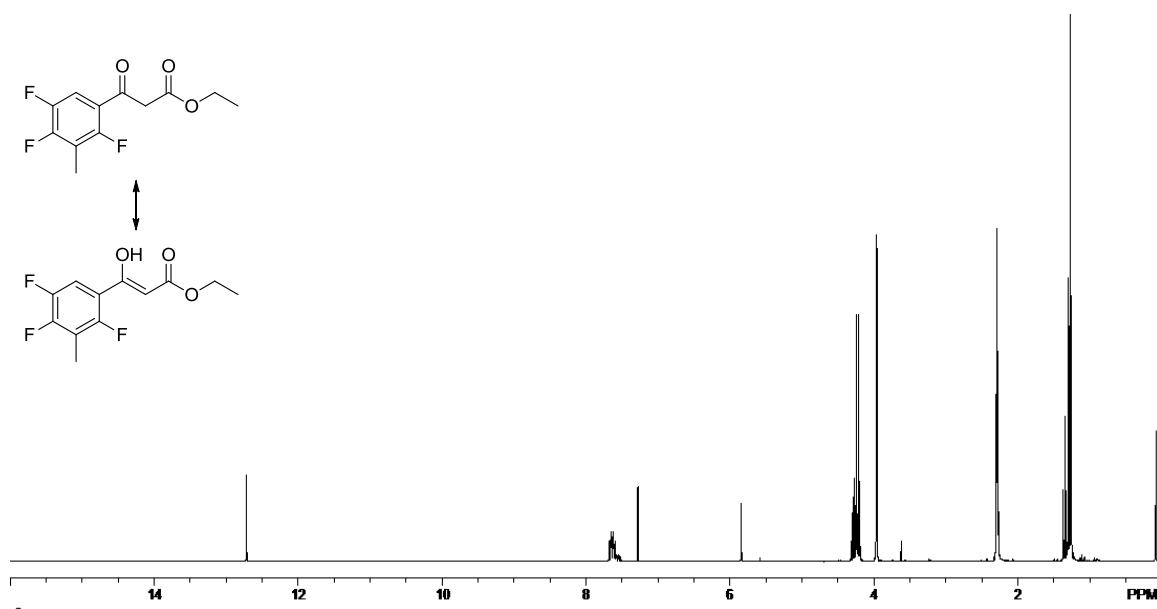
Figure A 4. ^{1}H NMR of **10** (HS-I-143) in CDCl$_3$.
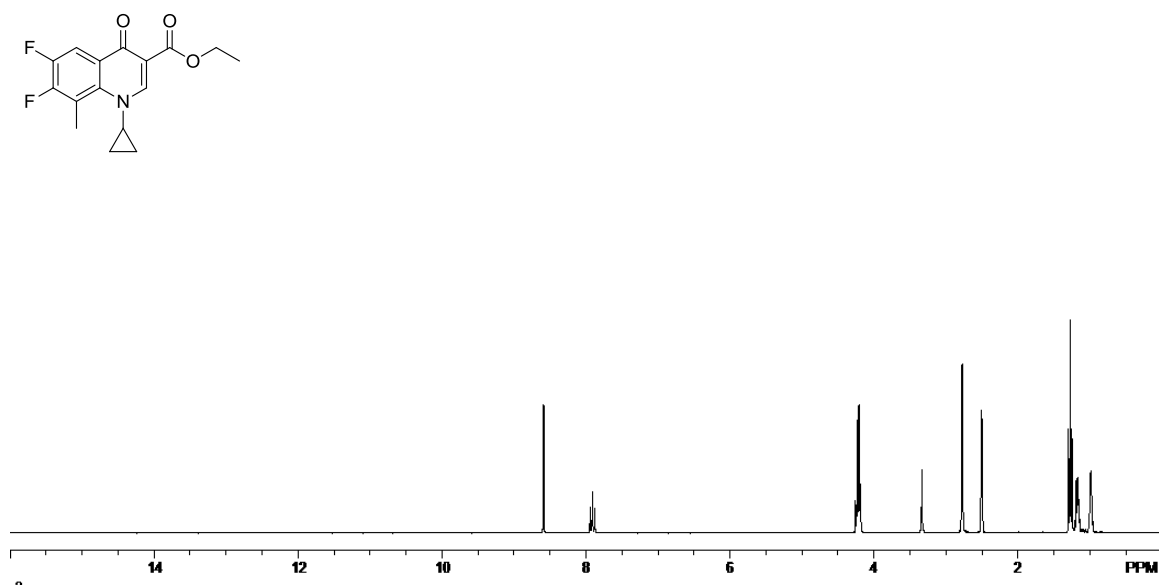
Figure A 5. ^{1}H NMR of **13 e.** (HS-I-147) in DMSO.
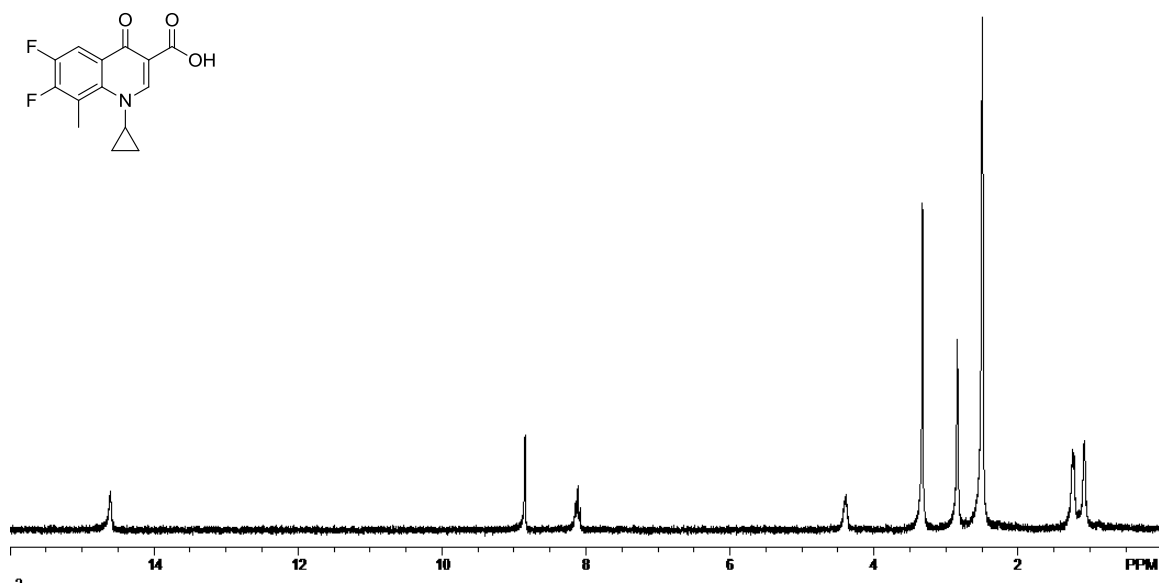
Figure A 6. ^{1}H NMR of **13** (HS-I-297) in DMSO.
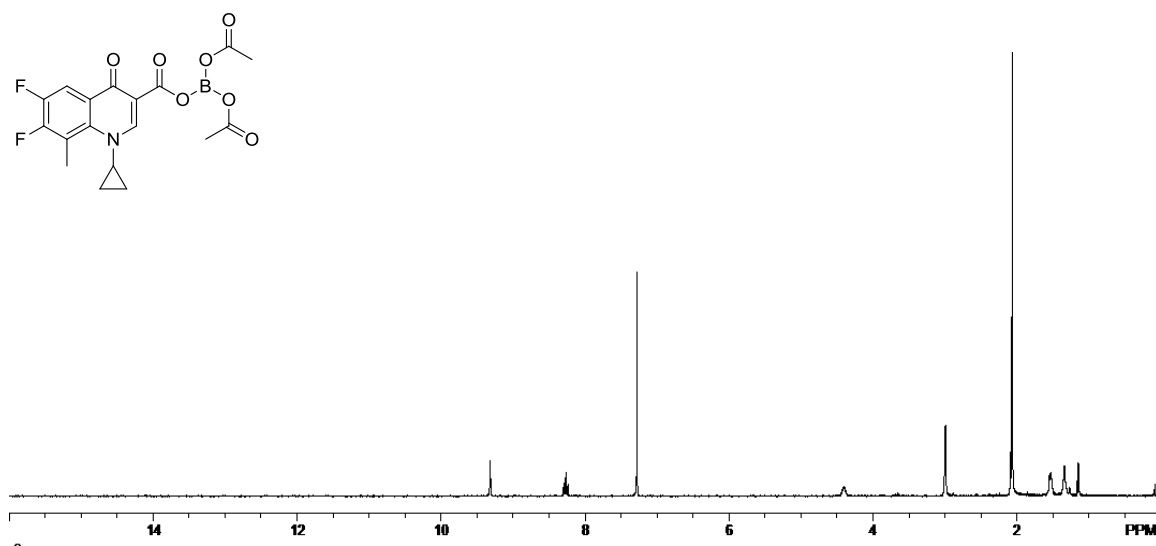
Figure A 7. ^{1}H NMR of **13 b.e.** (HS-I-301) in CDCl$_3$. Residual diisopropyl ether (δ = 1.15, d).
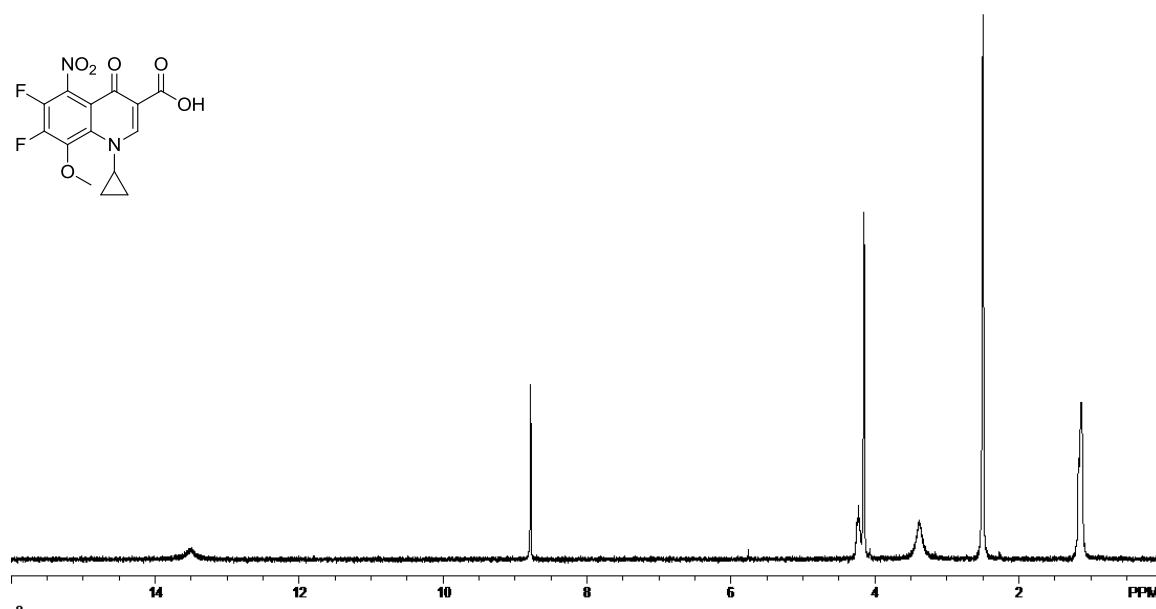
Figure A 8. ^{1}H NMR of **16** (HS-IIa-127) in DMSO.
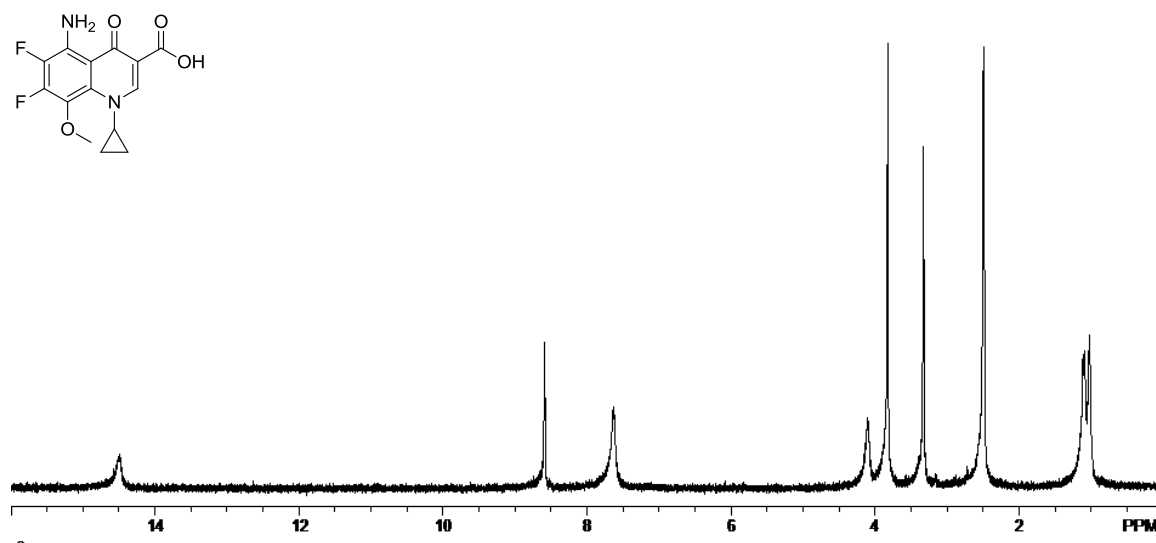
Figure A 9. ^{1}H NMR of **17** (HS-IIa-129) in DMSO.
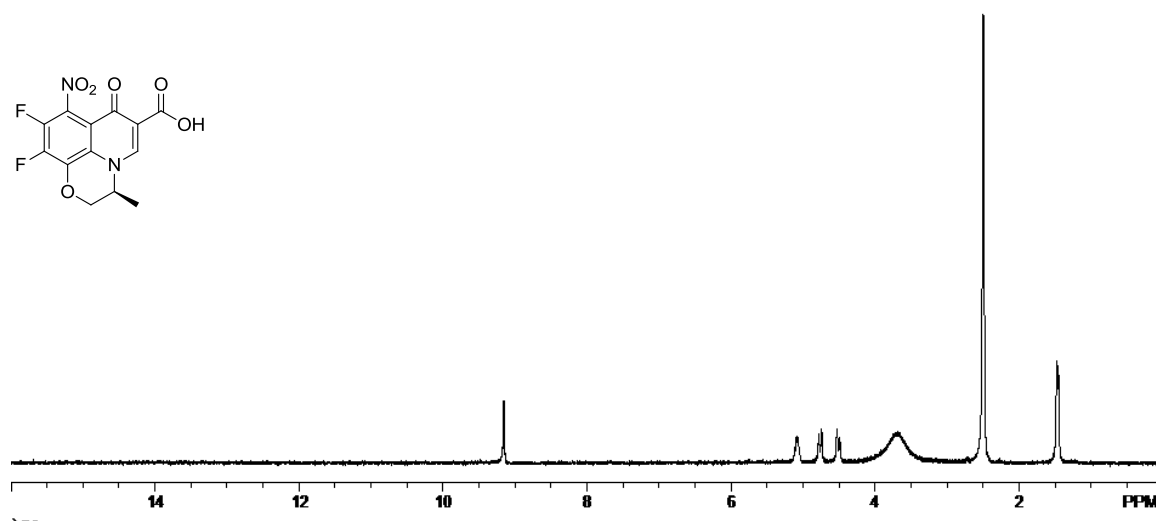
Figure A 10. ^{1}H NMR of **18** (HS-IIa-187) in DMSO.
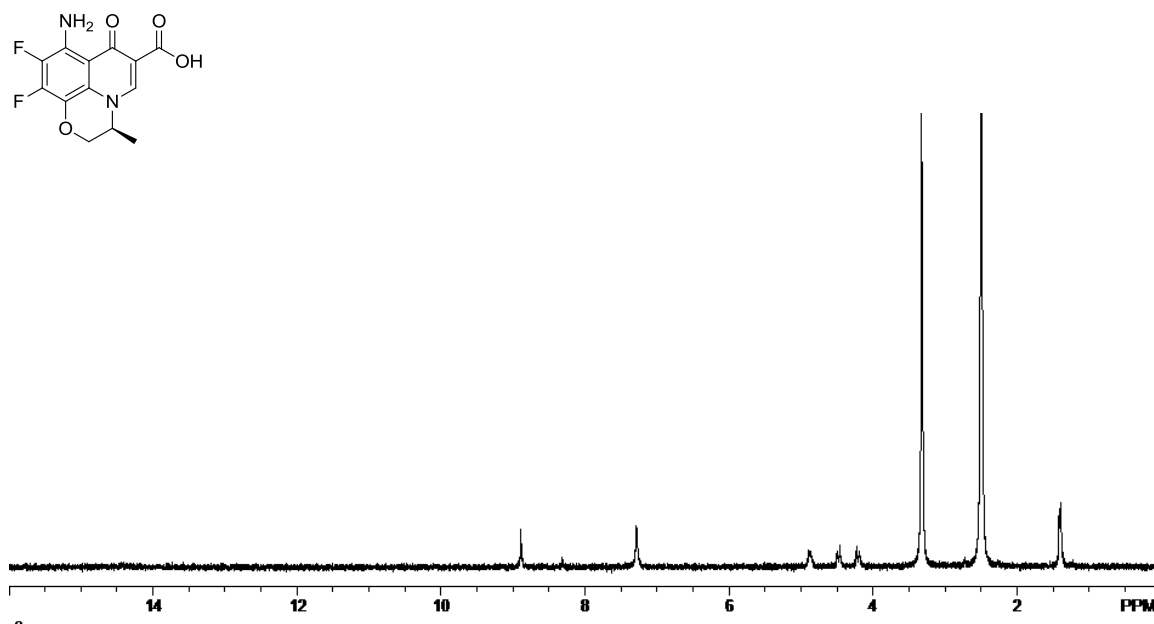
Figure A 11. ^{1}H NMR of **19** (HS-IIa-189) in DMSO.
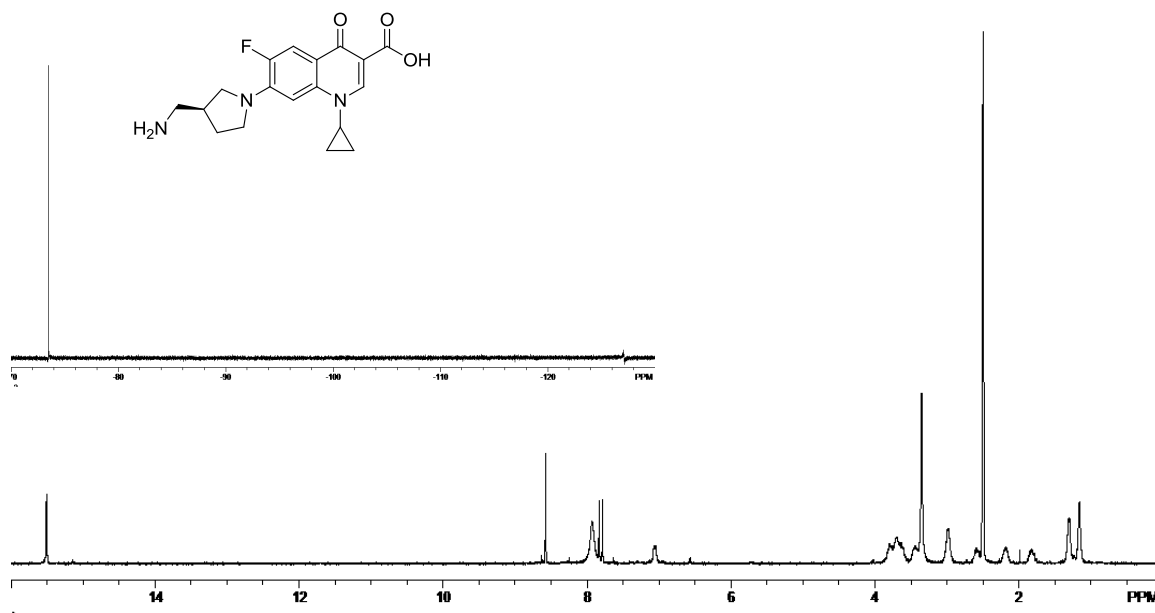
Figure A 12. ^{1}H NMR of **24** (HS-IIIa-35) in DMSO; ^{19}F NMR inset.
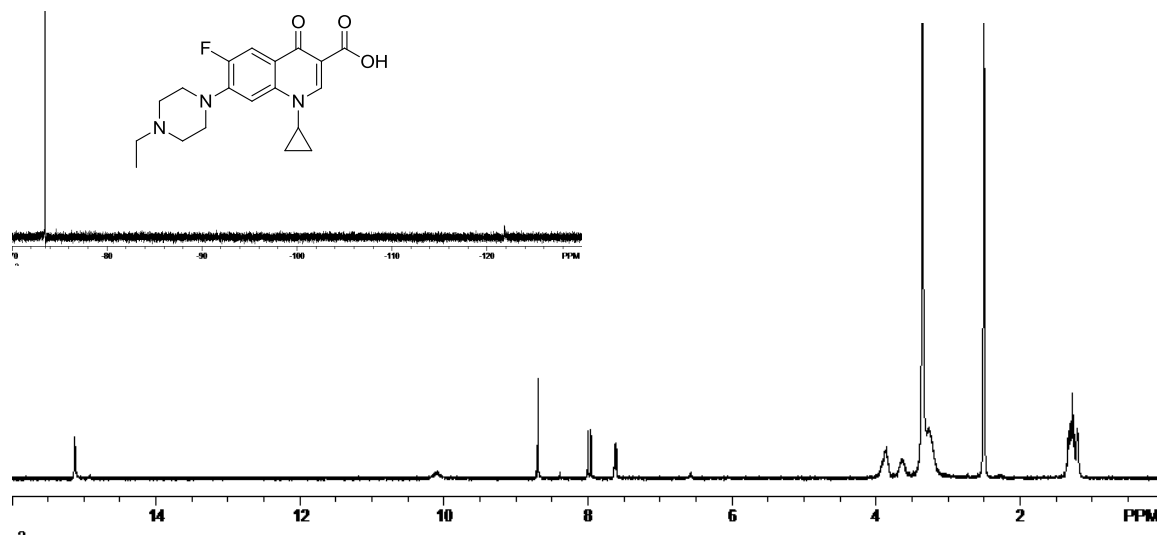
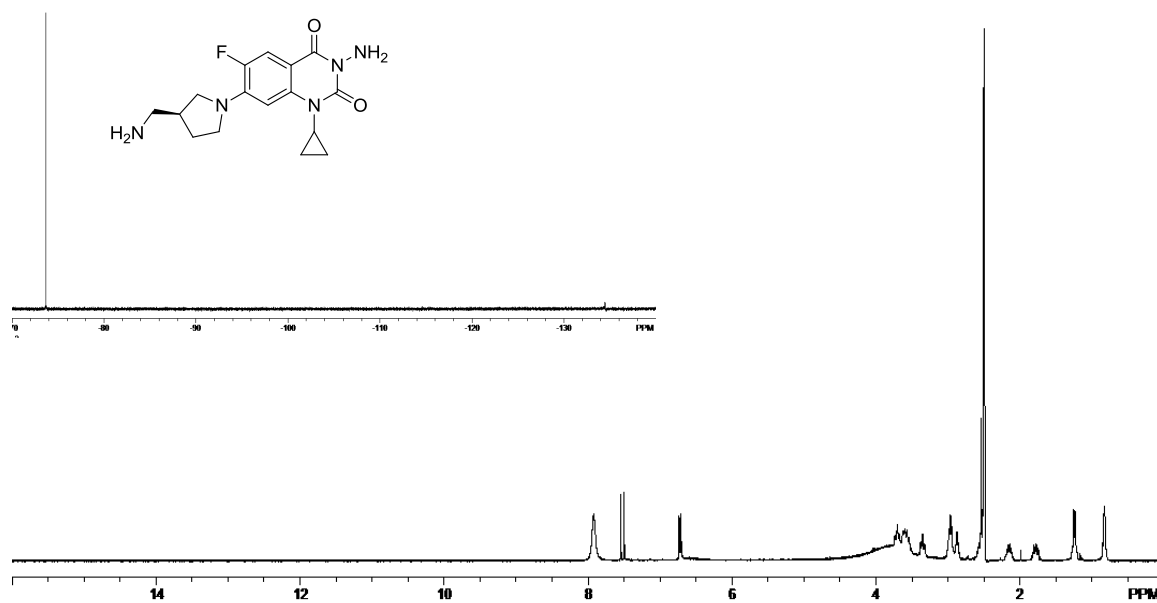Figure A 13. ^{1}H NMR of **25** (HS-IIa-165) in DMSO; ^{19}F NMR inset.
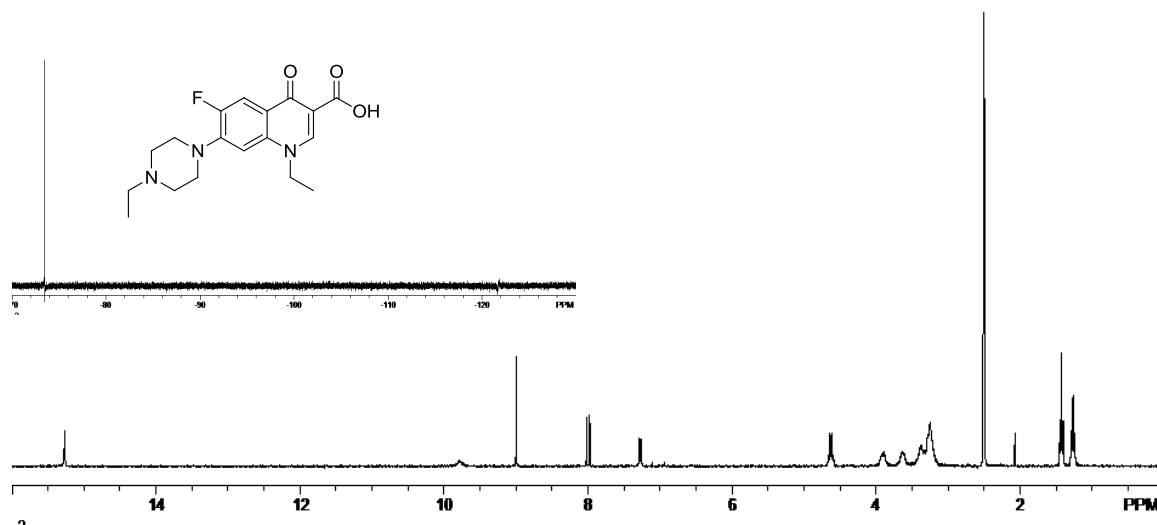
Figure A 14. ^{1}H NMR of **26** (HS-IIa-161) in DMSO; ^{19}F NMR inset.
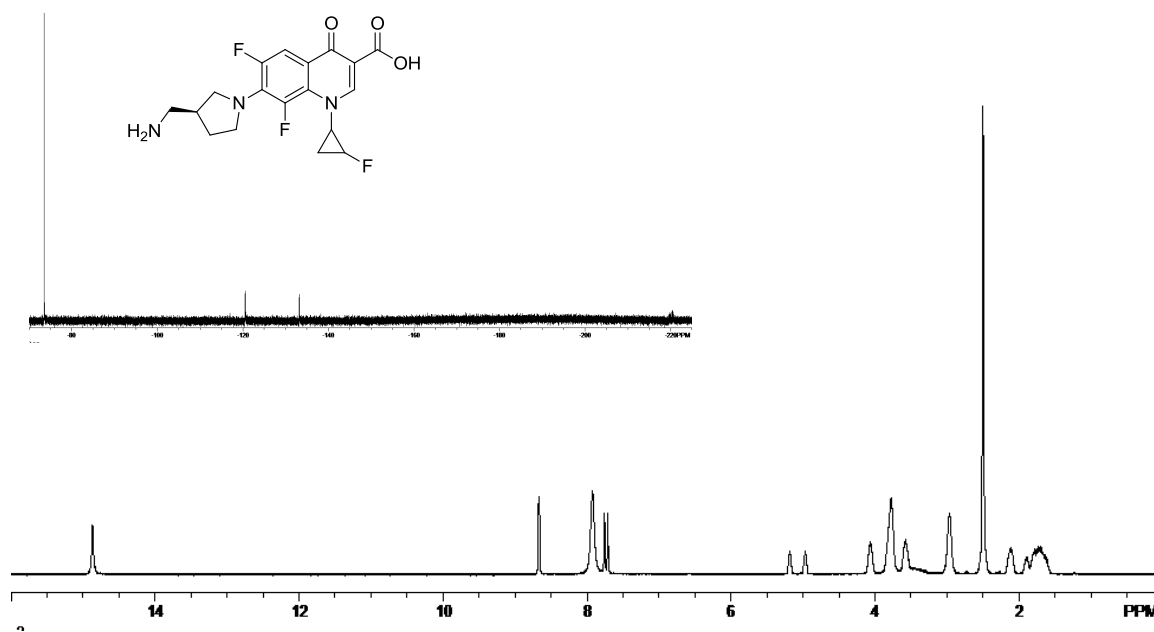
Figure A 15. ^{1}H NMR of **27** (HS-IIIa-39) in DMSO; ^{19}F NMR inset.
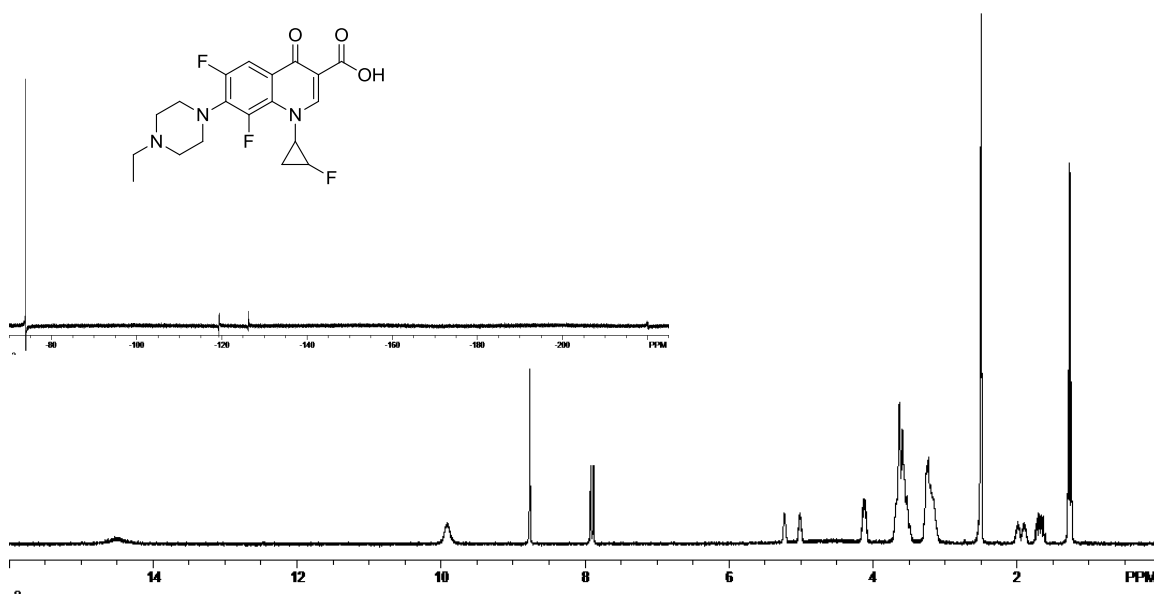
Figure A 16. ^{1}H NMR of **28** (HS-IIa-181) in DMSO; ^{19}F NMR inset.
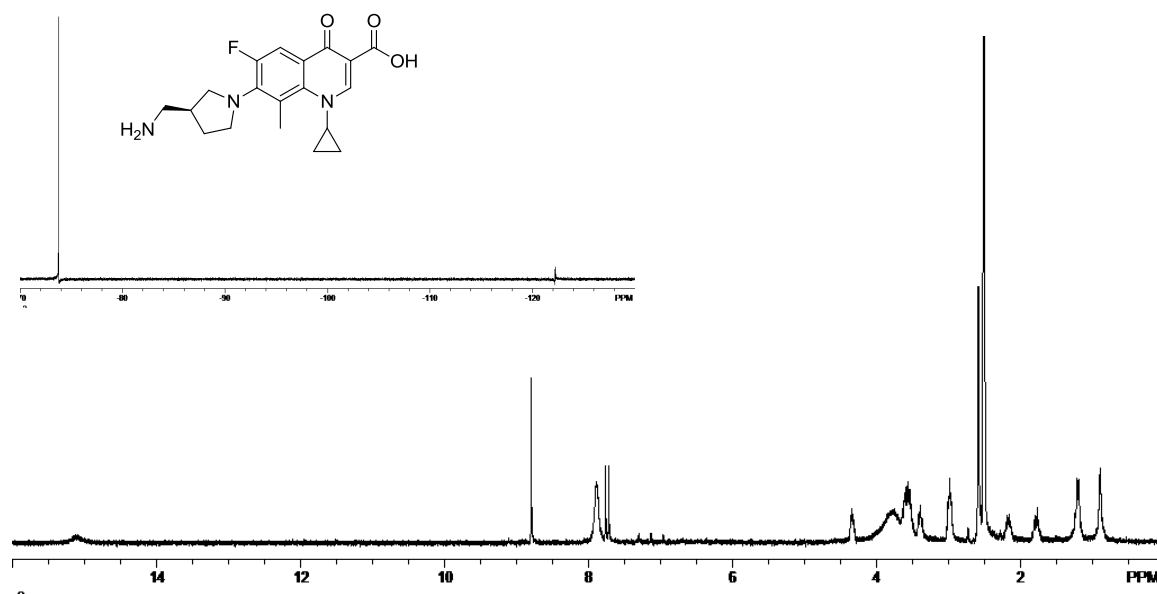
Figure A 17. ^{1}H NMR of **29** (HS-I-303) in DMSO; ^{19}F NMR inset.
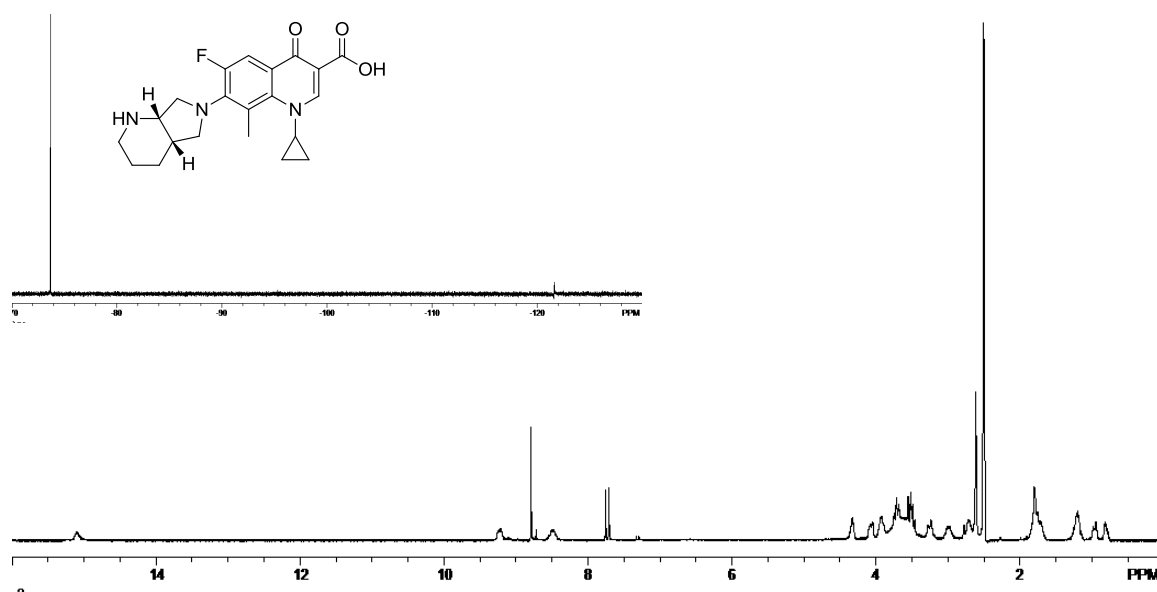
Figure A 18. ^{1}H NMR of **30** (HS-IIa-45) in DMSO; ^{19}F NMR inset.
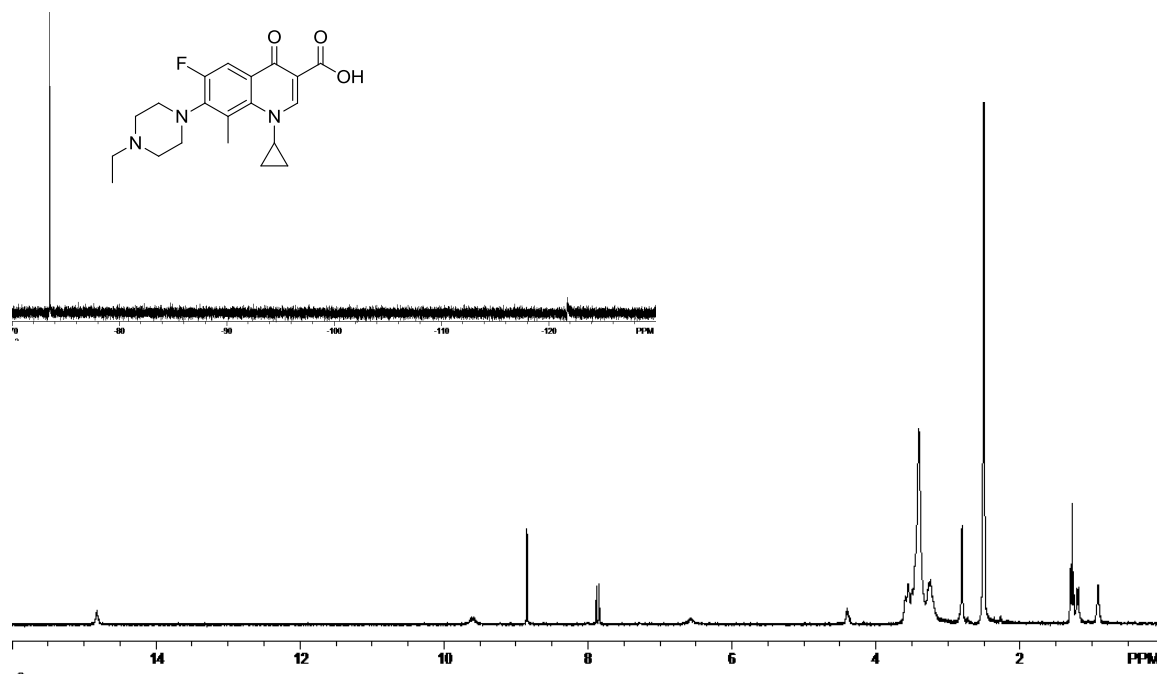
Figure A 19. ^{1}H NMR of **31** (HS-IIa-119) in DMSO; ^{19}F NMR inset.
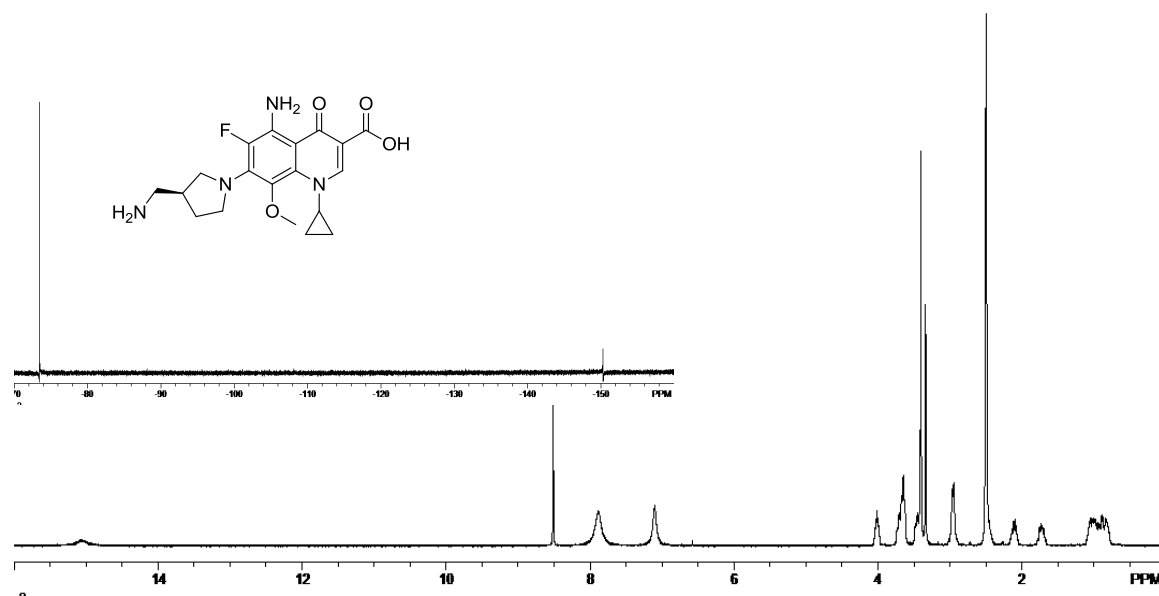
Figure A 20. ^{1}H NMR of **34** (HS-IIIa-41) in DMSO; ^{19}F NMR inset.
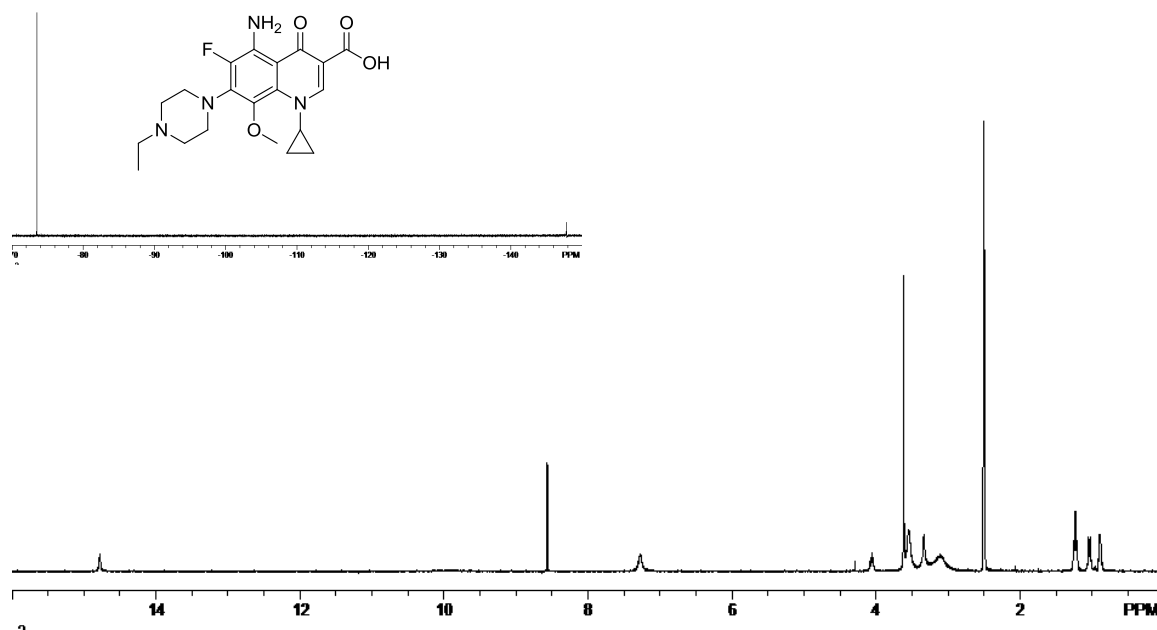
Figure A 21. ¹H NMR of **35** (HS-IIa-141) in DMSO; ¹⁹F NMR inset.
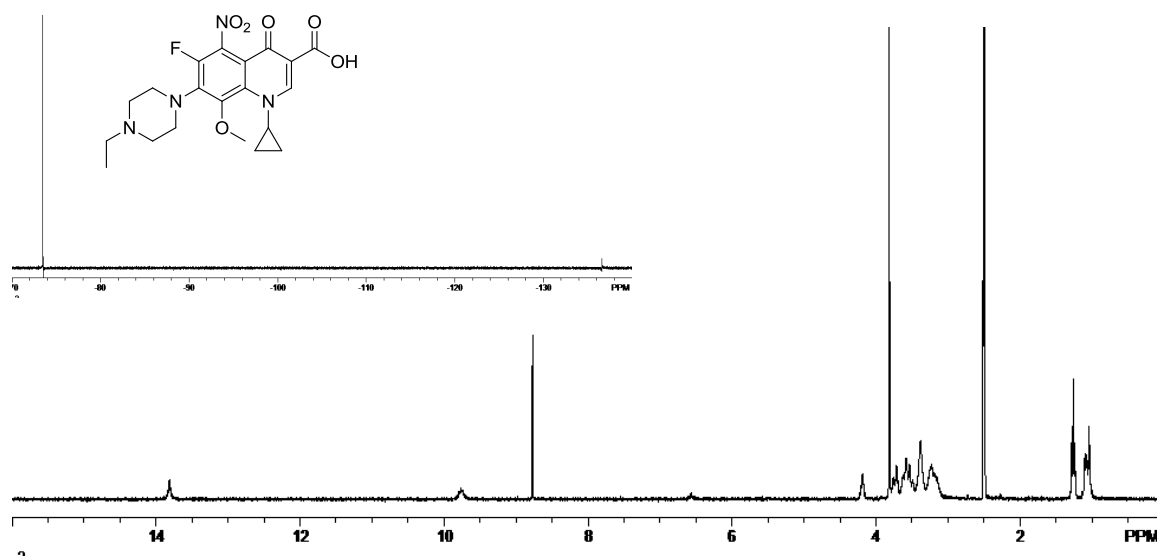
Figure A 22. ¹H NMR of **36** (HS-IIa-143) in DMSO; ¹⁹F NMR inset.
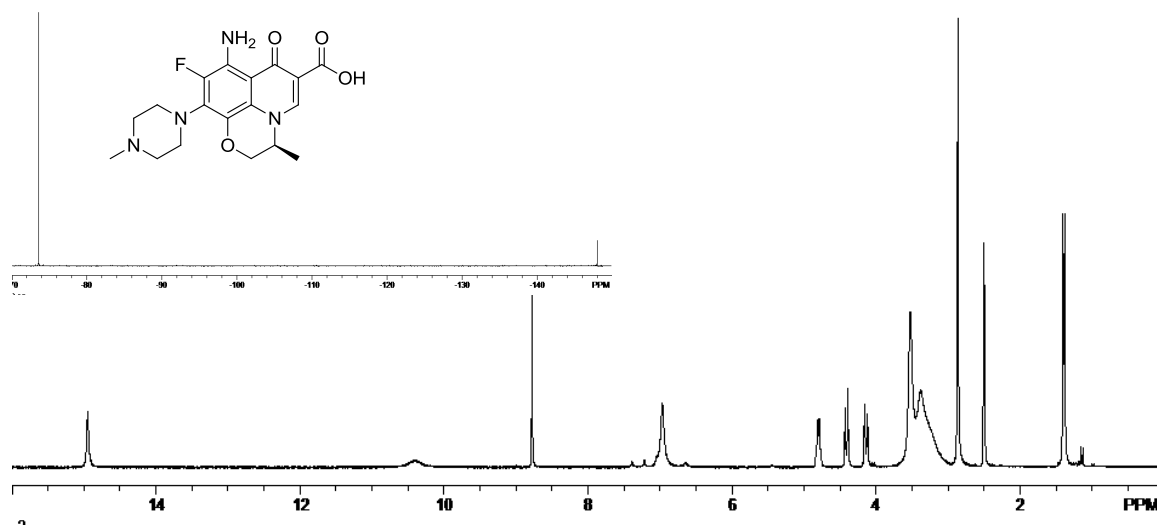
Figure A 23. ^{1}H NMR of **37** (HS-IIa-191, antofloxacin) in DMSO; ^{19}F NMR inset.
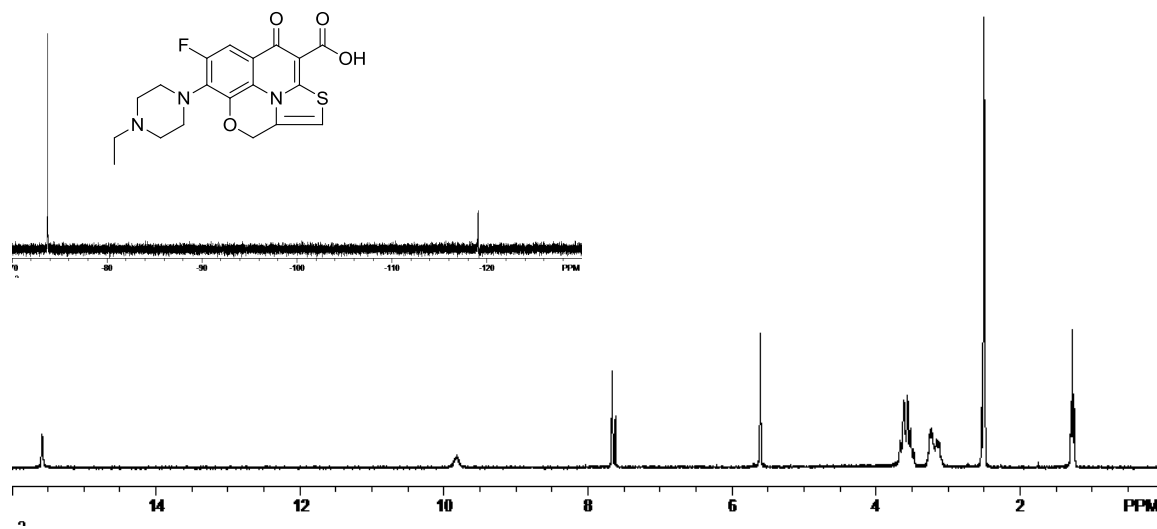
Figure A 24. ^{1}H NMR of **38** (HS-IIa-183) in DMSO; ^{19}F NMR inset.
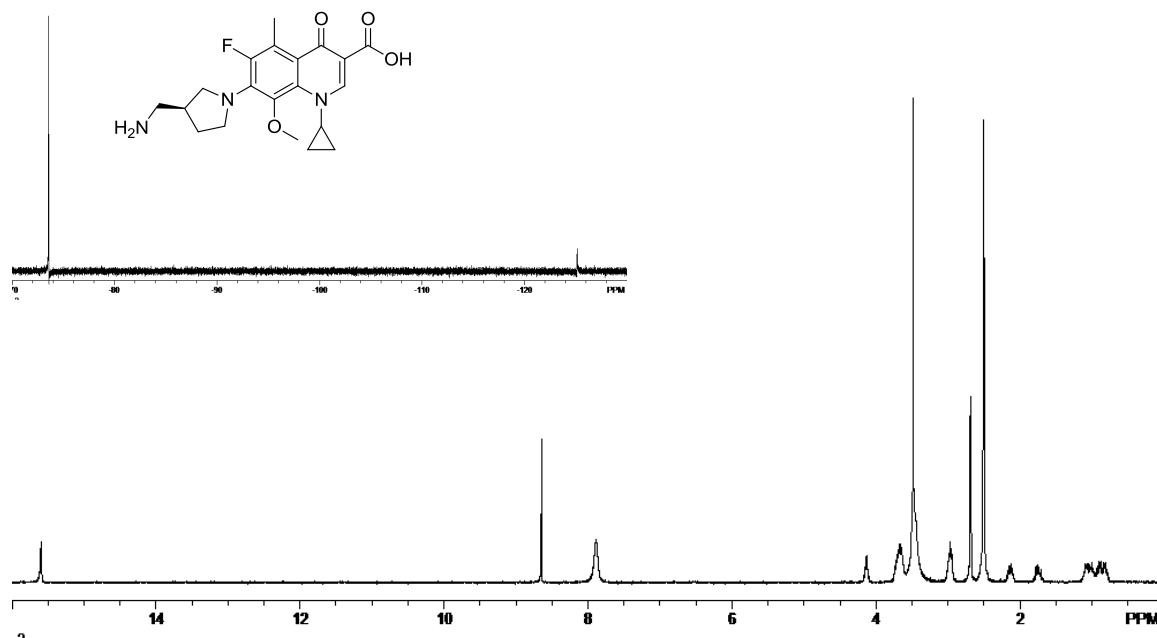
Figure A 25. ^{1}H NMR of **39** (HS-IIa-215) in DMSO; ^{19}F NMR inset.
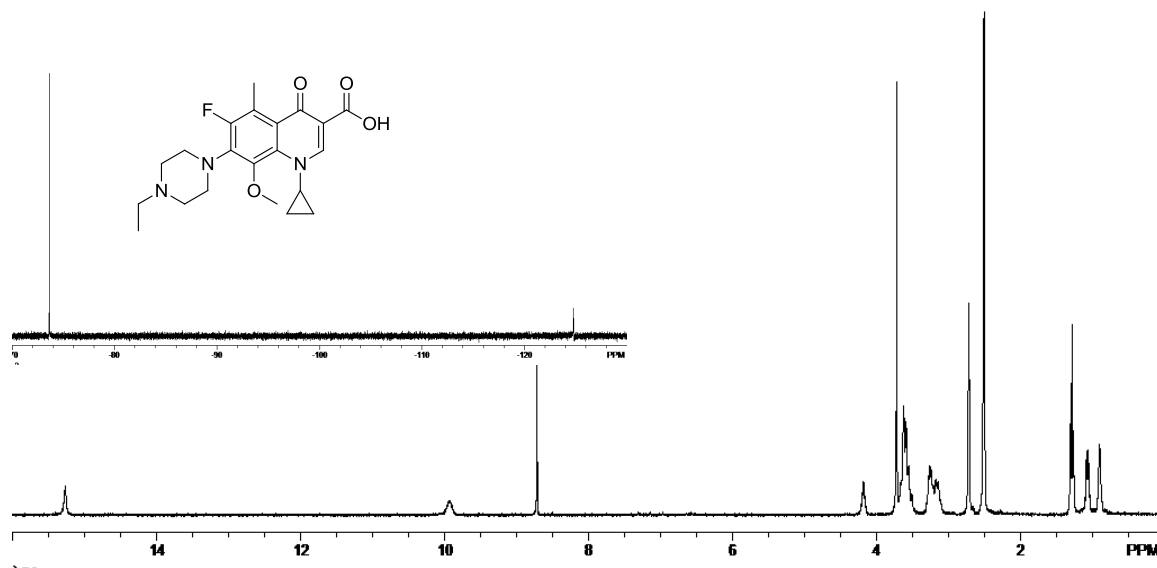
Figure A 26. ^{1}H NMR of **40** (HS-IIa-213) in DMSO; ^{19}F NMR inset.
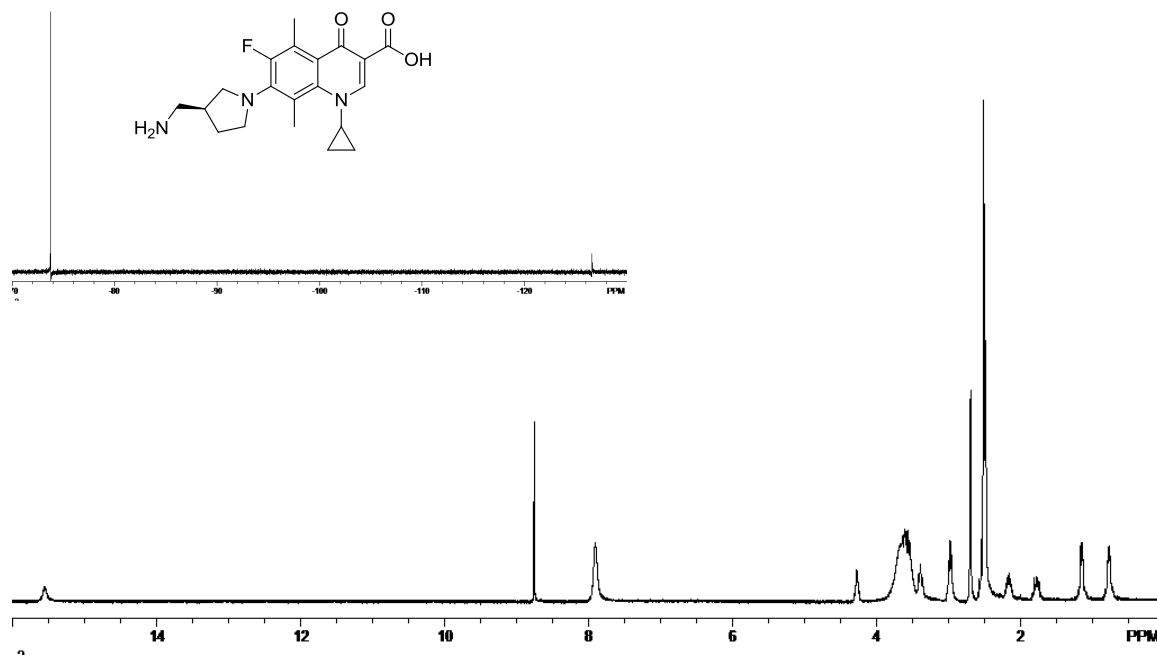
Figure A 27. ^{1}H NMR of **41** (HS-IIa-219) in DMSO; ^{19}F NMR inset.
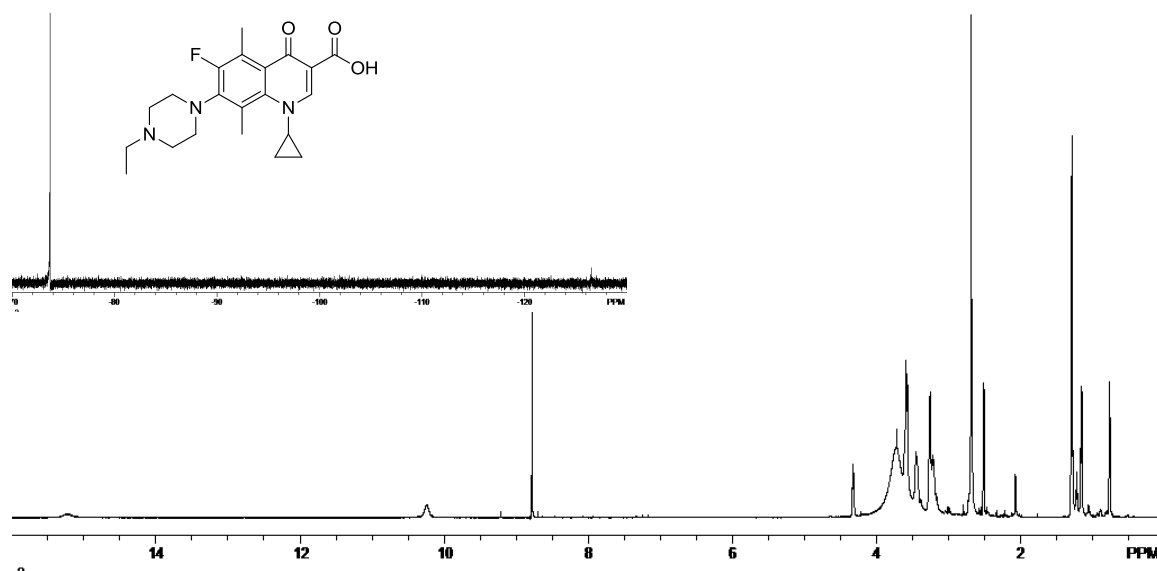
Figure A 28. ^{1}H NMR of **42** (HS-IIa-221) in DMSO; ^{19}F NMR inset.
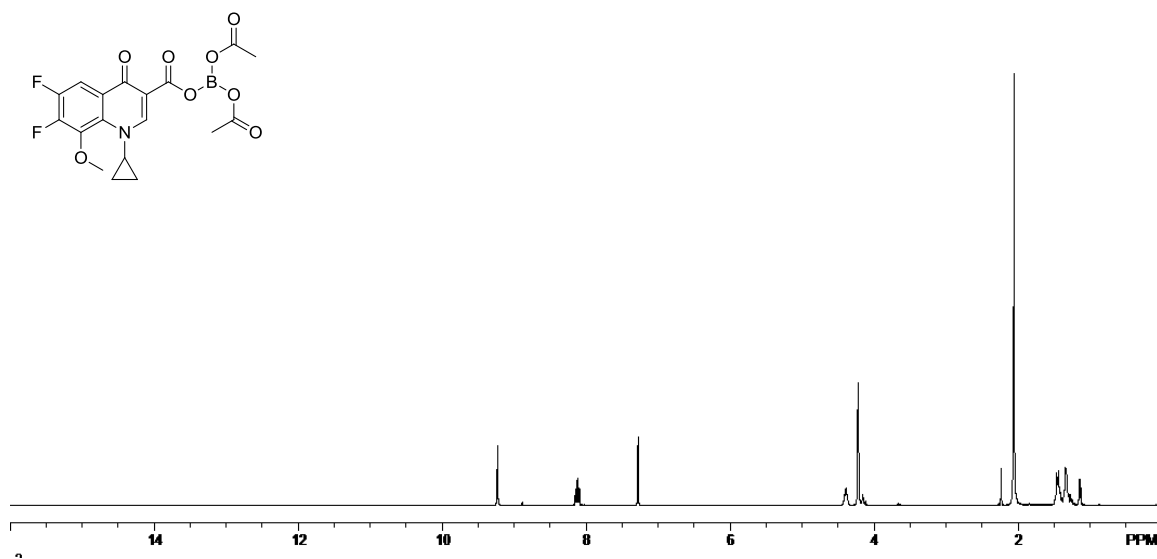
Figure A 29. ^{1}H NMR of **62 b.e.** (HS-IIa-89) in CDCl$_3$.
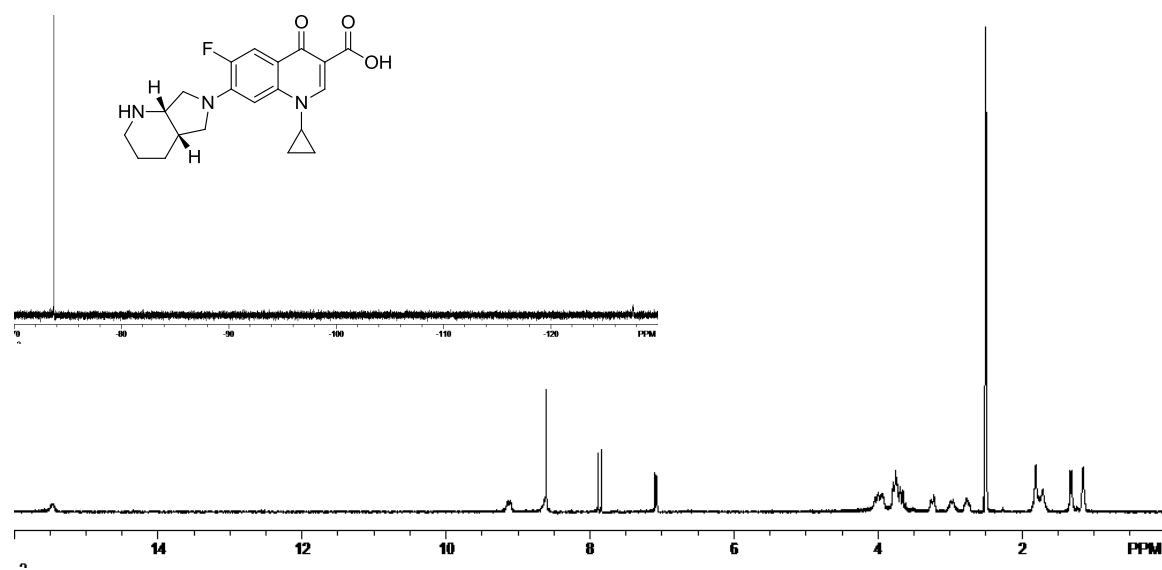
Figure A 30. ^{1}H NMR of **50** (HS-IIa-239) in DMSO; ^{19}F NMR inset.
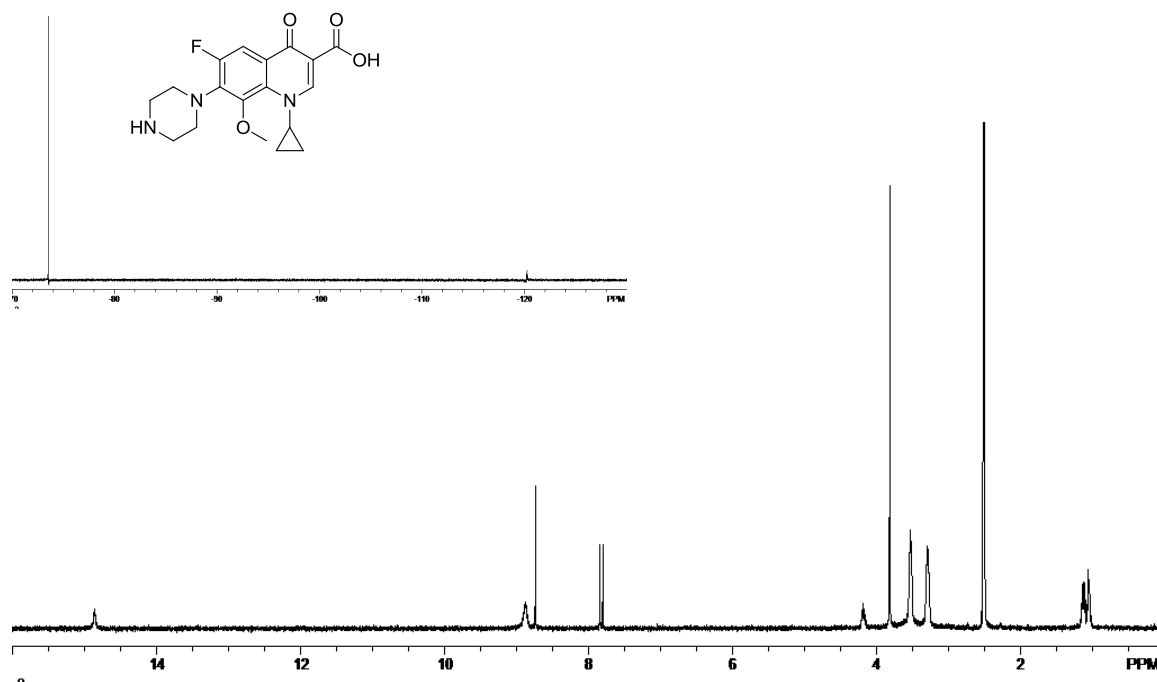
Figure A 31. ^{1}H NMR of **52** (HS-IIa-101) in DMSO; ^{19}F NMR inset.
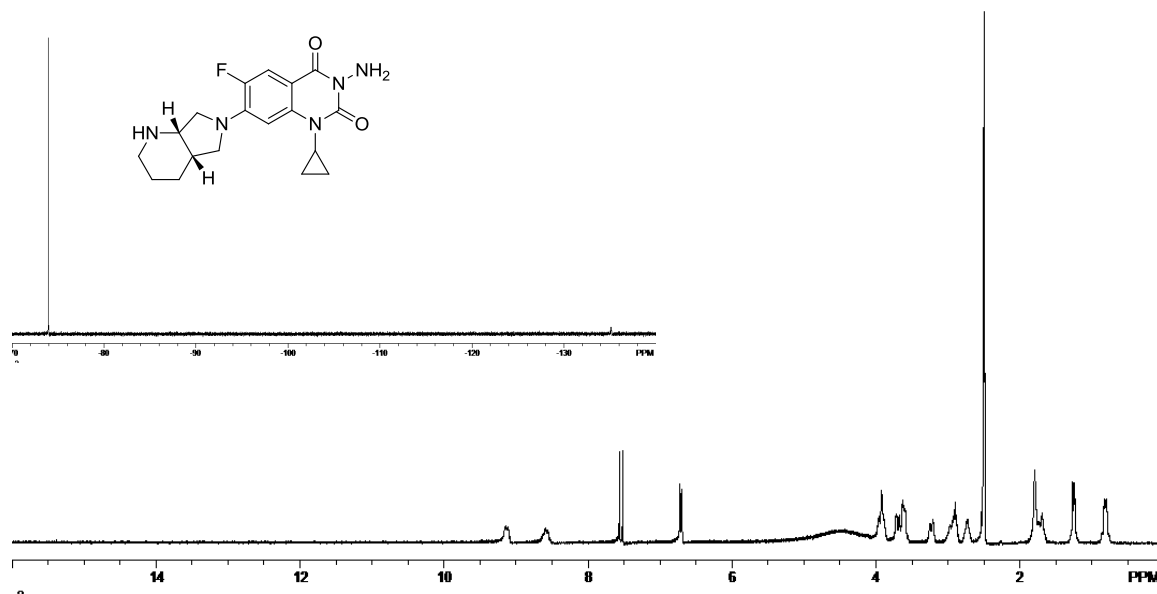
Figure A 32. ^{1}H NMR of **53** (HS-IIa-247) in DMSO; ^{19}F NMR inset.

Figure A 33. ^{1}H NMR of **54** (HS-IIa-245) in DMSO; ^{19}F NMR inset.
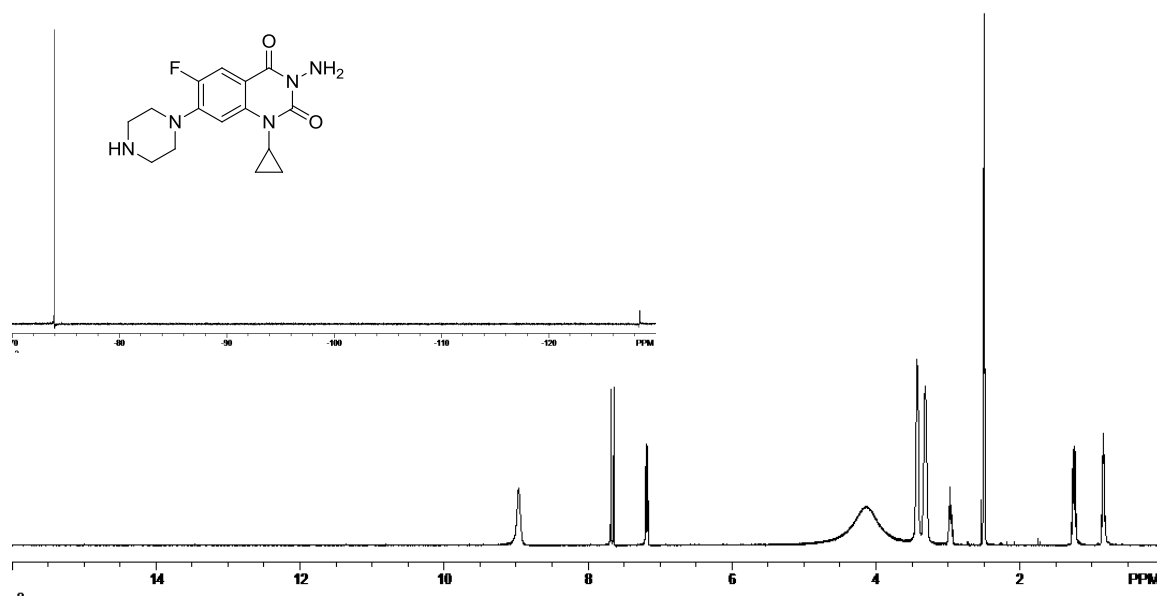
Figure A 34. ^{1}H NMR of **55** (HS-IIa-249) in DMSO; ^{19}F NMR inset.
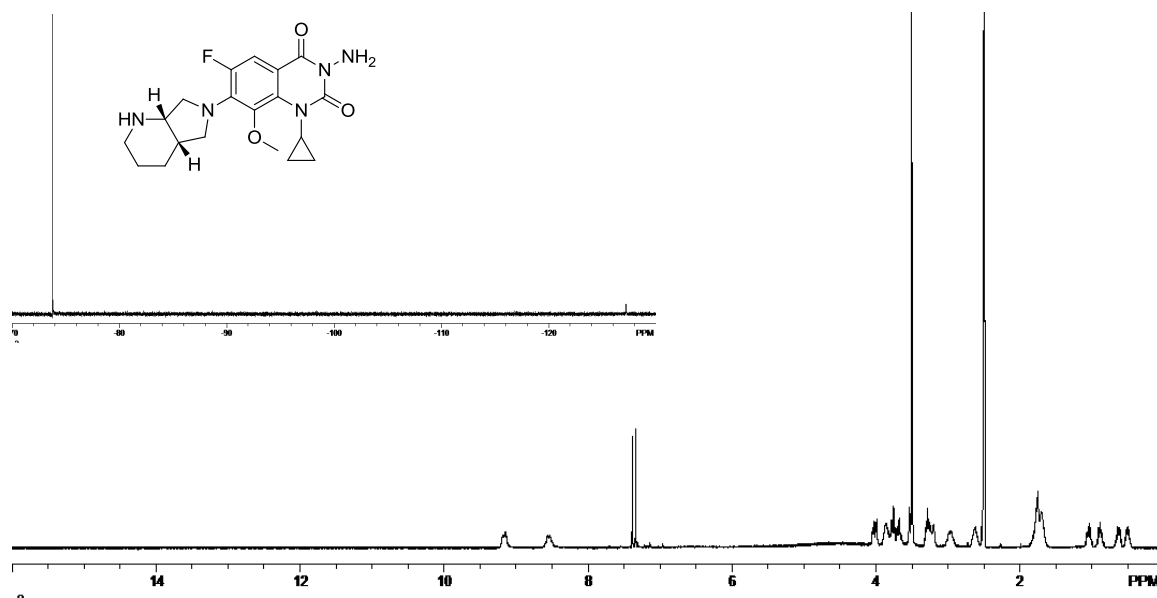
Figure A 35. ^{1}H NMR of **59** (HS-IIa-251) in DMSO; ^{19}F NMR inset.
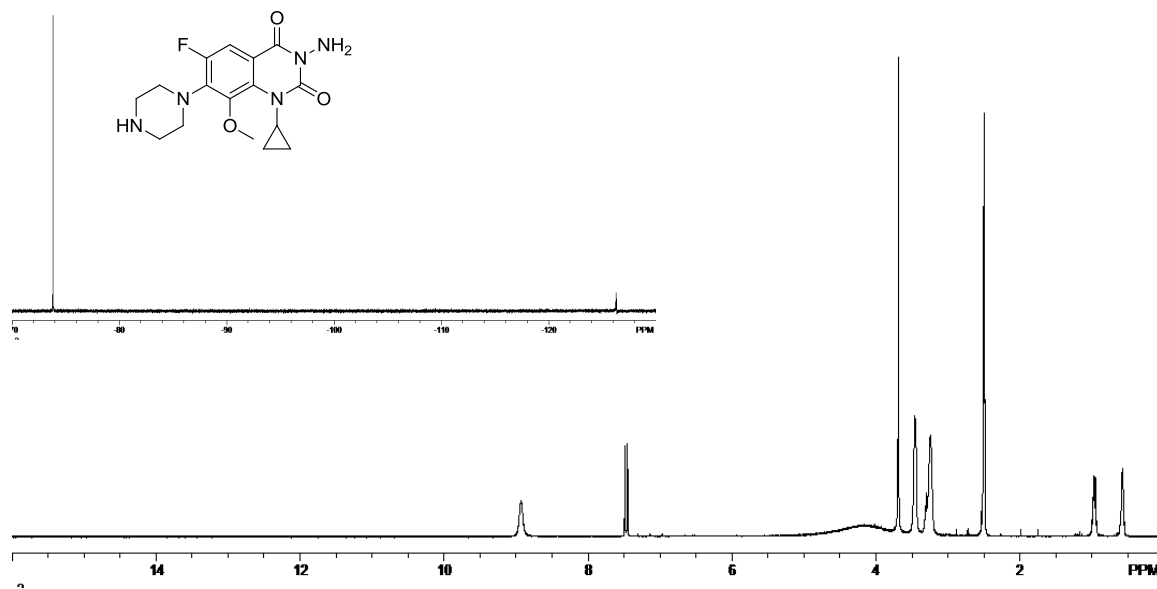
Figure A 36. ^{1}H NMR of **61** (HS-IIa-253) in DMSO; ^{19}F NMR inset.
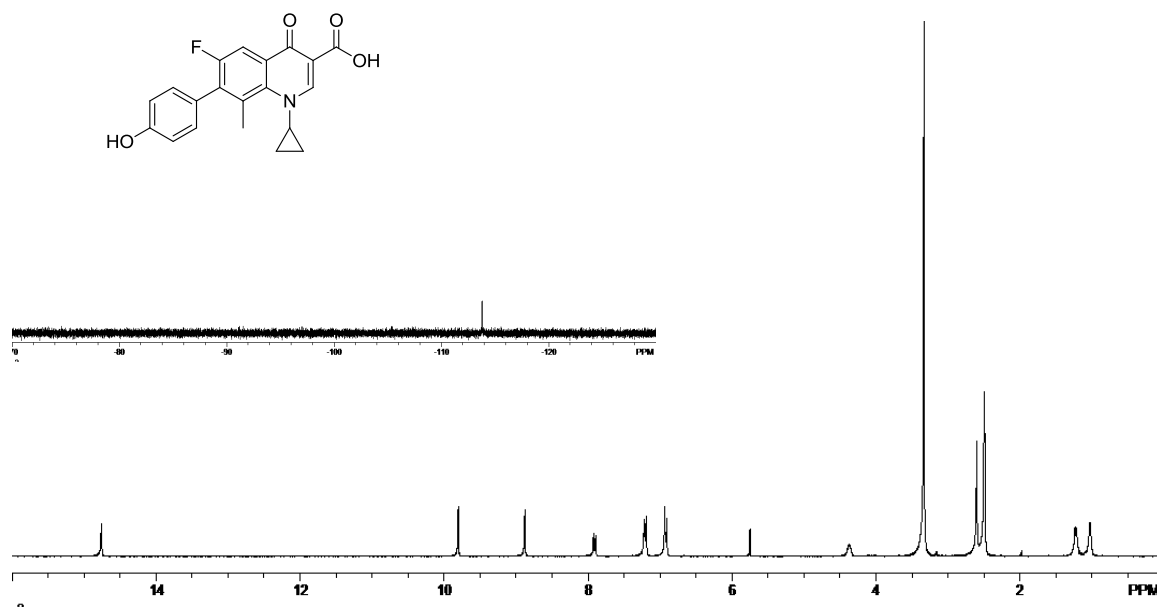
Figure A 37. ^{1}H NMR of **67** (HS-IIIa-23) in DMSO; ^{19}F NMR inset. Residual DCM was removed prior to testing.
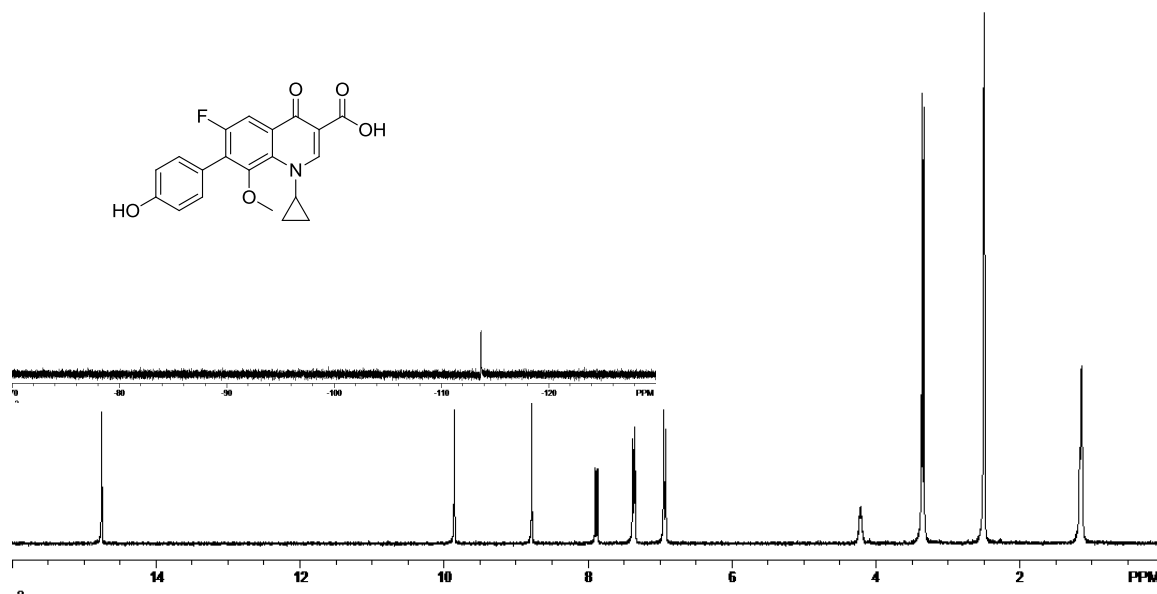
Figure A 38. ^{1}H NMR of **68** (HS-IIIa-27) in DMSO; ^{19}F NMR inset.

APPENDIX B. LETHAL ACTIVITY OF FLUOROQUINOLONES IN

THE PRESENCE AND ABSENCE OF CHLORAMPHENICOL

The lethality experiments in Appendix B were performed by M. Malik and A. Manzar in the Drlica lab at the University of Medicine and Dentistry of New Jersey and the raw data, as they provided it, is shown here.
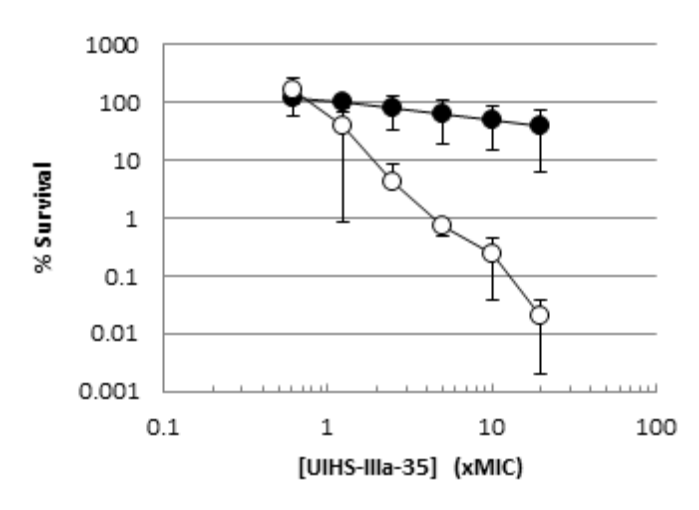
Figure B 1. Lethal activity of **24** UIHS-IIIa-35 in the presence and absence of chloramphenicol. Survival of *E. coli* was measured as a function of **24** concentration expressed as a multiple of the MIC in the presence (filled circles) or absence (open circles) of chloramphenicol, an inhibitor of protein synthesis. The error bars represent standard deviations of the means shown.
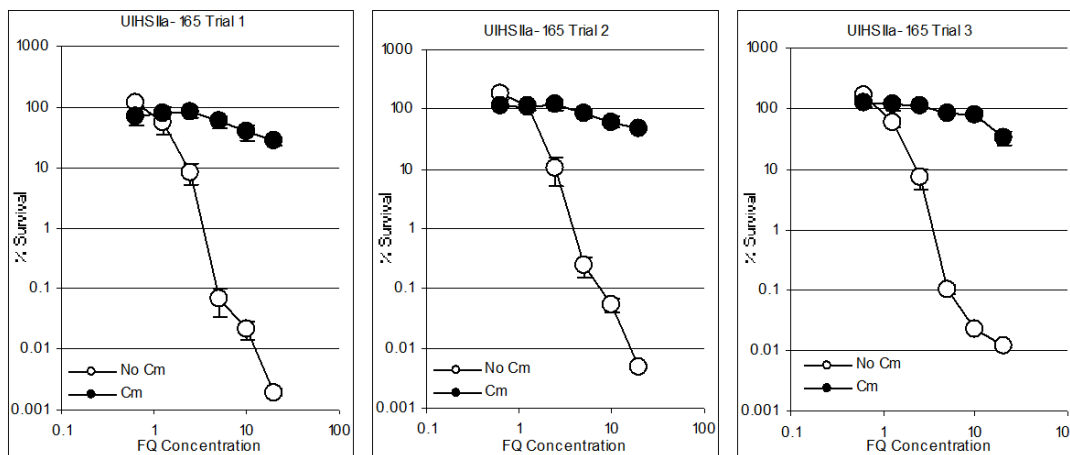
Figure B 2. Lethal activity of **25** UIHS-IIa-165 in the presence and absence of chloramphenicol. Survival of *E. coli* (y-axis) was measured as a function of **25** concentration expressed as a multiple of the MIC (x-axis) in the presence (filled circles) or absence (open circles) of chloramphenicol, an inhibitor of protein synthesis. The error bars represent standard deviations of the means shown for each of the three trials.
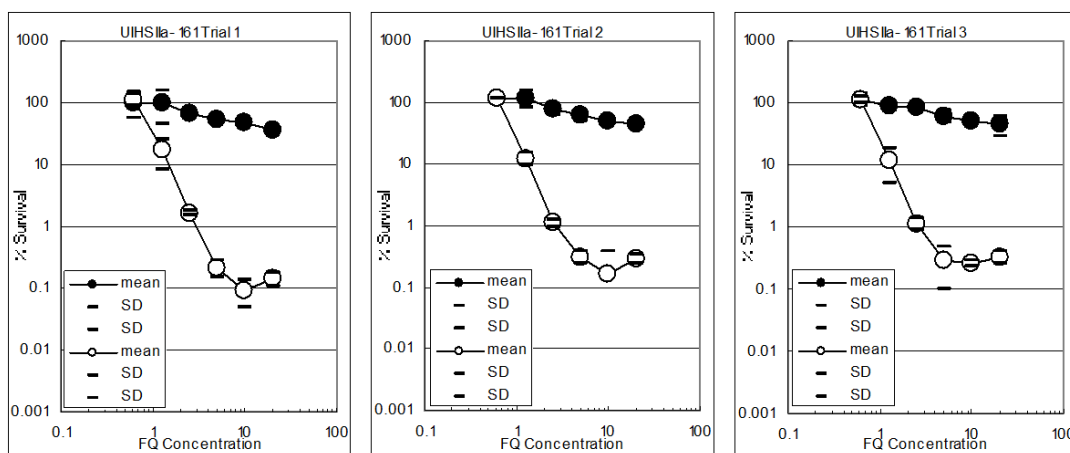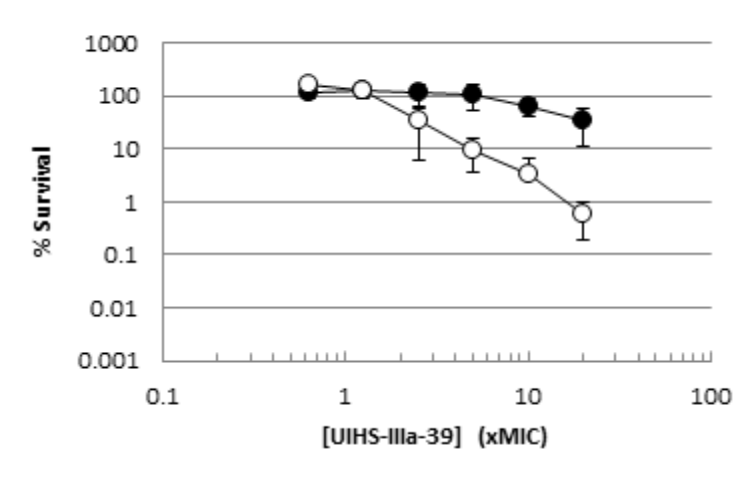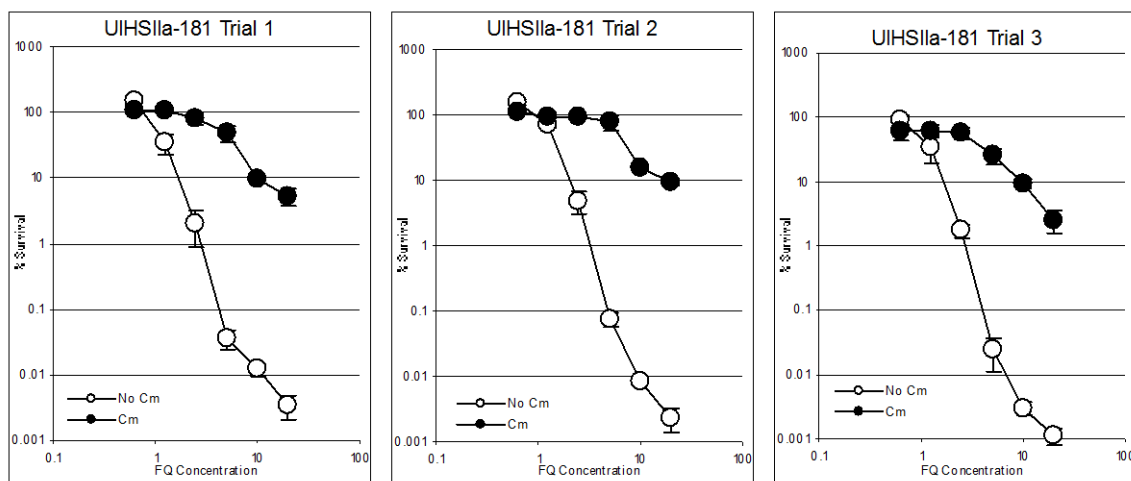

Figure B 3. Lethal activity of **26** UIHS-IIa-161 in the presence and absence of chloramphenicol. Survival of *E. coli* (y-axis) was measured as a function of **26** concentration expressed as a multiple of the MIC (x-axis) in the presence (filled circles) or absence (open circles) of chloramphenicol, an inhibitor of protein synthesis. The error bars represent standard deviations of the means shown for each of the three trials.
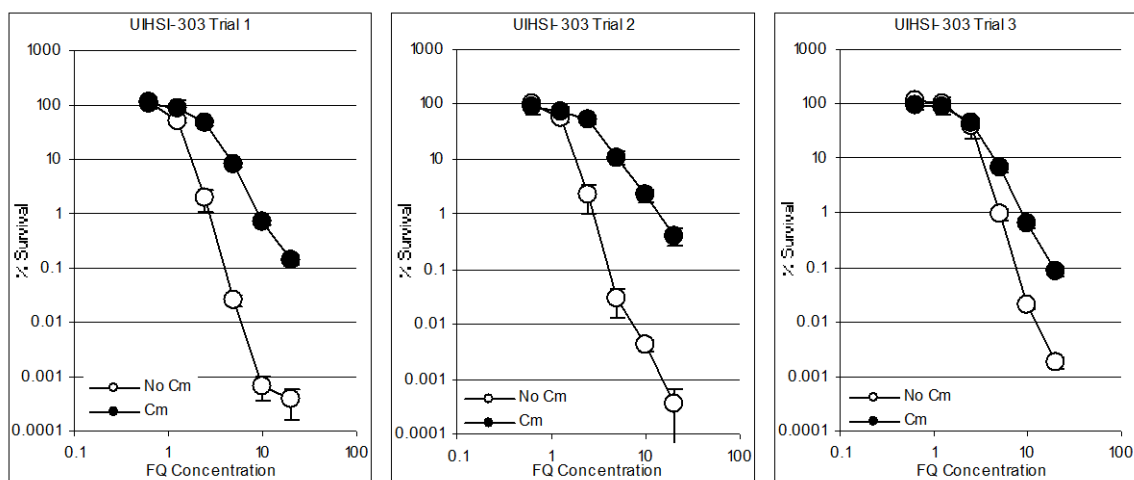
Figure B 4. Lethal activity of **27** UIHS-IIIa-39 in the presence and absence of chloramphenicol. Survival of *E. coli* was measured as a function of **27** concentration expressed as a multiple of the MIC in the presence (filled circles) or absence (open circles) of chloramphenicol, an inhibitor of protein synthesis. The error bars represent standard deviations of the means shown.

Figure B 5. Lethal activity of **28** UIHS-IIa-181 in the presence and absence of chloramphenicol. Survival of *E. coli* (y-axis) was measured as a function of **28** concentration expressed as a multiple of the MIC (x-axis) in the presence (filled circles) or absence (open circles) of chloramphenicol, an inhibitor of protein synthesis. The error bars represent standard deviations of the means shown for each of the three trials.
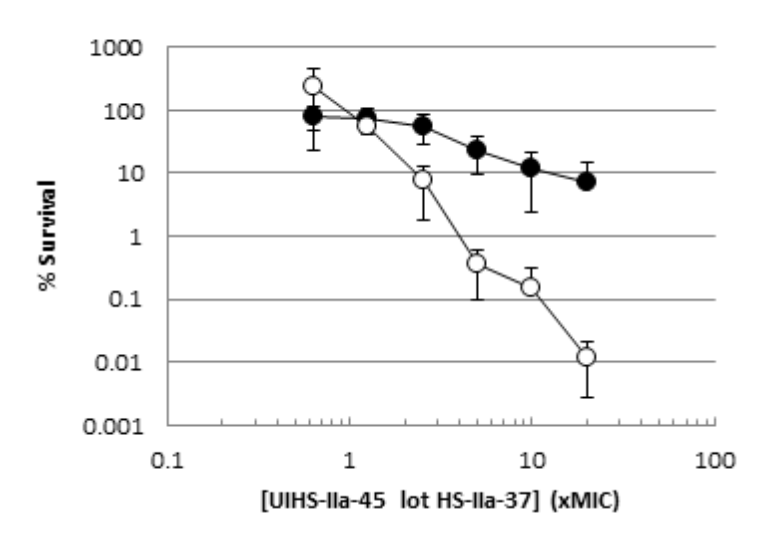
Figure B 6. Lethal activity of **29** UIHS-I-303 in the presence and absence of chloramphenicol. Survival of *E. coli* (y-axis) was measured as a function of **29** concentration expressed as a multiple of the MIC (x-axis) in the presence (filled circles) or absence (open circles) of chloramphenicol, an inhibitor of protein synthesis. The error bars represent standard deviations of the means shown for each of the three trials.
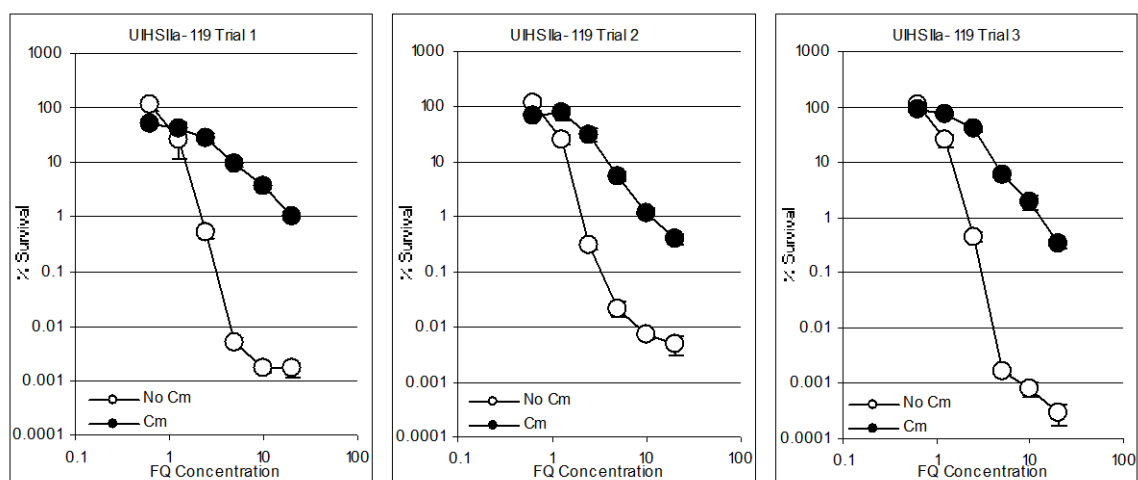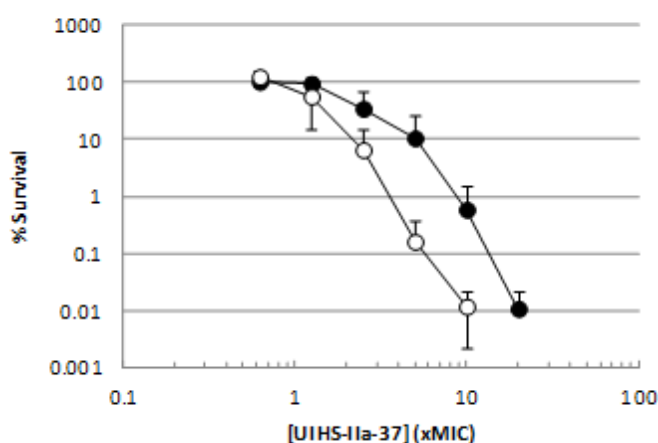

Figure B 7. Lethal activity of **30** UIHS-IIa-45 in the presence and absence of chloramphenicol. Survival of *E. coli* was measured as a function of **30** concentration expressed as a multiple of the MIC in the presence (filled circles) or absence (open circles) of chloramphenicol, an inhibitor of protein synthesis. The error bars represent standard deviations of the means shown.

Figure B 8. Lethal activity of **31** UIHS-IIa-119 in the presence and absence of chloramphenicol. Survival of *E. coli* (y-axis) was measured as a function of **31** concentration expressed as a multiple of the MIC (x-axis) in the presence (filled circles) or absence (open circles) of chloramphenicol, an inhibitor of protein synthesis. The error bars represent standard deviations of the means shown for each of the three trials.

Figure B 9. Lethal activity of **32** UING5-249 in the presence and absence of chloramphenicol. Survival of *E. coli* was measured as a function of **32** concentration expressed as a multiple of the MIC in the presence (filled circles) or absence (open circles) of chloramphenicol, an inhibitor of protein synthesis. The error bars represent standard deviations of the means shown.
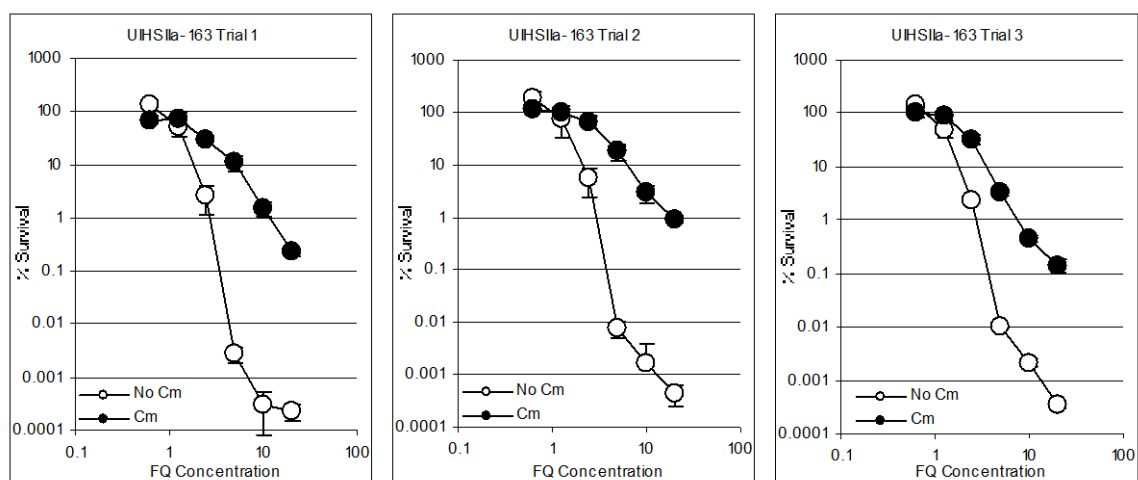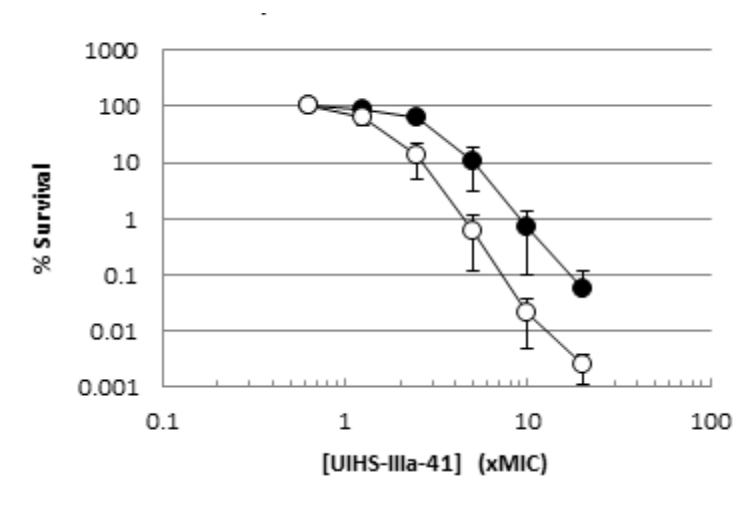
Figure B 10. Lethal activity of **33** PD161144 in the presence and absence of chloramphenicol. Survival of *E. coli* (y-axis) was measured as a function of **33** concentration expressed as a multiple of the MIC (x-axis) in the presence (filled circles) or absence (open circles) of chloramphenicol, an inhibitor of protein synthesis. The error bars represent standard deviations of the means shown for each of the three trials.

Figure B 11. Lethal activity of **34** UIHS-IIIa-41 in the presence and absence of chloramphenicol. Survival of *E. coli* was measured as a function of **34** concentration expressed as a multiple of the MIC in the presence (filled circles) or absence (open circles) of chloramphenicol, an inhibitor of protein synthesis. The error bars represent standard deviations of the means shown.
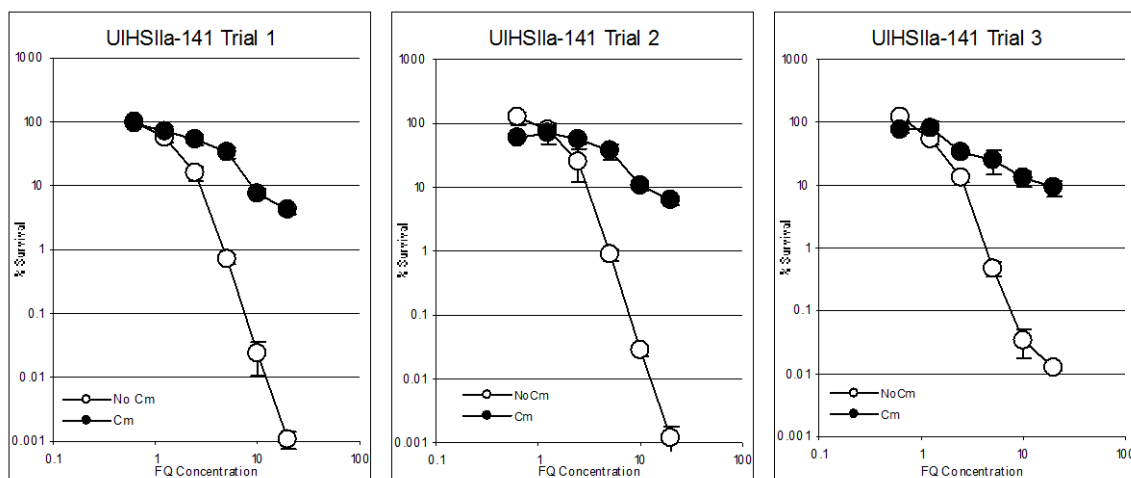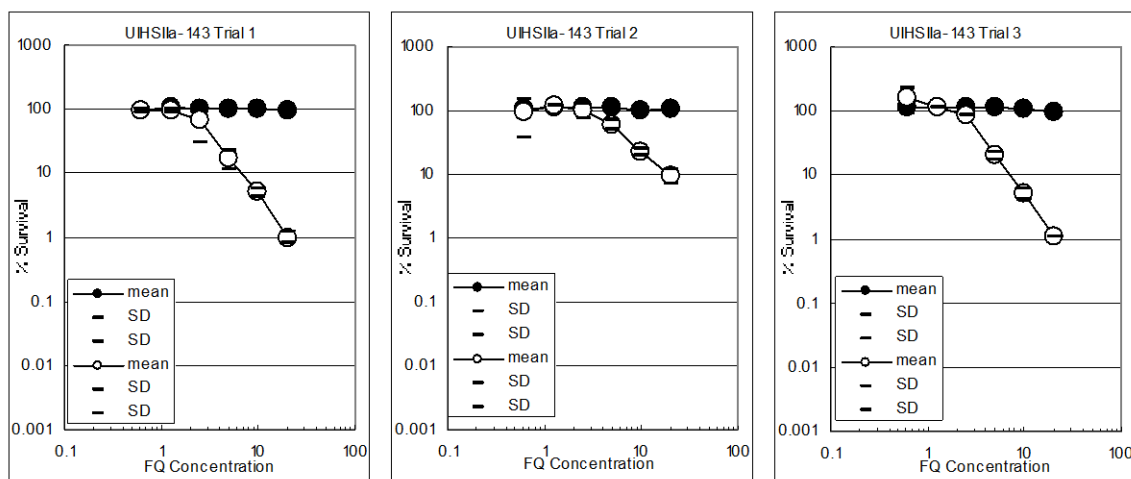
Figure B 12. Lethal activity of **35** UIHS-IIa-141 in the presence and absence of chloramphenicol. Survival of *E. coli* (y-axis) was measured as a function of **35** concentration expressed as a multiple of the MIC (x-axis) in the presence (filled circles) or absence (open circles) of chloramphenicol, an inhibitor of protein synthesis. The error bars represent standard deviations of the means shown for each of the three trials.

Figure B 13. Lethal activity of **36** UIHS-IIa-143 in the presence and absence of chloramphenicol. Survival of *E. coli* (y-axis) was measured as a function of **36** concentration expressed as a multiple of the MIC (x-axis) in the presence (filled circles) or absence (open circles) of chloramphenicol, an inhibitor of protein synthesis. The error bars represent standard deviations of the means shown for each of the three trials.
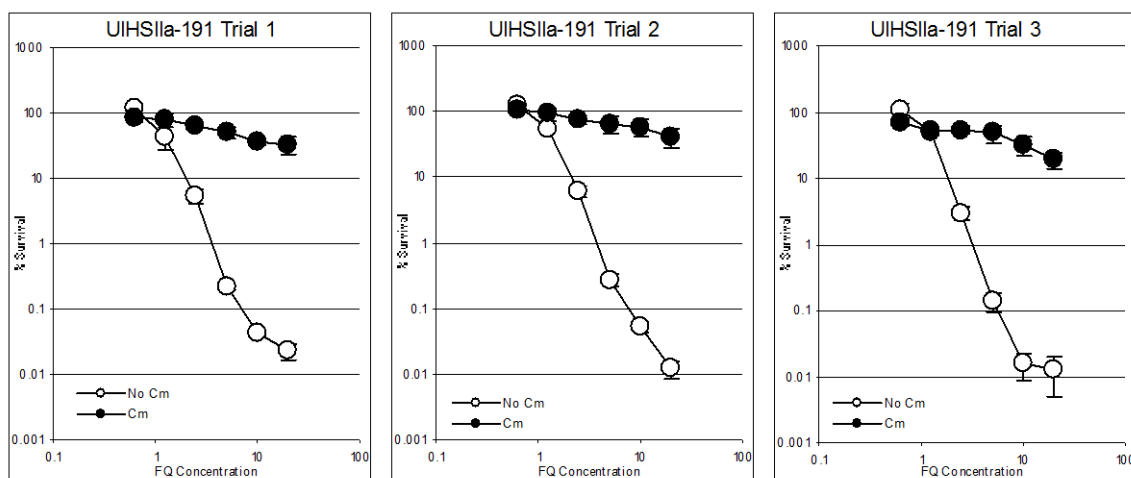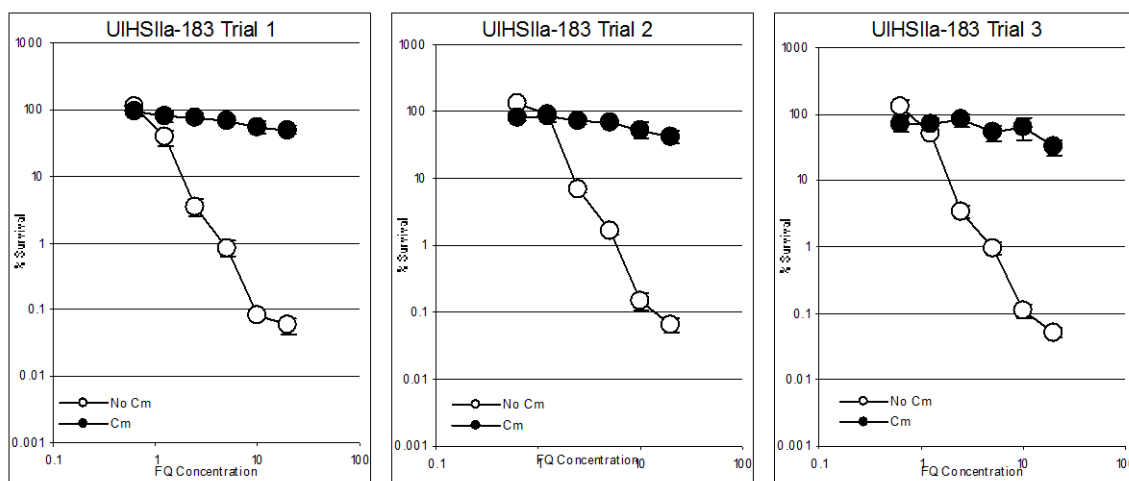
Figure B 14. Lethal activity of **37** UIHS-IIa-191 (antofloxacin) in the presence and absence of chloramphenicol. Survival of *E. coli* (y-axis) was measured as a function of **37** concentration expressed as a multiple of the MIC (x-axis) in the presence (filled circles) or absence (open circles) of chloramphenicol, an inhibitor of protein synthesis. The error bars represent standard deviations of the means shown for each of the three trials.

Figure B 15. Lethal activity of **38** UIHS-IIa-183 (antofloxacin) in the presence and absence of chloramphenicol. Survival of *E. coli* (y-axis) was measured as a function of **38** concentration expressed as a multiple of the MIC (x-axis) in the presence (filled circles) or absence (open circles) of chloramphenicol, an inhibitor of protein synthesis. The error bars represent standard deviations of the means shown for each of the three trials.
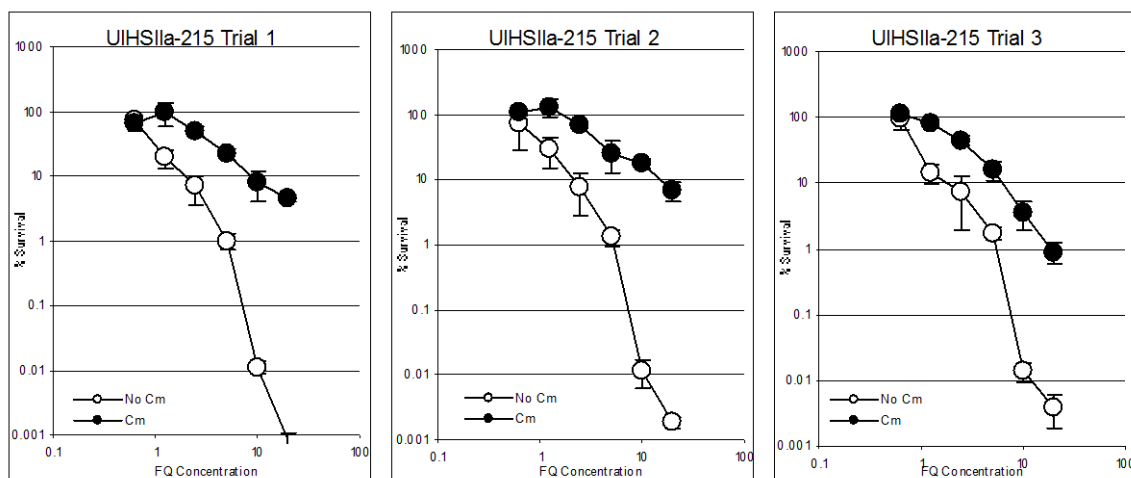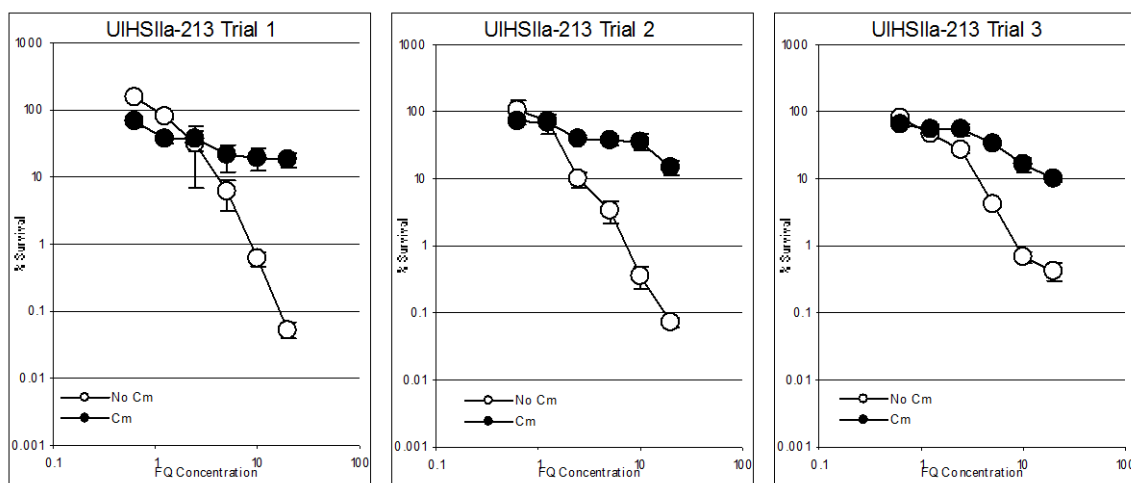
Figure B 16. Lethal activity of **39** UIHS-IIa-215 in the presence and absence of chloramphenicol. Survival of *E. coli* (y-axis) was measured as a function of **39** concentration expressed as a multiple of the MIC (x-axis) in the presence (filled circles) or absence (open circles) of chloramphenicol, an inhibitor of protein synthesis. The error bars represent standard deviations of the means shown for each of the three trials.
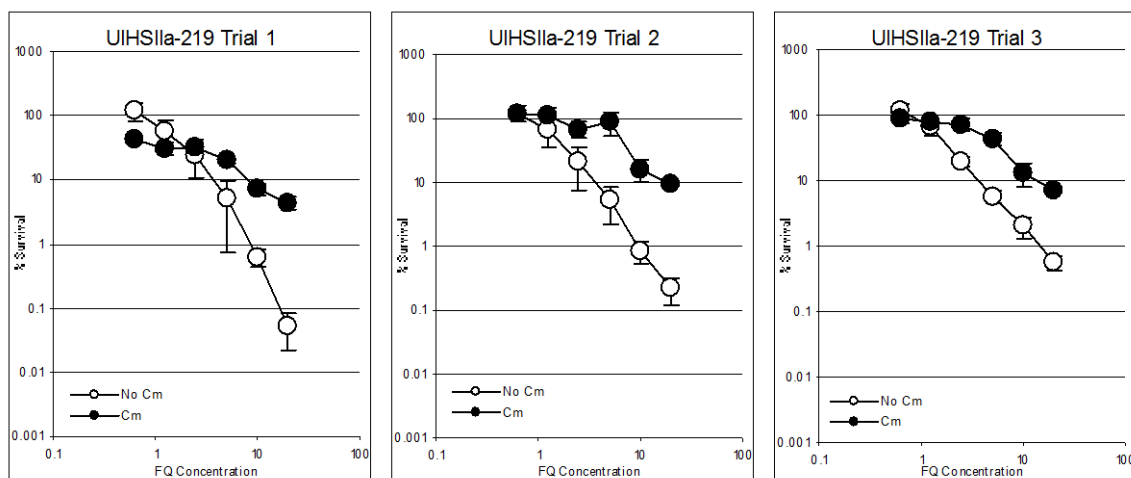

Figure B 17. Lethal activity of **40** UIHS-IIa-213 in the presence and absence of chloramphenicol. Survival of *E. coli* (y-axis) was measured as a function of **40** concentration expressed as a multiple of the MIC (x-axis) in the presence (filled circles) or absence (open circles) of chloramphenicol, an inhibitor of protein synthesis. The error bars represent standard deviations of the means shown for each of the three trials.
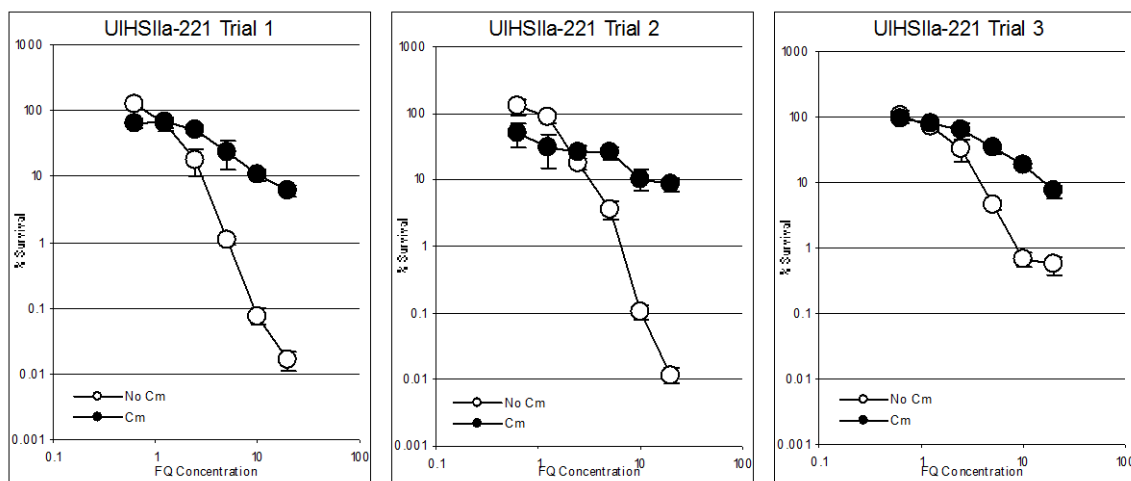
Figure B 18. Lethal activity of **41** UIHS-IIa-219 in the presence and absence of chloramphenicol. Survival of *E. coli* (y-axis) was measured as a function of **41** concentration expressed as a multiple of the MIC (x-axis) in the presence (filled circles) or absence (open circles) of chloramphenicol, an inhibitor of protein synthesis. The error bars represent standard deviations of the means shown for each of the three trials.

Figure B 19. Lethal activity of **42** UIHS-IIa-221 in the presence and absence of chloramphenicol. Survival of *E. coli* (y-axis) was measured as a function of **42** concentration expressed as a multiple of the MIC (x-axis) in the presence (filled circles) or absence (open circles) of chloramphenicol, an inhibitor of protein synthesis. The error bars represent standard deviations of the means shown for each of the three trials.
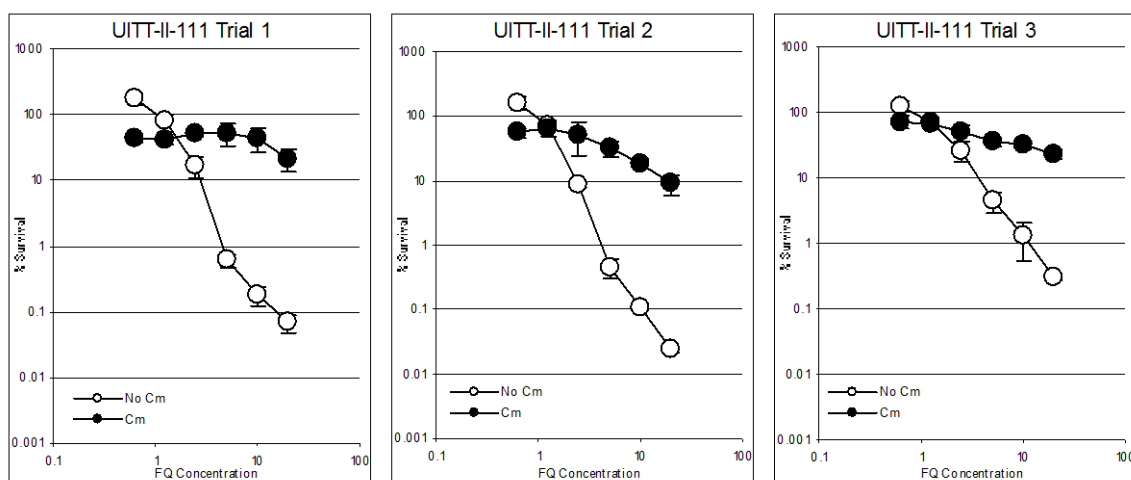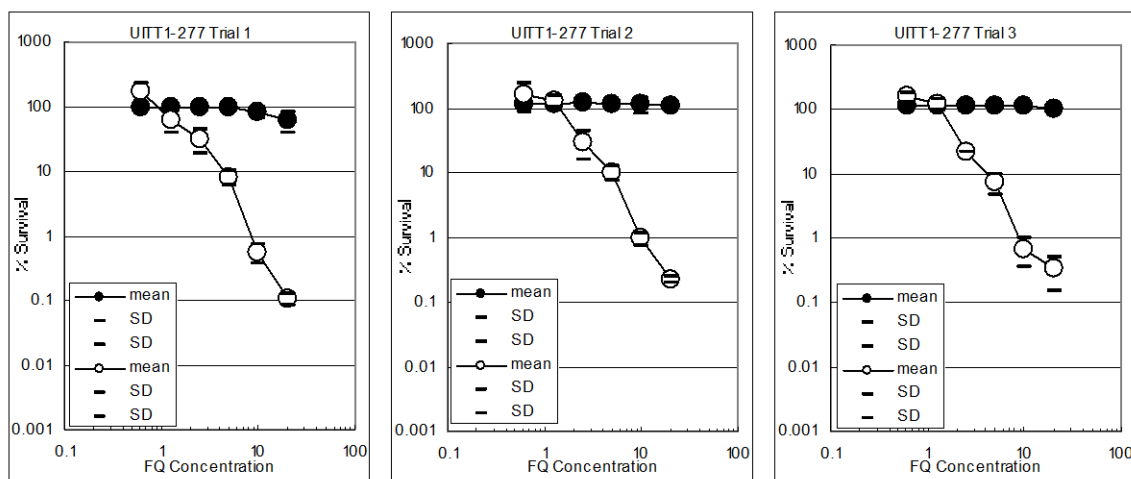
Figure B 20. Lethal activity of **43** UITT-I-111 in the presence and absence of chloramphenicol. Survival of *E. coli* (y-axis) was measured as a function of **43** concentration expressed as a multiple of the MIC (x-axis) in the presence (filled circles) or absence (open circles) of chloramphenicol, an inhibitor of protein synthesis. The error bars represent standard deviations of the means shown for each of the three trials.
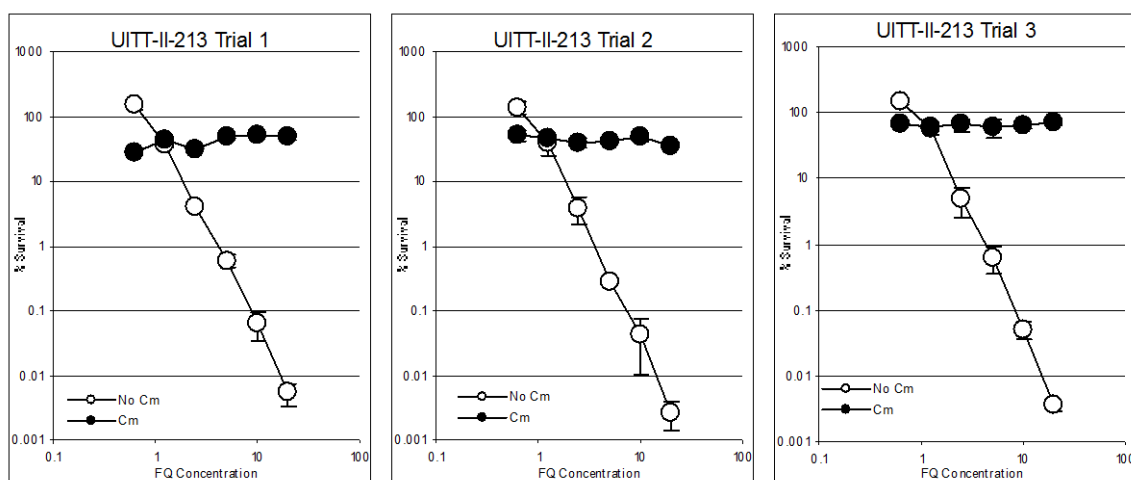

Figure B 21. Lethal activity of **44** UITT-I-277 in the presence and absence of chloramphenicol. Survival of *E. coli* (y-axis) was measured as a function of **44** concentration expressed as a multiple of the MIC (x-axis) in the presence (filled circles) or absence (open circles) of chloramphenicol, an inhibitor of protein synthesis. The error bars represent standard deviations of the means shown for each of the three trials.
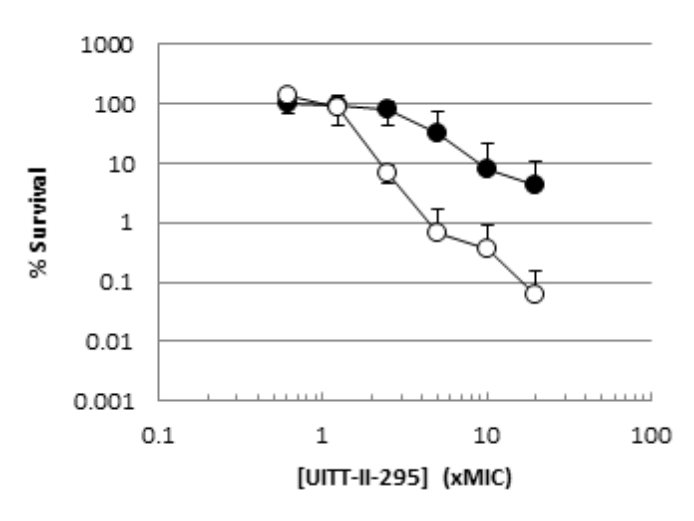
Figure B 22. Lethal activity of **45** UITT-I-195 in the presence and absence of chloramphenicol. Survival of *E. coli* (y-axis) was measured as a function of **45** concentration expressed as a multiple of the MIC (x-axis) in the presence (filled circles) or absence (open circles) of chloramphenicol, an inhibitor of protein synthesis. The error bars represent standard deviations of the means shown for each of the three trials.

Figure B 23. Lethal activity of **46** UITT-II-295 in the presence and absence of chloramphenicol. Survival of *E. coli* was measured as a function of **46** concentration expressed as a multiple of the MIC in the presence (filled circles) or absence (open circles) of chloramphenicol, an inhibitor of protein synthesis. The error bars represent standard deviations of the means shown.
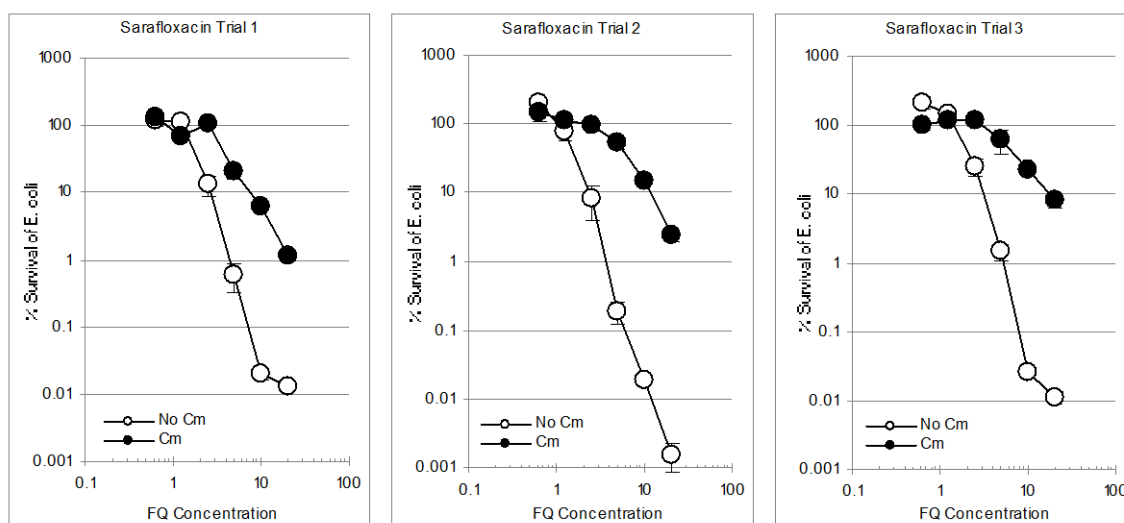
Figure B 24. Lethal activity of sarafloxacin in the presence and absence of chloramphenicol. Survival of *E. coli* (y-axis) was measured as a function of sarafloxacin concentration expressed as a multiple of the MIC (x-axis) in the presence (filled circles) or absence (open circles) of chloramphenicol, an inhibitor of protein synthesis. The error bars represent standard deviations of the means shown for each of the three trials.
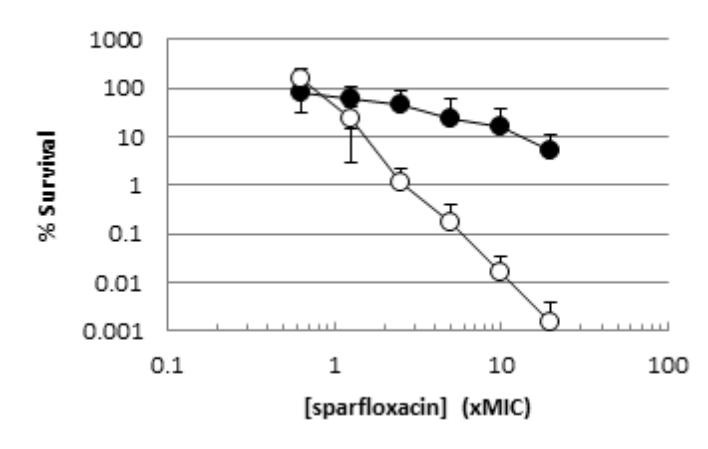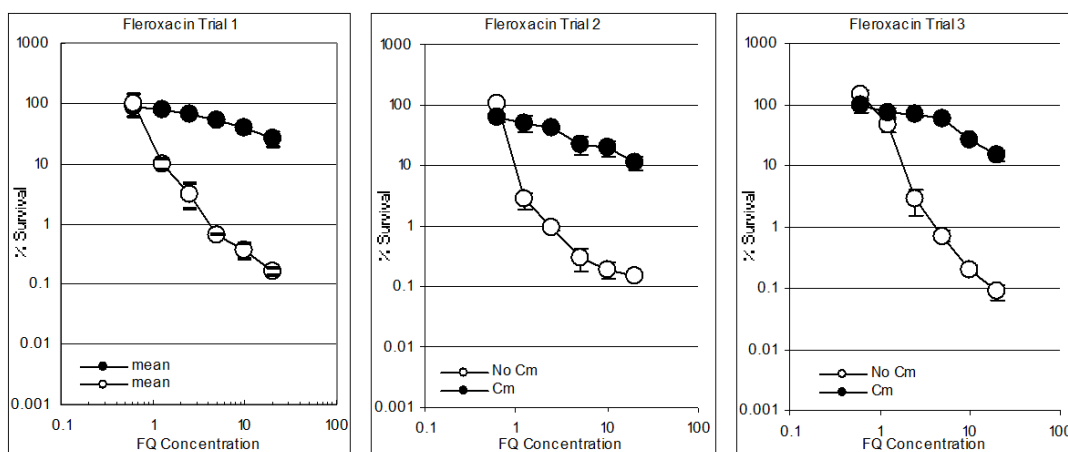

Figure B 25. Lethal activity of sparfloxacin in the presence and absence of chloramphenicol. Survival of *E. coli* was measured as a function of sparfloxacin concentration expressed as a multiple of the MIC in the presence (filled circles) or absence (open circles) of chloramphenicol, an inhibitor of protein synthesis. The error bars represent standard deviations of the means shown.

Figure B 26. Lethal activity of fleroxacin in the presence and absence of chloramphenicol. Survival of *E. coli* (y-axis) was measured as a function of fleroxacin concentration expressed as a multiple of the MIC (x-axis) in the presence (filled circles) or absence (open circles) of chloramphenicol, an inhibitor of protein synthesis. The error bars represent standard deviations of the means shown for each of the three trials.
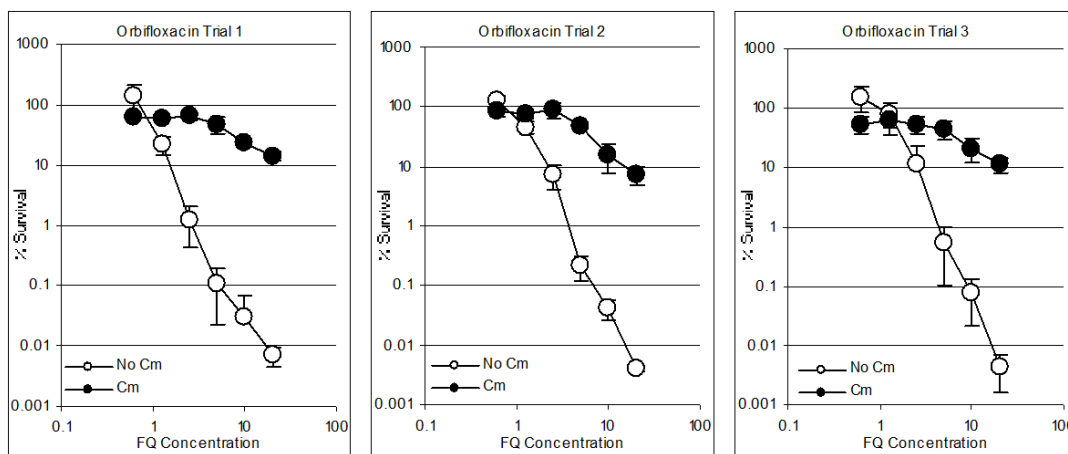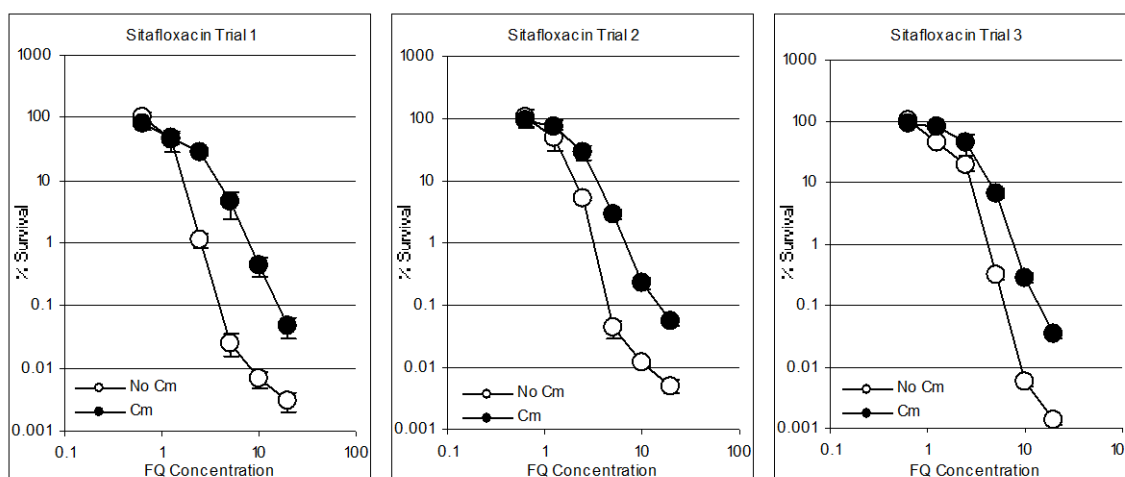

Figure B 27. Lethal activity of orbifloxacin in the presence and absence of chloramphenicol. Survival of *E. coli* (y-axis) was measured as a function of orbifloxacin concentration expressed as a multiple of the MIC (x-axis) in the presence (filled circles) or absence (open circles) of chloramphenicol, an inhibitor of protein synthesis. The error bars represent standard deviations of the means shown for each of the three trials.
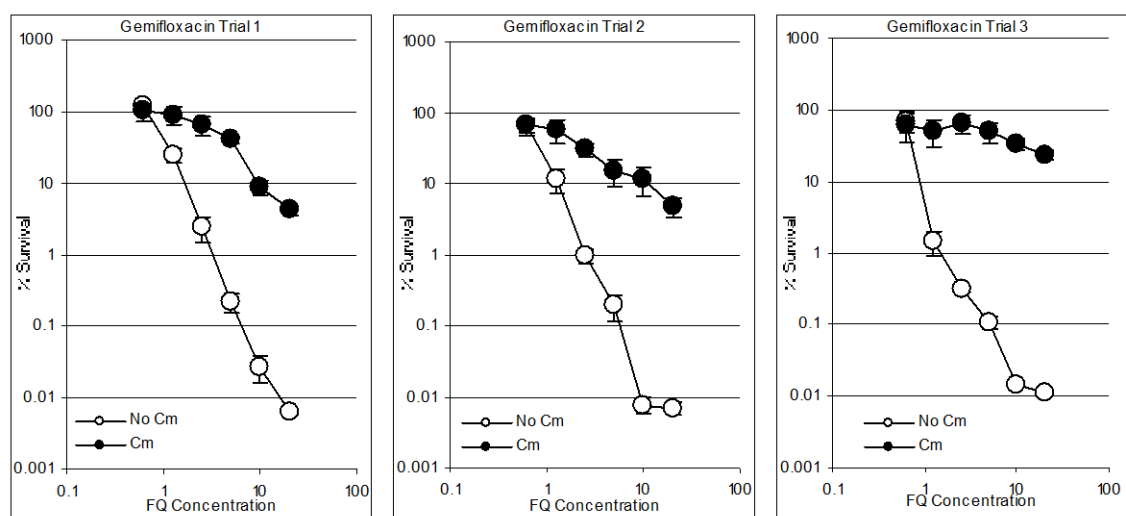
Figure B 28. Lethal activity of sitafloxacin in the presence and absence of chloramphenicol. Survival of *E. coli* (y-axis) was measured as a function of sitafloxacin concentration expressed as a multiple of the MIC (x-axis) in the presence (filled circles) or absence (open circles) of chloramphenicol, an inhibitor of protein synthesis. The error bars represent standard deviations of the means shown for each of the three trials.
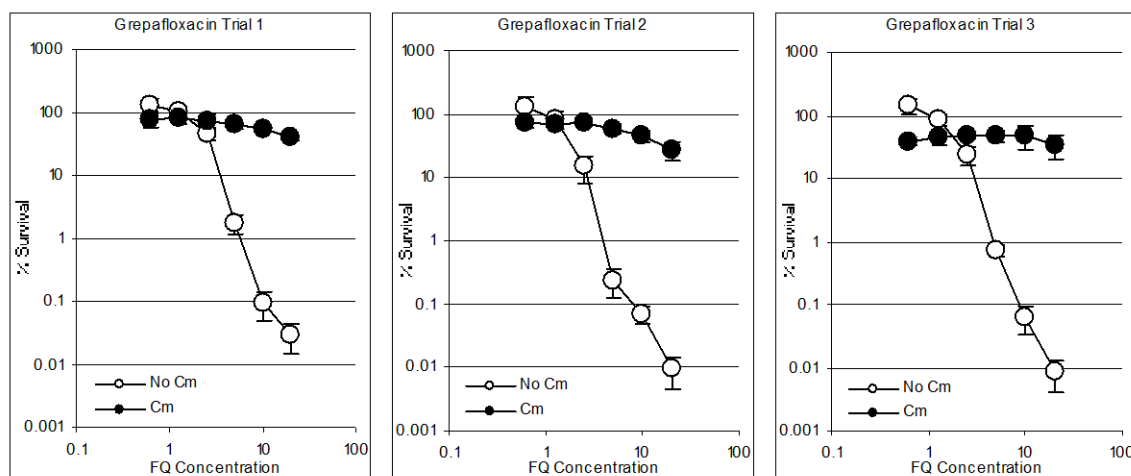

Figure B 29. Lethal activity of gemifloxacin in the presence and absence of chloramphenicol. Survival of *E. coli* (y-axis) was measured as a function of gemifloxacin concentration expressed as a multiple of the MIC (x-axis) in the presence (filled circles) or absence (open circles) of chloramphenicol, an inhibitor of protein synthesis. The error bars represent standard deviations of the means shown for each of the three trials.
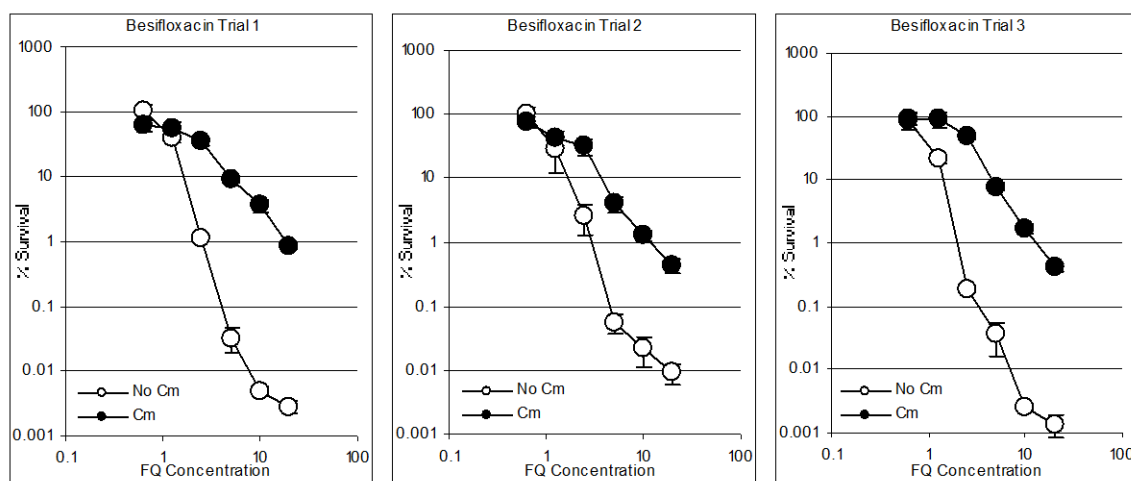
Figure B 30. Lethal activity of grepafloxacin in the presence and absence of chloramphenicol. Survival of *E. coli* (y-axis) was measured as a function of grepafloxain concentration expressed as a multiple of the MIC (x-axis) in the presence (filled circles) or absence (open circles) of chloramphenicol, an inhibitor of protein synthesis. The error bars represent standard deviations of the means shown for each of the three trials.
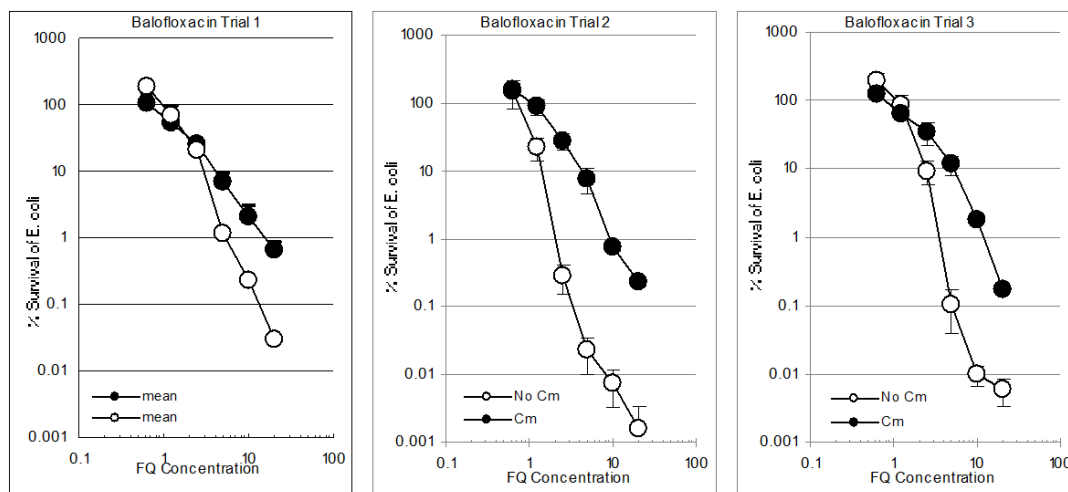

Figure B 31. Lethal activity of balofloxacin in the presence and absence of chloramphenicol. Survival of *E. coli* (y-axis) was measured as a function of balofloxacin concentration expressed as a multiple of the MIC (x-axis) in the presence (filled circles) or absence (open circles) of chloramphenicol, an inhibitor of protein synthesis. The error bars represent standard deviations of the means shown for each of the three trials.

Figure B 32. Lethal activity of balofloxacin in the presence and absence of chloramphenicol. Survival of *E. coli* (y-axis) was measured as a function of balofloxacin concentration expressed as a multiple of the MIC (x-axis) in the presence (filled circles) or absence (open circles) of chloramphenicol, an inhibitor of protein synthesis. The error bars represent standard deviations of the means shown for each of the three trials.
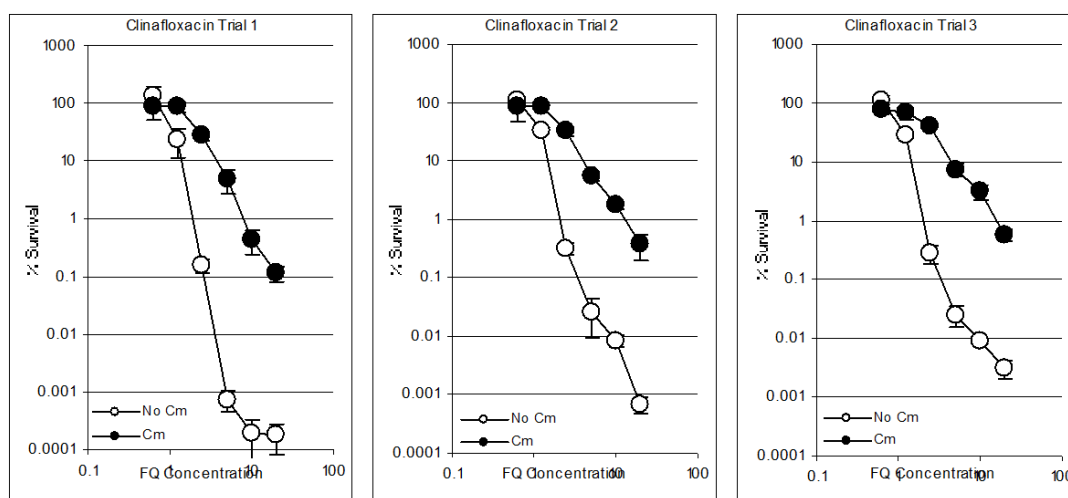

Figure B 33. Lethal activity of clinafloxacin in the presence and absence of chloramphenicol. Survival of *E. coli* (y-axis) was measured as a function of clinafloxacin concentration expressed as a multiple of the MIC (x-axis) in the presence (filled circles) or absence (open circles) of chloramphenicol, an inhibitor of protein synthesis. The error bars represent standard deviations of the means shown for each of the three trials.
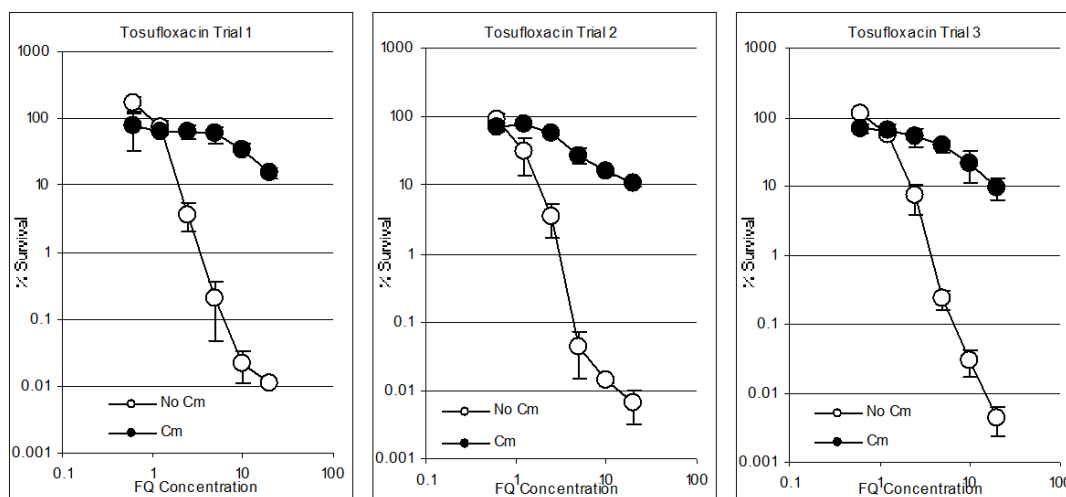
Figure B 34. Lethal activity of tosufloxacin in the presence and absence of chloramphenicol. Survival of *E. coli* (y-axis) was measured as a function of tosufloxacin concentration expressed as a multiple of the MIC (x-axis) in the presence (filled circles) or absence (open circles) of chloramphenicol, an inhibitor of protein synthesis. The error bars represent standard deviations of the means shown for each of the three trials.
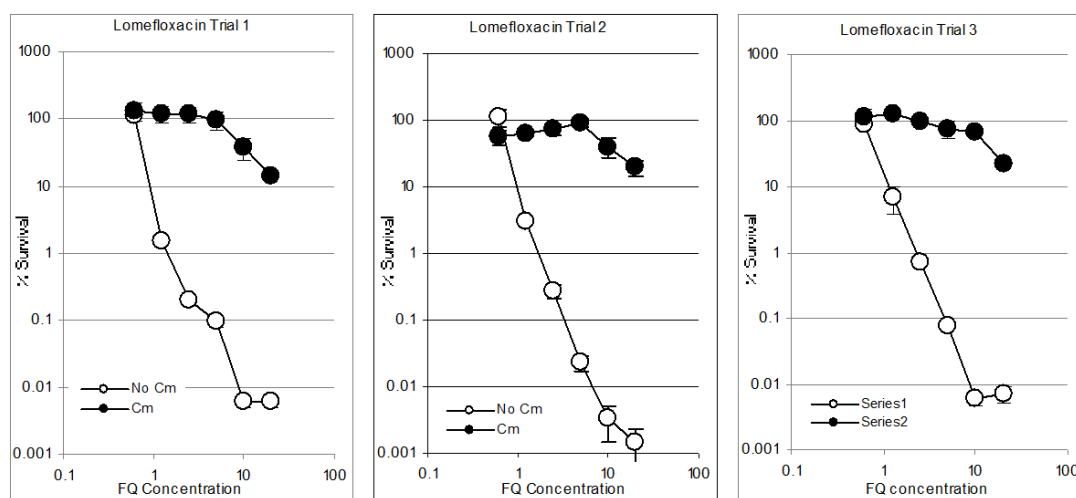

Figure B 35. Lethal activity of lomefloxacin in the presence and absence of chloramphenicol. Survival of *E. coli* (y-axis) was measured as a function of tosufloxacin concentration expressed as a multiple of the MIC (x-axis) in the presence (filled circles) or absence (open circles) of chloramphenicol, an inhibitor of protein synthesis. The error bars represent standard deviations of the means shown for each of the three trials
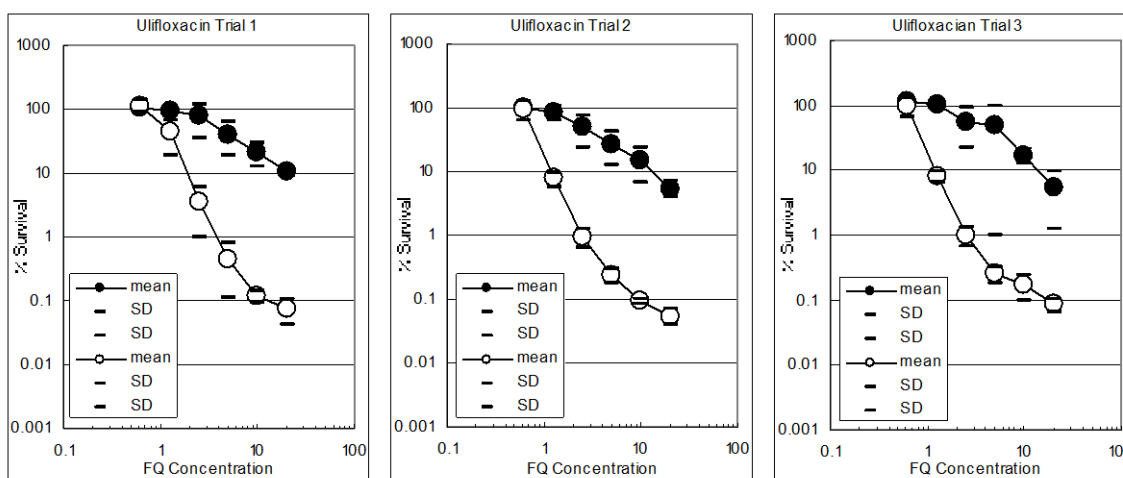
Figure B 36. Lethal activity of ulifloxacin in the presence and absence of chloramphenicol. Survival of *E. coli* (y-axis) was measured as a function of ulifloxacin concentration expressed as a multiple of the MIC (x-axis) in the presence (filled circles) or absence (open circles) of chloramphenicol, an inhibitor of protein synthesis. The error bars represent standard deviations of the means shown for each of the three trials.
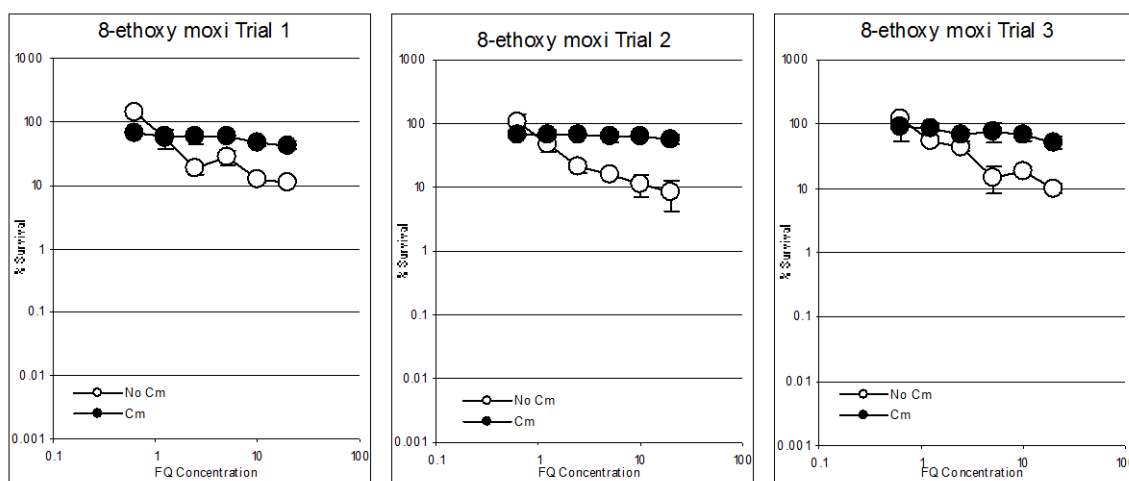

Figure B 37. Lethal activity of 8-ethoxy moxifloxacin in the presence and absence of chloramphenicol. Survival of *E. coli* (y-axis) was measured as a function of 8-ethoxy moxifloxacin concentration expressed as a multiple of the MIC (x-axis) in the presence (filled circles) or absence (open circles) of chloramphenicol, an inhibitor of protein synthesis. The error bars represent standard deviations of the means shown for each of the three trials.
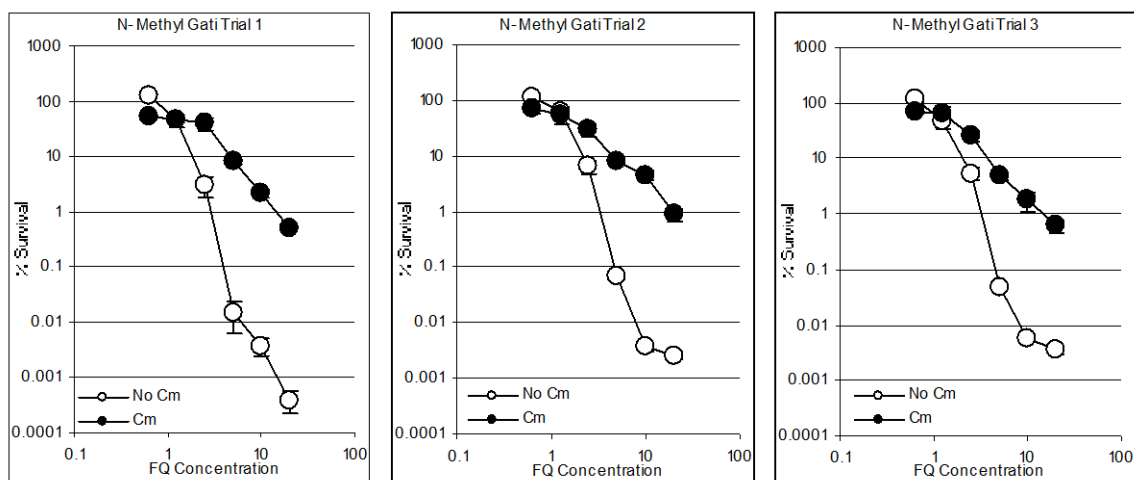
Figure B 38. Lethal activity of N-methyl gatifloxacin in the presence and absence of chloramphenicol. Survival of *E. coli* (y-axis) was measured as a function of N-methyl gatifloxacin concentration expressed as a multiple of the MIC (x-axis) in the presence (filled circles) or absence (open circles) of chloramphenicol, an inhibitor of protein synthesis. The error bars represent standard deviations of the means shown for each of the three trials.

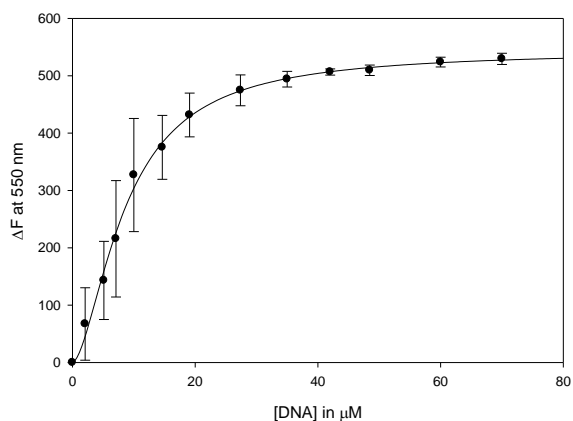APPENDIX C. FLUORESCENCE-BASED DNA BINDING PLOTS

Figure C 1. Binding curve of ciprofloxacin **72** to SS DNA in the absence of Mg^{2++}.
$K_{app} = 36.78 \pm 8.1$ µM, $R^2 = 0.996$; N = 1.67, $B_{max} = 543.6$.
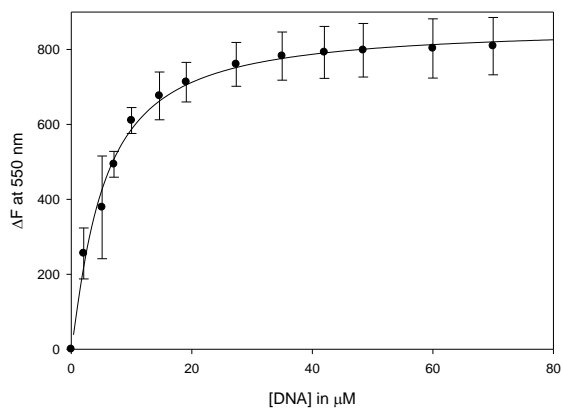

Figure C 2. Binding curve of ciprofloxacin **72** to SS DNA in the presence of Mg^{2++}.
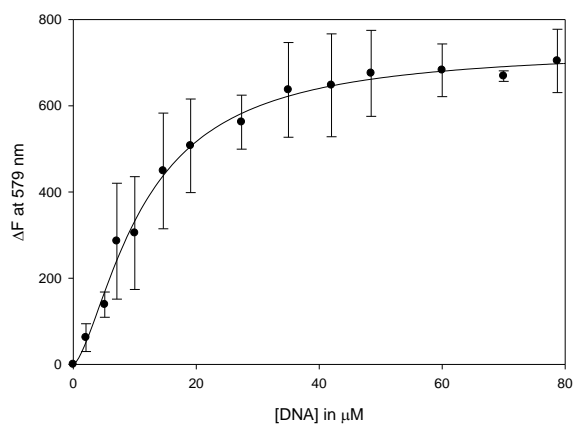$K_{app} = 6.79 \pm 1.1$ µM, $R^2 = 0.994$; N = 1.17, $B_{max} = 860$.

Figure C 3. Binding curve of moxifloxacin **73** to SS DNA in the absence of Mg^{2++}.
K$_{app}$ = 40.25 ±11.1 µM, R^2 = 0.994; N = 1.52, B$_{max}$ = 733.7.
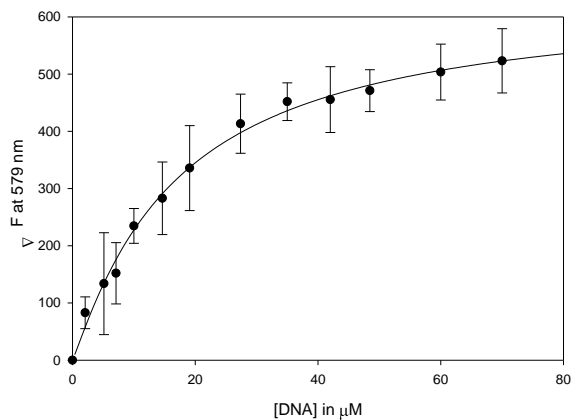

Figure C 4. Binding curve of moxifloxacin **73** to SS DNA in the presence of Mg^{2++}.
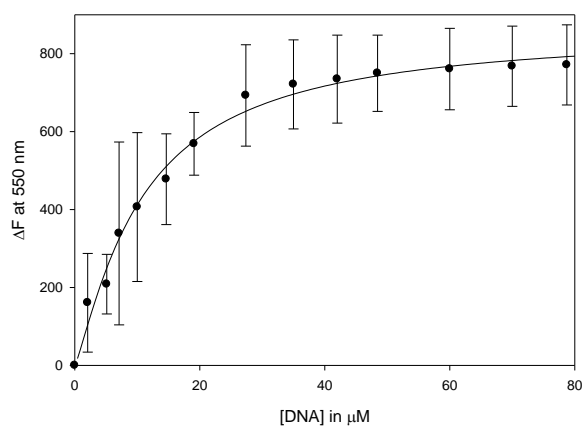K$_{app}$ = 22.17 ±3.7 µM, R^2 = 0.995; N = 1.09, B$_{max}$ = 634.9.

Figure C 5. Binding curve of DNP-cipro **74** to SS DNA in the absence of Mg^{2++}.
K_{app} = 17.67 ±4.5 μM, R^2 = 0.989; N = 1.21, B_{max} = 864.7.

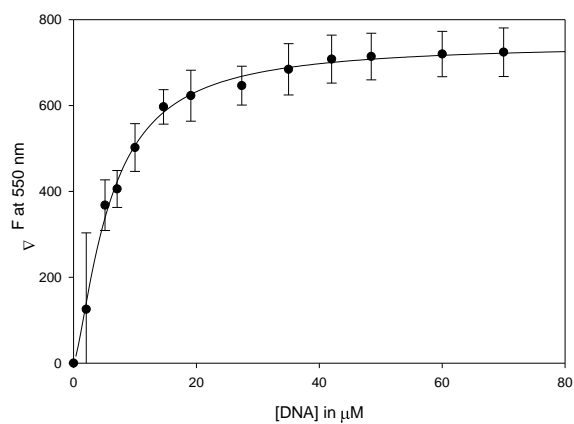Figure C 6. Binding curve of DNP-cipro **74** to SS DNA in the presence of Mg^{2++}.
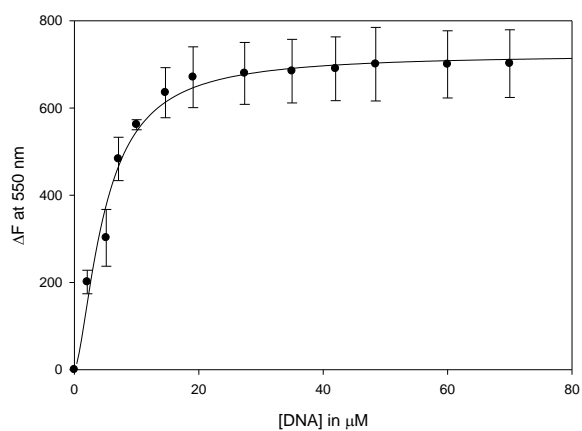K_{app} = 11.93 ±1.8 μM, R^2 = 0.997; N = 1.41, B_{max} = 743.9.

Figure C 7. Binding curve of ciprofloxacin **72** to DS DNA in the absence of Mg^{2++}.
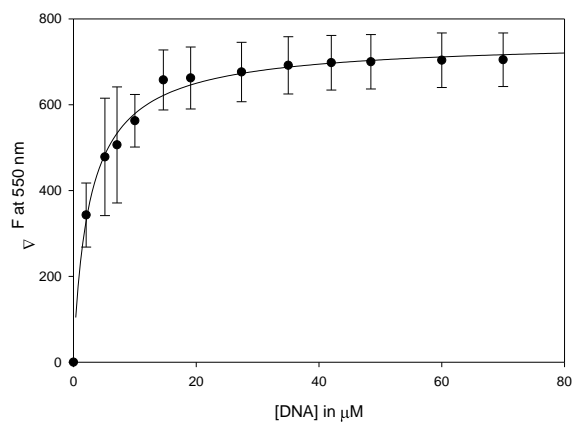$K_{app} = 11.59 \pm 4.0$ µM, $R^2 = 0.984$; N = 1.56, $B_{max} = 722.5$.

Figure C 8. Binding curve of ciprofloxacin **72** to DS DNA in the presence of Mg^{2++}.
$K_{app} = 2.51 \pm 0.3$ µM, $R^2 = 0.925$; N = 0.925, $B_{max} = 751.9$.
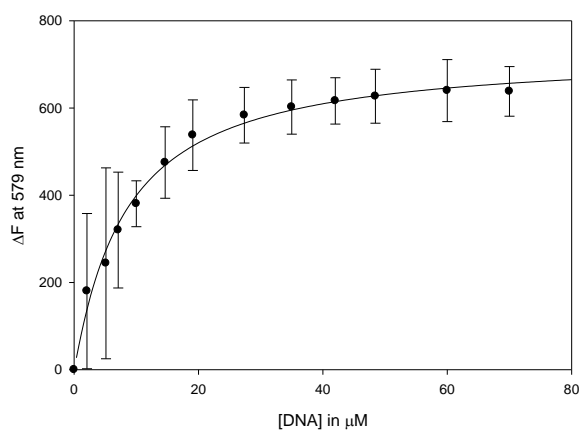
Figure C 9. Binding curve of moxifloxacin **73** to DS DNA in the absence of Mg^{2++}.
$K_{app} = 9.17 \pm 1.7$ μM, $R^2 = 0.991$, N = 1.05, $B_{max} = 726.7$.
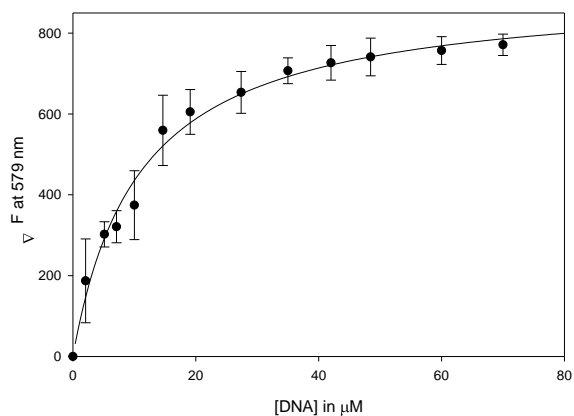
Figure C 10. Binding curve of moxifloxacin **73** toDSS DNA in the presence of Mg^{2++}.
$K_{app} = 10.71 \pm 2.3$ μM, $R^2 = 0.987$; N = 0.991, $B_{max} = 910.9$.
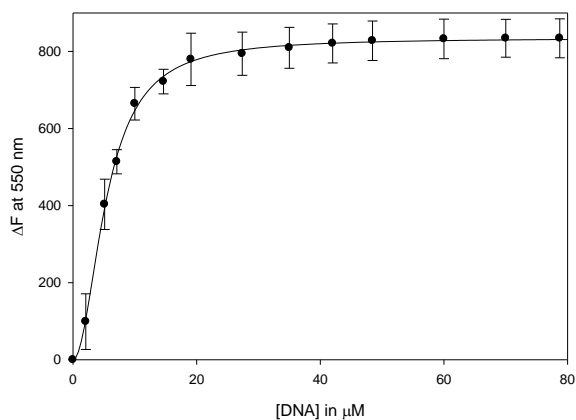
Figure C 11. Binding curve of DNP-cipro **74** to DS DNA in the absence of Mg^{2++}.
$K_{app} = 30.28 \pm 3.8$ μM, $R^2 = 0.999$; N = 2.02, $B_{max} = 834.7$.

Figure C 12. Binding curve of DNP-cipro **74** to DS DNA in the presence of Mg^{2++}.
$K_{app} = 6.89 \pm 0.6$ μM, $R^2 = 0.998$; N = 1.35, $B_{max} = 636.4$.
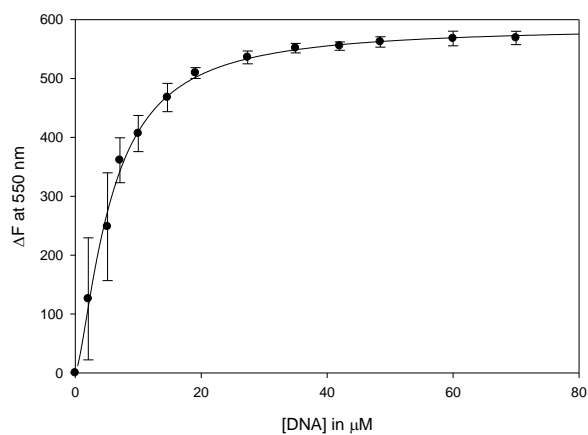
Figure C 13. Binding curve of ciprofloxacin **72** to nicked DNA in the absence of Mg^{2++}.
K_{app} = 12.13 ±1.8 μM, R^2 = 0.990; N = 1.45, B_{max} = 587.9.
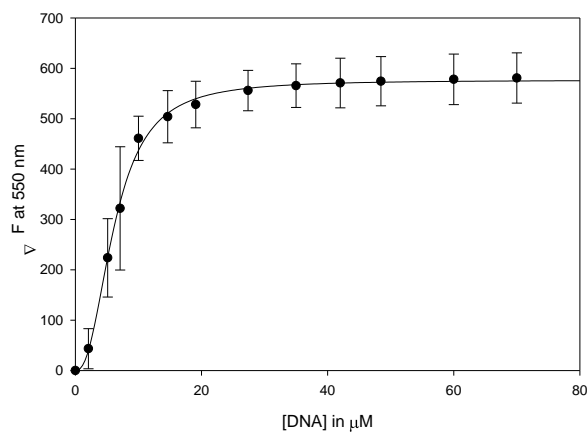
Figure C 14. Binding curve of ciprofloxacin **72** to nicked DNA in the presence of Mg^{2++}.
K_{app} = 76.67 ±18.2 μM, R^2 = 0.998; N = 2.38, B_{max} = 576.7.
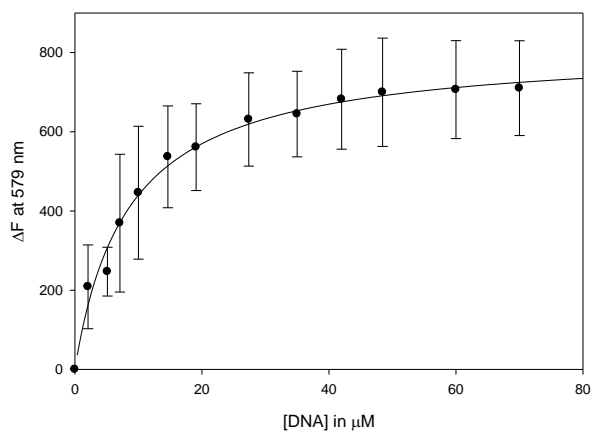
Figure C 15. Binding curve of moxifloxacin **73** to nicked DNA in the absence of Mg^{2++}.
$K_{app} = 8.24 \pm 1.6$ μM, $R^2 = 0.989$; N = 0.98, $B_{max} = 816.0$.
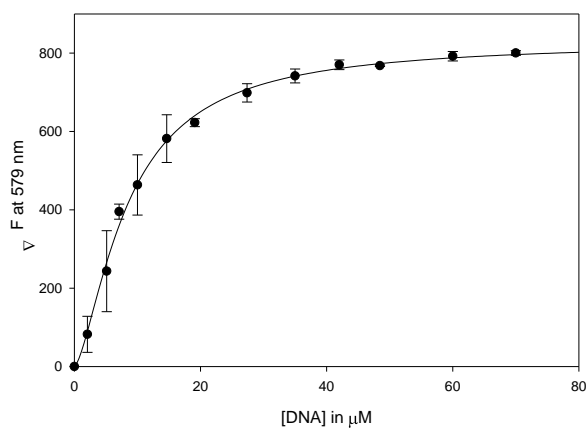
Figure C 16. Binding curve of moxifloxacin **73** to nicked DNA in the presence of Mg^{2++}.
$K_{app} = 24.55 \pm 4.0$ μM, $R^2 = 0.997$; N = 1.50, $B_{max} = 829.9$.
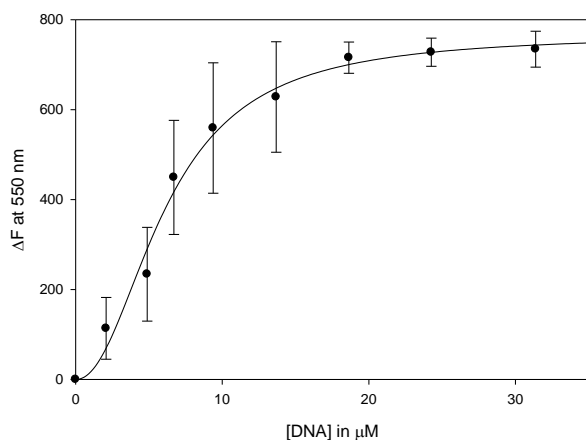
Figure C 17. Binding curve of DNP-cipro **74** to nicked DNA in the absence of Mg^{2++}. $K_{app} = 47.60 \pm 27.6$ µM, $R^2 = 0.989$; N = 2.12, $B_{max} = 767.2$.
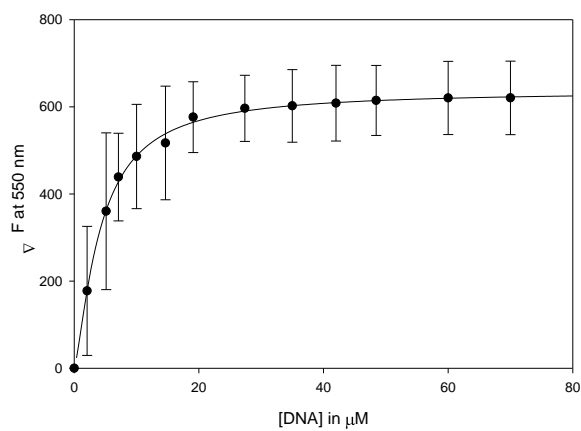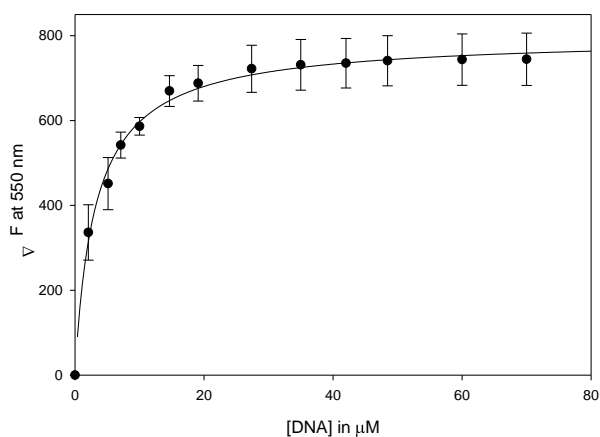

Figure C 18. Binding curve of DNP-cipro **74** to nicked DNA in the presence of Mg^{2++}. $K_{app} = 3.08 \pm 0.4$ µM, $R^2 = 0.995$; N = 0.96, $B_{max} = 798.8$.

APPENDIX D. MELTING TEMPERATURE (T_M) CURVES
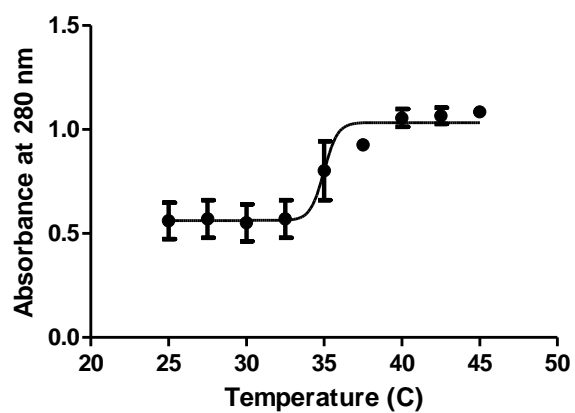
Figure D 1. T_m curve of DS DNA. $T_m = 35.3 \pm 1.0$ °C.
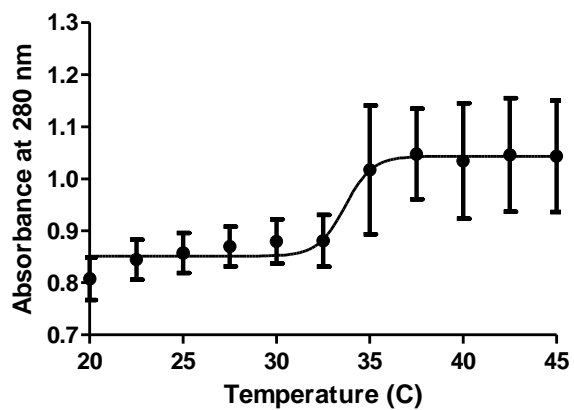
Figure D 2. T_m curve of nicked (N_1) DNA. $T_m = 33.9 \pm 0.9$ °C.
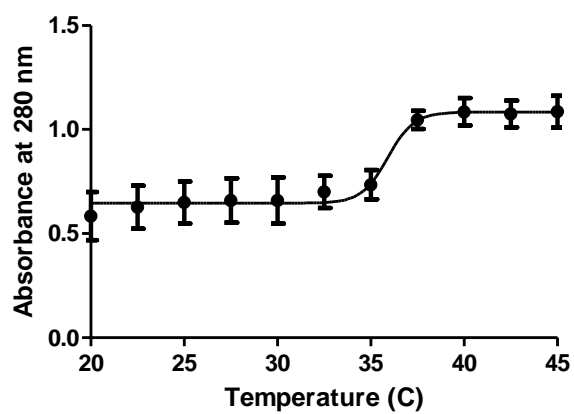
Figure D 3. T_m curve of nicked (N_2) DNA. $T_m = 35.9 \pm 0.8$ °C.
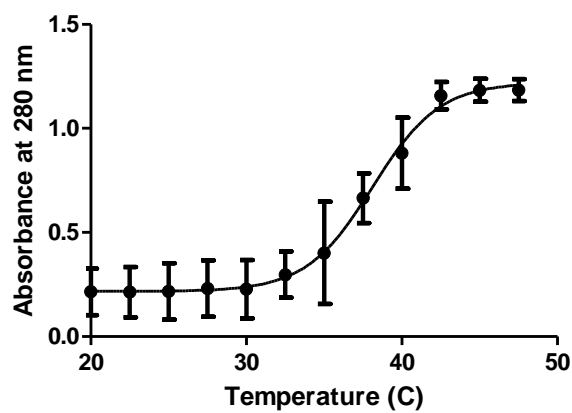
Figure D 4. T_m curve of DS DNA with EtBr at 20:1 DNA:EtBr. $T_m = 37.7 \pm 1.1$ °C.
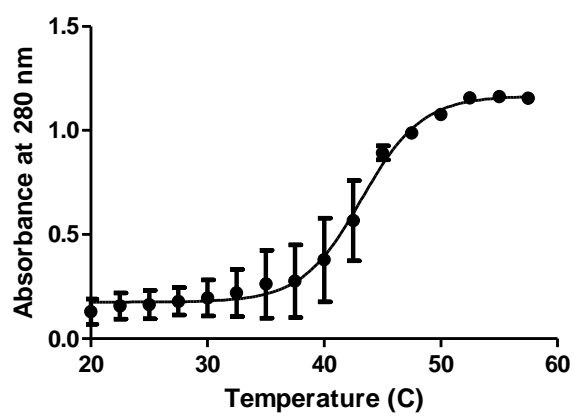
Figure D 5. T_m curve of DS DNA with EtBr at 1:1 DNA:EtBr. $T_m = 43.0 \pm 0.9$ °C.
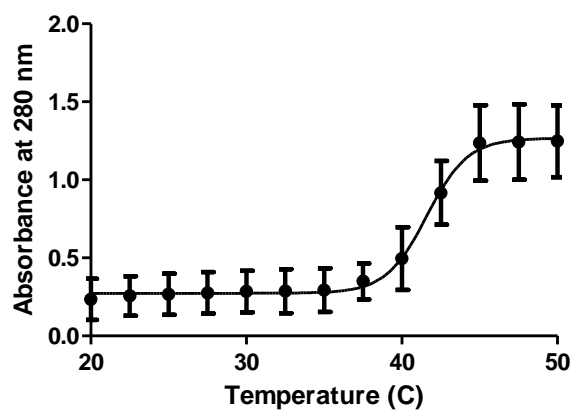
Figure D 6. T_m curve of nicked (N_1) DNA with EtBr at 20:1 DNA:EtBr. $T_m = 41.6 \pm 0.3$ °C.
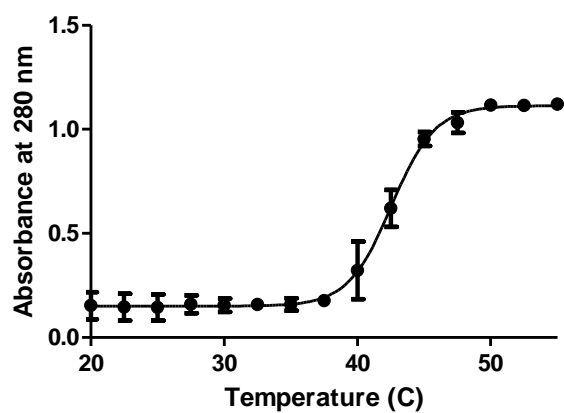
Figure D 7. T_m curve of nicked (N_1) DNA with EtBr at 1:1 DNA:EtBr. $T_m = 42.5 \pm 0.5$ °C.
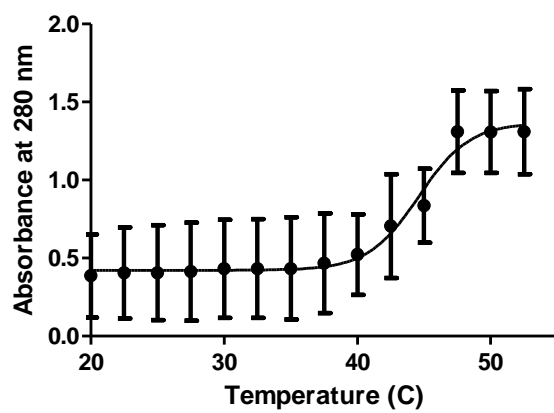
Figure D 8. T_m curve of nicked (N_2) DNA with EtBr at 20:1 DNA:EtBr. $T_m = 44.6 \pm 0.1$ °C.
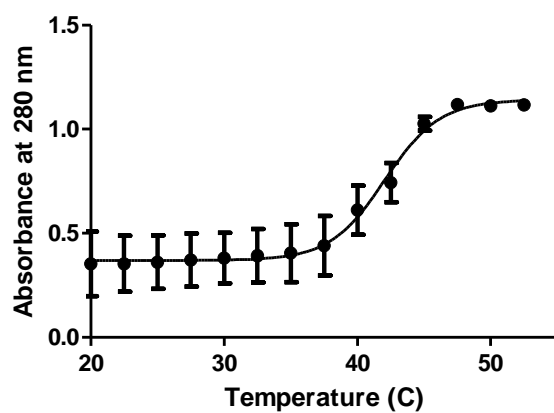
Figure D 9. T_m curve of nicked (N_2) DNA with EtBr at 1:1 DNA:EtBr. $T_m = 42.0 \pm$ 0.6 °C.
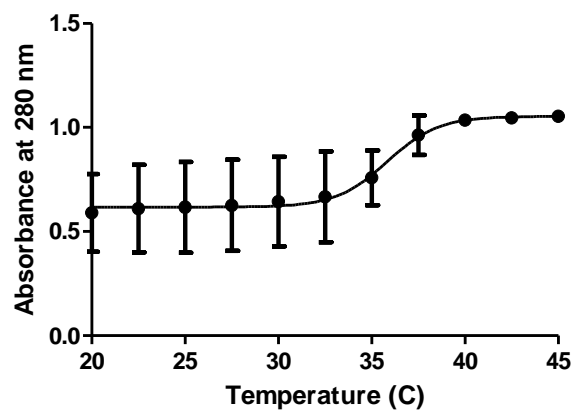
Figure D 10. T_m curve of DS DNA with ciprofloxacin **72** at 20:1 DNA:**72**. $T_m = 35.7 \pm$ 0.3 °C.
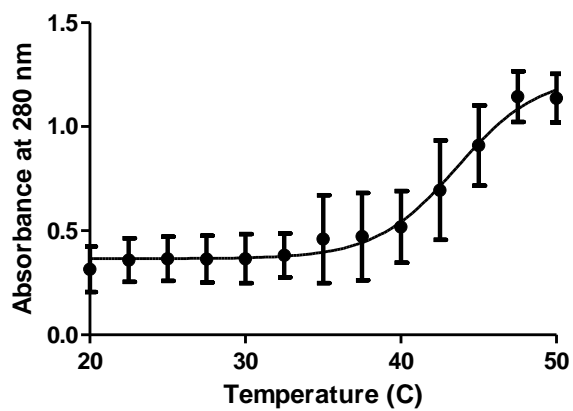
Figure D 11. T_m curve of DS DNA with ciprofloxacin **72** at 1:1 DNA:**72**. $T_m = 43.5 \pm$ 1.6 °C.

Figure D 12. T_m curve of nicked (N_1) DNA with ciprofloxacin **72** at 20:1 DNA:**72**. $T_m = 34.1 \pm 0.5$ °C.
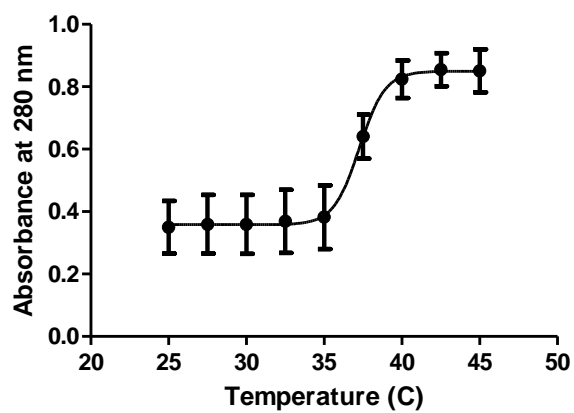
Figure D 13. T_m curve of nicked (N_1) DNA with ciprofloxacin **72** at 1:1 DNA:**72**. $T_m = 37.5 \pm 1.3$ °C.
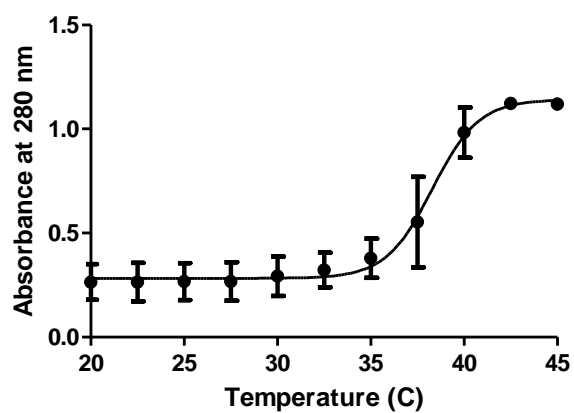
Figure D 14. T_m curve of nicked (N_2) DNA with ciprofloxacin **72** at 20:1 DNA:**72**. $T_m = 38.3 \pm 1.2$ °C.
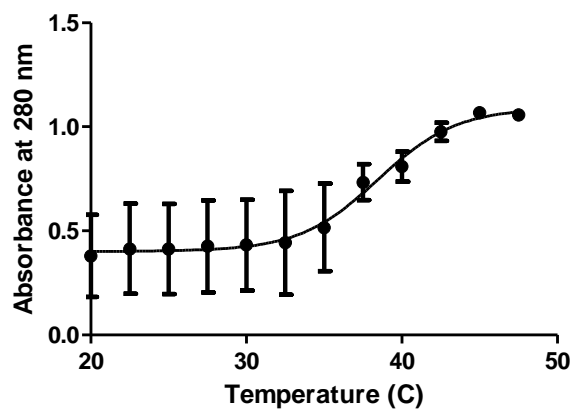
Figure D 15. T_m curve of nicked (N_2) DNA with ciprofloxacin **72** at 1:1 DNA:**72**. T_m = 38.9 ± 1.4 °C.
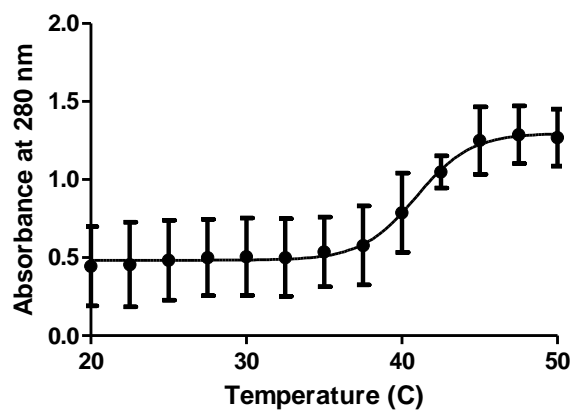
Figure D 16. T_m curve of DS DNA with moxifloxacin **73** at 20:1 DNA:**73**. T_m = 41.0 ± 0.2 °C.
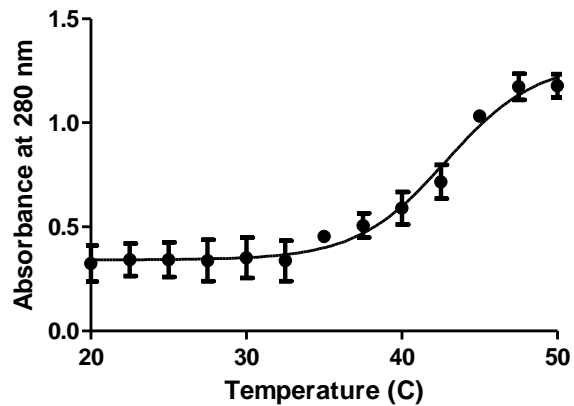
Figure D 17. T_m curve of DS DNA with moxifloxacin **73** at 1:1 DNA:**73**. $T_m = 42.9 \pm 0.7\ °C$
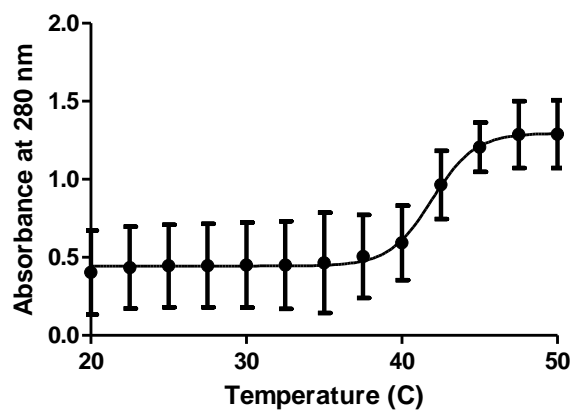
Figure D 18. T_m curve of nicked (N_1) DNA with moxifloxacin **73** at 20:1 DNA:**73**. $T_m = 41.9 \pm 0.4\ °C$.
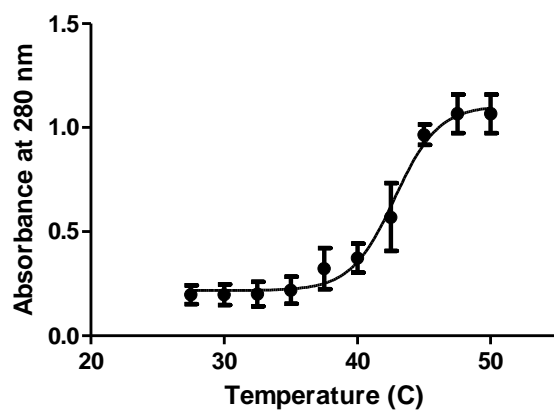
Figure D 19. T_m curve of nicked (N_1) DNA with moxifloxacin **73** at 1:1 DNA:**73**. T_m = 42.6 ± 1.5 °C.
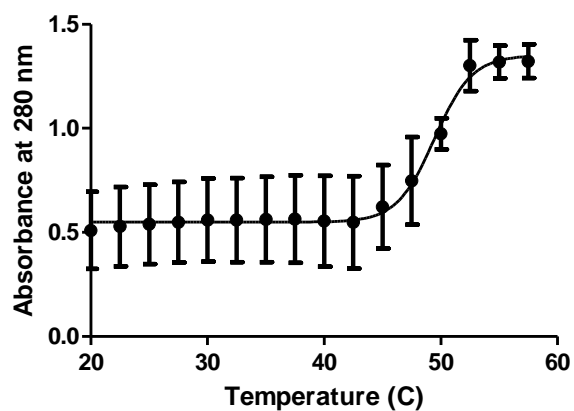
Figure D 20. T_m curve of nicked (N_2) DNA with moxifloxacin **73** at 20:1 DNA:**73**. T_m = 49.5 ± 0.5 °C.
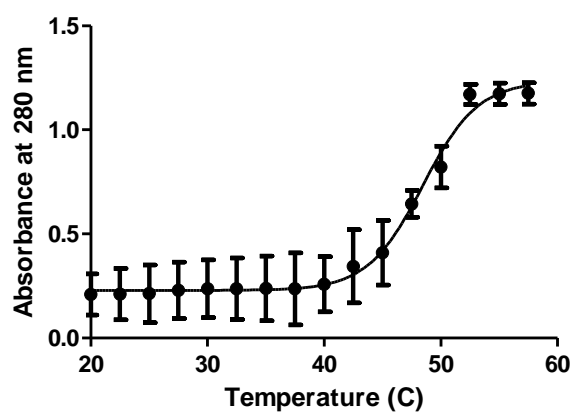
Figure D 21. T_m curve of nicked (N_2) DNA with moxifloxacin **73** at 1:1 DNA:**73**. T_m = 48.4 ± 0.9 °C.
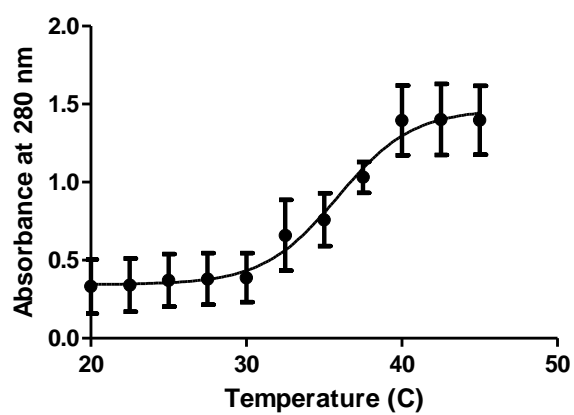
Figure D 22. T_m curve of DS DNA with UIHS-IIa-101 **52** at 20:1 DNA:**52**. T_m = 35.9 ± 0.2 °C.
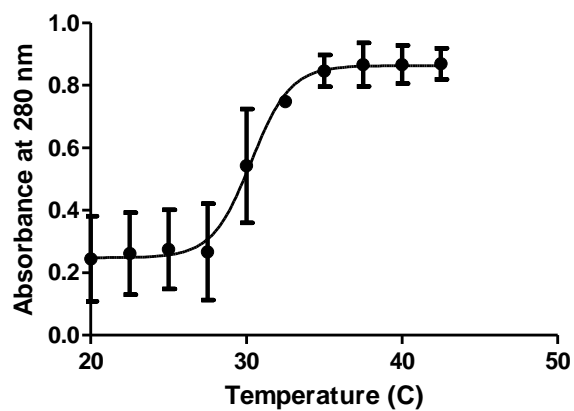
Figure D 23. T_m curve of DS DNA with UIHS-IIa-101 **52** at 1:1 DNA:**52**. $T_m = 30.3 \pm 0.5$ °C.

Figure D 24. T_m curve of nicked (N_1) DNA with UIHS-IIa-101 **52** at 20:1 DNA:**52**. $T_m = 33.8 \pm 0.7$ °C.

Figure D 25. T_m curve of nicked (N_1) DNA with UIHS-IIa-101 **52** at 1:1 DNA:**52**. T_m = 32.6 ± 1.0 °C.

Figure D 26. T_m curve of nicked (N_2) DNA with UIHS-IIa-101 **52** at 20:1 DNA:**52**. T_m = 33.6 ± 0.4 °C.
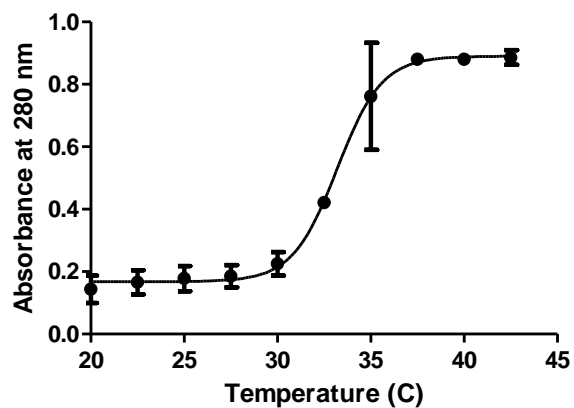
Figure D 27. T_m curve of nicked (N_2) DNA with UIHS-IIa-101 **52** at 1:1 DNA:**52**. $T_m = 33.3 \pm 0.5$ °C.

Figure D 28. T_m curve of DS DNA with UIHS-IIa-239 **50** at 20:1 DNA:**50**. $T_m = 33.9 \pm 0.5$ °C.
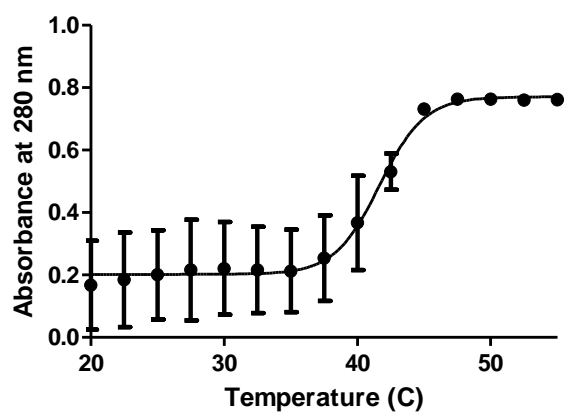
Figure D 29. T_m curve of DS DNA with UIHS-IIa-239 **50** at 1:1 DNA:**50**. $T_m = 41.6 \pm 0.8$ °C.
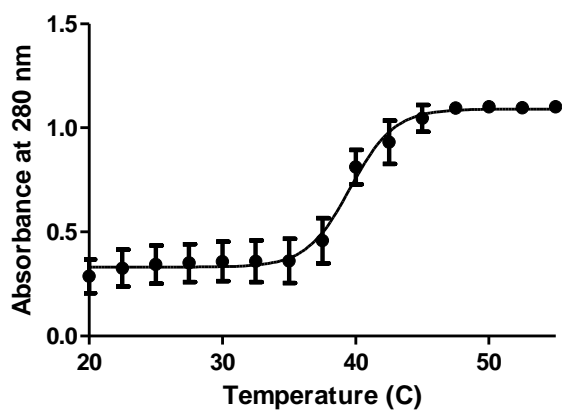
Figure D 30. T_m curve of nicked (N_1) DNA with UIHS-IIa-239 **50** at 20:1 DNA:**50**. $T_m = 39.7 \pm 0.8$ °C.
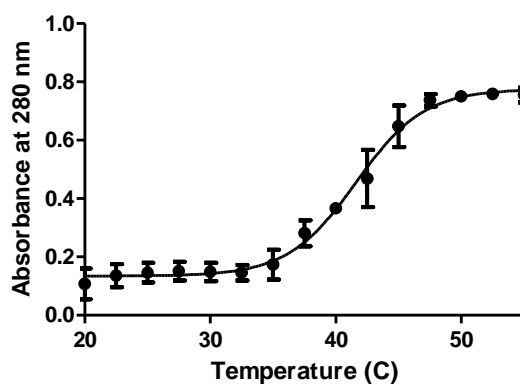
Figure D 31. T_m curve of nicked (N_1) DNA with UIHS-IIa-239 **50** at 1:1 DNA:**50**. T_m = 41.7 ± 1.2 °C.
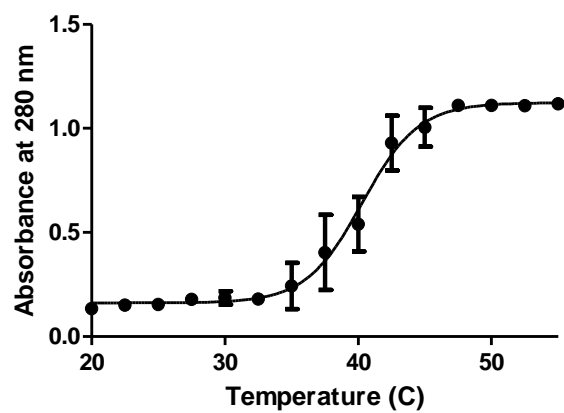
Figure D 32. T_m curve of nicked (N2) DNA with UIHS-IIa-239 **50** at 20:1 DNA:**50**. T_m = 40.2 ± 1.2 °C.
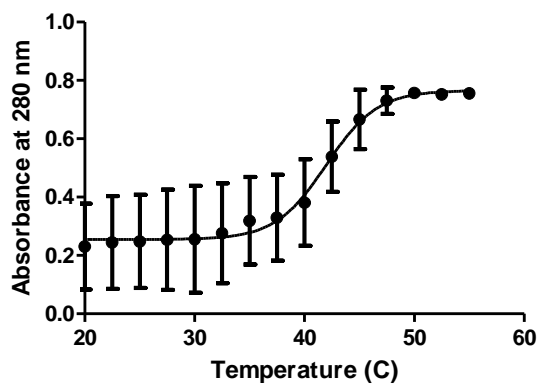
Figure D 33. T_m curve of nicked (N_2) DNA with UIHS-IIa-239 **50** at 1:1 DNA:**50**. T_m = 41.9 ± 0.5 °C.
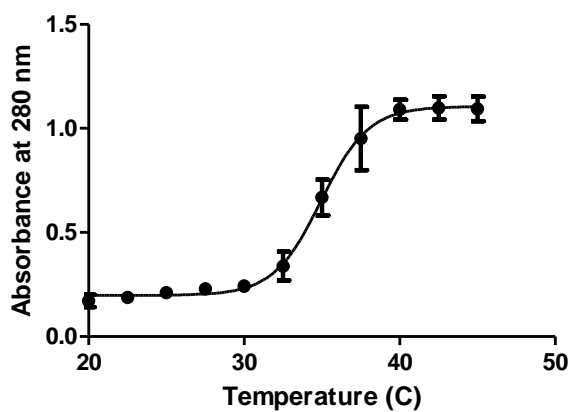
Figure D 34. T_m curve of DS DNA with UIJR-I-048 **57** at 20:1 DNA:**57**. T_m = 39.7 ± 1.3 °C.
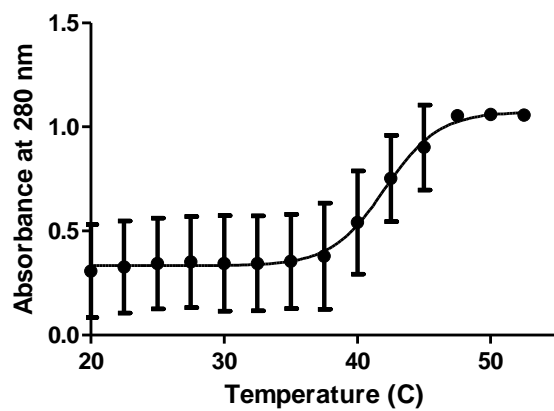
Figure D 35. T_m curve of DS DNA with UIJR-I-048 **57** at 1:1 DNA:**57**. $T_m = 34.1 \pm 0.9$ °C.
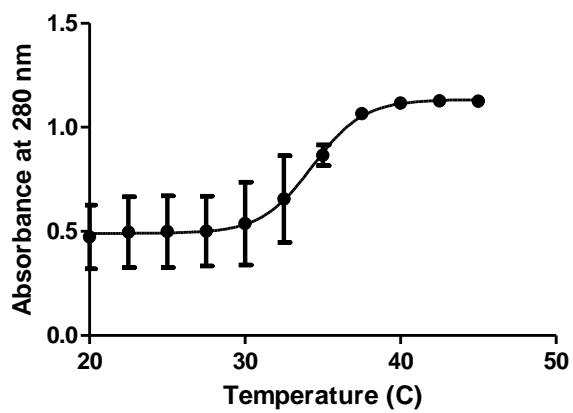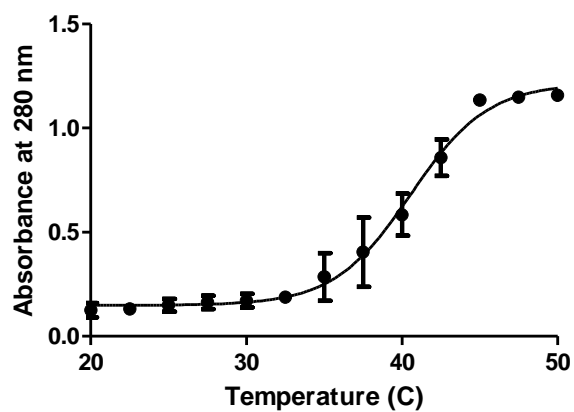

Figure D 36. T_m curve of nicked (N_1) DNA with UIJR-I-048 **57** at 20:1 DNA:**57**. $T_m = 41.3 \pm 0.8$ °C.
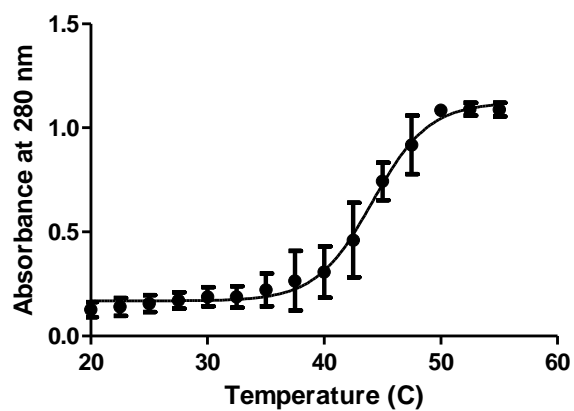
Figure D 37. T_m curve of nicked (N_1) DNA with UIJR-I-048 **57** at 1:1 DNA:**57**. T_m = 39.7 ± 1.0 °C.
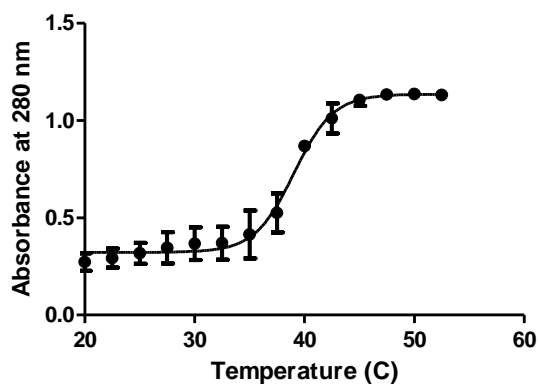
Figure D 38. T_m curve of nicked (N_2) DNA with UIJR-I-048 **57** at 20:1 DNA:**57**. T_m = 41.5 ± 0.7 °C.
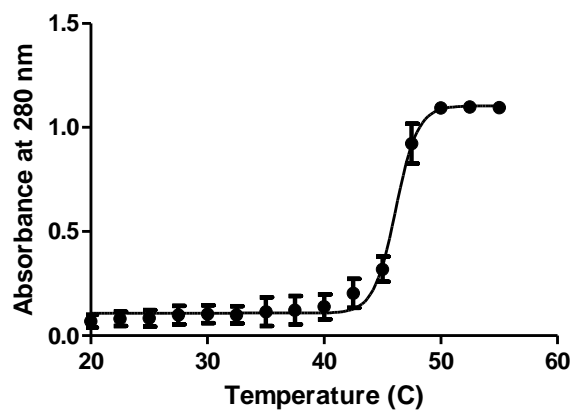
Figure D 39. T_m curve of nicked (N_2) DNA with UIJR-I-048 **57** at 1:1 DNA:**57**. T_m = 44.8 ± 0.2 °C.
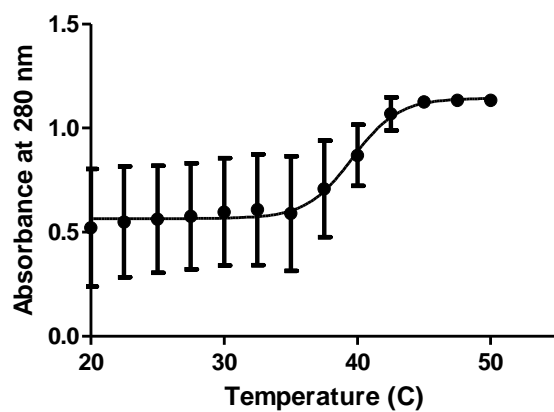
Figure D 40. T_m curve of DS DNA with UIHS-I-303 **29** at 20:1 DNA:**29**. T_m = 35.0 ± 0.4 °C
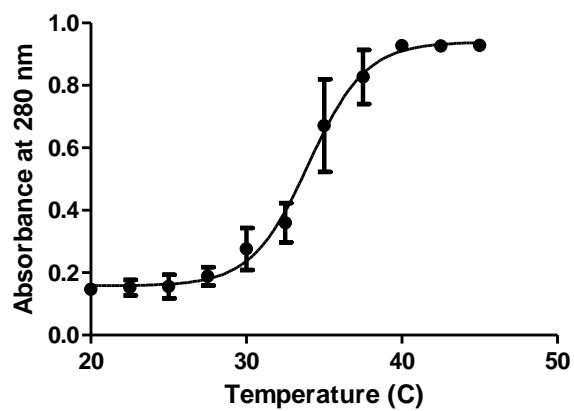
Figure D 41. T_m curve of DS DNA with UIHS-I-303 **29** at 1:1 DNA:**29**. $T_m = 41.9 \pm 1.0$ °C.
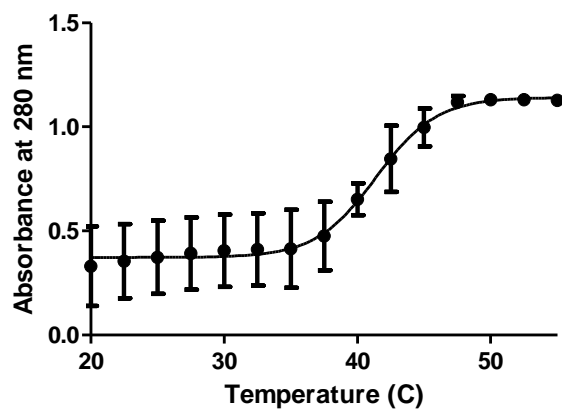
Figure D 42. T_m curve of nicked (N_1) DNA with UIHS-I-303 **29** at 20:1 DNA:**29**. $T_m = 40.5 \pm 0.7$ °C.
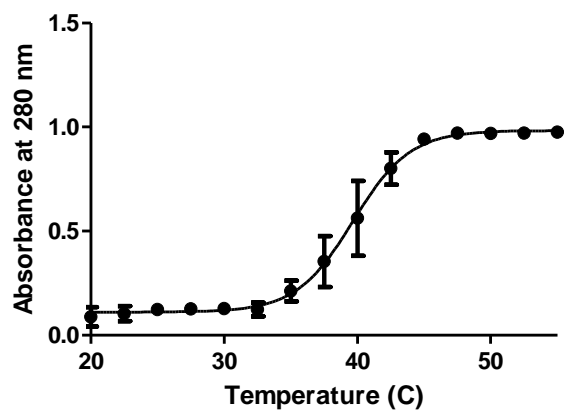
Figure D 43. T_m curve of nicked (N_1) DNA with UIHS-I-303 **29** at 1:1 DNA:**29**. $T_m =$ 44.0 ± 1.2 °C.
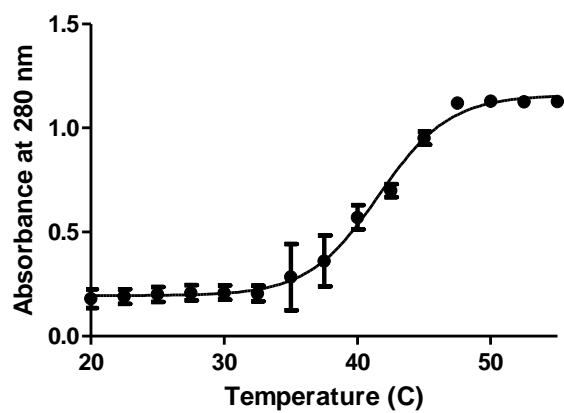
Figure D 44. T_m curve of nicked (N_2) DNA with UIHS-I-303 **29** at 20:1 DNA:**29**. $T_m =$ 38.9 ± 0.3 °C.

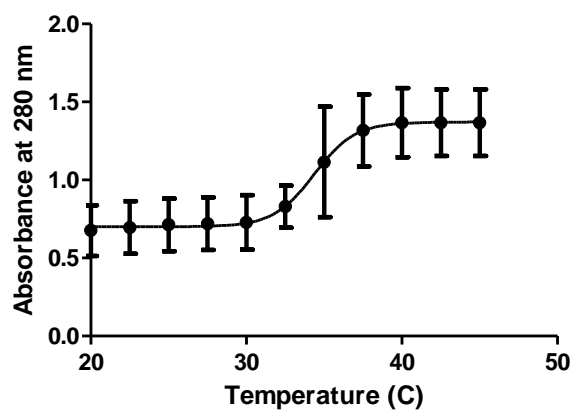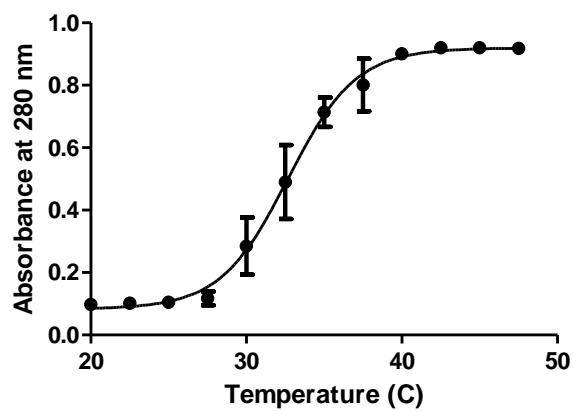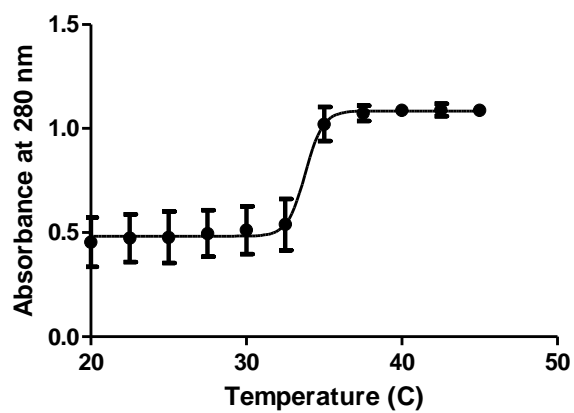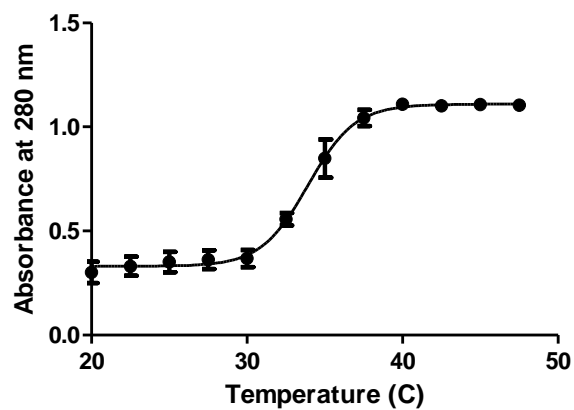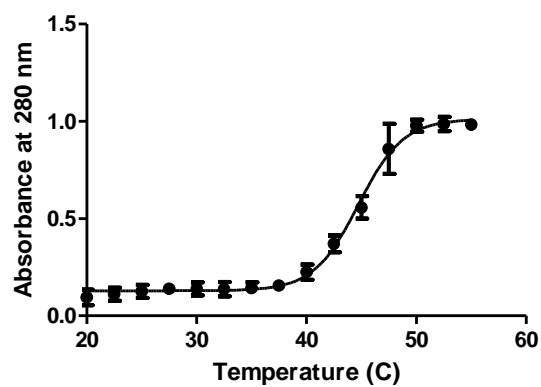Figure D 45. T_m curve of nicked (N_2) DNA with UIHS-I-303 **29** at 1:1 DNA:**29**. $T_m = 46.1 \pm 0.3°C$.

REFERENCES

1.   Silver, L.L., *Challenges of Antibacterial Discovery.* Clinical Microbiology Reviews, 2011. **24**(1): p. 71-109.

2.   Walsh, C. and G. Wright, *Introduction: antibiotic resistance.* Chemical reviews, 2005. **105**(2): p. 391-4.

3.   Livermore, D.M., *Has the era of untreatable infections arrived?* The Journal of antimicrobial chemotherapy, 2009. **64 Suppl 1**: p. i29-36.

4.   Fridkin, S.K., H.A. Hill, N.V. Volkova, J.R. Edwards, R.M. Lawton, R.P. Gaynes, and J.E. McGowan, Jr., *Temporal changes in prevalence of antimicrobial resistance in 23 US hospitals.* Emerging infectious diseases, 2002. **8**(7): p. 697-701.

5.   Lowy, F.D., *Antimicrobial resistance: the example of Staphylococcus aureus.* The Journal of clinical investigation, 2003. **111**(9): p. 1265-73.

6.   Rhomberg, P.R. and R.N. Jones, *Summary trends for the Meropenem Yearly Susceptibility Test Information Collection Program: a 10-year experience in the United States (1999-2008).* Diagnostic microbiology and infectious disease, 2009. **65**(4): p. 414-26.

7.   Agrawal, D., Z.F. Udwadia, C. Rodriguez, and A. Mehta, *Increasing incidence of fluoroquinolone-resistant Mycobacterium tuberculosis in Mumbai, India.* The international journal of tuberculosis and lung disease : the official journal of the International Union against Tuberculosis and Lung Disease, 2009. **13**(1): p. 79-83.

8.   Cooper, B.S., G.F. Medley, S.P. Stone, C.C. Kibbler, B.D. Cookson, J.A. Roberts, G. Duckworth, R. Lai, and S. Ebrahim, *Methicillin-resistant Staphylococcus aureus in hospitals and the community: stealth dynamics and control catastrophes.* Proceedings of the National Academy of Sciences of the United States of America, 2004. **101**(27): p. 10223-8.

9.   Reese, L., *Nalidixic Acid (Neggram) in the Treatment of Urinary Infections.* Canadian Medical Association journal, 1965. **92**: p. 394-7.

10.   Mitscher, L.A., *Bacterial topoisomerase inhibitors: quinolone and pyridone antibacterial agents.* Chemical reviews, 2005. **105**(2): p. 559-92.

11.   Appelbaum, P.C. and A. Bryskier, *Quinolones*, in *Antiobiotic and Chemotherapy : Anti-Infective Agents and Their Use in Therapy*, G.D. Finch RG, Norrby SR, Whitley RJ, Editor 2010, Elsevier: Edinburgh. p. 306-325.

12.   Katzung, B.G., A.J. Trevor, and S.B. Masters, *Chapter 46. Sulfonamides, Trimethoprim, and Fluoroquinolones.*, in *Pharmacology: Examination and Board Review.*, B.G. Katzung, A.J. Trevor, and S.B. Masters, Editors. 2010, McGraw-Hill: New York.

13.   Drlica, K., H. Hiasa, R. Kerns, M. Malik, A. Mustaev, and X. Zhao, *Quinolones: Action and Resistance Updated.* Current Topics in Medicinal Chemistry, 2009. **9**: p. 981-998.

14.   Wiles, J., B. Bradbury, and M. Pucci, *New Quinolone Antibiotics: A Survey of the Literature from 2005-2010.* Expert Opinion on Therapeutic Patents, 2010. **20**(10): p. 1295-1319.

15.   Champoux, J.J., *DNA topoisomerases: structure, function, and mechanism.* Annual review of biochemistry, 2001. **70**: p. 369-413.

16.   Hooper, D.C., *Emerging mechanisms of fluoroquinolone resistance.* Emerging infectious diseases, 2001. **7**(2): p. 337-41.

17.   Heddle, J.G., F.M. Barnard, L.M. Wentzell, and A. Maxwell, *The Interaction of Drugs with DNA Gyrase: A Model for the Molecular Basis of Quinolone Action.* Nucleosides, Nucleotides, and Nucleic Acids, 2000. **19**(8): p. 1249-1264.

18.   Drlica, K., M. Malik, R.J. Kerns, and X. Zhao, *Quinolone-Mediated Bacterial Death.* Antimicrobial Agents and Chemotherapy, 2008. **52**(2): p. 385-392.

19.   Malik, M., X. Zhao, and K. Drlica, *Lethal fragmentation of bacterial chromosomes mediated by DNA gyrase and quinolones.* Molecular Microbiology, 2006. **61**(3): p. 810-25.

20.   Laponogov, I., M.K. Sohi, D.A. Veselkov, X.-S. Pan, R. Sawhney, A.W. Thompson, K.E. McAuley, L.M. Fisher, and M.R. Sanderson, *Structural insight into the quinolone-DNA cleavage complex of type IIA topoisomerases.* Nature Structural & Molecular Biology, 2009. **16**(6): p. 667-669.

21.   Bax, B.D., P.F. Chan, D.S. Eggleston, A. Fosberry, D.R. Gentry, F. Gorrec, I. Giordano, M.M. Hann, A. Hennessy, M. Hibbs, J. Huang, E. Jones, J. Jones, K.K. Brown, C.J. Lewis, E.W. May, M.R. Saunders, O. Singh, C.E. Spitzfaden, C. Shen, A. Shillings, A.F. Theobald, A. Wohlkonig, N.D. Pearson, and M.N. Gwynn, *Type IIA topoisomerase inhibition by a new class of antibacterial agents.* Nature, 2010. **466**(7309): p. 935-940.

22.   Wohlkonig, A., P.F. Chan, A.P. Fosberry, P. Homes, J. Huang, M. Kranz, V.R. Leydon, A.J. Shillings, M.N. Gwynn, and B.D. Bax, *Structural basis of quinolone inhibition of type IIA topoisomerases and target-mediated resistance.* Nature Structural & Molecular Biology, 2010. **17**(9): p. 1152-1153.

23.   Shen, L.L., L.A. Mitscher, P.N. Sharms, T.J. O'Donnell, D.W.T. Chu, C.S. Cooper, T. Rosen, and A.G. Pernet, *Mechanism of Inhibition of DNA Gyrase by Quinolone Antibacterials: A Cooperative Drug-DNA Binding Model.* Biochemistry, 1989. **28**: p. 3886-3894.

24.   Domagala, J.M., L.D. Hanna, C.L. Heifetz, M.P. Hutt, T.F. Mich, J.P. Sanchez, and M. Solomon, *New structure-activity relationships of the quinolone antibacterials using the target enzyme. The development and application of a DNA gyrase assay.* Journal of Medicinal Chemistry, 1986. **29**(3): p. 394-404.

25. Heddle, J. and A. Maxwell, *Quinolone-Binding Pocket of DNA Gyrase: Role of GyrB.* Antimicrobial Agents and Chemotherapy, 2002. **46**(6): p. 1805-1815.

26. Yoshida, H., M. Bogaki, M. Nakamura, and S. Nakamura, *Quinolone resistance-determining region in the DNA gyrase gyrA gene of Escherichia coli.* Antimicrobial Agents and Chemotherapy, 1990. **34**(6): p. 1271-2.

27. Morais Cabral, J.H., A.P. Jackson, C.V. Smith, N. Shikotra, A. Maxwell, and R.C. Liddington, *Crystal structure of the breakage-reunion domain of DNA gyrase.* Nature, 1997. **388**(6645): p. 903-6.

28. Low, D.E., *Quinolone Resistance and Its Clinical Relevance*, in *Quinolone Antimicrobial Agents*, E.R. David C Hooper, Editor 2003, ASM Press: Washington DC. p. 355-386.

29. Peterson, L.R., *Quinolone Resistance in Clinical Practice: Occurrence and Importance*, in *Quinolone Antimicrobials Agents*, J.S.W. David C Hooper, Editor 1993, American Society for Microbiology: Washington DC. p. 119-137.

30. Sulochana, S., S. Narayanan, C.N. Paramasivan, C. Suganthi, and P.R. Narayanan, *Analysis of Fluoroquinolone Resistance in Clinical Isolates of Mycobacterium tuberculosis from India.* Journal of Chemotherapy, 2007. **19**(2): p. 166-171.

31. Zhao, X., J.-Y. Wang, C. Xu, Y. Dong, J. Zhou, J. Domagala, and K. Drlica, *Killing of Staphylococcus aureus by C-8 Methoxy Fluoroquinolones.* Antimicrobial Agents and Chemotherapy, 1998. **42**(4): p. 956-958.

32. Lu, T., X. Zhao, X. Li, A. Drlica-Wagner, J.-Y. Wang, J. Domagala, and K. Drlica, *Enhancement of Fluoroquinolone Activity by C-8 Halogen and Methoxy Moieties: Action against a Gyrase Resistance Mutant of Mycobacterium smegmatis and a Gyrase-Topoisomerase IV Double Mutant of Staphylococcus aureus.* Antimicrobial Agents and Chemotherapy, 2001. **45**(10): p. 2703-2709.

33. Dong, Y., C. Xu, X. Zhao, J. Domagala, and K. Drlica, *Fluoroquinolone Action against Mycobacteria: Effects of C-8 Substituents on Growth, Survival, and Resistance.* Antimicrobial Agents and Chemotherapy, 1998. **42**(11): p. 2978-2984.

34. Malik, M., K.R. Marks, A. Mustaev, X. Zhao, K. Chavda, R.J. Kerns, and K. Drlica, *Fluoroquinolone and Quinazolinedione Activities against Wild-Type and Gyrase Mutant Strains of Mycobacterium smegmatis.* Antimicrobial Agents and Chemotherapy, 2011. **55**(5): p. 2335-2343.

35. Malik, M., S. Hussain, and K. Drlica, *Effect of Anaerobic Growth on Quinolone Lethality with Escherichia coli.* Antimicrobial Agents and Chemotherapy, 2007. **51**(1): p. 28-34.

36. Malik, M., T. Lu, X. Zhao, A. Singh, C.M. Hattan, J. Domagala, R. Kerns, and K. Drlica, *Lethality of Quinolones against Mycobacterium smegmatis in the Presence or Absence of Chloramphenicol.* Antimicrobial Agents and Chemotherapy, 2005. **49**(5): p. 2008-2014.

37. Lewin, C.S. and S.G.B. Amyes, *The Bactericidal Activity of Dr-3355, an Optically-Active Isomer of Ofloxacin.* Journal of Medical Microbiology, 1989. **30**(3): p. 227-231.

38. Lewin, C.S., S.G.B. Amyes, and J.T. Smith, *Bactericidal Activity of Enoxacin and Lomefloxacin against Escherichia-Coli Kl16.* European Journal of Clinical Microbiology & Infectious Diseases, 1989. **8**(8): p. 731-733.

39. Lewin, C.S. and S.G.B. Amyes, *Conditions Required for the Bactericidal Activity of Fleroxacin and Pefloxacin against Escherichia-Coli Kl16.* Journal of Medical Microbiology, 1990. **32**(2): p. 83-86.

40. Malik, M. and K. Drlica, *Moxifloxacin Lethality against Mycobacterium tuberculosis in the Presence and Absence of Chloramphenicol.* Antimicrobial Agents and Chemotherapy, 2006. **50**(8): p. 2842-2844.

41. Malik, M., K.R. Marks, H.A. Schwanz, N. German, K. Drlica, and R.J. Kerns, *Effect of N-1/C-8 Ring Fusion and C-7 Ring Structure on Fluoroquinolone Lethality.* Antimicrobial Agents and Chemotherapy, 2010. **54**(12): p. 5214-5221.

42. Anquetin, G., J. Greiner, and P. Vierling, *Synthesis of mono- and di-substituted 2,4,5-trifluorobenzoic acid synthons, key precursors for biologically active 6-fluoroquinolones.* Tetrahedron, 2005. **61**(35): p. 8394-8404.

43. Masuzawa, K., S. Suzue, K. Hirai, and T. Ishizaki, *Preparation of 8-alkoxyquinolonecarboxylic acids as antibacterials with selective toxicity*, 1987, Kyorin Pharmaceutical Co., Ltd., Japan . p. 44 pp.

44. Zhang, Z. and W. Zhou, *Arylation of nitromethane: masked nucleophilic formylation of fluoroquinolones.* Tetrahedron Letters, 2005. **46**(22): p. 3855-3858.

45. Sternglanz, R., S. DiNardo, K.A. Voelkel, Y. Nishimura, Y. Hirota, K. Becherer, L. Zumstein, and J.C. Wang, *Mutations in the gene coding for Escherichia coli DNA topoisomerase I affect transcription and transposition.* Proceedings of the National Academy of Sciences, 1981. **78**(5): p. 2747-2751.

46. Mock, M. and A. Fouet, *ANTHRAX.* Annual Review of Microbiology, 2001. **55**(1): p. 647-671.

47. Bossi, P., A. Tegnell, A. Baka, F. Van Loock, J. Hendriks, A. Werner, H. Maidhof, and G. Gouvras, *Bichat guidelines for the clinical management of anthrax and bioterrorism-related anthrax.* Euro surveillance : bulletin europeen sur les maladies transmissibles = European communicable disease bulletin, 2004. **9**(12): p. E3-4.

48. Waterer, G.W. and H. Robertson, *Bioterrorism for the respiratory physician.* Respirology, 2009. **14**(1): p. 5-11.

49. Schwartz, M., *Dr. Jekyll and Mr. Hyde: A short history of anthrax.* Molecular Aspects of Medicine, 2009. **30**(6): p. 347-355.

50.   Aldred, K.J., S.A. McPherson, P. Wang, R.J. Kerns, D.E. Graves, C.L. Turnbough, Jr., and N. Osheroff, *Drug interactions with Bacillus anthracis topoisomerase IV: biochemical basis for quinolone action and resistance.* Biochemistry, 2012. **51**(1): p. 370-81.

51.   Brook, I., T.B. Elliott, H.I. Pryor Ii, T.E. Sautter, B.T. Gnade, J.H. Thakar, and G.B. Knudson, *In vitro resistance of Bacillus anthracis Sterne to doxycycline, macrolides and quinolones.* International Journal of Antimicrobial Agents, 2001. **18**(6): p. 559-562.

52.   Price, L.B., A. Vogler, T. Pearson, J.D. Busch, J.M. Schupp, and P. Keim, *In vitro selection and characterization of Bacillus anthracis mutants with high-level resistance to ciprofloxacin.* Antimicrobial Agents and Chemotherapy, 2003. **47**(7): p. 2362-5.

53.   Grohs, P., I. Podglajen, and L. Gutmann, *Activities of different fluoroquinolones against Bacillus anthracis mutants selected in vitro and harboring topoisomerase mutations.* Antimicrobial Agents and Chemotherapy, 2004. **48**(8): p. 3024-7.

54.   Bast, D.J., A. Athamna, C.L. Duncan, J.C.S. de Azavedo, D.E. Low, G. Rahav, D. Farrell, and E. Rubinstein, *Type II topoisomerase mutations in Bacillus anthracis associated with high-level fluoroquinolone resistance.* Journal of Antimicrobial Chemotherapy, 2004. **54**(1): p. 90-94.

55.   Oppegard, L.M., K.R. Steck, J.D. Rosen, H.A. Schwanz, K. Drlica, R.J. Kerns, and H. Hiasa, *Comparison of In Vitro Activities of Fluoroquinolone-Like 2,4- and 1,3-Diones.* Antimicrobial Agents and Chemotherapy, 2010. **54**(7): p. 3011-3014.

56.   Anderson, V.E., T.D. Gootz, and N. Osheroff, *Topoisomerase IV catalysis and the mechanism of quinolone action.* The Journal of biological chemistry, 1998. **273**(28): p. 17879-85.

57.   Anderson, V.E., R.P. Zaniewski, F.S. Kaczmarek, T.D. Gootz, and N. Osheroff, *Quinolones inhibit DNA religation mediated by Staphylococcus aureus topoisomerase IV. Changes in drug mechanism across evolutionary boundaries.* The Journal of biological chemistry, 1999. **274**(50): p. 35927-32.

58.   Robinson, M.J., B.A. Martin, T.D. Gootz, P.R. McGuirk, M. Moynihan, J.A. Sutcliffe, and N. Osheroff, *Effects of quinolone derivatives on eukaryotic topoisomerase II. A novel mechanism for enhancement of enzyme-mediated DNA cleavage.* The Journal of biological chemistry, 1991. **266**(22): p. 14585-92.

59.   Drlica, K. and X. Zhao, *DNA gyrase, topoisomerase IV, and the 4-quinolones.* Microbiology and molecular biology reviews : MMBR, 1997. **61**(3): p. 377-92.

60.   Barnard, F.M. and A. Maxwell, *Interaction between DNA gyrase and quinolones: effects of alanine mutations at GyrA subunit residues Ser(83) and Asp(87).* Antimicrobial Agents and Chemotherapy, 2001. **45**(7): p. 1994-2000.

61.   Anderson, V.E., R.P. Zaniewski, F.S. Kaczmarek, T.D. Gootz, and N. Osheroff, *Action of quinolones against Staphylococcus aureus topoisomerase IV: basis for DNA cleavage enhancement.* Biochemistry, 2000. **39**(10): p. 2726-32.

62. Pan, X.-S., K.A. Gould, and L.M. Fisher, *Probing the Differential Interactions of Quinazolinedione PD 0305970 and Quinolones with Gyrase and Topoisomerase IV.* Antimicrobial Agents and Chemotherapy, 2009. **53**(9): p. 3822-3831.

63. Mortensen, D.S., S.M. Perrin-Ninkovic, R. Harris, B.G.S. Lee, G. Shevlin, M. Hickman, G. Khambatta, R.R. Bisonette, K.E. Fultz, and S. Sankar, *Discovery and SAR exploration of a novel series of imidazo[4,5-b]pyrazin-2-ones as potent and selective mTOR kinase inhibitors.* Bioorganic & Medicinal Chemistry Letters, 2011. **21**(22): p. 6793-6799.

64. Fortune, J.M. and N. Osheroff, *Merbarone inhibits the catalytic activity of human topoisomerase IIalpha by blocking DNA cleavage.* The Journal of biological chemistry, 1998. **273**(28): p. 17643-50.

65. Noble, C.G., F.M. Barnard, and A. Maxwell, *Quinolone-DNA Interaction: Sequence-Dependent Binding to Single-Stranded DNA Reflects the Interaction within the Gyrase-DNA Complex.* Antimicrobial Agents and Chemotherapy, 2003. **47**(3): p. 854-862.

66. Bailly, C., P. Colson, and C. Houssier, *The orientation of norfloxacin bound to double-stranded DNA.* Biochemical and Biophysical Research Communications, 1998. **243**(3): p. 844-8.

67. Ni, Y., S. Du, and S. Kokot, *Molecular spectroscopy and chemometrics: an analytical study of synergistic effects of drugs--interaction between fluoroquinolones and DNA.* The Analyst, 2009. **134**(9): p. 1840-7.

68. Son, G.S., J.-A. Yeo, M.-S. Kim, S.K. Kim, A. Holmen, B. Akerman, and B. Norden, *Binding mode of norfloxacin to calf thymus DNA.* Journal of the American Chemical Society, 1998. **120**: p. 6451-6457.

69. Son, G.-S., J.-A. Yeo, J.-M. Kim, S.K. Kim, H.R. Moon, and W. Nam, *Base specific complex formation of norfloxacin with DNA.* Biophysical Chemistry, 1998. **74**: p. 225-236.

70. Sortino, S. and G. Condorelli, *Complexes between fluoroquinolones and calf thymus DNA: binding mode and photochemical reactivity.* New Journal of Chemistry, 2002. **26**: p. 250-258.

71. Shen, L.L. and A.G. Pernet, *Mechanism of inhibition of DNA gyrase by analogues of nalidixic acid: the target of the drugs is DNA.* Proceedings of the National Academy of Sciences of the United States of America, 1985. **82**(2): p. 307-11.

72. Palu, G., S. Valisena, G. Ciarrocchi, B. Gatto, and M. Palumbo, *Quinolone binding to DNA is mediated by magnesium ions.* Proceedings of the National Academy of Sciences, 1992. **89**: p. 9671-9675.

73. Kampranis, S.C. and A. Maxwell, *The DNA Gyrase-Quinolone Complex.* Journal of Biological Chemistry, 1998. **273**(35): p. 22615-22626.

74. Tornaletti, S. and A.M. Pedrini, *Studies on the interaction of 4-quinolones with DNA by DNA unwinding experiments.* Biochimica et biophysica acta, 1988. **949**(3): p. 279-87.

75.   Tornaletti, S. and A.M. Pedrini, *DNA unwinding induced by nalidixic acid binding to DNA.* Biochemical Pharmacology, 1988. **37**(9): p. 1881-1882.

76.   Laponogov, I., X.-S. Pan, D.A. Veselkov, K.E. McAuley, L.M. Fisher, and M.R. Sanderson, *Structural Basis of Gate-DNA Breakage and Resealing by Type II Topoisomerases.* PLoS ONE, 2010. **5**(6).

77.   Richter, S.N., G. Giaretta, V. Comuzzi, E. Leo, L.A. Mitchenall, L.M. Fisher, A. Maxwell, and M. Palumbo, *Hot-spot consensus of fluoroquinolone-mediated DNA cleavage by Gram-negative and Gram-positive type II DNA topoisomerases.* Nucleic Acids Research, 2007. **35**(18): p. 6075-6085.

78.   Marians, K.J. and H. Hiasa, *Mechanism of Quinolone Action.* Journal of Biological Chemistry, 1997. **272**(14): p. 9401-9409.

79.   Mergny, J.L. and L. Lacroix, *Analysis of thermal melting curves.* Oligonucleotides, 2003. **13**(6): p. 515-37.

80.   Miller, J.H., *Experiments in molecular genetics*1972, Cold Spring Harbor, N.Y.: Cold Spring Harbor Laboratory. xvi, 466 p.

81.   Tran, T.P., E.L. Ellsworth, B.M. Watson, J.P. Sanchez, H.D.H. Showalter, J.R. Rubin, M.A. Sier, J. Yip, D.Q. Nguyen, P. Bird, and R. Singh, *A Facile Synthesis of Substituted 3-Amino-1H-Quinazoline -2,4-Diones.* Journal of Heterocyclic Chemistry, 2005. **42**: p. 669-674.

82.   Beylin, V., D.C. Boyles, T.T. Curran, D. Macikenas, R.V. Parlett, and D. Vrieze, *The Preparation of Two, Preclinical Amino-quinazolinediones as Antibacterial Agents.* Organic Process Research & Development, 2007. **11**: p. 441-449.

83.   Masuzawa, K., S. Suzue, K. Hirai, and T. Ishizaki, *Quinolonecarboxylic acid derivatives and their preparation*, 1990, Kyorin Pharmaceutical Co., Ltd.: United States.

84.   Baker, W.R., S. Cai, M. Dimitroff, L. Fang, K.K. Huh, D.R. Ryckman, X. Shang, R.M. Shawar, and J.H. Therrien, *A prodrug approach toward the development of water soluble fluoroquinolones and structure--activity relationships of quinoline-3-carboxylic acids.* Journal of Medicinal Chemistry, 2004. **47**(19): p. 4693-709.

85.   Miyamoto, H., H. Ueda, T. Otsuka, S. Aki, H. Tamaoka, M. Tominaga, and K. Nakagawa, *Studies on antibacterial agents. III. Synthesis and antibacterial activities of substituted 1,4-dihydro-8-methyl-4-oxoquinoline-3-carboxylic acids.* Chemical & Pharmaceutical Bulletin, 1990. **38**(9): p. 2472-5.

86.   Yang, Y., R. Ji, Z. Hu, K. Chen, and J. Wu, *Synthesis and structure-activity relationships of levofloxacin analogs.* Yaoxue Xuebao, 1999. **34**(Copyright (C) 2012 American Chemical Society (ACS). All Rights Reserved.): p. 197-202.

87.   Li, B., O.M. Cociorva, T. Nomanbhoy, Q. Li, K. Nakamura, M. Nomura, K. Okada, K. Yumoto, M. Liyanage, M.C. Zhang, A. Aban, A.K. Szardenings, J.W. Kozarich, Y. Kohno, and K.R. Shreder, *6-Position optimization of tricyclic 4-quinolone-based inhibitors of glycogen synthase kinase-3β: Discovery of nitrile derivatives with picomolar potency.* Bioorg. Med. Chem. Lett., 2012. **22**(Copyright (C) 2012 American Chemical Society (ACS). All Rights Reserved.): p. 1005-1008.

88.   Sanchez, J.P., J.M. Domagala, S.E. Hagen, C.L. Heifetz, M.P. Hutt, J.B. Nichols, and A.K. Trehan, *Quinolone antibacterial agents. Synthesis and structure-activity relationships of 8-substituted quinoline-3-carboxylic acids and 1,8-naphthyridine-3-carboxylic acids.* Journal of Medicinal Chemistry, 1988. **31**(5): p. 983-91.

89.   Grohe, K. and H. Heitzer, *Cycloaracylation of enamines. I. Synthesis of 4-quinolone-3-carboxylic acids.* Liebigs Ann. Chem., 1987(Copyright (C) 2012 American Chemical Society (ACS). All Rights Reserved.): p. 29-37.

90.   Koga, H., A. Itoh, S. Murayama, S. Suzue, and T. Irikura, *Structure-activity relationships of antibacterial 6,7- and 7,8-disubstituted 1-alkyl-1,4-dihydro-4-oxoquinoline-3-carboxylic acids.* Journal of Medicinal Chemistry, 1980. **23**(12): p. 1358-63.

91.   Takemura, M., H. Takahashi, K. Kawakami, K. Namba, M. Tanaka, and R. Miyauchi, *Preparation of oxoquinolinecarboxylic acid, oxonaphthyridinecarboxylic acid, and pyridobenzoxazinecarboxylic acid derivatives as antibacterial agents*, 2001, Daiichi Pharmaceutical Co., Ltd., Japan . p. 104 pp.

92.   Fujita, N., Y. Fukuda, J. Namikawa, M. Tominaga, and Y. Manabe, *Preparation of N-cyclopropyl-1,4-dihydro-4-oxoquinoline-3-carboxylic acids as bactericides*, 1989, Otsuka Pharmaceutical Co., Ltd., Japan . p. 29 pp.

93.   Petersen, U., A. Krebs, T. Schenke, T. Philipps, K. Grohe, K.d. Bremm, R. Endermann, K.G. Metzger, and I. Haller, *Preparation of (diazabicyclononyl)quinolones and related compounds as antibacterials*, 1993, Bayer A.-G., Germany . p. 68 pp.

94.   Bird, P., E.L. Ellsworth, D.Q. Nguyen, J.P. Sanchez, H.D.H. Showalter, R. Singh, M.A. Stier, T.P. Tran, B.M. Watson, and J. Yip, *Preparation of 3-aminoquinazoline-2,4-dione antibacterial agents*, 2001, Warner-Lambert Company, USA . p. 291 pp.

95.   German, N., M. Malik, J.D. Rosen, and R.J. Kerns, *Use of Gyrase Resistance Mutants to Guide Selection of 8-Methoxy-Quinazoline-2,4-Diones.* Antimicrobial Agents and Chemotherapy, 2008. **52**(11): p. 3915-3921.

96.   Renau, T.E., J.W. Gage, J.A. Dever, G.E. Roland, E.T. Joannides, M.A. Shapiro, J.P. Sanchez, S.J. Gracheck, J.M. Domagala, M.R. Jacobs, and R.C. Reynolds, *Structure-Activity Relationships of Quinolone Agents against Mycobacteria: Effect of Structural Modifications at the 8 Position.* Antimicrobial Agents and Chemotherapy, 1996. **40**(10): p. 2363-2368.